SRNS-STI-2008-00057
Revision 0

International Study of Aluminum Impacts on Crystallization in U.S. High Level Waste Glass

K. M. Fox, D. K. Peeler, T. B. Edwards, D. R. Best, I. A. Reamer, R. J. Workman and J.C. Marra

Pacific Northwest National Laboratory
B. J. Riley, J. D. Vienna, J. V. Crum, J. Matyas, A. B. Edmondson, J. B. Lang, N. M. Ibarra and A. Fluegel

V.G. Khlopin Radium Institute
A. Aloy, A.V. Trofimenko and R. Soshnikov

September 2008

Environmental & Chemical Process Technology
Savannah River National Laboratory
Aiken, SC 29808

This document was prepared in conjunction with work accomplished under Contract No. DE-AC09-08SR22470 with the U.S. Department of Energy.

SRNL
SAVANNAH RIVER NATIONAL LABORATORY

DISCLAIMER

This document was prepared in conjunction with work accomplished under Contract No. DE-AC09-08SR22470 with the U.S. Department of Energy.

Keywords: *waste glass formulation, crystallization, aluminum retention*

Retention: *permanent*

International Study of Aluminum Impacts on Crystallization in U.S. High Level Waste Glass

K. M. Fox, D. K. Peeler, T. B. Edwards, D. R. Best, I. A. Reamer, R. J. Workman and J.C. Marra

Pacific Northwest National Laboratory
B. J. Riley, J. D. Vienna, J. V. Crum, J. Matyas, A. B. Edmondson, J. B. Lang, N. M. Ibarra and A. Fluegel

V.G. Khlopin Radium Institute
A. Aloy, A.V. Trofimenko and R. Soshnikov

September 2008

Environmental & Chemical Process Technology
Savannah River National Laboratory
Aiken, SC 29808

This document was prepared in conjunction with work accomplished under Contract No. DE-AC09-08SR22470 with the U.S. Department of Energy.

EXECUTIVE SUMMARY

The objective of this task was to develop glass formulations for (Department of Energy) DOE waste streams with high aluminum concentrations to avoid nepheline formation while maintaining or meeting waste loading and/or waste throughput expectations as well as satisfying critical process and product performance related constraints. Liquidus temperatures and crystallization behavior were carefully characterized to support model development for higher waste loading glasses. The experimental work, characterization, and data interpretation necessary to meet these objectives were performed among three partnering laboratories: the V.G. Khlopin Radium Institute (KRI), Pacific Northwest National Laboratory (PNNL) and Savannah River National Laboratory (SRNL).

Projected glass compositional regions that bound anticipated Defense Waste Processing Facility (DWPF) and Hanford high level waste (HLW) glass regions of interest were developed and used to generate glass compositions of interest for meeting the objectives of this study. A thorough statistical analysis was employed to allow for a wide range of waste glass compositions to be examined while minimizing the number of glasses that had to be fabricated and characterized in the laboratory. The glass compositions were divided into two sets, with 45 in the test matrix investigated by the U.S. laboratories and 30 in the test matrix investigated by KRI. Fabrication and characterization of the US and KRI-series glasses were generally handled separately. This report focuses mainly on the US-series glasses.

Glasses were fabricated and characterized by SRNL and PNNL. Crystalline phases were identified by X-ray diffraction (XRD) in the quenched and canister centerline cooled (CCC) glasses and were generally iron oxides and spinels, which are not expected to impact durability of the glass. Nepheline was detected in five of the glasses after the CCC heat treatment.

Chemical composition measurements for each of the glasses were conducted following an analytical plan. A review of the individual oxides for each glass revealed that there were no errors in batching significant enough to impact the outcome of the study. A comparison of the measured compositions of the replicates indicated an acceptable degree of repeatability as the percent differences for most of the oxides were less than 5% and percent differences for all of the oxides were less than 10 wt%.

Chemical durability was measured using the Product Consistency Test (PCT). All but two of the study glasses had normalized leachate for boron (NL [B]) values that were well below that of the Environmental Assessment (EA) reference glass. The two highest NL [B] values were for the CCC versions of glasses US-18 and US-27 (10.498 g/L and 15.962 g/L, respectively). Nepheline crystallization was identified by qualitative XRD in five of the US-series glasses. Each of these five glasses (US-18, US-26, US-27, US-37 and US-43) showed a significant increase in NL [B] values after the CCC heat treatment. This reduction in durability can be attributed to the formation of nepheline during the slow cooling cycle and the removal of glass formers from the residual glass network.

The liquidus temperature (T_L) of each glass in the study was determined by both optical microscopy and XRD methods. The correlation coefficient of the measured XRD T_L data versus the measured optical T_L data was very good ($R^2 = 0.9469$). Aside from a few outliers, the two datasets aligned very well across the entire temperature range (829 °C to 1312 °C for optical data and 813 °C to 1310 °C for XRD crystal fraction data). The data also correlated well with the predictions of a PNNL T_L model. The correlation between the measured and calculated data had

a higher degree of merit for the XRD crystal fraction data than for the optical data (higher R^2 value of 0.9089 versus 0.8970 for the optical data).

The SEM-EDS analysis of select samples revealed the presence of undissolved RuO_2 in all glasses due to the low solubility of RuO_2 in borosilicate glass. These particles tended to form agglomerates with varying sizes and shapes that were located close to the bottom of crucibles.

The results of this study provide further insight into the ability of borosilicate waste glass to incorporate increased (>16 wt %) concentrations of aluminum. The glass composition and properties data will be incorporated into a database of glass composition-property relationships (ComPro) to support further optimization of waste glass compositions at DOE sites.

TABLE OF CONTENTS

LIST OF TABLES

LIST OF FIGURES

LIST OF ABBREVIATIONS

ARM	Approved Reference Material
CCC	Canister Centerline Cooled
DOE	Department of Energy
DWPF	Defense Waste Processing Facility
EA	Environmental Assessment
EDS	Energy Dispersive Spectroscopy
FC	Furnace Controller
HLW	High Level Waste
HROM	High Resolution Optical Microscopy
ICP-AES	Inductively Coupled Plasma – Atomic Emission Spectroscopy
INL	Idaho National Laboratory
KRI	V.G. Khlopin Radium Institute
LM	Lithium Metaborate
LROM	Low Resolution Optical Microscopy
LWO	Liquid Waste Organization
NL	Normalized Leachate
NQARD	Nuclear Quality Assurance Requirements and Description
PCT	Product Consistency Test
PF	Peroxide Fusion
PNNL	Pacific Northwest National Laboratory
PSAL	Process Science Analytical Laboratory
SEM	Scanning Electron Microscopy
QA	Quality Assurance
SRNL	Savannah River National Laboratory
SRS	Savannah River Site
T_a	Amorphous Temperature
TC	Thermocouple
T_c	Crystallization Temperature
ThS	Thin Section
T_L	Liquidus Temperature
UT	Uniform Temperature
XRD	X-ray Diffraction

1.0 Introduction

The United States Department of Energy (DOE) is currently processing (or planning to process) high-level waste (HLW) through Joule-heated melters at the Savannah River Site (SRS) and Hanford. The process combines the HLW sludge with prefritted or mined mineral glass forming additives that are subsequently melted. The molten glass is poured into stainless steel canisters to create the final waste form. In preparation for the qualification and receipt of each sludge batch, development and definition of various tank blending and/or washing strategies have been or will be initiated. The various strategies are contemplated in an effort to meet critical site objectives or constraints that include tank volume space, transfer options, and settling issues. Although these objectives or constraints are critical, the ability to meet both process and product performance criteria associated with the final waste form must also be maintained. The product performance issues relate to the durability of the glass waste form. Process related issues (e.g., liquidus temperature, viscosity, electrical conductivity, and melting rate) ultimately dictate the efficiency and effectiveness of the melter operation.

Tank retrieval and blending strategies at both the SRS and Hanford have identified high Al_2O_3 concentration waste streams that are scheduled to be processed through their respective HLW vitrification facilities. For example, the Liquid Waste Organization (LWO) at SRS provided compositional projections for the next two sludge batches (Sludge Batch 4 and Sludge Batch 5) to be processed in the Defense Waste Processing Facility (DWPF). These streams have Al_2O_3 concentrations of approximately 25-40 wt% (on a calcined oxide basis). In addition, physical limitations in the Tank Farms and/or settling issues associated with the sludge coupled with the need to maintain feed for DWPF have prevented advanced washing which has resulted in relatively high Na_2O (approximately 22-26 wt%) and SO_4^{2-} (approximately 0.8-1.6 wt%) concentrations. Current Hanford projections suggest that Al_2O_3 concentrations in sludge could be much greater than those currently projected for DWPF, with Al_2O_3 concentrations as high as 80 wt%.

While it is well known that the addition of small amounts of Al_2O_3 to borosilicate glass generally enhances the durability of the waste form (through creation of network-forming tetrahedral Na^+-$[AlO_{4/2}]^-$ pairs), nepheline ($NaAlSiO_4$) formation, which depends in part on the Al_2O_3 concentration, can result in a severe deterioration of the chemical durability of the glass through residual glass compositional changes. The primary driver for this reduction in durability is the fact that nepheline removes three moles of glass forming oxides (Al_2O_3 and $2SiO_2$) from the continuous glass phase per each mole of Na_2O consumed. Nepheline formation produces an Al_2O_3 and SiO_2 deficient continuous glass matrix (relative to the same composition which is void of crystals), which reduces the durability of the final product. The magnitude of the reduction ultimately depends on the extent of crystallization and on the initial glass composition.

The formation of nepheline and/or other aluminum/silicon-containing crystals is a potential for both DWPF and Hanford due to the projected compositional views recently evaluated coupled with the frit development strategy (e.g., higher alkali frits have lead to enhanced melt rates at DWPF for those sludge batches). Although durability is obviously a critical constraint that the HLW glass must meet, other process related issues must also be considered. Additionally, the inclusion of higher concentrations of Al_2O_3 will generally increase the liquidus temperature of the melt and decrease the processing rate.

2.0 Objective

The objective of this task was to develop glass formulations for DOE waste streams with high aluminum concentrations to avoid nepheline formation while maintaining or meeting waste loading and/or waste throughput expectations as well as satisfying critical process and product performance related constraints. Secondary objectives of this task were to assess the SO_4^{2-} solubility limit for the DWPF compositions and spinel settling for the Hanford compositions. Liquidus temperatures and crystallization behavior were carefully characterized to support model development for higher waste loading glasses.

The experimental work, characterization, and data interpretation necessary to meet these objectives were performed among three partnering laboratories: the V.G. Khlopin Radium Institute (KRI), Pacific Northwest National Laboratory (PNNL) and Savannah River National Laboratory (SRNL).

3.0 Quality Assurance (QA)

This project was performed in accordance with the applicable criteria of 10 CFR 830.120, Subpart A, *Quality Assurance Criteria* and DOE/RW-0333P requirements. The PNNL QA Program implemented for this project was the *Nuclear Quality Assurance Requirements and Description (NQARD)* document. The NQARD is an NQA-1 based program (which meets DOE/RW-0333P requirements) with a graded approach for applying QA controls. The NQARD manual includes a program description section, followed by a set of QA implementing procedures.[1] The SRNL work scope was performed in accordance with Savannah River Site Manual 1Q, *Quality Assurance,* with supplemental QA requirements as defined by Manual L1, Section 8.21, *Supplemental QA Requirements for DOE/RW-0333P*. Additional detail of the QA measures applied to this study can be found in the Test Plan.[2]

4.0 Experimental Procedure

4.1 Selection of Study Glass Compositions

A total of 67 individual glass compositions (75 glasses including replicates) were selected for this study. A thorough description of the process used to select these glasses is available in a separate document,[3] although a brief summary will be provided here. Projected glass compositional regions that bound anticipated DWPF and Hanford glass regions of interest were developed and used to generate glass compositions of interest for meeting the objectives of this study (i.e., the incorporation of larger concentrations of aluminum, as well as improved sulfur retention and minimization of detrimental crystallization). A thorough statistical analysis was employed to allow for a wide range of waste glass compositions to be examined while minimizing the number of glasses that had to be fabricated and characterized in the laboratory. The glass compositions were divided into two sets, with 45 in the test matrix investigated by the U.S. laboratories (US-xx series glasses) and 30 in the test matrix investigated by KRI (KRI-xx series glasses). Fabrication and characterization of the US and KRI-series glasses were generally handled separately. SRNL and PNNL supported work on the US-series glasses, while KRI performed all work on the KRI-series glasses. This report will therefore focus mainly on the US-series glasses. A complete description of the results from the KRI-series glasses can be found in the final report from Aloy et al.,[4] which is included in the appendices.

The targeted compositions for the 45 US-series glasses in this study are given in Table 4-1.

Table 4-1. Target Compositions of the US-Series Glasses.

Glass Identifier	Al_2O_3	B_2O_3	CaO	Cr_2O_3	Fe_2O_3	K_2O	Li_2O	MgO	MnO	Na_2O	NiO	PbO	RuO_2	SO_3	SiO_2	SrO	TiO_2	ZnO	ZrO_2
US-01	0.1493	0.0789	0.0000	0.0030	0.0859	0.0100	0.0562	0.0050	0.0250	0.1237	0.0006	0.0010	0.0002	0.0000	0.4553	0.0010	0.0000	0.0000	0.0050
US-02	0.1600	0.1686	0.0000	0.0000	0.0659	0.0000	0.0529	0.0000	0.0063	0.1233	0.0000	0.0000	0.0002	0.0000	0.4168	0.0000	0.0000	0.0010	0.0050
US-03	0.1600	0.1731	0.0100	0.0000	0.0653	0.0100	0.0407	0.0050	0.0000	0.0788	0.0029	0.0010	0.0002	0.0000	0.4421	0.0010	0.0100	0.0000	0.0000
US-04	0.1600	0.1129	0.0100	0.0000	0.0827	0.0100	0.0374	0.0050	0.0219	0.1033	0.0000	0.0010	0.0002	0.0050	0.4338	0.0010	0.0100	0.0010	0.0050
US-05	0.1599	0.1670	0.0070	0.0000	0.0816	0.0100	0.0200	0.0050	0.0241	0.0958	0.0000	0.0010	0.0002	0.0050	0.4064	0.0010	0.0100	0.0010	0.0050
US-06	0.1600	0.1406	0.0100	0.0000	0.0815	0.0100	0.0247	0.0050	0.0300	0.1078	0.0000	0.0000	0.0002	0.0050	0.4142	0.0010	0.0100	0.0000	0.0000
US-07	0.1600	0.1349	0.0100	0.0000	0.0730	0.0100	0.0266	0.0050	0.0300	0.1067	0.0020	0.0010	0.0002	0.0050	0.4188	0.0010	0.0100	0.0010	0.0050
US-08	0.1519	0.0956	0.0000	0.0000	0.0975	0.0100	0.0486	0.0000	0.0244	0.0981	0.0000	0.0010	0.0002	0.0050	0.4577	0.0000	0.0100	0.0000	0.0000
US-09	0.1337	0.1505	0.0100	0.0030	0.1088	0.0000	0.0200	0.0050	0.0000	0.1411	0.0000	0.0010	0.0002	0.0050	0.4117	0.0000	0.0100	0.0000	0.0000
US-10	0.1412	0.1099	0.0100	0.0000	0.1069	0.0100	0.0200	0.0050	0.0274	0.1267	0.0000	0.0010	0.0002	0.0050	0.4198	0.0010	0.0100	0.0010	0.0050
US-11	0.1370	0.1998	0.0100	0.0000	0.0776	0.0100	0.0200	0.0050	0.0300	0.0669	0.0000	0.0010	0.0002	0.0050	0.4366	0.0000	0.0000	0.0010	0.0000
US-12	0.1324	0.1608	0.0100	0.0014	0.0874	0.0100	0.0600	0.0000	0.0000	0.1116	0.0184	0.0000	0.0002	0.0050	0.3913	0.0010	0.0050	0.0010	0.0045
US-13	0.1600	0.1457	0.0100	0.0000	0.0730	0.0100	0.0215	0.0050	0.0280	0.1153	0.0028	0.0010	0.0002	0.0000	0.4165	0.0000	0.0100	0.0010	0.0000
US-14	0.1302	0.1790	0.0040	0.0000	0.0941	0.0100	0.0574	0.0050	0.0260	0.1122	0.0000	0.0007	0.0002	0.0000	0.3652	0.0000	0.0100	0.0010	0.0050
US-15	0.1000	0.1780	0.0050	0.0030	0.0500	0.0100	0.0200	0.0000	0.0000	0.1500	0.0000	0.0010	0.0002	0.0050	0.4659	0.0010	0.0100	0.0010	0.0000
US-16	0.1332	0.1881	0.0100	0.0008	0.0903	0.0100	0.0256	0.0000	0.0248	0.0630	0.0000	0.0000	0.0002	0.0000	0.4391	0.0000	0.0100	0.0000	0.0050
US-17	0.1166	0.1178	0.0000	0.0011	0.0622	0.0000	0.0536	0.0050	0.0300	0.0858	0.0108	0.0000	0.0002	0.0000	0.4999	0.0010	0.0100	0.0010	0.0050
US-18	0.1600	0.0913	0.0100	0.0000	0.0975	0.0000	0.0495	0.0000	0.0300	0.1341	0.0000	0.0010	0.0002	0.0000	0.4145	0.0010	0.0100	0.0010	0.0000
US-19	0.1447	0.1440	0.0070	0.0007	0.0823	0.0078	0.0364	0.0033	0.0199	0.1080	0.0021	0.0007	0.0002	0.0028	0.4281	0.0006	0.0080	0.0007	0.0027
US-20	0.1447	0.1440	0.0070	0.0007	0.0823	0.0078	0.0364	0.0033	0.0199	0.1080	0.0021	0.0007	0.0002	0.0028	0.4281	0.0006	0.0080	0.0007	0.0027
US-21	0.1422	0.1375	0.0038	0.0008	0.0845	0.0075	0.0300	0.0037	0.0178	0.1075	0.0050	0.0008	0.0002	0.0012	0.4495	0.0008	0.0054	0.0003	0.0013
US-22	0.1334	0.1169	0.0075	0.0008	0.0947	0.0075	0.0500	0.0037	0.0225	0.1178	0.0092	0.0003	0.0002	0.0012	0.4240	0.0008	0.0075	0.0008	0.0013
US-23	0.1450	0.1332	0.0075	0.0008	0.0762	0.0025	0.0350	0.0012	0.0225	0.1168	0.0050	0.0008	0.0002	0.0037	0.4446	0.0003	0.0025	0.0008	0.0013
US-24	0.1450	0.1225	0.0075	0.0008	0.0779	0.0075	0.0300	0.0037	0.0225	0.1157	0.0050	0.0008	0.0002	0.0037	0.4443	0.0008	0.0075	0.0008	0.0038
US-25	0.1158	0.1625	0.0075	0.0022	0.0854	0.0029	0.0500	0.0037	0.0216	0.1088	0.0145	0.0003	0.0002	0.0037	0.4079	0.0008	0.0075	0.0008	0.0038
US-26	0.1883	0.1069	0.0100	0.0055	0.0500	0.0000	0.0600	0.0050	0.0000	0.1102	0.0000	0.0000	0.0002	0.0000	0.3805	0.0300	0.0100	0.0200	0.0235
US-27	0.1040	0.0648	0.0000	0.0100	0.1518	0.0100	0.0600	0.0050	0.0000	0.1687	0.0000	0.0000	0.0002	0.0050	0.4004	0.0000	0.0000	0.0200	0.0000
US-28	0.1747	0.1796	0.0000	0.0000	0.0572	0.0100	0.0200	0.0000	0.0000	0.1336	0.0000	0.0000	0.0002	0.0050	0.3597	0.0300	0.0100	0.0200	0.0000
US-29	0.1000	0.0873	0.0100	0.0067	0.0500	0.0100	0.0600	0.0050	0.0000	0.1868	0.0000	0.0100	0.0002	0.0000	0.4526	0.0118	0.0096	0.0000	0.0000
US-30	0.1265	0.1819	0.0100	0.0082	0.0533	0.0100	0.0600	0.0000	0.0350	0.0500	0.0000	0.0000	0.0002	0.0050	0.3752	0.0300	0.0100	0.0048	0.0400
US-31	0.1267	0.1452	0.0000	0.0000	0.1545	0.0000	0.0491	0.0050	0.0074	0.0710	0.0000	0.0100	0.0002	0.0050	0.3860	0.0300	0.0100	0.0000	0.0000
US-32	0.1000	0.1901	0.0100	0.0000	0.0500	0.0000	0.0600	0.0000	0.0400	0.0750	0.0000	0.0100	0.0002	0.0050	0.4397	0.0000	0.0000	0.0200	0.0000
US-33	0.1134	0.0500	0.0000	0.0100	0.0500	0.0000	0.0200	0.0050	0.0400	0.1976	0.0097	0.0100	0.0002	0.0050	0.4591	0.0300	0.0000	0.0000	0.0000
US-34	0.1000	0.1369	0.0000	0.0000	0.0639	0.0100	0.0242	0.0050	0.0400	0.2000	0.0000	0.0000	0.0002	0.0000	0.3499	0.0300	0.0000	0.0000	0.0400
US-35	0.1002	0.1996	0.0100	0.0052	0.1135	0.0000	0.0200	0.0050	0.0400	0.0794	0.0000	0.0000	0.0002	0.0000	0.3800	0.0270	0.0000	0.0200	0.0000
US-36	0.1286	0.1551	0.0021	0.0051	0.0976	0.0052	0.0242	0.0005	0.0121	0.1252	0.0056	0.0100	0.0002	0.0000	0.3884	0.0001	0.0001	0.0001	0.0400
US-37	0.1000	0.0577	0.0100	0.0000	0.1700	0.0000	0.0200	0.0000	0.0000	0.1889	0.0000	0.0100	0.0002	0.0000	0.3733	0.0000	0.0100	0.0200	0.0400
US-38	0.1000	0.0731	0.0079	0.0000	0.0500	0.0100	0.0200	0.0000	0.0400	0.1972	0.0291	0.0100	0.0002	0.0050	0.3975	0.0300	0.0100	0.0200	0.0000
US-39	0.1155	0.1635	0.0000	0.0000	0.0750	0.0100	0.0600	0.0050	0.0000	0.0500	0.0183	0.0100	0.0002	0.0000	0.4246	0.0080	0.0000	0.0200	0.0400
US-40	0.1552	0.1700	0.0000	0.0043	0.1142	0.0100	0.0251	0.0000	0.0276	0.1013	0.0000	0.0100	0.0002	0.0000	0.3730	0.0000	0.0092	0.0000	0.0000
US-41	0.1000	0.1555	0.0100	0.0000	0.1553	0.0100	0.0372	0.0000	0.0000	0.0652	0.0000	0.0100	0.0002	0.0000	0.4265	0.0300	0.0000	0.0000	0.0000
US-42	0.2000	0.0619	0.0100	0.0000	0.0500	0.0100	0.0600	0.0000	0.0400	0.1882	0.0000	0.0100	0.0002	0.0000	0.3549	0.0000	0.0000	0.0149	0.0000
US-43	0.1717	0.0864	0.0100	0.0000	0.0886	0.0100	0.0490	0.0050	0.0081	0.1029	0.0020	0.0100	0.0002	0.0050	0.3970	0.0047	0.0048	0.0045	0.0400
US-44	0.1280	0.1259	0.0056	0.0031	0.0886	0.0064	0.0405	0.0025	0.0183	0.1273	0.0036	0.0067	0.0002	0.0022	0.3955	0.0162	0.0047	0.0102	0.0146
US-45	0.1280	0.1259	0.0056	0.0031	0.0886	0.0064	0.0405	0.0025	0.0183	0.1273	0.0036	0.0067	0.0002	0.0022	0.3955	0.0162	0.0047	0.0102	0.0146

4.2 Glass Fabrication

Each study glass was prepared from the proper proportions of reagent-grade metal oxides, carbonates, H_3BO_3, and salts in 250 g batches. The raw materials were thoroughly mixed and placed into a 95% platinum / 5% gold, 250 mL crucible. The crucibles were placed into a high-temperature furnace at a target melt temperature of 1150 °C. The crucibles were removed from the furnace after an isothermal hold at 1150 °C for 1 hour. The molten glass was quenched by pouring onto a clean, stainless steel plate. Note that some of the glasses did not appear to have melted completely after holding at 1150 °C for 1 hour. Those glasses were re-melted at 1200 °C for 1 hour and then quenched.

Approximately 25 g of each glass was heat-treated to simulate cooling along the centerline of a DWPF-type canister to gauge the effects of thermal history on the product performance.[5] This cooling schedule is referred to as canister centerline cooling (CCC). Visual observations were recorded for each of the glasses both after quenching and at the completion of the CCC heat treatment.

4.3 Property Measurements

4.3.1 *X-Ray Diffraction Analysis*

Representative samples of each of the quenched and CCC glasses were submitted to SRNL Analytical Development for X-ray diffraction (XRD) analysis. Samples were run under conditions providing a detection limit of approximately 0.5 vol %. That is, if crystals (or undissolved batch material) were present at 0.5 vol % or greater, the diffractometer would not only be capable of detecting the crystals but would also allow a qualitative determination of the type of crystal(s) present. Otherwise, a characteristically high background signal (amorphous hump) devoid of crystalline spectral peaks indicates that the glass product is free of crystallization, suggesting either a completely amorphous product or that the degree of crystallization is below the detection limit.

4.3.2 *Compositional Analysis*

To confirm that the as-fabricated glasses met the target compositions, a representative sample from each quenched glass was submitted to the SRNL Process Science Analytical Laboratory (PSAL) for chemical analysis under the auspices of an analytical plan.[6] The plan identified the cations to be analyzed and the two dissolution techniques, sodium peroxide fusion (PF) and lithium-metaborate (LM), to be used. The samples prepared by LM were used to measure calcium (Ca), chromium (Cr), potassium (K), magnesium (Mg), manganese (Mn), sodium (Na), lead (Pb), sulfur (S), strontium (Sr), titanium (Ti), zinc (Zn), and zirconium (Zr) concentrations. Samples prepared by PF were used to measure aluminum (Al), boron (B), iron (Fe), lithium (Li), nickel (Ni), and silicon (Si) concentrations. Each glass was prepared in duplicate for each of the two cation dissolution techniques. All of the prepared samples were analyzed twice for each element of interest by Inductively Coupled Plasma – Atomic Emission Spectroscopy (ICP-AES), with the instrumentation being re-calibrated between the duplicate analyses. The analytical plan was developed in such a way as to provide the opportunity to evaluate potential sources of bias and error. Glass standards were also intermittently measured to assess the performance of the ICP-AES instrument over the course of these analyses.

4.3.3 *Durability Testing*

A 7-day Product Consistency Test (PCT) was performed in triplicate on each quenched and CCC glass to assess chemical durability using Method A of the PCT procedure.[7] Also included in the

experimental test matrix was the Environmental Assessment (EA) glass, the Approved Reference Material (ARM) glass, and blanks from the sample cleaning batch. Samples were ground, washed, and prepared according to the standard procedure. The resulting solutions were sampled (filtered and acidified) and analyzed under the auspices of three analytical plans.[8-10] Samples of a multi-element standard solution were also included in the analytical plans as a check on the accuracy of the ICP-AES instrument. Normalized release rates were calculated based on the target and measured compositions using the average of the logs of the leachate concentrations.

4.3.4 *Liquidus Temperature*

Liquidus temperature (T_L) measurements were performed on the 45 study glasses using the uniform temperature (UT) method as described in PNNL procedure GDL-LQT.[11] Using this procedure, the quenched glass was crushed and sieved to a size fraction from 4.0 mm to 0.425 mm (-5 to +40 mesh, respectively). The captured chunks were then cleaned three times with ethanol using an ultrasonic bath. The UT analyses for these samples were completed by:

- Placing the glass in a covered, square platinum boat with a side length of about 13 mm
- Heat treating for 24 ± 2 hours at temperature (shorter times are used at higher temperatures)
- Quenching the boat on steel plate
- Recording initial observations by optical microscopy with the glass still in the platinum boat
- Grinding the glass with 5 wt% CaF_2 for quantitative XRD analysis

XRD measurements for all glasses were performed with a Scintag PAD V diffractometer using Cu K_α radiation (λ = 1.5406 Å, 45 kV, and 40 mA) and equipped with a Peltier-cooled Si(Li) solid state detector. The experiments were done using $\theta - 2\theta$ geometry in a step-scan approach from 10° to 60° 2θ with a step size of 0.04° 2θ and a dwell time of 6 seconds per step. Each sample was loaded into a 12-position automatic sample changer. Jade 6® and RIQAS® software[a] were used to process and identify phase assemblages. PNNL's standard procedure for XRD analysis[12] was used to guide these measurements.

Optional portions of the method include thin-sectioning and analysis using high-power optical microscopy or SEM analysis.

4.4 Scanning Electron Microscopy

A select group of the US-series glasses, US-01, US-03 to US-09, and US-14 (see compositions in Table 4-1) were analyzed by Scanning Electron Microscopy (SEM) and Energy Dispersive Spectroscopy (EDS) to identify crystalline phases and insoluble metal species. The glasses were subjected to heat-treatments at various temperatures for 24 ± 2 hrs in 1.2 × 1.2 × 1.2 cm Pt-10% Rh crucibles. Samples were removed from the crucibles and cut in half. Cross-sections were ground, polished and coated by sputtering with gold-palladium for SEM and EDS analysis.

[a] Materials Data, Inc., Livermore, CA.

5.0 Results and Discussion

5.1 Visual Observations and XRD Results

Visual observations for each of the study glasses were recorded both after quenching and at the completion of the CCC heat treatment. These observations are listed in Table 5-1. Crystallization in the glasses is described as a haze, streaks or swirls. Glasses that are described as clean or homogeneous indicate that no crystallization was observable by the unaided eye. XRD results for the quenched and CCC version of each glass are also provided in Table 5-1. The XRD results generally agree with the visual observations, although there are some cases where crystallization occurred only on the surface of the glass and may not have existed in a significant enough volume fraction to be detected by XRD. The phases identified by XRD are generally iron oxides and spinels, which are not expected to impact durability of the glass.[13] Nepheline was detected in five of the glasses after the CCC heat treatment (highlighted in the table): US-18, US-26, US-27, US-37 and US-43. The impact of the nepheline crystallization on the durability of the glasses will be explored in the following sections.

Table 5-1. Visual Observations and XRD Results for the US-Series Glasses.

Glass	T_{Melt} (°C)	Heat Treatment	Visual Observations	XRD Results
US-01	1150	quenched	Crucible – clean with bubbles; Patty – black, shiny, homogeneous	amorphous
		CCC	Surface – very light shiny black haze; Bulk – clean	Fe_3O_4, $NiFe_2O_4$, SiO_2
US-02	1150	quenched	Crucible – clean with bubbles; Patty – black, shiny, homogeneous	amorphous
		CCC	Surface – black, shiny, clean; Bulk – clean	Fe_3O_4, $NiFe_2O_4$, SiO_2
US-03	1150	quenched	Crucible – clean with bubbles; Patty – black, shiny, homogeneous	amorphous
		CCC	Surface – multiple crystals; Bulk – multiple crystals	Fe_2O_3
US-04	1150	quenched	Crucible – clean with bubbles; Patty – black, shiny, homogeneous	amorphous
		CCC	Surface – chocolate brown; Bulk – black and shiny	amorphous
US-05	1150	quenched	Crucible – several spots of undissolved material; Patty – black and shiny with some silvery spots/pits on the surface, thin white film on bottom	amorphous
		CCC	Surface – chocolate brown with clusters of crystals; Bulk – chocolate brown	Fe_3O_4, Fe_2O_3
US-06	1150	quenched	Crucible – clean with bubbles; Patty – black, shiny, homogeneous	amorphous
		CCC	Surface – chocolate brown with clusters of crystals; Bulk – black and shiny	Fe_2O_3 (Hematite)
US-07	1150	quenched	Crucible – few spots of undissolved material; Patty – black, shiny, homogeneous	amorphous
		CCC	Surface – chocolate brown with clusters of shiny crystals; Bulk – black and shiny	Fe_3O_4, $NiFe_2O_4$
US-08	1150	quenched	Crucible – few spots of undissolved material; Patty – black, shiny, homogeneous	amorphous
		CCC	Surface – brown with crystals; Bulk – black, shiny, clean	amorphous
US-09	1150	quenched	Crucible – few spots of undissolved material; Patty – black, shiny, homogeneous	amorphous
		CCC	Surface – clear shellac with crystals under surface, also circular clusters of crystals; Bulk – solid medium brown	Fe_2O_3
US-10	1150	quenched	Crucible – clean with bubbles; Patty – black, shiny, homogeneous	amorphous
		CCC	Surface – dull matte with crystals; Bulk – devitrified	Fe_2O_3
US-11	1150	quenched	Crucible – few spots of undissolved material; Patty – some surface pits and white film on bottom	amorphous
		CCC	Surface and Bulk – totally devitrified	Fe_2O_3

Table 5-1. Visual Observations and XRD Results for the US-Series Glasses. (continued)

Glass	T_{Melt} (°C)	Heat Treatment	Visual Observations	XRD Results
US-12	1150	quenched	Crucible – clean with bubbles; Patty – black, shiny, homogeneous	amorphous
		CCC	Surface – black matte; Bulk – crystals	Fe_3O_4, $NiFe_2O_4$
US-13	1150	quenched	Crucible – few spots of undissolved material; Patty – clean	amorphous
		CCC	Surface – large metallic circles with crystals; Bulk – crystals	Fe_3O_4, $NiFe_2O_4$
US-14	1150	quenched	Crucible – clean; Patty – Clean, homogeneous	amorphous
		CCC	Surface – shiny haze with crystals along the melt line; Bulk – clean	Fe_3O_4, $NiFe_2O_4$
US-15	1200	quenched	Crucible – green glass with some brown streaks; Patty – translucent green glass with some brown streaks	amorphous
		CCC	Surface – dark, shiny; Bulk – green, clean	Fe_3O_4
US-16	1200	quenched	Crucible – two small spots of undissolved material; Patty – black, shiny, homogeneous	$NiFe_2O_4$, Fe_2O_3
		CCC	Surface – green, hazy sheen with small silver crystals; Bulk – crystals throughout	Fe_2O_3
US-17	1150	quenched	Crucible – two spots of undissolved material; Patty – black, shiny, clean	amorphous
		CCC	Surface – shiny with crystals; Bulk – bottom layer chocolate brown and crystallized, top layer black, shiny, clean	Fe_3O_4, $NiFe_2O_4$
US-18	1150	quenched	Crucible – four small spots of undissolved material; Patty – black, shiny, homogeneous	amorphous
		CCC	Surface and Bulk – totally crystallized	$NaAlSiO_4$
US-19	1150	quenched	Crucible – three spots of undissolved material; Patty – black, shiny, homogeneous	amorphous
		CCC	Surface – shiny, silver spots of crystals; Bulk – clean	Fe_3O_4
US-20	1150	quenched	Crucible – three spots of undissolved material; Patty – black, shiny, homogeneous	amorphous
		CCC	Surface – shiny, silver spots of crystals; Bulk – thin layer of crystals along surfaces in contact with crucible	Fe_3O_4
US-21	1150	quenched	Crucible – four small spots of undissolved material and bubbles; Patty – black, shiny, homogeneous	amorphous
		CCC	Surface – brown with a lot of metallic crystals; Bulk – crystals	Fe_3O_4, $NiFe_2O_4$
US-22	1150	quenched	Crucible – two spots of undissolved material; Patty – black, shiny, homogeneous	amorphous
		CCC	Surface – hazy sheen with a few metallic crystals; Bulk – crystals	Fe_3O_4, $NiFe_2O_4$, SiO_2

Table 5-1. Visual Observations and XRD Results for the US-Series Glasses. (continued)

Glass	T_{Melt} (°C)	Heat Treatment	Visual Observations	XRD Results
US-23	1150	quenched	Crucible – four spots of undissolved material with bubbles; Patty – black, shiny, homogeneous	amorphous
		CCC	Surface – brown with metallic crystals; Bulk – clean	Fe_3O_4, $NiFe_2O_4$
US-24	1150	quenched	Crucible – three spots of undissolved material; Patty – black, shiny, clean, homogeneous	amorphous
		CCC	Surface – chocolate brown with crystals; Bulk – clean	Fe_3O_4, $NiFe_2O_4$
US-25	1150	quenched	Crucible – two spots of undissolved material; Patty – clean, black, shiny, homogeneous	amorphous
		CCC	Surface – hazy sheen; Bulk – crystals throughout	Fe_3O_4, $NiFe_2O_4$
US-26	1200	quenched	Crucible – green glass with some undissolved material; Patty – dark with some undissolved solids and some metallic streaks	Fe_3O_4
		CCC	Surface – brown with pitted crystals; Bulk – crystals	Fe_3O_4, $NiFe_2O_4$, $NaAlSiO_4$
US-27	1150	quenched	Crucible – clean with bubbles; Patty – very light amount of possible salt layer on surface	Fe_3O_4
		CCC	Surface – gold and yellow crystals; Bulk – crystals throughout	Fe_3O_4, $NiFe_2O_4$, $NaAlSiO_4$
US-28	1150	quenched	Crucible – one spot of undissolved material; Patty – black, shiny, clean, homogeneous	amorphous
		CCC	Surface – broken bubbles in small section of melt line, otherwise clean; Bulk – clean	amorphous
US-29	1150	quenched	Crucible – green glass with some darker green on bottom; Patty – clean, homogeneous	amorphous
		CCC	Surface – dark and shiny with five small spots of crystals; Bulk – clean	amorphous
US-30	1200	quenched	Crucible – two spots of undissolved material; Patty – shiny silver streaks on surface, bulk clean	Fe_3O_4
		CCC	Surface – hazy sheen with clusters of crystals along melt line; Bulk – crystals	Fe_3O_4, $MnFeO_4$
US-31	1150	quenched	Crucible – clean; Patty – black, shiny, a few light brown surface streaks	amorphous
		CCC	Surface – covered with metallic crystals; Bulk – completely devitrified	Fe_2O_3
US-32	1150	quenched	Crucible – clean with bubbles; Patty – black, shiny, homogeneous	amorphous
		CCC	Surface – black, shiny, homogeneous; Bulk - clean	amorphous
US-33	1150	quenched	Crucible – clean; Patty – some silvery, hazy swirls on surface, bulk black and shiny	Fe_3O_4
		CCC	Surface – covered with silvery/goldish swirls of crystals; Bulk – crystals	Fe_3O_4, $NiFe_2O_4$
US-34	1150	quenched	Crucible – clean; Patty – clean	amorphous
		CCC	Surface – covered with shiny crystals; Bulk – crystals	amorphous

Table 5-1. Visual Observations and XRD Results for the US-Series Glasses. (continued)

Glass	T_{Melt} (°C)	Heat Treatment	Visual Observations	XRD Results
US-35	1200	quenched	Crucible – clean with bubbles; Patty – black, shiny, homogeneous	Fe_3O_4
		CCC	Surface – covered with shiny crystalline haze; Bulk – crystals	$(Zn,Mn,Fe)(Fe,Mn)_2O_4$
US-36	1150	quenched	Crucible – a few silver streaks; Patty – black, shiny with some silver swirls on surface	$NiFe_2O_4$
		CCC	Surface – covered with shiny crystals, some dull crystals along melt line; Bulk – crystals	Fe_3O_4, $NiFe_2O_4$
US-37	1150	quenched	Crucible – clean with bubbles; Patty – black, shiny, homogeneous	amorphous
		CCC	Surface – dull, reddish/brown crystals; Bulk – devitrified	$NaAlSiO_4$, Fe_3O_4
US-38	1150	quenched	Crucible – clean with bubbles; Patty – milky haze on surface, bulk black, shiny and clean	amorphous
		CCC	Surface – matte finish; Bulk – crystals	NiO, Fe_3O_4
US-39	1150	quenched	Crucible – clean; Patty – black, shiny, homogeneous	amorphous
		CCC	Surface – chocolate brown crystals; Bulk – chocolate brown color with crystals	Fe_3O_4, $NiFe_2O_4$
US-40	1150	quenched	Crucible – clean; Patty – dark brown surface, bulk was a lighter brown with a thin layer of black shiny glass on the bottom	Fe_2O_3, Fe_3O_4
		CCC	Surface – shiny crystals under surface; Bulk – crystals	Fe_2O_3
US-41	1150	quenched	Crucible – clean; Patty – black, shiny, homogeneous	amorphous
		CCC	Surface – Purple, sparkly crystals, pitted; Bulk – shiny crystals throughout	Fe_2O_3
US-42	1150	quenched	Crucible – haze on surface, no undissolved; Patty – dull, brownish haze on surface, bulk clean	amorphous
		CCC	Surface – covered with shiny/reddish crystals; Bulk – completely devitrified	nepheline
US-43	1150	quenched	Crucible – light beige streaks on surface; Patty – shiny brown with a few beige streaks	amorphous
		CCC	Surface – dull, matte, covered with crystals; Bulk – devitrified	$Na_{6.65}Al_{6.24}Si_{9.76}O_{32}$, Fe_2O_3
US-44	1150	quenched	Crucible – two spots of undissolved material; Patty – dark, shiny, homogeneous	amorphous
		CCC	Surface – black, shiny, a few tiny spots of crystals; Bulk – crystals	Fe_3O_4
US-45	1150	quenched	Crucible – three spots of undissolved material; Patty – dark, shiny, homogeneous	amorphous
		CCC	Surface – Black, shiny, a few tiny spots of crystals; Bulk – crystals	Fe_3O_4

5.2 Chemical Composition Analysis

Chemical composition measurements for these glasses were conducted by the SRNL PSAL following an analytical plan.[6] The elemental concentrations were converted to oxide concentrations by multiplying the values for each element by the gravimetric factor for the corresponding oxide. During this process, each elemental concentration that was determined to be below the detection limit of the analytical procedures used by the PSAL was reduced to half of that detection limit as the oxide concentration was determined.

As detailed in the summary by Edwards,[14] the oxide measurements of the study glasses were bias corrected for the effect of the ICP-AES calibration on each of the analytical blocks. The four measurements for each oxide for each glass (over both preparation methods) were averaged to determine a representative chemical composition for each glass. These determinations were conducted both for the measured and for the bias-corrected data. A sum of oxides was also computed for each glass based upon both the measured and bias-corrected values.

Table 5-2 provides a summary of the average, bias-corrected concentration of each oxide for each glass. All of the sums of oxides for the study glasses fall within the interval of 95 to 105 wt%, indicating good confidence in the analyses. Table 5-2 also provides the percent difference (when the targeted concentration for the oxide is at least 0.5 wt%) between the measured bias-corrected concentrations and the targeted concentrations. A review of the individual oxides for each glass reveals that there were no errors in batching significant enough to impact the outcome of the study.

The chemical compositions of glasses US-44 and US-45 can be compared as a measure of repeatability of the batching process since these glasses were duplicates; that is, they had the same target compositions. A comparison indicates an acceptable degree of repeatability as the percent differences for most of the oxides are less than 5% and percent differences for all of the oxides are less than 10 wt%.

Table 5-2. Bias-Corrected Chemical Composition Data for the US-Series Glasses and Percent Differences from the Target Values.

Glass ID	Al_2O_3	B_2O_3	CaO	Cr_2O_3	Fe_2O_3	K_2O	Li_2O	MgO	MnO	Na_2O	NiO	PbO	SiO_2	SO_3	SrO	TiO_2	ZnO	ZrO_2	Sum
US-01	15.389	8.190	0.131	0.265	8.811	0.884	5.712	0.559	2.674	13.799	0.062	0.060	44.045	0.062	0.090	0.014	0.006	0.463	101.216
	3.10%	3.80%			2.60%	-11.6%	1.70%		7.10%	11.50%			-3.30%						1.20%
US-02	16.355	16.043	0.069	0.024	6.561	0.053	5.137	0.009	0.617	12.660	0.021	0.005	40.456	0.062	0.036	0.068	0.123	0.458	98.759
	2.20%	-4.80%			-0.40%		-2.90%		-2.70%	2.60%			-2.90%						-1.20%
US-03	16.359	17.213	1.010	0.016	6.649	0.839	4.071	0.543	0.068	8.272	0.307	0.093	44.120	0.062	0.088	1.025	0.006	0.007	100.747
	2.30%	-0.60%	1.10%		1.90%	-16.1%	0.00%			4.90%			-0.20%			2.70%			0.80%
US-04	16.676	11.158	0.987	0.017	7.978	0.837	3.788	0.535	2.298	11.108	0.007	0.090	42.575	0.396	0.089	1.007	0.095	0.430	100.071
	4.30%	-1.10%	-1.20%		-3.50%	-16.2%	1.20%		5.00%	7.50%			-1.90%			0.90%			0.10%
US-05	16.456	16.370	0.696	0.017	7.948	0.885	2.020	0.539	2.545	10.162	0.007	0.091	39.287	0.284	0.113	1.061	0.097	0.495	99.072
	2.90%	-2.00%	-1.00%		-2.60%	-11.4%	1.00%		5.70%	6.10%			-3.30%			6.40%			-0.90%
US-06	16.523	13.986	0.984	0.018	7.925	0.880	2.513	0.537	3.223	10.564	0.007	0.005	42.120	0.351	0.107	0.982	0.018	0.024	100.765
	3.30%	-0.60%	-1.50%		-2.80%	-11.9%	1.60%		7.50%	-2.00%			1.70%			-1.70%			0.80%
US-07	16.305	13.114	0.981	0.013	6.767	0.850	2.598	0.540	3.086	11.082	0.208	0.090	43.442	0.360	0.087	1.011	0.097	0.423	101.054
	1.90%	-2.80%	-1.80%		-7.30%	-14.9%	-2.30%		2.90%	3.90%			3.70%			1.20%			1.10%
US-08	15.825	9.577	0.132	0.040	9.083	0.832	4.926	0.051	2.363	10.143	0.007	0.082	44.050	0.380	0.180	0.938	0.133	0.154	98.894
	4.20%	0.20%			-6.80%	-16.8%	1.30%		-3.10%	3.40%			-3.80%			-6.10%			-1.10%
US-09	14.037	15.097	0.956	0.223	10.602	0.053	2.087	0.541	0.069	12.911	0.007	0.089	41.899	0.390	0.016	1.013	0.006	0.007	100.003
	5.00%	0.30%	-4.40%		-2.60%		4.30%			-8.50%			1.80%			1.30%			0.00%
US-10	14.693	11.104	0.998	0.017	10.257	0.879	2.085	0.540	2.893	12.992	0.007	0.088	40.747	0.398	0.090	1.022	0.099	0.437	99.347
	4.00%	1.00%	0.00%		-4.00%	-12.0%	4.20%		5.70%	2.50%			-2.90%			2.40%			-0.60%
US-11	14.713	20.008	1.036	0.015	7.014	0.867	2.057	0.555	3.284	6.916	0.007	0.093	45.619	0.249	0.006	0.009	0.102	0.012	102.561
	7.40%	0.20%	3.60%		-9.60%	-13.3%	2.90%		9.50%	3.40%			4.50%						2.60%
US-12	13.938	15.884	1.053	0.117	8.935	0.905	6.066	0.009	0.068	12.482	1.944	0.005	40.564	0.456	0.094	0.547	0.111	0.439	103.617
	5.30%	-1.20%	5.30%		2.20%	-9.50%	1.10%			11.90%	5.80%		3.70%						3.60%
US-13	16.547	14.553	0.995	0.020	7.050	0.847	2.220	0.542	2.987	12.006	0.294	0.088	43.101	0.062	0.006	1.021	0.102	0.036	102.477
	3.40%	-0.10%	-0.40%		-3.40%	-15.2%	3.00%		6.70%	4.10%			3.50%			2.20%			2.50%
US-14	13.587	17.685	0.465	0.009	10.051	0.865	5.810	0.538	2.718	11.160	0.007	0.063	37.117	0.062	0.006	1.030	0.107	0.459	101.739
	4.40%	-1.20%			6.80%	-13.5%	1.20%		4.60%	-0.60%			1.60%			3.10%			1.80%
US-15	10.537	17.897	0.609	0.227	5.132	0.845	2.030	0.009	0.068	15.674	0.007	0.089	46.591	0.408	0.090	0.996	0.098	0.024	101.330
	5.40%	0.60%			2.70%	-15.5%	1.50%			4.50%			0.00%			-0.40%			1.40%
US-16	13.889	18.816	0.997	0.080	8.856	0.894	2.598	0.009	2.634	6.690	0.015	0.005	43.370	0.062	0.006	1.029	0.006	0.486	100.442
	4.30%	0.00%	-0.30%		-1.90%	-10.5%	1.70%		6.10%	6.20%			-1.20%			2.90%			0.50%
US-17	11.942	11.287	0.073	0.087	7.303	0.053	5.227	0.533	3.071	8.867	1.097	0.005	47.124	0.062	0.085	1.016	0.104	0.409	98.345
	2.50%	-4.10%			17.40%		-2.50%		2.40%	3.30%	1.20%		-5.70%			1.60%			-1.60%
US-18	16.864	9.267	0.925	0.011	9.544	0.053	4.998	0.009	3.240	12.607	0.007	0.090	43.066	0.062	0.096	1.030	0.112	0.006	101.989
	5.40%	1.50%	-7.40%		-2.10%		0.90%		8.00%	-6.00%			3.90%			3.00%			2.00%
US-19	14.877	13.961	0.730	0.055	7.923	0.689	3.647	0.364	2.008	11.245	0.209	0.066	40.951	0.263	0.060	0.836	0.067	0.227	98.179
	2.80%	-3.10%	4.30%		-3.70%	-11.3%	0.30%		1.00%	4.10%			-4.30%			3.90%			-1.80%
US-20	14.848	14.014	0.816	0.065	8.327	0.672	3.625	0.362	2.059	11.143	0.214	0.065	41.109	0.254	0.058	0.835	0.072	0.278	98.814
	2.60%	-2.70%	16.70%		1.20%	-13.5%	-0.30%		3.60%	3.20%			-4.00%			3.70%			-1.20%
US-21	15.158	13.697	0.405	0.058	7.914	0.639	3.095	0.404	1.848	11.347	0.489	0.075	46.106	0.127	0.075	0.558	0.037	0.103	102.134
	6.60%	-0.40%			-6.40%	-14.7%	3.10%		3.90%	5.50%	-2.30%		2.60%			2.80%			2.20%

Table 5-2. Bias-Corrected Chemical Composition Data for the US-Series Glasses and Percent Differences from the Target Values. (continued)

Glass ID	Al_2O_3	B_2O_3	CaO	Cr_2O_3	Fe_2O_3	K_2O	Li_2O	MgO	MnO	Na_2O	NiO	PbO	SiO_2	SO_3	SrO	TiO_2	ZnO	ZrO_2	Sum
US-22	13.878	11.602	0.768	0.078	9.440	0.650	5.025	0.416	2.316	13.016	0.947	0.030	42.670	0.140	0.071	0.797	0.087	0.123	102.053
	4.00%	-0.70%	2.60%		-0.30%	-13.2%	0.50%		3.00%	10.50%	3.10%		0.60%			6.40%			2.10%
US-23	14.860	13.111	0.746	0.065	6.941	0.223	3.488	0.137	2.350	12.454	0.505	0.078	44.318	0.331	0.030	0.273	0.091	0.137	100.139
	2.50%	-1.60%	-0.50%		-8.90%		-0.30%		4.50%	6.60%			-0.30%						0.20%
US-24	15.252	12.258	0.768	0.057	7.602	0.669	3.145	0.399	2.454	12.201	0.502	0.077	43.185	0.325	0.072	0.759	0.082	0.384	100.189
	5.20%	0.10%	2.60%		-2.40%	-10.6%	4.80%		9.10%	5.40%	0.10%		-2.80%			1.30%			0.20%
US-25	12.279	16.128	0.781	0.145	8.434	0.270	5.036	0.406	2.219	11.622	1.412	0.031	40.043	0.337	0.082	0.793	0.105	0.361	100.483
	6.00%	-0.70%	4.20%		-1.20%		0.70%		2.50%	6.80%	-2.60%		-1.80%			5.70%			0.50%
US-26	19.201	10.429	1.003	0.402	5.114	0.053	5.923	0.522	0.068	11.285	0.007	0.005	38.642	0.062	2.528	1.002	1.696	2.040	99.982
	2.00%	-2.40%	0.30%	-26.7%	2.30%		-1.30%			2.40%			1.50%		-15.7%	0.20%	-15.2%	-13.2%	0.00%
US-27	10.812	6.676	0.030	0.820	15.146	0.905	5.879	0.530	0.068	17.868	0.007	0.019	39.803	0.483	0.006	0.011	1.733	0.420	101.217
	3.90%	3.00%		-18.0%	-0.20%	-9.40%	-2.00%			5.90%			-0.60%				-13.4%		1.20%
US-28	17.717	17.637	0.038	0.007	5.618	0.841	2.051	0.009	0.067	13.709	0.007	0.005	36.896	0.381	2.481	1.019	1.758	0.013	100.254
	1.40%	-1.80%			-1.80%	-15.80	2.60%			2.70%			2.60%		-17.3%	1.90%	-12.1%		0.30%
US-29	10.441	8.543	1.012	0.542	4.875	0.874	5.934	0.537	0.068	18.814	0.007	1.301	44.137	0.062	1.076	0.979	0.008	0.007	99.214
	4.40%	-2.10%	1.20%	-19.30	-2.50%	-12.6%	-1.10%			0.70%		30.10%	-2.50%		-8.50%	1.50%			-0.80%
US-30	13.165	18.374	1.053	0.569	5.403	0.879	6.053	0.009	3.752	5.453	0.007	0.005	39.059	0.458	2.690	1.050	0.454	3.576	102.009
	4.10%	1.00%	5.40%	-30.5%	1.40%	-12.0%	0.90%		7.30%	9.10%			4.10%		-10.3%	5.00%		-10.6%	2.00%
US-31	13.472	14.224	0.062	0.013	14.859	0.053	4.992	0.518	0.777	8.022	0.025	0.877	40.030	0.368	2.537	1.027	0.006	0.011	101.874
	6.40%	-2.00%			-3.80%		1.70%		4.80%	13.00%		-12.2%	3.70%		-15.4%	2.70%			1.90%
US-32	10.653	18.938	1.014	0.016	5.045	0.053	6.268	0.009	4.594	7.829	0.007	0.894	44.534	0.411	0.006	0.009	1.773	0.044	102.097
	6.50%	-0.40%	1.40%		0.90%		4.50%		14.90%	4.40%		-10.5%	1.30%				-11.3%		2.10%
US-33	12.205	5.355	0.038	0.708	5.033	0.053	2.089	0.577	4.460	19.458	0.992	0.900	47.795	0.506	2.608	0.009	0.120	0.006	102.912
	7.60%	7.10%		-29.2%	0.70%		4.50%		11.50%	-1.50%	2.80%	-10.0%	4.10%		-13.1%				2.90%
US-34	10.492	13.621	0.034	0.009	6.398	0.929	2.442	0.537	4.294	19.339	0.007	0.005	36.505	0.062	2.685	0.009	0.006	3.505	100.879
	4.90%	-0.50%			0.20%	-7.10%	0.90%		7.40%	-3.30%			4.30%		-10.5%			-12.3%	0.90%
US-35	10.482	19.694	1.022	0.428	11.344	0.053	2.061	0.537	4.304	8.447	0.012	0.005	38.785	0.062	2.339	0.009	1.756	0.009	101.350
	4.70%	-1.30%	2.30%	-17.3%	-0.10%		3.10%		7.60%	6.40%			2.10%		-13.5%		-12.2%		1.40%
US-36	13.117	15.337	0.385	0.383	9.734	0.494	2.439	0.049	1.174	13.355	0.553	0.918	38.895	0.062	0.006	0.025	0.014	3.472	100.409
	2.00%	-1.10%		-25.1%	-0.30%	-4.60%	0.70%		-2.60%	6.70%	-1.00%	-8.20%	0.10%					-13.2%	0.40%
US-37	10.711	6.196	1.013	0.009	17.569	0.053	2.049	0.009	0.068	19.151	0.013	0.881	38.701	0.062	0.041	1.020	1.746	3.431	102.724
	7.10%	7.40%	1.30%		3.40%		2.40%			1.40%		-11.8%	3.70%			2.00%	-12.7%	-14.2%	2.70%
US-38	10.468	7.361	0.798	0.013	5.477	0.886	2.083	0.009	4.204	18.343	3.165	0.883	40.195	0.483	2.649	1.011	1.764	0.019	99.810
	4.70%	0.60%	1.10%		9.60%	-11.4%	4.20%		5.10%	-7.00%	8.90%	-11.7%	1.10%		-11.7%	1.10%	-11.8%		-0.20%
US-39	12.079	15.852	0.023	0.011	7.325	0.927	5.993	0.538	0.068	5.006	1.915	0.911	40.840	0.062	0.729	0.009	1.785	3.526	97.596
	4.60%	-3.00%			-2.40%	-7.30%	-0.10%			0.10%	4.70%	-8.90%	-3.80%		-8.60%		-10.7%	-11.8%	-2.40%
US-40	16.088	16.968	0.051	0.308	11.157	0.887	2.554	0.009	2.945	10.661	0.007	0.921	38.486	0.062	0.006	0.945	0.012	0.007	102.072
	3.70%	-0.20%			-2.30%	-11.3%	1.70%		6.70%	5.20%		-7.80%	3.20%			2.40%			2.10%
US-41	10.238	15.224	1.019	0.015	14.818	0.883	3.707	0.009	0.069	6.884	0.013	0.894	41.681	0.062	2.593	0.009	0.006	0.013	98.137
	2.40%	-2.10%	1.90%		-4.60%	-11.60	-0.50%			5.60%		-10.6%	-2.30%		-13.6%				-1.80%
US-42	20.833	6.381	0.975	0.007	5.122	0.861	6.044	0.009	4.415	18.720	0.007	0.887	36.583	0.059	0.006	0.009	1.369	0.012	102.298
	4.20%	3.10%	-2.50%		2.50%	-13.9%	0.70%		10.40%	-0.50%		-11.3%	3.10%				-8.00%		2.30%

Table 5-2. Bias-Corrected Chemical Composition Data for the US-Series Glasses and Percent Differences from the Target Values. (continued)

Glass ID	Al_2O_3	B_2O_3	CaO	Cr_2O_3	Fe_2O_3	K_2O	Li_2O	MgO	MnO	Na_2O	NiO	PbO	SiO_2	SO_3	SrO	TiO_2	ZnO	ZrO_2	Sum
US-43	17.964	8.692	0.987	0.007	9.099	0.866	4.968	0.529	0.752	11.014	0.203	0.888	38.865	0.409	0.416	0.494	0.441	3.367	99.959
	4.60%	0.50%	-1.30%		2.70%	-13.3%	1.30%		-7.40%	7.00%		-11.2%	-2.10%					-15.8%	0.00%
US-44	13.826	12.378	0.606	0.255	8.775	0.567	4.462	0.275	1.866	13.354	0.374	0.607	38.240	0.228	1.407	0.488	0.965	1.308	99.980
	8.00%	-1.70%	9.20%		-1.00%	-11.3%	10.20%		1.70%	4.90%		-8.90%	-3.30%		-13.1%		-5.70%	-10.7%	0.00%
US-45	13.488	12.779	0.584	0.250	8.924	0.589	4.122	0.266	1.898	12.958	0.366	0.591	40.330	0.222	1.434	0.488	0.961	1.313	101.562
	5.40%	1.50%	5.10%		0.70%	-7.90%	1.80%		3.50%	1.80%		-11.3%	2.00%		-11.5%		-6.20%	-10.3%	1.60%

5.3 Chemical Durability Analysis

The results of the PCT for each of the study glasses in terms of the normalized leachate (NL) releases for each of the four elements of interest are given in Table 5-3 as a function of heat treatment. All but two of the study glasses have normalized leachate for boron (NL [B]) values that are well below that of the EA reference glass (16.695 g/L).[15] The two highest NL [B] values are for the CCC versions of glasses US-18 and US-27 (10.498 g/L and 15.962 g/L, respectively). Note the similarity of PCT results for US-44 and US-45. These two glasses had the same targeted composition, and their PCT results differ by less than 0.1 g/L for any of the four elements over all of the compositional views and heat treatments, indicating good reproducibility in fabrication and characterization of the study glasses.

Nepheline crystallization was identified by qualitative XRD in five of the US-series glasses (see Section 5.1). Each of these five glasses (US-18, US-26, US-27, US-37 and US-43) shows a significant increase in NL [B] after the CCC heat treatment. This reduction in durability can be attributed to the formation of nepheline during the slow cooling cycle and the removal of glass formers from the residual glass network.

Five other glasses in the study showed elevated NL [B] values after both quenching and the CCC heat treatment (glasses US-14, US-15, US-32, US-34 and US-35). While there are likely to be compositional drivers responsible for this reduced durability, no clear trends in composition are apparent for this subset of the study glasses.

Table 5-3. PCT Results for Each of the US-Series Glasses by Heat Treatment, Normalized Using the Bias-Corrected Composition Data.

Glass ID	Heat Treatment	NL [B] (g/L)	NL [Li] (g/L)	NL [Na] (g/L)	NL [Si] (g/L)
US-01	CCC	0.446	0.533	0.454	0.407
US-01	quenched	0.454	0.545	0.478	0.418
US-02	CCC	1.468	1.264	0.742	0.354
US-02	quenched	1.821	1.562	0.871	0.354
US-03	CCC	0.326	0.475	0.157	0.256
US-03	quenched	0.358	0.427	0.232	0.271
US-04	CCC	0.335	0.451	0.264	0.248
US-04	quenched	0.353	0.494	0.266	0.257
US-05	CCC	0.500	0.672	0.338	0.283
US-05	quenched	0.347	0.688	0.186	0.249
US-06	CCC	0.308	0.441	0.279	0.220
US-06	quenched	0.338	0.501	0.296	0.225
US-07	CCC	0.331	0.462	0.259	0.217
US-07	quenched	0.364	0.527	0.283	0.226
US-08	CCC	0.407	0.527	0.314	0.370
US-08	quenched	0.433	0.600	0.314	0.395
US-09	CCC	0.441	0.510	0.286	0.240
US-09	quenched	0.431	0.534	0.439	0.275
US-10	CCC	0.345	0.460	0.369	0.245
US-10	quenched	0.352	0.476	0.381	0.251
US-11	CCC	0.796	0.888	0.494	0.220
US-11	quenched	0.328	0.561	0.246	0.186
US-12	CCC	1.765	1.478	0.979	0.370
US-12	quenched	1.286	1.106	0.800	0.342
US-13	CCC	0.299	0.421	0.280	0.216
US-13	quenched	0.352	0.485	0.317	0.233

Table 5-3. PCT Results for Each of the US-Series Glasses by Heat Treatment, Normalized Using the Bias-Corrected Composition Data. (continued)

Glass ID	Heat Treatment	NL [B] (g/L)	NL [Li] (g/L)	NL [Na] (g/L)	NL [Si] (g/L)
US-14	CCC	2.650	2.200	1.577	0.333
US-14	quenched	3.162	2.618	1.846	0.334
US-15	CCC	3.627	3.051	2.007	0.232
US-15	quenched	4.623	3.867	2.512	0.217
US-16	CCC	0.864	0.925	0.426	0.269
US-16	quenched	0.640	0.788	0.292	0.254
US-17	CCC	0.503	0.579	0.302	0.399
US-17	quenched	0.514	0.641	0.279	0.415
US-18	CCC	10.498	8.136	3.540	0.830
US-18	quenched	0.516	0.590	0.620	0.389
US-19	CCC	0.427	0.533	0.328	0.312
US-19	quenched	0.458	0.579	0.330	0.335
US-20	CCC	0.429	0.552	0.334	0.312
US-20	quenched	0.458	0.595	0.344	0.325
US-21	CCC	0.398	0.543	0.292	0.293
US-21	quenched	0.419	0.587	0.301	0.350
US-22	CCC	0.536	0.545	0.517	0.414
US-22	quenched	0.570	0.569	0.466	0.357
US-23	CCC	0.445	0.566	0.335	0.323
US-23	quenched	0.457	0.610	0.338	0.353
US-24	CCC	0.407	0.522	0.335	0.305
US-24	quenched	0.395	0.532	0.320	0.299
US-25	CCC	1.423	1.228	0.865	0.432
US-25	quenched	1.155	1.026	0.731	0.348
US-26	CCC	3.691	2.579	1.184	0.325
US-26	quenched	0.430	0.527	0.409	0.261
US-27	CCC	15.962	7.281	7.039	2.316
US-27	quenched	1.213	1.050	1.475	0.835
US-28	CCC	1.402	1.226	0.884	0.272
US-28	quenched	1.738	1.467	1.023	0.260
US-29	CCC	1.568	1.389	1.736	0.760
US-29	quenched	1.868	1.486	2.074	0.791
US-30	CCC	0.634	0.616	0.405	0.244
US-30	quenched	0.569	0.567	0.358	0.219
US-31	CCC	0.314	0.486	0.178	0.241
US-31	quenched	0.508	0.625	0.262	0.275
US-32	CCC	2.828	2.258	1.444	0.334
US-32	quenched	3.579	2.849	1.787	0.337
US-33	CCC	0.321	0.544	0.864	0.356
US-33	quenched	0.338	0.498	0.911	0.342
US-34	CCC	3.865	3.169	2.811	0.430
US-34	quenched	4.176	3.389	3.067	0.450
US-35	CCC	4.012	3.440	2.367	0.215
US-35	quenched	0.812	0.883	0.596	0.203
US-36	CCC	0.812	0.783	0.463	0.238
US-36	quenched	0.658	0.688	0.395	0.226
US-37	CCC	1.982	1.621	1.395	0.503
US-37	quenched	0.676	0.645	0.919	0.384
US-38	CCC	0.794	0.781	1.207	0.487
US-38	quenched	0.785	0.688	1.164	0.429
US-39	CCC	0.451	0.518	0.182	0.287
US-39	quenched	0.511	0.552	0.220	0.285

Table 5-3. PCT Results for Each of the US-Series Glasses by Heat Treatment, Normalized Using the Bias-Corrected Composition Data. (continued)

Glass ID	Heat Treatment	NL [B] (g/L)	NL [Li] (g/L)	NL [Na] (g/L)	NL [Si] (g/L)
US-40	CCC	1.543	1.366	0.794	0.283
US-40	quenched	1.096	1.057	0.608	0.290
US-41	CCC	0.287	0.493	0.170	0.211
US-41	quenched	0.333	0.493	0.198	0.217
US-42	CCC	0.897	1.987	3.664	0.190
US-42	quenched	1.259	1.088	1.664	0.690
US-43	CCC	1.745	1.755	0.491	0.352
US-43	quenched	0.403	0.587	0.336	0.287
US-44	CCC	0.520	0.516	0.471	0.301
US-44	quenched	0.532	0.514	0.477	0.292
US-45	CCC	0.446	0.538	0.452	0.278
US-45	quenched	0.467	0.559	0.485	0.280

5.4 Liquidus Temperature

5.4.1 *Select Visual Observations of the Quenched Glasses*

Glass composition US-40 appears to be located outside the glass formation range as it is homogeneous at the bottom of the pour patty and inhomogeneous in all other locations, recognizable through different colors visible by eye (Figure 5-1). US-40 may have crystallized or phase separated quickly during pouring. In addition, glass composition US-43 appears to be incompletely melted because it does not have a homogeneous color. A liquidus temperature therefore cannot be determined for these glasses.

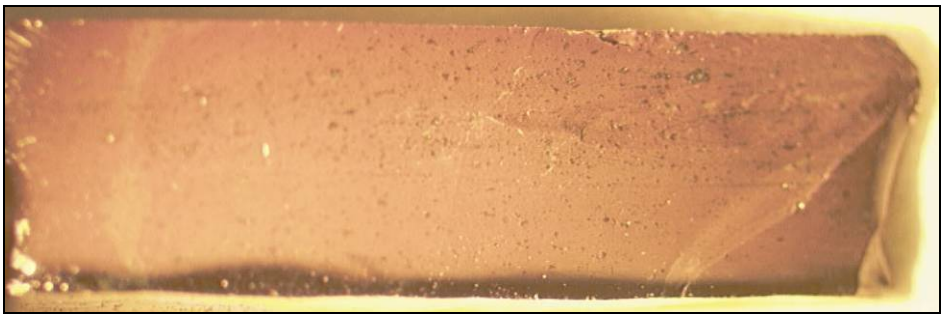

Figure 5-1. US-40 as-received after quenching on a steel plate. Crystallization is visible in the bulk of the glass, while a homogeneous region formed in contact with the steel plate at the bottom of the sample.

5.4.2 *Furnace calibrations*

The calibration of the furnaces used for isothermal T_L measurements at PNNL was verified prior to the start of experiments. Temperature calibration data are given in Table 5-4. Homogeneity of the temperature gradient within each furnace was found to be sufficient to provide reliable measurements.

In addition, T_L standard glasses were measured to verify the correct furnace temperatures and correct execution of the experimental procedure. The T_L of the ARG-1 and Zr-9 standard glasses

have been measured in a Round Robin study with Monarch Laboratories and Idaho National Laboratory (INL). Data from the Round Robin study are listed in Table 5-5. The T_L determination of Zr-9 is complicated by the fact that small crystals appear like air bubbles. Therefore, Zr-9 may be heat-treated several days to allow the crystals to grow. The measured T_L for each standard glass for each of the furnaces used are given at the bottom of Table 5-4, and are in reasonable agreement with the Round Robin values shown in Table 5-5.

Table 5-4. Furnace calibrations at PNNL. The T_L of SRM-773 is 990°C (standard certificate).

	Furnace			
	25	12	5	10
Calibration date using SRM 773	Sept. 22, 2006	Oct. 5, 2006	Nov. 4, 2006	Nov. 18, 2006
Thermocouple (TC) reading in °C	993	991	1009	1008
Furnace controller (FC) reading in °C	984	989	1006	1010
T_L (SRM-773) - TC	-3	-1	-19	-18
TC-FC in °C at FC = 800°C	7	5	4	-9
TC-FC in °C at FC = 900°C	6	2	4	-
TC-FC in °C at FC = 1000°C	9	4	3	-
TC-FC in °C at FC = 1100°C	10	2	4	-
TC-FC in °C at FC = 1200°C	8	-1	4	-
TC-FC in °C at FC = 1300°C	6	-1	4	-
TC-FC in °C at FC = 1400°C	5	2	4	-
Temperature homogeneity at ~1000°C using Ferro temperature control rings	below detection limit (4°C)	~ 4-8°C	~ 4-8°C	~ 4-8°C
T_L in °C, Zr-9	962	963	965	973
T_L in °C, ARG-1	1039	1043	1037	1042

Table 5-5. T_L of ARG-1 and Zr-9 from a Round Robin Study with Monarch Laboratories and INL.

	ARG-1, T_L in °C	Zr-9, T_L in °C
PNNL, measured previously	1028.3	960
Monarch Labs	1030	967
	1031	969
	1038	973
INL	1046	956
	1046	966

5.4.3 *Initial Optical Microscopy Observations*

The glasses were analyzed by both low and high resolution optical microscopy following isothermal heat treatments. Select micrographs are described below, followed by a summary of observations for all of the US-series glasses.

Select Low Resolution Optical Microscopy Observations

Select Low Resolution Optical Microscopy (LROM) observations are provided below. The observations are detailed in the captions accompanying each micrograph.

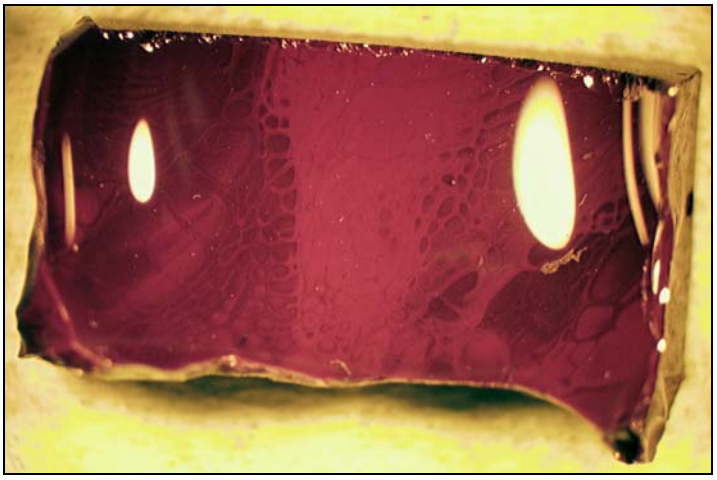

Figure 5-2. Brown crystal striations in the bulk of glass US-03 after heat treating at 854 °C (sample length approximately 12 mm).

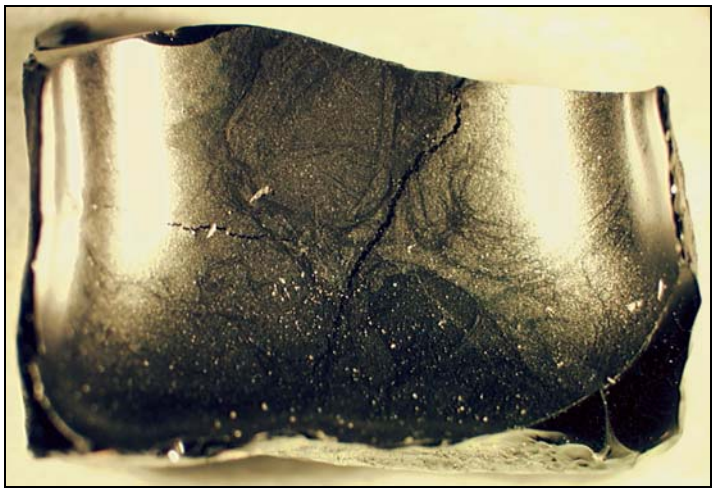

Figure 5-3. Surface of glass US-08 covered with grey crystals after heat treating at 904 °C (sample length approximately 12 mm).

Figure 5-4. Glittering crystals in the bulk of glass US-11 after heat treating at 904 °C.

Figure 5-5. White crystal agglomerates on the surface of glass US-13 while still in the platinum crucible after heat treating at 1056 °C (exaggerated colors, black glass).

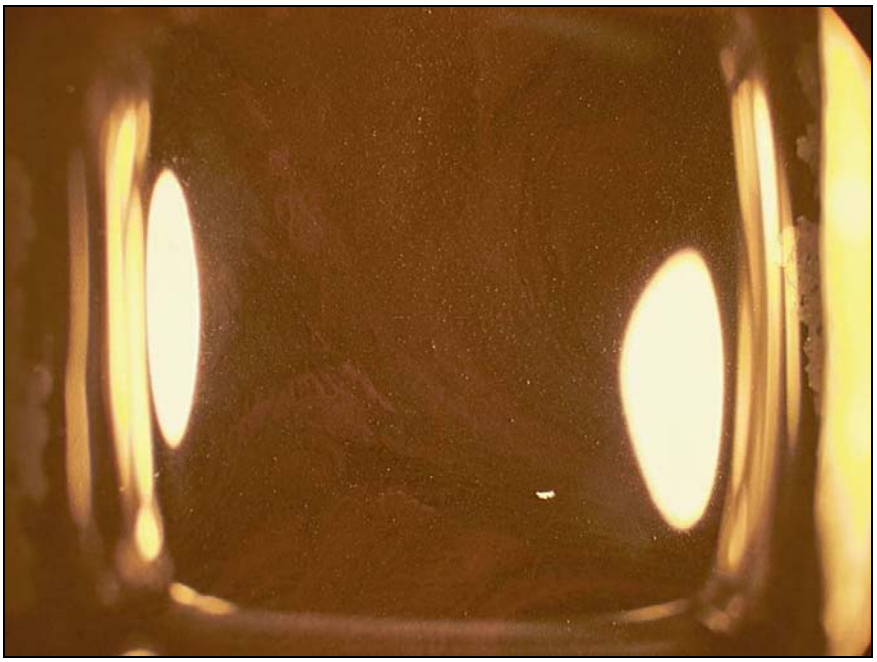

Figure 5-6. Tiny, bright crystals on the surface and brown crystal striations in the bulk of glass US-19 while still in the platinum crucible after heat treating at 904 °C (sample length approximately 12 mm).

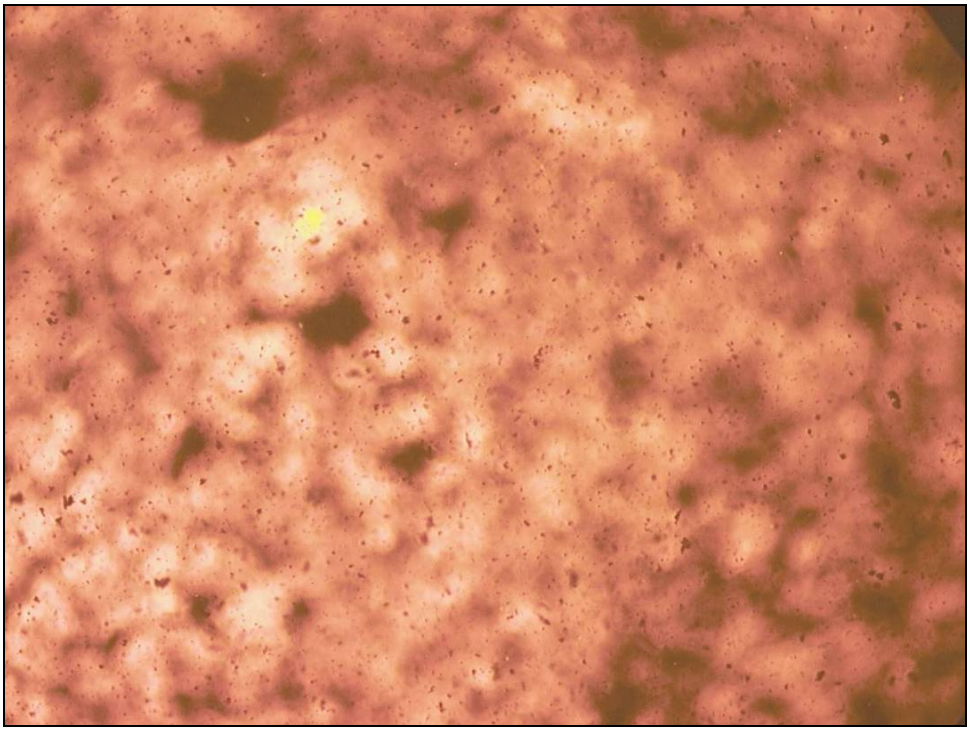

Figure 5-7. Many black crystal agglomerates in the bulk of glass US-26 while still in the platinum crucible after heat treating at 1157 °C.

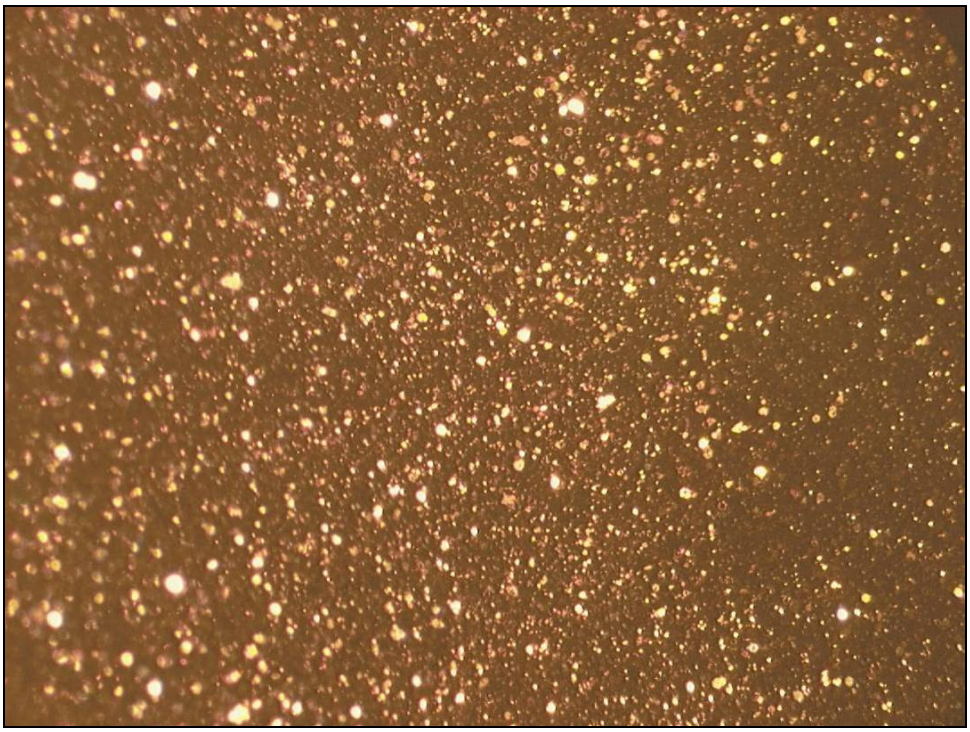

Figure 5-8. Surface of glass US-41 covered by hexagonal crystals while still in the platinum crucible after heat treating at 1007 °C.

Select High Resolution Optical Microscopy Observations

Initial High Resolution Optical Microscopy (HROM) observations are provided below. The observations are detailed in the captions accompanying each micrograph.

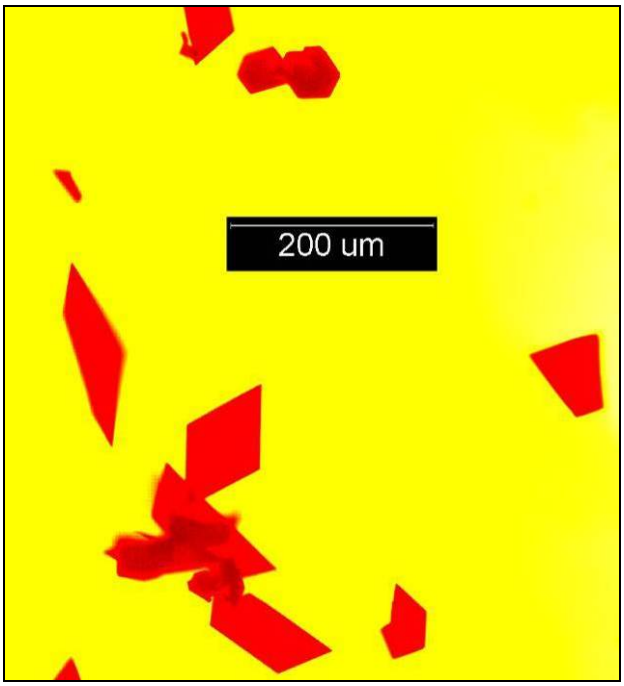

Figure 5-9. Hematite in glass US-09 after heat treating at 1157 °C. Colors in the image are not original: the crystals appear very dark red.

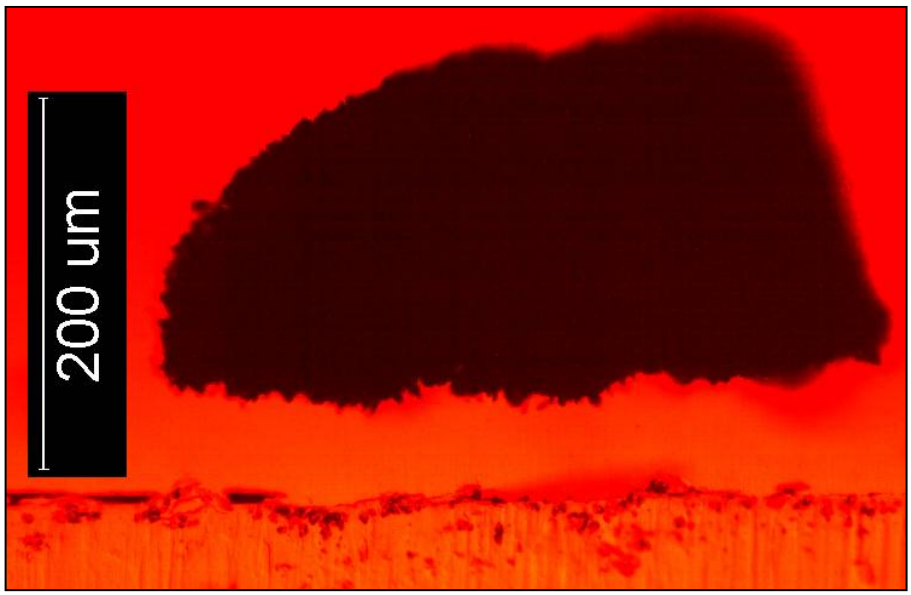

Figure 5-10. Large, black agglomerate of undissolved noble metals in glass US-09 after heat treating at 1157 °C. Colors in the image are not original: the glass appears light yellow and the crystal agglomerate is black.

Summary of Optical Microscopy Observations

The complete optical microscopy observations for each of the US-series glasses are provided in Table 5-6 below as a function of heat treatment temperature.

Table 5-6. Initial LROM Observations of Surface and Bulk Crystallization in the US-Series Glasses.

Glass ID	853 °C	904 °C	954 °C
US-01	grey crystal film on surface	grey crystal film on surface	fine crystal striations on surface
US-02	few black crystals in bulk	few black crystals in bulk	fine crystal layer on surface, black spots in bulk
US-03	brown crystal striations in bulk	brown crystal striations in bulk	brown crystal striations, tiny crystals on surface
US-04	grey crystal film on surface	brown crystal striations in bulk	brown crystal striations, tiny crystals on surface
US-05	glass appears grey in bulk, many crystals	glass appears grey in bulk, many crystals	grey crystal film on surface, brown crystals in bulk and on surface
US-06	grey crystal film on surface	grey crystal film on surface, brown crystals in bulk	brown crystal striations in bulk, some glittering crystals on surface
US-07	grey crystal film on surface	grey crystals on surface and in bulk	grey crystals on surface and in bulk
US-08	grey crystal film on surface	grey crystal film on surface	partly grey crystal film on surface
US-09	glittering crystals in bulk	glittering crystals in bulk	glittering crystals in bulk
US-10	grey crystal film on surface	grey crystal film on surface	brown crystal striations in bulk
US-11	glittering crystals in bulk	glittering crystals in bulk	glittering crystals in bulk
US-12	brown crystal striations in bulk, few grey crystals in surface	brown crystal striations in bulk	brown crystal striations in bulk
US-13	partly grey crystal cover on surface	many tiny bright crystals on surface, in one place still continuous grey crystal cover	many tiny bright crystals on surface
US-14	triangular crystals on surface	homogeneous	/
US-15	crystals on surface and in bulk, striations	black crystal agglomerates in bulk	black crystal agglomerates in bulk

Table 5-6. Initial LROM Observations of Surface and Bulk Crystallization in the US-Series Glasses. (continued)

GLASS ID	1007 °C	1058 °C	1108 °C
US-01	white crystal agglomerates on surface and in bulk	very few white crystal agglomerates on surface	one tiny white crystal agglomerate on surface, 2-3 tiny bright spots
US-02	black crystal agglomerates in bulk	few black crystal agglomerates in bulk	homogeneous
US-03	many black crystals in bulk	black crystal agglomerates in bulk	very few white crystal agglomerates on surface, black agglomerates in bulk
US-04	many white crystals in bulk	few black crystal agglomerates in bulk	few black crystal agglomerates in bulk
US-05	many glittering crystals in bulk	white crystal agglomerates on surface and in bulk	few white crystal agglomerates on surface and in bulk, 1 bright tiny spot
US-06	white crystal agglomerates on surface and in bulk	few white crystal agglomerates on surface and in bulk	few white crystal agglomerates on surface, black agglomerates in bulk
US-07	few glittering crystals in bulk	few white crystal agglomerates on surface	very few white crystal agglomerates on surface and in bulk
US-08	few white crystal agglomerates on surface and in bulk	few white crystal agglomerates on surface and in bulk	very few white crystal agglomerates on surface and in bulk
US-09	few glittering crystals in bulk	few black crystal agglomerates in bulk, few white crystal agglomerates on surface	very few black crystal agglomerates in bulk
US-10	few white crystal agglomerates on surface and in bulk	few white crystal agglomerates on surface and in bulk	very few white crystal agglomerates on surface
US-11	few white and glittering crystals in bulk	few white crystal agglomerates on surface and in bulk	very few white crystal agglomerates on surface and in bulk
US-12	tiny white crystals on surface and in bulk	tiny white crystals on surface and in bulk	extremely few and tiny white spots (crystals?)
US-13	many tiny bright crystals on surface	white crystal agglomerates on surface	few white crystal agglomerates on surface, few black crystal agglomerates in bulk
US-14	/	/	/
US-15	black crystal agglomerates in bulk	black crystal agglomerates in bulk	few black crystal agglomerates in bulk

Table 5-6. Initial LROM Observations of Surface and Bulk Crystallization in the US-Series Glasses. (continued)

Glass ID	1157 °C	1206 °C
US-01	glass very dark, no crystals on surface, maybe homogeneous	/
US-02	/	/
US-03	very few black crystal agglomerates in bulk	homogeneous
US-04	very few white crystal agglomerates on surface	homogeneous
US-05	homogeneous	/
US-06	very few black crystal agglomerates in bulk	homogeneous
US-07	homogeneous	/
US-08	homogeneous	/
US-09	homogeneous	/
US-10	homogeneous	/
US-11	homogeneous	/
US-12	homogeneous	/
US-13	homogeneous	/
US-14	/	/
US-15	homogeneous	/

Table 5-6. Initial LROM Observations of Surface and Bulk Crystallization in the US-Series Glasses. (continued)

Glass ID	853 °C	904 °C	954 °C
US-16	glass appears grey, many crystals	cell-like crystal striations on surface	grey, cell-like crystal striations
US-17	silver crystal cover on surface	partly silver crystal cover on surface, brown crystal striations in bulk	grey-brown crystal striations
US-18	grey crystal cover on surface	silver crystal cover on surface	partly grey crystal cover on surface
US-19	partly silver crystal cover on surface, brown crystal striations in bulk	tiny bright crystals on surface, brown crystal striations in bulk	tiny bright crystals on surface, brown crystal striations in bulk
US-20	partly grey crystal cover on surface, crystal striations in bulk	tiny bright crystals on surface, brown crystal striations in bulk	tiny bright crystals on surface, brown crystal striations in bulk
US-21	partly grey crystal cover on surface, brown crystal striations in bulk	tiny bright crystals on surface, brown crystal striations in bulk	many tiny bright crystals on surface
US-22	partly grey crystal cover on surface, grey crystal striations in bulk	partly grey crystal cover on surface, grey crystal striations in bulk	grey crystal striations in bulk
US-23	silver crystal cover on surface	partly grey crystal cover on surface	tiny bright crystals on surface, brown crystal striations in bulk
US-24	partly grey crystal cover on surface, brown crystal striations in bulk	tiny bright crystals on surface, brown crystal striations in bulk	tiny bright crystals on surface, brown crystal striations in bulk
US-25	grey-brown crystal striations in bulk	grey-brown crystal striations in bulk	grey-brown crystal striations in bulk
US-26	brown and white crystals on surface	brown and white crystals on surface	red-brown crystal striations in bulk, white crystal agglomerates on surface
US-27	brown and white crystals on surface	brown and white crystals on surface	partly grey crystal cover on surface
US-28	many black crystal agglomerates in bulk, some white crystal agglomerates on surface	many black crystal agglomerates in bulk	black crystal agglomerates in bulk
US-29	many small black crystal agglomerates in bulk	black crystal agglomerates in bulk, small needle-like crystals on surface	few black crystal agglomerates in bulk
US-30	many white crystal agglomerates on surface	white crystal agglomerates on surface	white crystal agglomerates on surface

Table 5-6. Initial LROM Observations of Surface and Bulk Crystallization in the US-Series Glasses. (continued)

Glass ID	1007 °C	1058 °C	1108 °C
US-16	tiny bright crystals on surface, grey striations	tiny bright crystals on surface, glass appears grey, many crystals	big and very bright spots on surface
US-17	brown crystal striations in bulk, one big and very bright crystal agglomerate on surface	few big and very bright spots on surface	homogeneous
US-18	very few black crystal agglomerates in bulk	homogeneous	/
US-19	bright crystals on surface and in bulk	white crystal agglomerates on surface	white crystal agglomerates on surface, black crystal agglomerates in bulk
US-20	white crystals on surface and in bulk	very bright spots on surface	few white crystal agglomerates on surface, few black crystal agglomerates in bulk
US-21	many tiny bright crystals on surface	white crystal agglomerates on surface and in bulk	white crystal agglomerates on surface, black crystal agglomerates in bulk
US-22	many tiny bright crystals on surface	many bright agglomerates on surface and in bulk	glass appear homogeneous on surface and in bulk, except one white spot on surface
US-23	tiny bright crystals on surface and in bulk	white crystal agglomerates on surface and in bulk	white crystal agglomerates on surface, black crystal agglomerates in bulk
US-24	tiny bright crystals on surface, brown crystal striations in bulk	white crystal agglomerates on surface and in bulk	few white crystal agglomerates on surface, few black crystal agglomerates in bulk
US-25	many tiny bright crystals on surface	many bright tiny crystals on surface	very few white crystal agglomerates on surface, too dark to see in bulk
US-26	many white and brown crystals	many white and brown crystals	many black crystal agglomerates in bulk
US-27	white crystal agglomerates on surface, black crystal agglomerates in bulk	black crystal agglomerates in bulk	black crystal agglomerates in bulk
US-28	black crystal agglomerates in bulk	black crystal agglomerates in bulk	homogeneous
US-29	one small black crystal agglomerate in bulk	homogeneous	/
US-30	white crystal agglomerates on surface	many tiny white spots on surface	many black crystal agglomerates in bulk

Table 5-6. Initial LROM Observations of Surface and Bulk Crystallization in the US-Series Glasses. (continued)

Glass ID	1157 °C	1206 °C	1254 °C
US-16	many big black crystal agglomerates	many big black crystal agglomerates	/
US-17	/	/	/
US-18	/	/	/
US-19	homogeneous	/	/
US-20	homogeneous	/	/
US-21	homogeneous	/	/
US-22	homogeneous	/	/
US-23	homogeneous	/	/
US-24	homogeneous	/	/
US-25	homogeneous	/	/
US-26	many black crystal agglomerates in bulk	some black crystal agglomerates in bulk	homogeneous
US-27	homogeneous	/	/
US-28	/	/	/
US-29	/	/	/
US-30	many big black crystal agglomerates in bulk	many black crystal agglomerates in bulk	big black crystal agglomerates

Table 5-6. Initial LROM Observations of Surface and Bulk Crystallization in the US-Series Glasses. (continued)

Glass ID	853 °C	904 °C	954 °C
US-31	silver crystal cover on surface	silver crystal cover on surface	white crystal agglomerates cover surface
US-32	many white crystal agglomerates on surface and in bulk	tiny white crystals on surface and in bulk	tiny white crystals on surface, black crystal agglomerates in bulk
US-33	silver crystal cover on surface	partly silver crystal cover on surface	white crystal agglomerates on surface
US-34	homogeneous	homogeneous	/
US-35	brown crystal striations, tiny white spots on surface	tiny white and brown crystals on surface	tiny white and brown crystals on surface
US-36	brown crystal striations, white crystal agglomerates on surface	brown crystal striations, white crystal agglomerates on surface	brown crystal striations, white crystal agglomerates on surface
US-37	brown crystal cover on surface	partly brown crystal cover on surface, brown crystal striations in bulk, white crystal agglomerates on surface	many white crystal agglomerates on surface and in bulk
US-38	grey crystal cover on surface	silver crystal cover on surface	silver crystal cover on surface
US-39	small regular red crystal striations, partly grey crystal cover on surface	regular circular red crystal striations with white crystal agglomerates in center	regular circular red crystal striations with white crystal agglomerates in center
US-40	on hold, fast crystallization		
US-41	surface covered by hexagonal crystals	surface covered by hexagonal crystals	surface covered by hexagonal crystals
US-42	dull grey crystal cover on surface	grey crystal cover on surface	many white crystal agglomerates on surface
US-43	/	/	/
US-44	partly grey crystal cover on surface	many tiny white spots on surface	many tiny white spots on surface
US-45	partly grey crystal cover on surface	many tiny white spots on surface	many tiny white spots on surface

Table 5-6. Initial LROM Observations of Surface and Bulk Crystallization in the US-Series Glasses. (continued)

Glass ID	1007 °C	1058 °C	1108 °C
US-31	many single crystals on surface	many single crystals on surface	homogeneous
US-32	two small black crystal agglomerates in bulk	one small black crystal agglomerate in bulk	homogeneous
US-33	many tiny white spots on surface	many tiny white spots on surface	many tiny white spots on surface
US-34	/	/	/
US-35	tiny white and brown crystals on surface	tiny white and brown crystals on surface	many tiny white spots on surface
US-36	many tiny white spots on surface	many single crystals on surface	many black crystal agglomerates in bulk
US-37	tiny white spots on surface and in bulk	homogeneous	/
US-38	many small white spots on surface	many small white spots on surface	many small white spots on surface
US-39	single crystals cover surface	single crystals cover surface	homogeneous
US-40	on hold, fast crystallization		
US-41	surface covered by hexagonal crystals	white crystal agglomerates on surface and in bulk	few white crystal agglomerates on surface
US-42	many white crystal agglomerates on surface	many white crystal agglomerates on surface	many white crystal agglomerates on surface
US-43	/	/	/
US-44	many tiny white spots on surface	few white crystal agglomerates on surface	homogeneous
US-45	many tiny white spots on surface	white crystal agglomerates on surface	homogeneous

Table 5-6. Initial LROM Observations of Surface and Bulk Crystallization in the US-Series Glasses. (continued)

Glass ID	1157 °C	1206 °C	1254 °C
US-31	/	/	
US-32	/	/	
US-33	many tiny white spots on surface	homogeneous	
US-34	/	/	
US-35	many white crystal agglomerates on surface, many black crystal agglomerates in bulk	many big black crystal agglomerates in bulk	
US-36	many big black crystal agglomerates in bulk	many big black crystal agglomerates in bulk	
US-37	/	/	
US-38	many small white spots on surface	many small white spots on surface	many small white spots on surface
US-39	/	/	
US-40	on hold, fast crystallization		
US-41	homogeneous	/	/
US-42	many white crystal agglomerates on surface	many white crystal agglomerates on surface	grey crystal cover on surface
US-43	/	many big white crystal agglomerates in bulk	
US-44	/	/	/
US-45	/	/	/

5.4.4 *Uniform Temperature Heat Treatments and Observations*

Uniform temperature heat treatments were made on 44 of the US-series glasses (glass US-40 was excluded) in order to determine T_L optically. These data are presented in Table 5-7 where the amorphous temperature (T_a), the crystallization temperature (T_c), and T_L are presented along with the predicted T_L (using models prior to the commencement of this study). The measured crystal fraction T_L and the crystalline phases measured using quantitative XRD for each glass (as discussed in the next section) are included in this table as well. Detailed data for optical heat treatment specimens are available in Appendix A.

Table 5-7. Predicted and Measured Liquidus Temperatures.

Glass ID	Predicted T_L (°C)	T_c-T_a (°C)	Optical T_L (°C)	T_L by XRD Crystal Fraction (°C)	XRD Primary & Secondary Phases
US-01	1048	1049-1057	1053	1019	Spinel
US-02	882	753-764	759	BDL*	Baddelyite (optical)
US-03	1009	995-1000	997	1018	Spinel
US-04	1050	946-954	950	956	Spinel
US-05	1050	1019-1027	1023	1025	Hematite
US-06	1037	1001-1008	1005	968	Spinel
US-07	1050	1022-1029	1026	1018	Spinel
US-08	1042	994-1000	997	981	Spinel
US-09	1027	1157-1169	1163	1091	Hematite
US-10	1050	995-1001	998	998	Spinel
US-11	1017	1000-1006	1003	976	Spinel, hematite
US-12	1050	1082-1086	1084	1062	Spinel
US-13	1030	1022-1029	1026	1034	Spinel
US-14	882	869-879	874	880	Spinel
US-15	786	890-901	895	913	Spinel
US-16	1050	1120-1126	1124	1136	Hematite, spinel
US-17	1050	1040-1049	1045	1031	Spinel
US-18	1007	982-994	988	1026	Spinel
US-19	1007	1029-1040	1035	1052	Spinel
US-20	1007	1001-1007	1004	1006	Spinel
US-21	1050	1070-1074	1072	1071	Spinel
US-22	1043	1086-1095	1091	1050	Spinel
US-23	1021	1030-1035	1032	1032	Spinel
US-24	1050	1049-1056	1052	1024	Spinel
US-25	1050	1080-1086	1083	1074	Spinel
US-26	1150	1205-1206	1206	1167	Spinel
US-27	1113	1079-1086	1082	1077	Spinel
US-28	928	826-831	829	813	Spinel, nepheline, nosean
US-29	804	879-890	885	BDL*	Spinel
US-30	1150	1235-1247	1241	1251	Spinel, zircon
US-31	1121	1107-1118	1113	1125	Hematite
US-32	814	753-764	759	BDL*	Spinel

Table 5-7. Predicted and Measured Liquidus Temperatures. (continued)

Glass ID	Predicted T_L (°C)	T_c-T_a (°C)	Optical T_L (°C)	T_L by XRD Crystal Fraction (°C)	XRD Primary & Secondary Phases
US-33	1121	1001-1007	1004	1017	Spinel, nosean
US-34	764	826-840	832	BDL*	Spinel
US-35	1118	1309-1318	1312	1310	Spinel
US-36	1150	1235-1247	1238	1253	Spinel
US-37	1044	1001-1007	1004	1036	Spinel
US-38	1004	1056-1067	1062	1038	Spinel, NiO
US-39	1150	1107-1110	1109	1105	Spinel, zircon
US-40	1144	no glass formation	no glass formation	N/A	N/A
US-41	1066	1058-1067	1063	1046	Hematite
US-42	895	1017-1028	1023	1037	Spinel, nepheline
US-43	1147	1217-1225	1221	1245	Zircon, Li_2SiO_3, spinel
US-44	1038	1095-1101	1098	1112	Spinel
US-45	1038	1070-1074	1072	1072	Spinel

*Four glasses (US-02, US-29, US-32, and US-34) don't have a value listed for the T_L calculated from XRD crystal fraction data and therefore are listed as "BDL" for *below detection limit* where the quantity of crystals in the heat treatments for a particular glass was too low to get a data fit.

5.5 Crystallinity vs. Temperature Using XRD (Crystal Fraction Method)

5.5.1 *Quantitative XRD Analysis*

Several heat treatment specimens were analyzed by XRD for each glass in order to obtain a meaningful extrapolation of crystal fraction versus temperature. A summary of the volume fractions of crystalline phases identified in each glass after the CCC heat treatment is provided in Table 5-8. Detailed data for crystal fraction as a function of temperature for each glass is available in Appendix B.

Table 5-8. Identified Crystalline Phases and Their Concentrations (vol%) in the CCC Glasses.

Glass ID	Crystalline Phases	Glass ID	Crystalline Phases	Glass ID	Crystalline Phases
US-01	WC (inhomogeneity from milling)	US-16	Hematite (Fe_2O_3) –2.23	US-31	Hematite (Fe_2O_3) – 3.19
US-02	WC (inhomogeneity from milling)	US-17	Spinel – 0.34	US-32	none
US-03	Hematite (Fe_2O_3) – 0.15, WC (inhomogeneity from milling)	US-18	Nepheline ($Na_{7.11}Al_{7.2}Si_{8.8}O_{32}$) – 4.7	US-33	Spinel – 0.39
US-04	none	US-19	none	US-34	none
US-05	Spinel – 2.44, Hematite (Fe_2O_3) – 0.44, Perovskite ($CaFe_3Ti_4O_{12}$) – 0.48	US-20	none	US-35	Spinel – 3.13
US-06	Spinel – 0.24, WC (inhomogeneity from milling)	US-21	Spinel – 0.15	US-36	Spinel – 0.93
US-07	none	US-22	Spinel – 0.34	US-37	Nepheline ($Na_{6.65}Al_{6.24}Si_{9.76}O_{32}$) – 12.5, Spinel – 0.78
US-08	none	US-23	none	US-38	Bunsenite (NiO) – 0.22vol%, Spinel – 0.2
US-09	none	US-24	none	US-39	Spinel – 1.17vol%
US-10	Hematite (Fe_2O_3) – 0.19	US-25	Spinel – 0.88	US-40	Spinel – 0.64vol%, Hematite (Fe_2O_3) – 2.18
US-11	Hematite (Fe_2O_3) – 1.06 + another crystalline phase (61-2808 LiCl ?)	US-26	Spinel – 0.93, Nepheline ($Na_{6.8}Al_{6.3}Si_{9.7}O_{32}$) – 0.9	US-41	Hematite (Fe_2O_3) – 2.08
US-12	Spinel – 0.93	US-27	Nepheline ($Na_{2.8}K_{0.66}Ca_{0.32}Al_{3.82}Si_{4.18}O_{15.3}$) – 11.8, Li_2SiO_3 – 4.05, Nosean ($Na_8Al_6Si_6O_{24}SO_4$) – 1.05, Spinel – 0.88	US-42	Nepheline ($KNa_3(AlSiO_4)_4$), Li0.88Mn2O4, Tridymite (SiO_2), $Na_{0.68}Fe_{0.68}Si_{0.32}O_2$, $Al_{0.5}Si_{0.75}O_{0.25}$, Hematite ($Fe_2O_3$), Pb_2O_3
US-13	none	US-28	none	US-43	Nepheline ($Na_6K_{1.2}Al_{7.2}Si_{8.8}O_{32}$) – 17.8, Hematite ($Fe_2O_3$) – 1.06, Spinel – 0.49
US-14	none	US-29	none	US-44	Spinel – 0.39
US-15	none	US-30	Spinel – 1.12	US-45	Spinel – 0.24

[a]XRD pattern is too busy to determine amounts of crystalline phases with RIQAS

Spinel peak locations and intensities matched XRD patterns of following crystalline phases:

Magnetite (Fe_3O_4) – Glasses US-06, 12, 17, 21, 22, 25-27, 30, 33, 36-40, 44, and 45

$MnFe_2O_4$ – Glass US-05

$MgFe_2O_4$ – Glass US-43

$Zn_{0.6}Mn_{0.4}Fe_2O_4$ – Glass US-35

5.5.2 *Data Analysis*

The section provides a comparison of the data obtained using optical and crystal fraction (XRD) methods. The correlation coefficient of the measured XRD data versus the measured optical T_L data was $R^2 = 0.9469$. Aside from a few outliers, the two datasets aligned very well across the entire temperature range (829 °C to 1312 °C for optical data and 813 °C to 1310 °C for crystal fraction data). See Figure 5-11 for a comparison of the two measured datasets.

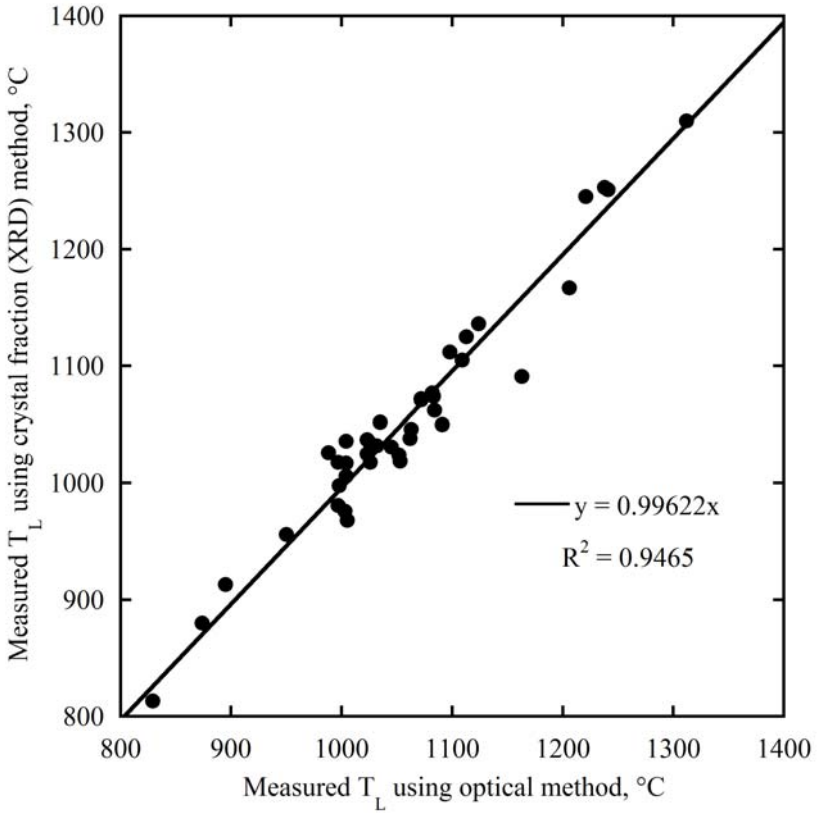

Figure 5-11. Comparison of T_L data obtained using XRD and optical methods.

Regression models were fit from the mass fraction data presented in Table 4-1 to both the measured optical and crystal fraction T_L data presented in Table 5-7 where spinel was listed as the primary phase and regression coefficients were produced. These coefficients are presented in Table 5-9.

Table 5-9. Regression Coefficients for Optical and Crystal Fraction Methods.

Component	Optical	XRD
Al_2O_3	2459	2245
B_2O_3	232.3	505.5
CaO	9007	8226
Cr_2O_3	34305	34764
Fe_2O_3	2236	1605
K_2O	5727	2622
Li_2O	-1784	-853
MnO	2467	2347
Na_2O	-806.2	-705.4
NiO	11034	8590
PbO	-7884	1589
SiO_2	1188	1111
SrO	688.6	-1806
TiO_2	-2639	1754
ZnO	2573	3139
ZrO_2	2712	2465
Others*	-16326	-12363

*Others coefficient includes MgO, RuO_2, and SO_3.

The component coefficients, r_i, presented in Table 5-9 were then used in Equation 1:

$$T_L(calc) = \sum_{i=1}^{n} m_i r_i \qquad [1]$$

along with the mass fraction of the *i*-th component in the glass, m_i (data from Table 4-1), and the resulting sum-product was the calculated T_L value for the given method (calculated for both optical and crystal fraction T_L data). These data were computed and the calculated values for both methods of T_L measurements are presented in Table 5-10. Outliers are listed in color in the table according to the difference in temperature between the measured and calculated values (red is >70 °C variation, orange is 55-70 °C variation, and yellow is 40-55 °C variation).

Table 5-10. Summary of measured T_L data for optical and crystal fraction methods for all glasses containing spinel as the primary phase as well as the calculated T_L values for both sets using Equation 1 with data presented in Table 4-1 and the coefficients presented in Table 5-9.

Glass ID	Optical Data			Crystal Fraction Data		
	Meas.	Calc.	ΔT	Meas.	Calc.	ΔT
US-01	1053	1068	15	1019	1025.5	7
US-03	997	1030	33	1018	1039.0	21
US-04	950	970	20	956	979.8	24
US-06	1005	981	24	968	979.5	12
US-07	1026	995	31	1018	1001.8	16
US-08	997	973	24	981	968.9	12
US-10	998	987	11	998	970.7	27
US-11	1003	1018	15	976	998.2	22
US-12	1084	1126	42	1062	1083.8	22
US-13	1026	1085	59	1034	1069.5	35
US-14	874	870	4	880	901.4	21
US-15	895	868	27	913	904.1	9
US-17	1045	1018	27	1031	1038.0	7
US-18	988	1058	70	1026	1056.2	30
US-19	1035	1003	32	1052	1002.3	50
US-20	1004	1003	1	1006	1002.3	4
US-21	1072	1063	9	1071	1031.8	39
US-22	1091	1076	15	1050	1047.0	3
US-23	1032	1044	12	1032	1025.4	7
US-24	1052	1037	15	1024	1023.9	0
US-25	1083	1045	38	1074	1052.1	22
US-26	1206	1159	47	1167	1143.7	23
US-27	1082	1111	29	1077	1081.9	5
US-28	829	884	55	813	838.3	25
US-30	1241	1298	57	1251	1266.2	15
US-33	1004	1059	55	1017	1060.5	44
US-36	1238	1222	16	1253	1237.5	16
US-37	1004	1036	32	1036	1065.5	30
US-38	1062	1064	2	1038	1026.2	12
US-39	1109	1107	2	1105	1129.5	25
US-42	1023	983	40	1037	1033.4	4
US-44	1098	1037	61	1112	1041.4	71
US-45	1072	1037	35	1072	1041.4	31

Using the data presented in Table 5-10, Figure 5-12 shows plots of the calculated versus measured data for both methods. The correlation between the measured and calculated data has a higher degree of merit for the crystal fraction data than for the optical data (higher R^2 value of 0.9089 versus 0.8970 for the optical data). The crystal fraction data only have 3 glasses with a calculated value differing from the corresponding measured value by ≥40 °C, whereas the optical data have 9 glasses, thus helping to explain the better fit to the crystal fraction data.

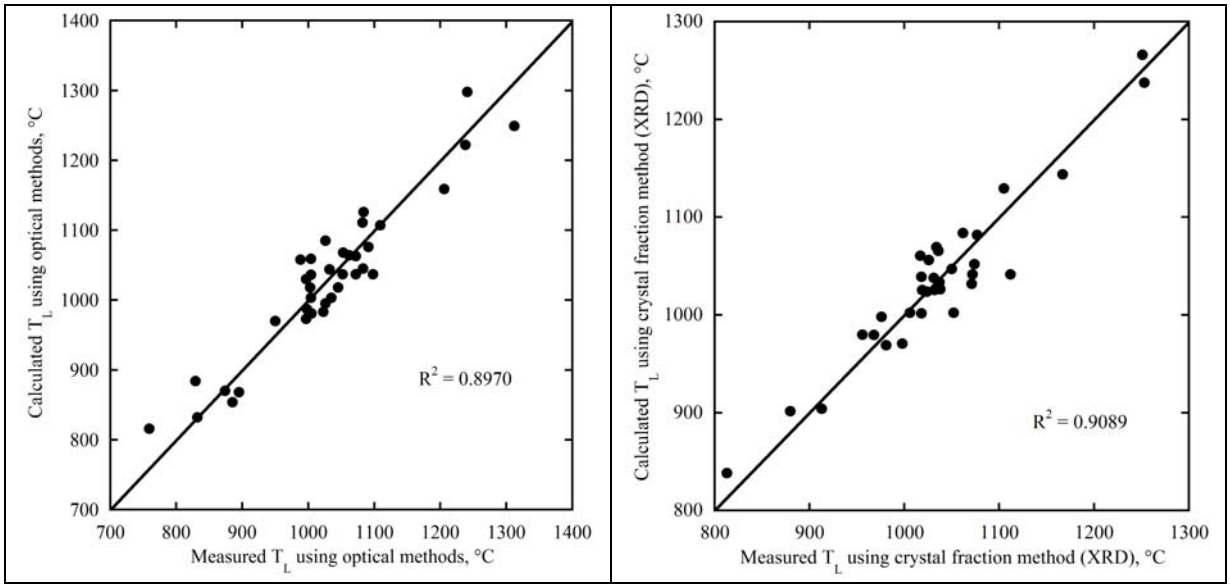

Figure 5-12. Calculated versus measured data obtained for both optical (left) and crystal fraction (right) methods.

The data calculated for the different methods are presented in Figure 5-13. The two methods predict T_L values that are in good agreement ($R^2 = 0.9135$).

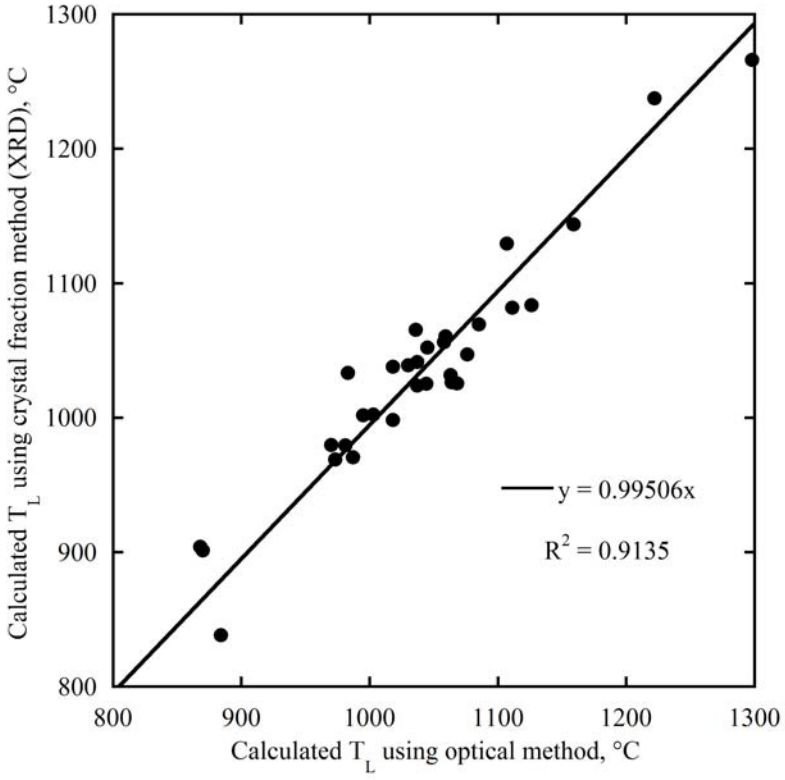

Figure 5-13. Comparison of calculated T_L data for both crystal fraction and optical methods.

5.6 SEM-EDS Analyses

The SEM-EDS analysis of coated samples revealed the presence of undissolved RuO_2 in all glasses due to the low solubility of RuO_2 in borosilicate glass. According to Schreiber et al.,[16] the solubility of RuO_2 in borosilicate glasses is lower than 0.001 wt% at melting temperatures from 1050 °C to 1150 °C. Most of the RuO_2 is present as approximately 1 μm diameter particles. These particles tend to form agglomerates with varying sizes and shapes that are located close to the bottom of crucible. Table 5-11 summarizes the phases identified and the number of RuO_2 agglomerates observed on the polished glass surfaces.

Table 5-11. Phases identified in borosilicate glasses US-01, US-03 to US-09, and US-14.

	US-01	US-03	US-04	US-05	US-06	US-07	US-08	US-09	US-14
Identified phases	Spinel Nepheline RuO_2 (5)[b]	RuO_2 (6)[b]	RuO_2 (5)[b]	RuO_2 (6)[b]	RuO_2 (1)[b]	RuO_2 (5)[b]	RuO_2 (3)[b]	RuO_2 (2)[b]	Spinel RuO_2 (6)[b]

[b] number of undissolved RuO_2 agglomerates

A series of SEM micrographs detailing the morphology of the RuO_2 agglomerates in each of the nine glasses selected for analysis is provided in Figure 5-14 through Figure 5-22. Locations are identified on some of the micrographs where semi-quantitative EDS spectra were recorded. The EDS data are provided after each corresponding figure, constituting Table 5-12 through Table 5-20.

There was only one RuO_2 agglomerate detected on the polished surface of glass US-06, compared to two on US-09, three on US-08, five on US-01, US-04, and US-07, and six agglomerates on the polished surfaces of glasses US-03, US-05, and US-14. Spinel crystallized in glasses US-01 and US-14. Nepheline crystals were present solely in glass US-01. Figure 5-14 shows spinel and nepheline crystals together with undissolved RuO_2 particles identified in glass US-01. The spinel crystals located on the shell of a bubble that formed next to the crucible wall contained a small concentration of Rh from the crucible. A much higher concentration of Rh was detected in the spinel crystals deposited along the crucible bottom in glass US-14 (see Table 5-20).

The EDS data shown in the tables below should be considered qualitative only because the detection of light elements such as B and O with EDS is limited. The scintillation counter detector cannot accurately separate and measure the characteristic X-rays of elements with atomic numbers lower than 11. Also, the detected low concentration of Na, Al, Si, Ti, Mn, and Fe in the 1 μm RuO_2 particles is attributed to the surrounding glass due to image drift during spectra acquisition and a large spot size.

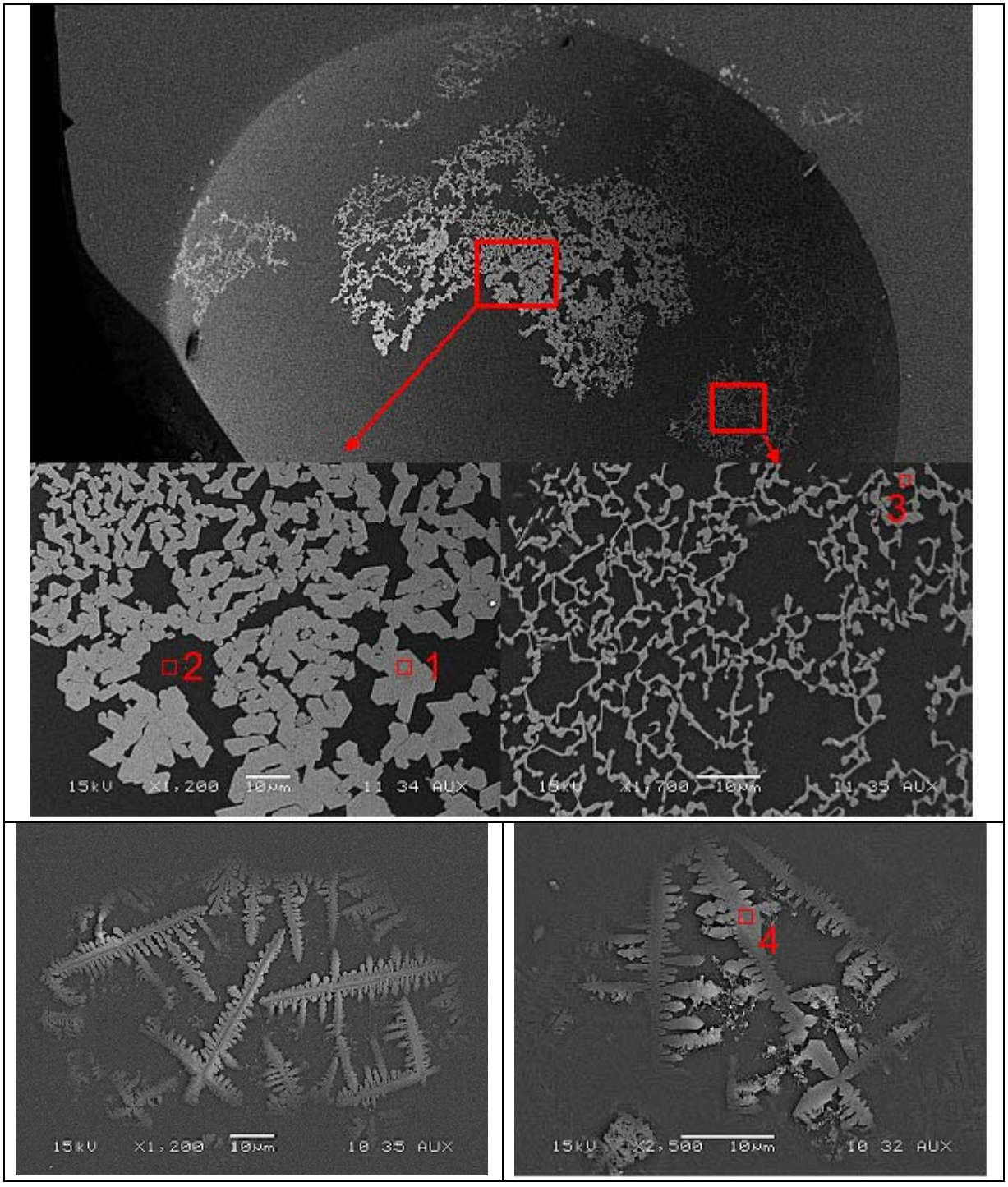

Figure 5-14. Spinel, Nepheline and Undissolved RuO_2 Agglomerates in Glass US-01 After Heat Treating at 1008 °C for 24 h.

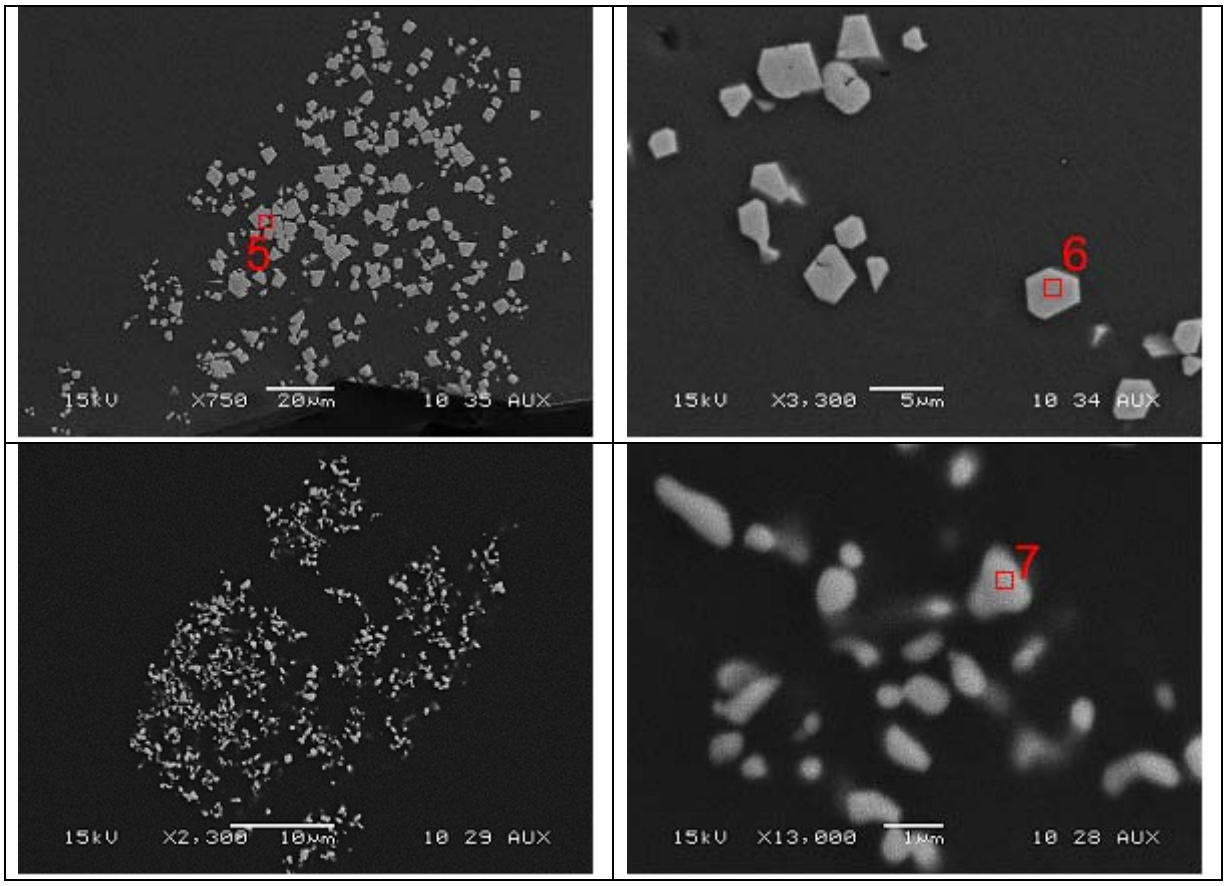

Figure 5-14. Spinel, Nepheline and Undissolved RuO2 Agglomerates in Glass US-01 After Heat Treating at 1008 °C for 24 h. (continued)

Table 5-12. Composition of Crystals, Particles, and the Surrounding Glass in US-01 Measured with EDS After Heat Treating at 1008 °C for 24 h.

Element	X1200_1	X1200_2	X1700_3	X2500_4	X750_5	X3300_6	X13000_7
	Atomic%						
O	21.03	26.04	28.03	7.35	18.70	24.17	29.82
Na	1.39	10.51	4.90	8.65			6.60
Mg	1.29	0.51	1.93	0.51	2.75	2.79	
Al	6.14	12.99	6.06	10.81	1.10	2.08	6.02
Si	15.21	39.63	10.74	32.82	1.00	1.25	14.59
Ru							38.40
Rh	3.64		1.26				
Cl				15.71			
K	0.50	1.04		17.53			
Cr	9.74		10.08		47.08	33.22	
Mn	13.01	2.36	11.19	1.68	14.54	14.26	1.54
Fe	26.18	6.92	24.21	4.95	13.63	20.63	3.03
Ni	1.88		1.60		1.20	1.60	

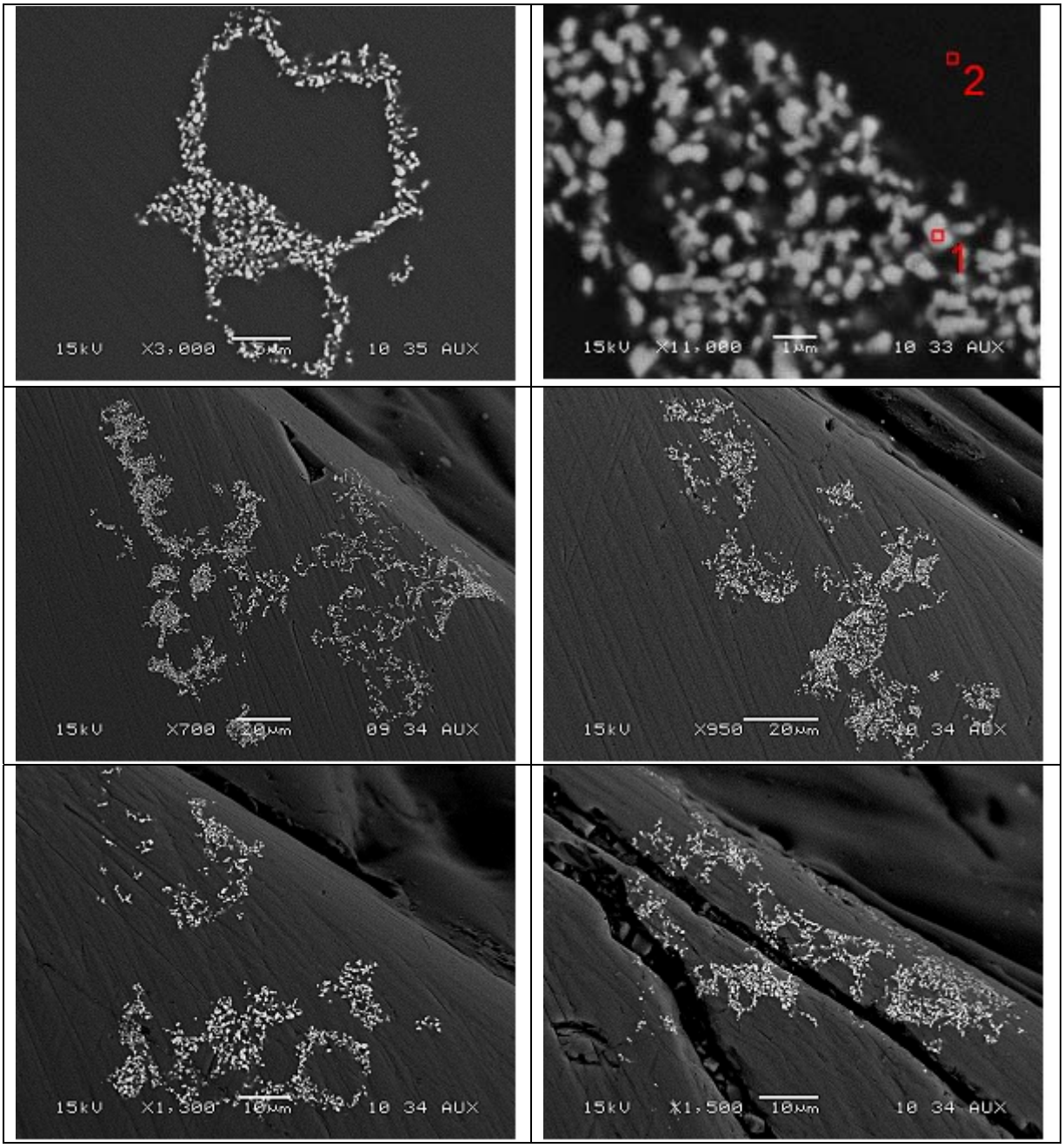

Figure 5-15. Undissolved RuO_2 Agglomerates in Glass US-03 After Heat Treating at 1107 °C for 24 h.

Table 5-13. Composition of Particles and the Surrounding Glass in US-03 Measured with EDS After Heat Treating at 1107 °C for 24 h.

Element	X11000_1	X11000_2
	Atomic%	
O	34.20	2.14
Na	2.68	6.02
Mg		0.55
Al	4.63	14.25
Si	9.33	40.34
K		0.78
Ca		0.83
Ru	47.43	
Ti		0.56
Fe	1.71	4.00
Ni		0.53

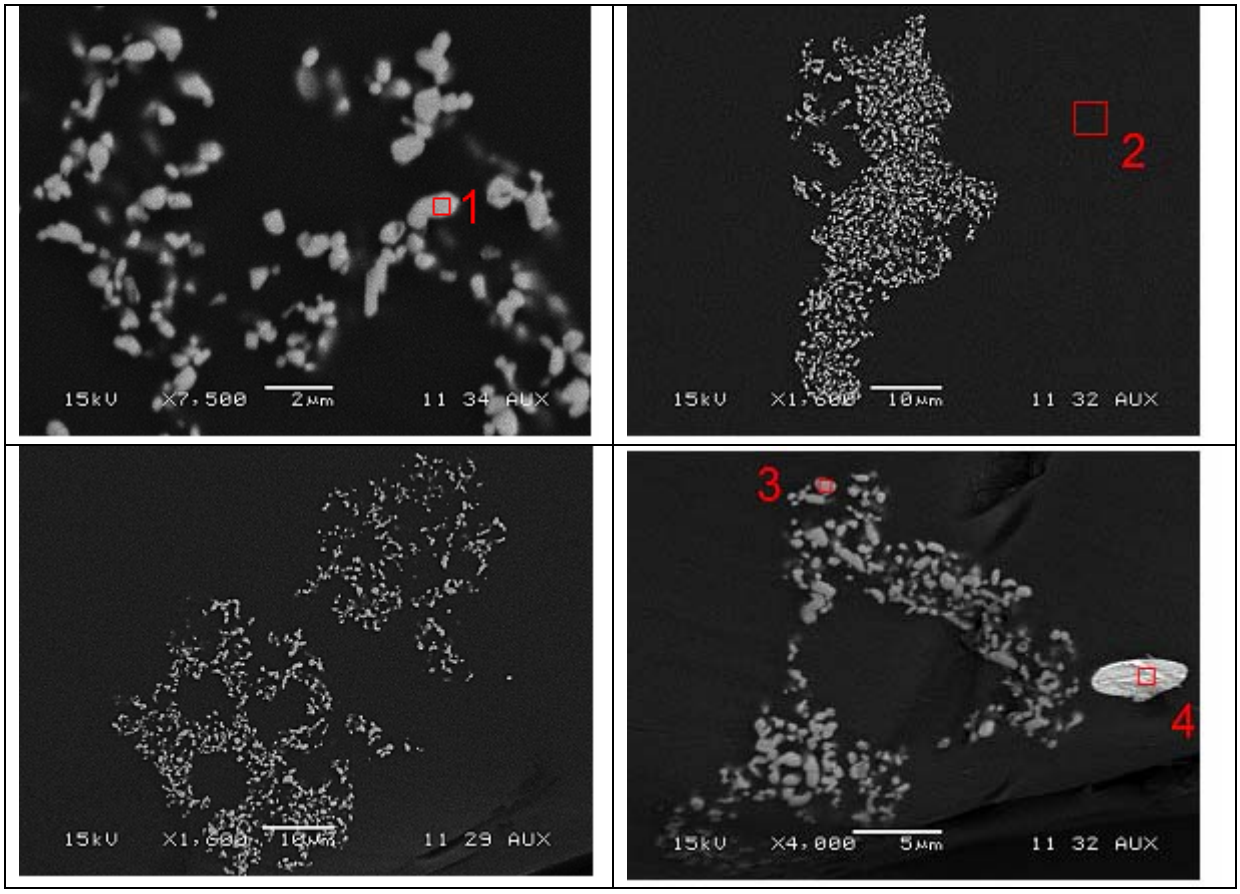

Figure 5-16. Undissolved RuO_2 Agglomerates in Glass US-04 After Heat Treating at 1107 °C for 24 h.

Table 5-14. Composition of Particles and the Surrounding Glass in US-04 Measured with EDS After Heat Treating at 1107 °C for 24 h.

Element	X7500_1	1600_2	X4000_3	X4000_4
	Atomic%			
O	33.73	32.07	33.42	
Na	4.77	9.64	4.55	
Mg		0.59		
Al	5.29	13.65	5.43	
Si	10.91	36.47	11.85	
Ru	43.42		41.68	
Pt				87.06
Rh				12.94
K		0.87		
Ca		0.76		
Ti		0.51		
Mn		1.30		
Fe	1.87	4.13	3.07	

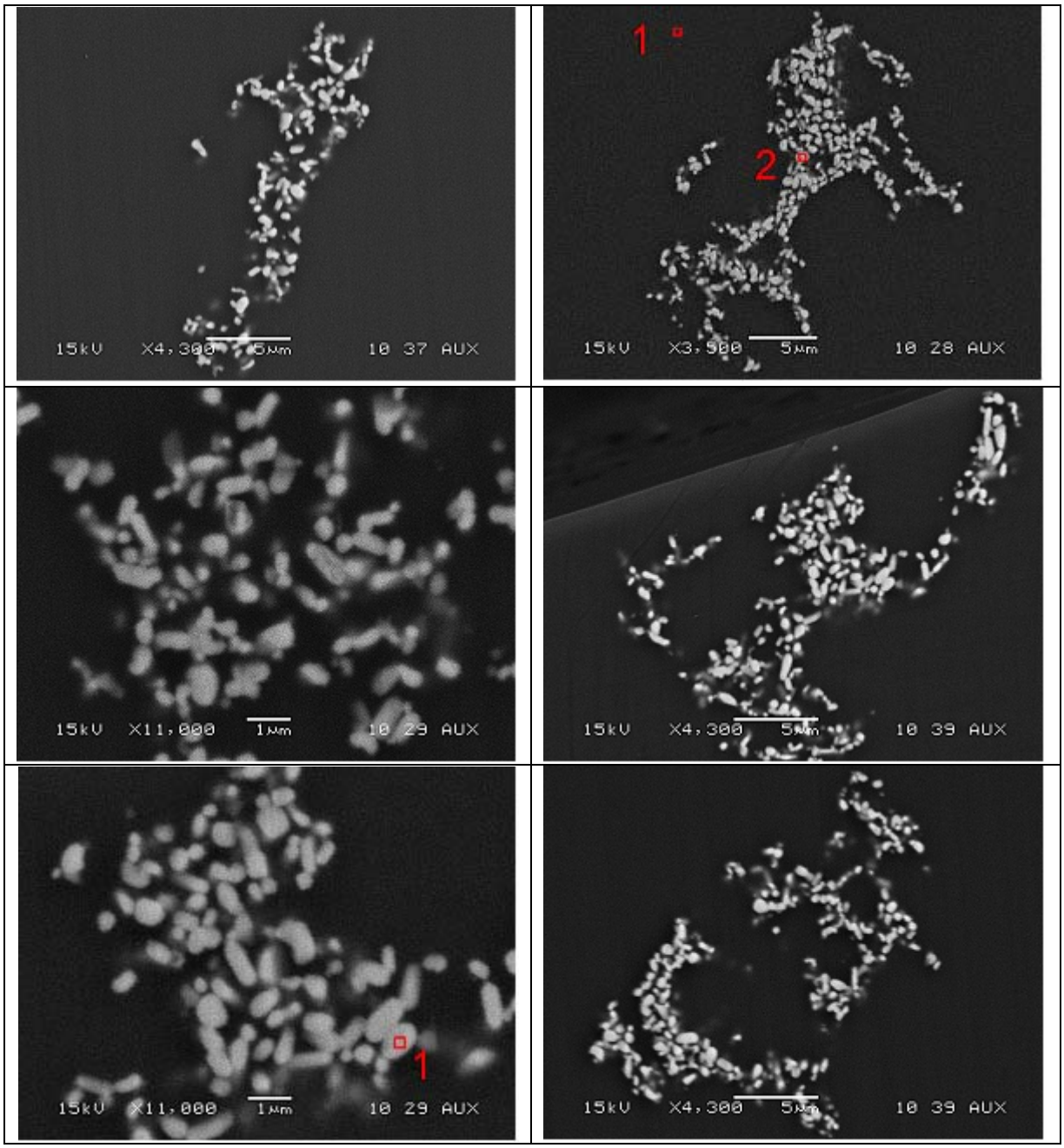

Figure 5-17. Undissolved RuO_2 Agglomerates in Glass US-05 After Heat Treating at 1107 °C for 24 h.

Table 5-15. Composition of Particles and the Surrounding Glass in US-05 Measured by EDS After Heat Treating at 1107 °C for 24 h.

Element	X3500_1	X3500_2	X11000_1
	Atomic%		
O	33.97	40.88	34.05
Na	5.96	5.04	3.69
Mg	0.75		
Al	14.43	5.58	5.82
Si	37.08	11.42	12.27
K	0.86		
Ca	0.53		
Ru		32.40	39.49
Ti	0.51	0.66	0.35
Mn	1.54	1.31	1.29
Fe	4.38	2.71	3.05

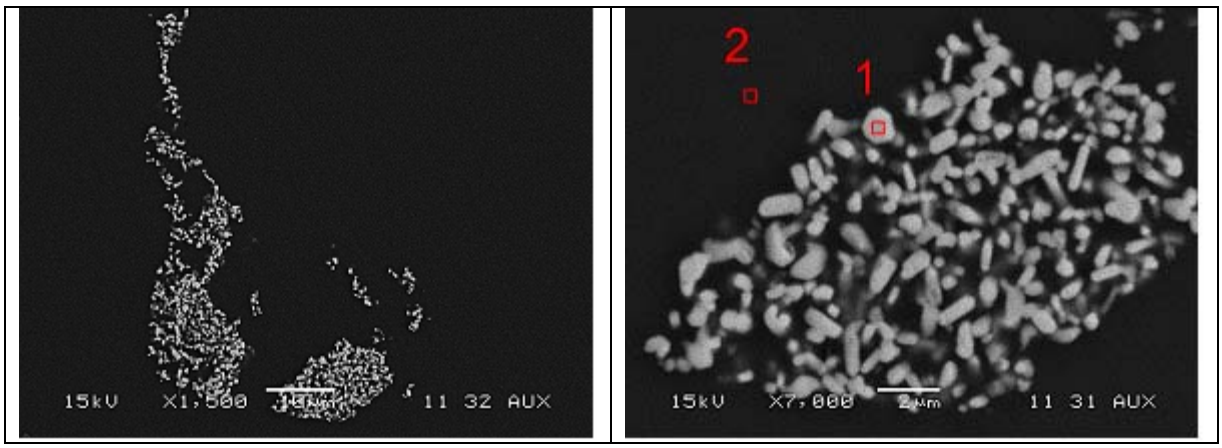

Figure 5-18. Undissolved RuO_2 Agglomerates in Glass US-06 After Heat Treating at 1107 °C for 24 h.

Table 5-16. Composition of Particles and the Surrounding Glass in US-06 Measured by EDS After Heat Treating at 1107 °C for 24 h.

Element	X7000_1	X7000_2
	Atomic%	
O	43.15	33.42
Na	5.40	8.06
Mg		0.59
Al	6.37	13.53
Si	13.03	35.21
K		1.06
Ca		0.92
Ti		0.62
Ru	28.88	
Mn	1.03	2.02
Fe	2.15	4.56

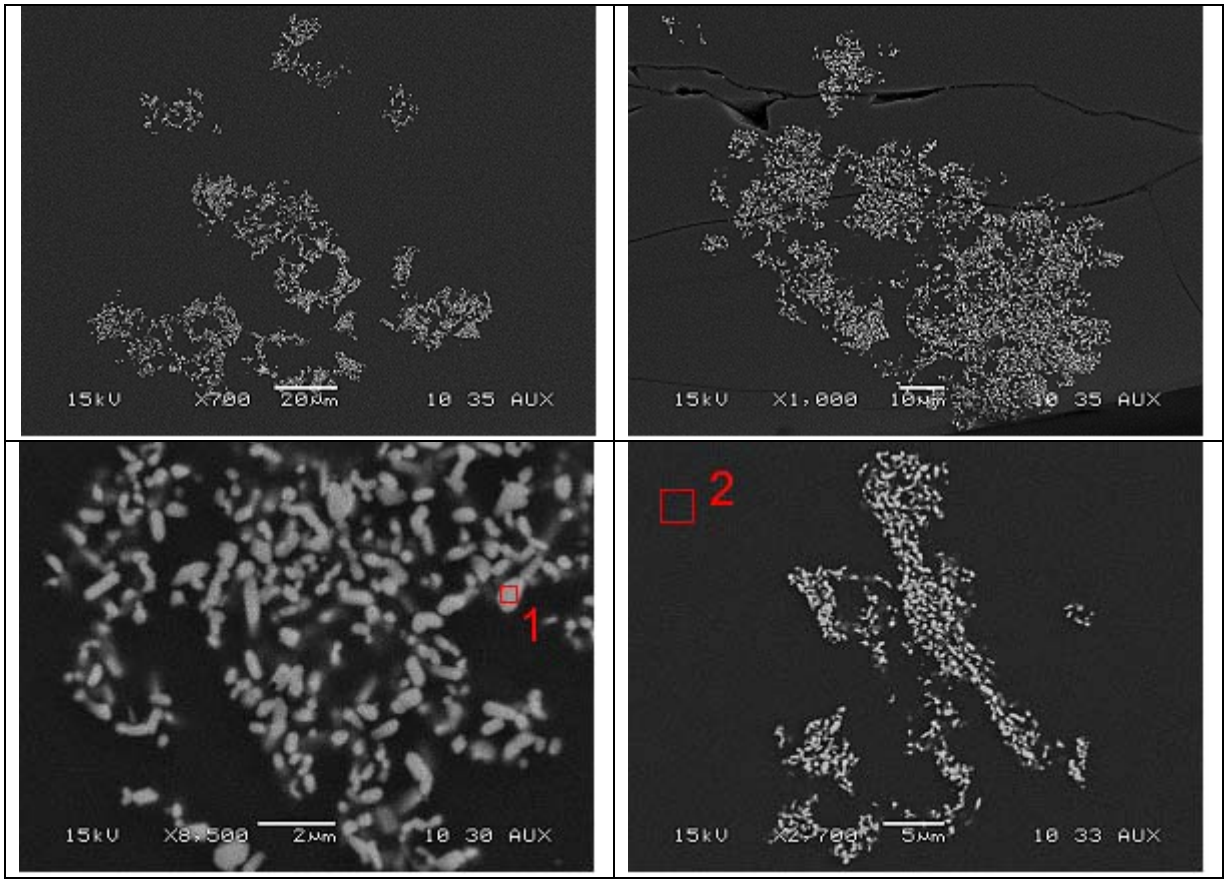

Figure 5-19. Undissolved RuO_2 Agglomerates in Glass US-07 After Heat Treating at 1058 °C for 24 h.

Table 5-17. Composition of Particles and the Surrounding Glass in US-07 Measured by EDS After Heat Treating at 1058 °C for 24 h.

Element	X8500_1	x2700_2
	Atomic%	
O	38.97	30.36
Na	7.15	8.67
Mg		0.86
Al	7.84	14.04
Si	16.88	37.34
Ru	26.20	
K		1.00
Ca		0.94
Ti		0.66
Mn	0.79	1.93
Fe	2.16	4.21

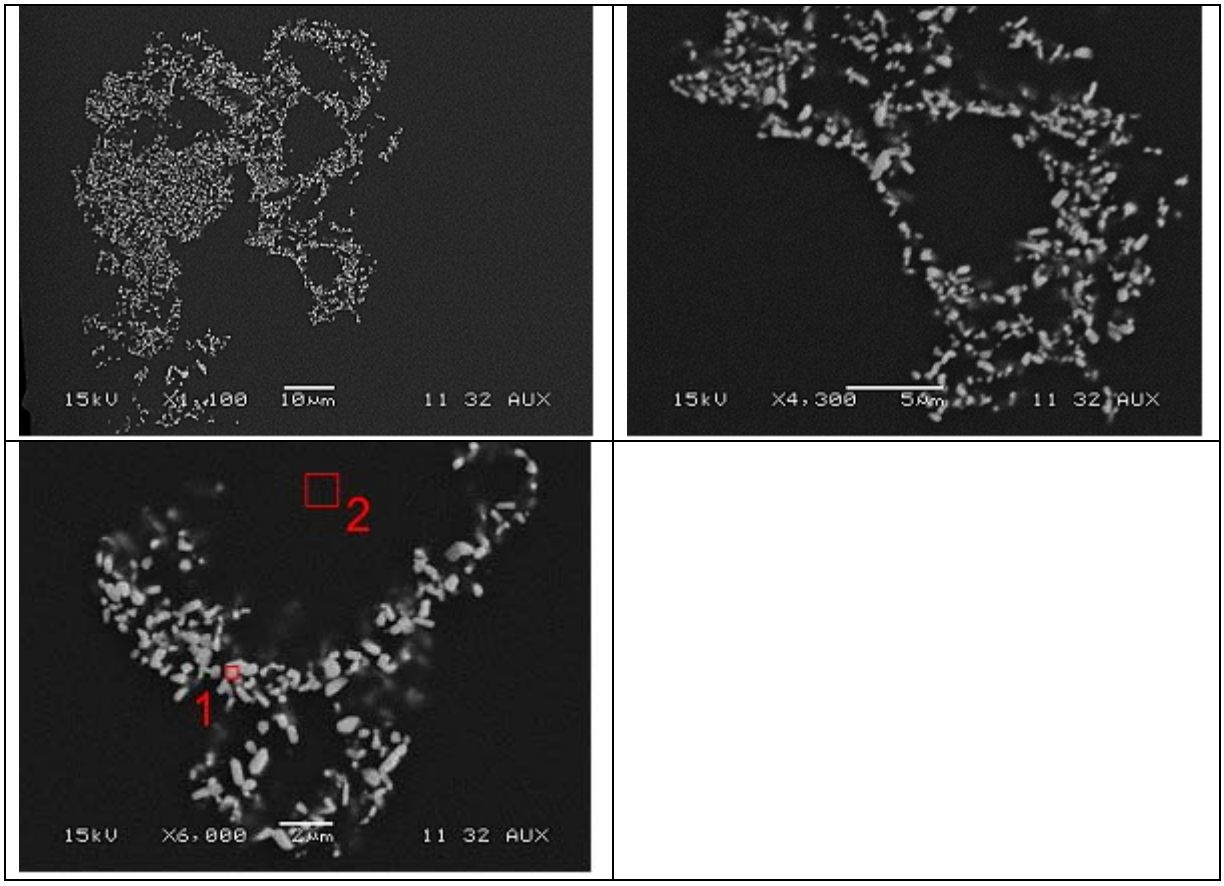

Figure 5-20. Undissolved RuO_2 Agglomerates in Glass US-08 After Heat Treating at 1058 °C for 24 h.

Table 5-18. Composition of Particles and the Surrounding Glass in US-08 Measured by EDS After Heat Treating at 1058 °C for 24 h.

Element	X6000_1	X6000_2
	Atomic%	
O	36.10	31.33
Na	4.88	7.72
Al	5.22	13.26
Si	13.31	39.81
Ru	36.04	
K		0.82
Ti	0.34	0.43
Mn	1.20	1.47
Fe	2.91	5.15

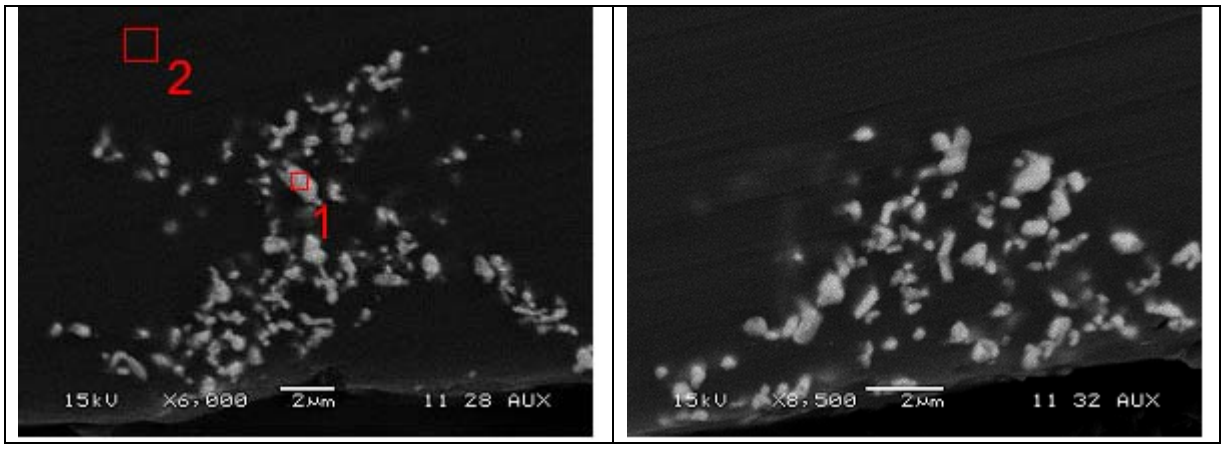

Figure 5-21. Undissolved RuO_2 Agglomerates in Glass US-09 After Heat Treating at 1107 °C for 24 h.

Table 5-19. Composition of Particles and the Surrounding Glass in US-09 Measured by EDS After Heat Treating at 1107 °C for 24 h.

Element	X6000_1	X6000_2
	Atomic%	
O	26.57	20.23
Na	5.19	5.28
Mg		0.82
Al	5.74	14.23
Si	15.13	46.58
Ru	42.10	
Ca		1.22
Ti		0.94
Cr	1.46	0.43
Fe	3.81	10.26

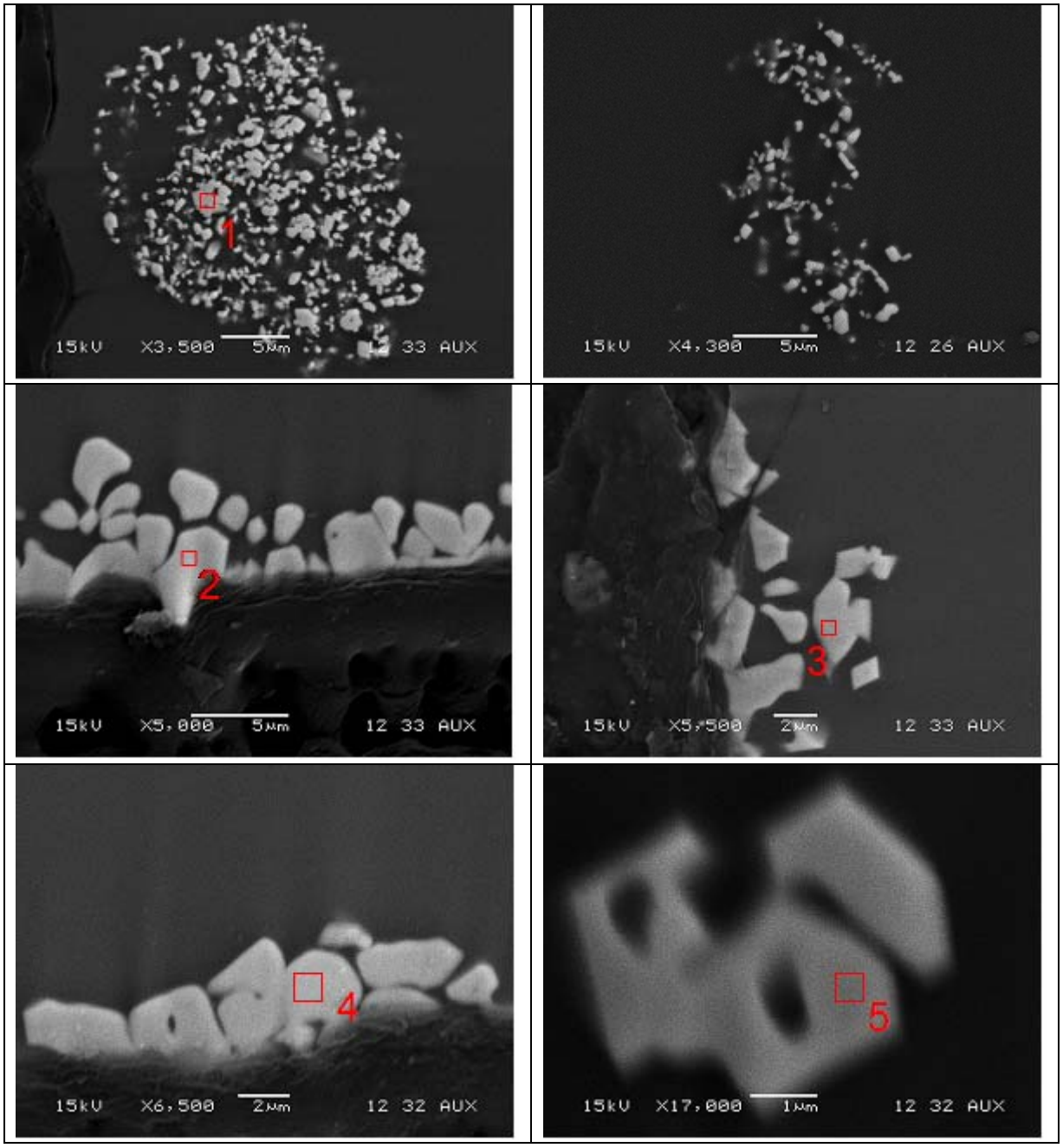

Figure 5-22. Undissolved RuO_2 Agglomerates and Spinel Crystals in Glass US-14 After Heat Treating at 954 °C for 24 h.

Table 5-20. Composition of Particles and Spinel Crystals in Glass US-14 Measured by EDS After Heat Treating at 954 °C for 24 h.

Element	X3500_1	x5500_4	X5000_2	x5500_3	X17000_5
	Atomic%				
O	37.77	15.93	15.33	15.32	27.56
Na	2.79	1.73	1.33	1.33	2.60
Mg		1.20	1.38	1.40	
Al	2.93	2.37	1.75	1.77	2.41
Si	7.50	3.00	1.47	1.50	3.34
Ru	46.88				
Rh		15.67	17.64	17.66	15.46
Ti		1.13	1.20	1.19	1.20
Mn		17.81	18.81	18.78	14.95
Fe	2.12	41.15	41.09	41.04	32.48

6.0 Summary

The objective of this task was to develop glass formulations for DOE waste streams with high aluminum concentrations to avoid nepheline formation while maintaining or meeting waste loading and/or waste throughput expectations as well as satisfying critical process and product performance related constraints. Liquidus temperatures and crystallization behavior were carefully characterized to support model development for higher waste loading glasses. The experimental work, characterization, and data interpretation necessary to meet these objectives were performed among three partnering laboratories: KRI, PNNL and SRNL.

Projected glass compositional regions that bound anticipated DWPF and Hanford HLW glass regions of interest were developed and used to generate glass compositions of interest for meeting the objectives of this study. A thorough statistical analysis was employed to allow for a wide range of waste glass compositions to be examined while minimizing the number of glasses that had to be fabricated and characterized in the laboratory. The glass compositions were divided into two sets, with 45 in the test matrix investigated by the U.S. laboratories and 30 in the test matrix investigated by KRI. Fabrication and characterization of the US and KRI-series glasses were generally handled separately. This report has focused mainly on the US-series glasses.

Glasses were fabricated and characterized by SRNL and PNNL. Crystalline phases were identified by XRD in the quenched and CCC glasses and were generally iron oxides and spinels, which are not expected to impact durability of the glass. Nepheline was detected in five of the glasses after the CCC heat treatment.

Chemical composition measurements each of the glasses were conducted following an analytical plan. A review of the individual oxides for each glass revealed that there were no errors in batching significant enough to impact the outcome of the study. A comparison of the measured compositions of the replicates indicated an acceptable degree of repeatability as the percent differences for most of the oxides were less than 5% and percent differences for all of the oxides were less than 10 wt%.

Chemical durability was measured using the PCT. All but two of the study glasses had NL [B] values that were well below that of the EA reference glass. The two highest NL [B] values were for the CCC versions of glasses US-18 and US-27 (10.498 g/L and 15.962 g/L, respectively). Nepheline crystallization was identified by qualitative XRD in five of the US-series glasses. Each of these five glasses (US-18, US-26, US-27, US-37 and US-43) shows a significant increase in NL [B] after the CCC heat treatment. This reduction in durability can be attributed to the formation of nepheline during the slow cooling cycle and the removal of glass formers from the residual glass network.

The liquidus temperature of each glass in the study was determined by both optical microscopy and XRD methods. The correlation coefficient of the measured XRD T_L data versus the measured optical T_L data was very good (R^2 = 0.9469). Aside from a few outliers, the two datasets aligned very well across the entire temperature range (829 °C to 1312 °C for optical data and 813 °C to 1310 °C for XRD crystal fraction data). The data also correlated well with the predictions of a T_L model. The correlation between the measured and calculated data had a higher degree of merit for the XRD crystal fraction data than for the optical data (higher R^2 value of 0.9089 versus 0.8970 for the optical data).

The SEM-EDS analysis of select samples revealed the presence of undissolved RuO_2 in all glasses due to the low solubility of RuO_2 in borosilicate glass. These particles tended to form agglomerates with varying sizes and shapes that were located close to the bottom of crucibles.

The results of this study provide further insight into the ability of borosilicate waste glass to incorporate increased concentrations of aluminum. The glass composition and properties data will be incorporated into a database of glass composition-property relationships (ComPro[a]) to support further optimization of waste glass compositions at DOE sites.

[a] Taylor, A. S., T. B. Edwards, J. C. George, T. K. Snyder and D. K. Peeler, "The SRNL Composition - Properties (ComPro™) Database," *U.S. Department of Energy Report WSRC-RP-2004-00704, Revision 0,* Westinghouse Savannah River Company, Aiken, SC (2004).

7.0 References

1. Barnes, B. O., "Pacific Northwest National Laboratory Quality Assurance Plan, Project 47607 – Task 6, LAW Glass Studies," *U.S. Department of Energy Report PNNL-QAP-47607, Revision 0,* Pacific Northwest National Laboratory, Richland, WA (2006).

2. Peeler, D. K. and T. B. Edwards, "Test Plan: Improved Alumina Solubility in US High Level Waste Glasses," *U.S. Department of Energy Report SRNL-PSE-2006-00275,* Washington Savannah River Company, Aiken, SC 2006).

3. Aloy, A., J. D. Vienna, K. M. Fox, T. B. Edwards and D. K. Peeler, "Glass Selection Strategy: Development of US and KRI Test Matrices," *U.S. Department of Energy Report WSRC-STI-2006-00205, Revision 0,* Washington Savannnah River Company, Aiken, SC (2006).

4. Aloy, A., "Final Report: Improved Retention of Aluminum, Chromium, and Sulfate in U.S. Waste Glasses," *U.S. Department of Energy Report SRNS-OS-2008-00001,* V.G. Khlopin Radium Institute, St. Petersburg, Russia (2008).

5. Marra, S. L. and C. M. Jantzen, "Characterization of Projected DWPF Glass Heat Treated to Simulate Canister Centerline Cooling," *U.S. Department of Energy Report WSRC-TR-92-142, Revision 1,* Westinghouse Savannah River Company, Aiken, SC (1993).

6. Edwards, T. B., "An Analytical Plan for Measuring the Chemical Compositions of Glasses from the Task #6 Study," *U.S. Department of Energy Report SRNL-SCS-2006-00036,* Washington Savannah River Company, Aiken, SC (2006).

7. Herman, C. C., T. B. Edwards, D. R. Best, D. M. Marsh and R. J. Workman, "Reduction of Constraints: Phase 2 Experimental Assessment for Sludge-Only Processing," *U.S. Department of Energy Report WSRC-TR-2002-00482, Revision 0,* Westinghouse Savannah River Company, Aiken, SC (2002).

8. Edwards, T. B., "An Analytical Plan for Measuring the PCT Solutions for the Third Set of Glasses from the Task #6 Study (U)," *U.S. Department of Energy Report SRNL-SCS-2006-00041,* Washington Savannah River Company, Aiken, SC (2006).

9. Edwards, T. B., "An Analytical Plan for Measuring the PCT Solutions for the Second Set of Glasses from the Task #6 Study," *U.S. Department of Energy Report SRNL-SCS-2006-00037,* Washington Savannah River Company, Aiken, SC (2006).

10. Edwards, T. B., "An Analytical Plan for Measuring the PCT Solutions for the First Set of Glasses from the Task #6 Study," *U.S. Department of Energy Report SRNL-SCS-2006-00035,* Washington Savannah River Company, Aiken, SC (2006).

11. "Standard Test Methods for Determining the Liquidus Temperature (TL) of Waste Glasses and Simulated Waste Glases," *U.S. Department of Energy Report PNNL Technical Procedure GDL-LQT, Revison 3,* Pacific Northwest National Laboratory, Richland, WA

12. "Quantitative and Semi-Quantitative Analysis using X-Ray Diffraction," *U.S. Department of Energy Report PNNL Technical Procedure GDL-XRD, Revision 0,* Pacific Northwest National Laboratory, Richland, WA

13. Bickford, D. F. and C. M. Jantzen, "Devitrification of SRL Defense Waste Glass," *Sci. Basis for Nuclear Waste Management VII, edited by G. L. McVay.* Elsevier, New York, pp. 557-565 (1984).

14. Edwards, T. B., "A Statistical Review of the Chemical Composition Measurements and PCT Results for the Glass Fabricated as Part of the US Test Matrix," *U.S. Department of Energy Report SRNL-SCS-2007-00029,* Washington Savannah River Company, Aiken, SC (2007).

15. Jantzen, C. M., N. E. Bibler, D. C. Beam, C. L. Crawford and M. A. Pickett, "Characterization of the Defense Waste Processing Facility (DWPF) Environmental Assessment (EA) Glass Standard Reference Material," *U.S. Department of Energy Report WSRC-TR-92-346, Revision 1,* Westinghouse Savannah River Company, Aiken, SC (1993).

16. Schreiber, H. D., F. A. Settle Jr., P. L. Jamison, J. P. Eckenrode and G. W. Headley, "Ruthenium in Glass-Forming Borosilicate Melts," *Journal of the Less-Common Metals,* **115** 145-154 (1986).

Appendix A

Heat Treatment Summaries for Optical Determination of Liquidus Temperature

The data below include some low resolution optical microscopy (LROM) observations and more detailed information from the high resolution optical microscopy (HROM) analyses using thin sections (ThS). Here, the heat treatments are listed with the type of observation (i.e., HROM or LROM), the temperature, and the observations that were made on that particular sample.

US-01:

- HROM ThS, 1156°C: homogeneous >>> lower temperature
- HROM ThS, 1107°C: black agglomerates of noble metals at bottom >>> lower temperature
- HROM ThS, 1057°C: black agglomerates of noble metals >>> lower temperature
- HROM ThS, 905°C: cubic crystals (spinels) >>> T_L between 905°C and 1057°C
- HROM ThS, 954°C: cubic crystals (spinels) >>> T_L between 954°C and 1057°C
- HROM ThS, 1008°C: black agglomerates of noble metals, few spinels >>> T_L between 1008°C and 1057°C
- HROM ThS, 1040°C: black agglomerates of noble metals, several spinels at bottom of sample >>> T_L between 1040°C and 1057°C
- HROM ThS, 1049°C: black agglomerates of noble metals at bottom of crucible, center of sample contains several spinels and black agglomerates of noble metals >>> T_L between 1049°C and 1057°C
- **T_L = 1053°C**

US-02:

- HROM ThS, 1285°C: homogeneous
- LROM, 1108°C: large black agglomerates of noble metals at bottom >>> lower temperature
- HROM ThS, 1008°C: black agglomerates of noble metals >>> lower temperature
- HROM ThS, 905°C: needles of noble metals >>> lower temperature
- HROM ThS, 954°C: needles of noble metals >>> lower temperature
- HROM ThS, 982°C: needles of noble metals and black agglomerates of noble metals >>> lower temperature
- HROM ThS, 995°C: needles of noble metals and black agglomerates of noble metals >>> lower temperature
- HROM ThS, 1001°C: black agglomerates of noble metals throughout specimen >>> lower temperature
- HROM ThS, 861°C: needles of noble metals throughout sample >>> lower temperature
- HROM ThS, 812°C: black agglomerates of noble metals throughout, very small undissolved particles everywhere >>> T_L less than 812°C
- HROM ThS, 764°C: black agglomerates of noble metals, lots of needles, undissolved material >>> T_L less than 764°C
- HROM ThS, 704°C: hematite on surface of sample, hematite throughout bulk, some spinel, black agglomerates of noble metals >>> T_L between 704°C and 764°C
- HROM ThS, 731°C: large prism-like clear crystals, needles throughout bulk >>> T_L between 731°C and 764°C
- HROM ThS, 753°C: lots of clear cubic crystals, some needles >>> T_L between 753°C and 764°C; **T_L = 759°C**

US-03:

- HROM ThS, 1206°C: black agglomerates of noble metals in bulk >>> lower temperature
- HROM ThS, 1056°C: black agglomerates of noble metals in bulk >>> lower temperature
- HROM ThS, 1009°C: black agglomerates of noble metals in bulk >>> lower temperature
- HROM ThS, 954°C: cubic crystals (spinels) >>> T_L between 954°C and 1009°C
- HROM ThS, 982°C: large agglomerates of cubic crystals (spinels) (~50), black agglomerates of noble metals at bottom of sample >>> T_L between 982°C and 1009°C
- HROM ThS, 995°C: black agglomerates of noble metals throughout sample >>> T_L between 995°C and 1009°C
- HROM ThS, 1000°C: several black agglomerates of noble metals in bulk, no crystals visible >>> T_L between 995°C and 1000°C
- **T_L = 997°C**

US-04:

- HROM ThS, 1205°C: homogeneous >>> lower temperature
- HROM ThS, 1156°C: homogeneous >>> lower temperature
- HROM ThS, 1056°C: black agglomerates of noble metals >>> lower temperature
- HROM ThS, 954°C: very tiny needles >>> T_L between 954°C and 1056°C
- HROM ThS, 1009°C: black agglomerates of noble metals >>> T_L between 954°C and 1009°C
- HROM ThS, 980°C: black agglomerates of noble metals, needles on side of sample (also, there were lots of really small anomalies in the sample that were too small to distinguish at 1000 x using HROM) >>> T_L between 980°C and 1009°C
- HROM ThS, 994°C: black agglomerates of noble metals >>> T_L between 980°C and 994°C
- HROM ThS, 1000°C: black agglomerates of noble metals, undissolved particulates throughout sample >>> T_L between 980°C and 994°C
- HROM ThS, 861°C: surface crystallization
- HROM ThS, 904°C: spinel everywhere, some hematite >>> T_L between 904°C and 954°C
- HROM ThS, 931°C: surface crystallization, spinel throughout, undissolved material throughout >>> T_L between 931°C and 954°C
- HROM ThS, 946°C: very large quantity of small undissolved particles, possibly a few cubic crystals (spinels) >>> T_L between 946°C and 954°C
- **T_L = 950°C**

US-05:

- HROM ThS, 1157°C: large black agglomerates of noble metals >>> lower temperature
- HROM ThS, 1056°C: large black agglomerates of noble metals, T_L possibly above 1056°C but verification advisable >>> temperature between 1056°C and 1156°C
- HROM ThS, 1109°C: large black agglomerates of noble metals, T_L possibly above 1109°C but verification advisable >>> temperature possibly between 1109°C and 1156°C
- HROM ThS, 1130°C: large black agglomerates of noble metals >>> T_L between questionable
- HROM ThS, 994°C:very crystallized with hematite and spinel, large black agglomerates of noble metals throughout bulk >>> T_L between 994°C and 1056°C
- HROM ThS, 1027°C: lots of crystals at base (round spinels) >>> T_L between 1027°C and 1056°C
- HROM ThS, 1043°C: several black agglomerates of noble metals, several clusters with round shaped objects >>> T_L between 994°C and 1027°C
- HROM ThS, 1013°C: hematite and cubic crystals (spinels) everywhere; few black agglomerates of noble metals >>> T_L between 1013°C and 1027°C
- HROM ThS, 1019°C: large black agglomerates of noble metals, few cubic crystals (spinels) >>> T_L between 1019°C and 1027°C
- **T_L = 1023°C**

US-06:

- HROM ThS, 1206°C: black agglomerates of noble metals in bulk >>> lower temperature
- HROM ThS, 1056°C: black agglomerates of noble metals at bottom and in bulk >>> lower temperature
- HROM ThS, 954°C: cubic crystals (spinels) >>> higher temperature
- HROM ThS, 1008°C: large black agglomerates of noble metals >>> T_L between 954°C and 1008°C
- HROM ThS, 982°C: cubic crystals (spinels) at middle of the bottom (~100 spinel agglomerate) >>> T_L between 982°C and 1008°C
- HROM ThS, 995°C: black agglomerates of noble metals, needles at bottom (large but few) >>> T_L between 995°C and 1008°C
- HROM ThS, 1001°C: black agglomerates of noble metals throughout bulk, submicron particles in areas (maybe spinels) >>> T_L between 1001°C and 1008°C
- **T_L = 1005°C**

US-07:

- HROM ThS, 1157°C: black agglomerates of noble metals >>> lower temperature
- HROM ThS, 1107°C: black agglomerates of noble metals >>> lower temperature
- HROM ThS, 1006°C: cubic crystals (spinels) >>> T_L between 1006°C and 1107°C
- HROM ThS, 1058°C: no cubic crystals, black agglomerates of noble metals at bottom of sample and ~10 throughout the bulk of the sample >>> T_L between 1006°C and 1058°C
- HROM ThS, 1015°C: lots of cubic crystals (spinels), black agglomerates of noble metals >>> T_L between 1015°C and 1058°C
- HROM ThS, 1029°C: black agglomerates of noble metals, no cubic crystals >>> T_L between 1015°C and 1029°C
- HROM ThS, 1022°C: large and small cubic crystals (spinel), RuO_2 agglomerates >>> T_L between 1022°C and 1029°C
- **T_L = 1026°C**

US-08:

- HROM ThS, 1157°C: large black agglomerates of noble metals >>> lower temperature
- HROM ThS, 1107°C: black agglomerates of noble metals >>> lower temperature
- HROM ThS, 1006°C: black agglomerates of noble metals >>> lower temperature
- HROM ThS, 903°C: cubic crystals (spinels) >>> T_L between 903°C and 1006°C
- HROM ThS, 954°C: streaks of cubic crystals (spinels) throughout the sample, needles at bottom of sample >>> T_L between 954°C and 1006°C
- HROM ThS, 980°C: black agglomerates of noble metals, chunks of cubic crystals (spinel) at bottom; small chunks of debris in bulk of sample – too small to distinguish at 1000 x >>> T_L between 980°C and 1006°C
- HROM ThS, 994°C: black agglomerates of noble metals, microscopic undissolved material (too small to distinguish at 1000 x) >>> T_L between 994°C and 1006°C
- HROM ThS, 1000°C: several black agglomerates of noble metals, small undissolved particulates throughout sample >>> T_L between 994°C and 1000°C
- **T_L = 997°C**

US-09:

- HROM ThS, 1157°C: large black agglomerates of noble metals, dark red prismatic crystals >>> higher temperature
- HROM ThS, 1202°C: homogeneous >>> T_L between 1157°C and 1202°C
- HROM ThS, 1232°C: homogeneous >>> T_L between 1157°C and 1202°C
- HROM ThS, 1180°C: sample clear aside from one black agglomerate of noble metals >>> T_L between 1157°C and 1180°C
- HROM ThS, 1169°C: no crystals, few black agglomerates of noble metals >>> T_L between 1157°C and 1169°C
- **T_L = 1163°C**

US-10:

- HROM ThS, 1157°C: homogeneous >>> lower temperature
- HROM ThS, 1107°C: few black agglomerates of noble metals >>> lower temperature
- HROM ThS, 1006°C: black agglomerates of noble metals >>> lower temperature
- HROM ThS, 954°C: cubic crystals (spinels) >>> T_L between 954°C and 1006°C
- HROM ThS, 982°C: streaks of tiny cubic crystals (spinels) throughout the bulk, black agglomerates of noble metals >>> T_L between 982°C and 1006°C
- HROM ThS, 995°C: black agglomerates of noble metals, needles at bottom, few large cubic clusters (spinels?) at base >>> T_L between 995°C and 1006°C
- HROM ThS, 1001°C: no cubic crystals, black agglomerates of noble metals throughout sample >>> T_L between 995°C and 1001°C
- **T_L = 998°C**

US-11:

- HROM ThS, 1157°C: few black agglomerates of noble metals >>> lower temperature
- HROM ThS, 1107°C: few black agglomerates of noble metals >>> lower temperature
- HROM ThS, 1006°C: black agglomerates of noble metals, some very small undissolved particles throughout bulk of sample >>> lower temperature
- HROM ThS, 903°C: many red hexagons (hematite), some cubic crystals >>> T_L between 903°C and 1006°C
- HROM ThS, 954°C: lots of crystals including hematite and a few cubic crystals (spinel) >>> T_L between 954°C and 1006°C
- HROM ThS, 980°C: lots of hematite and cubic crystals (spinels), black agglomerates of noble metals >>> T_L between 980°C and 1006°C
- HROM ThS, 994°C: lots of spinel and hematite (small to moderate in size), some hematite strings, black agglomerates of noble metals >>> T_L between 994°C and 1006°C
- HROM ThS, 1000°C: large spinel cluster at bottom of sample, black agglomerates of noble metals throughout bulk >>> T_L between 1000°C and 1006°C
- **T_L = 1003°C**

US-12:

- HROM ThS, 1157°C: black agglomerates of noble metals on bottom >>> lower temperature
- HROM ThS, 1107°C: homogeneous in small sample section >>> lower temperature
- HROM ThS, 1006°C: cubic crystals (spinels) >>> T_L between 1006°C and 1107°C
- HROM ThS, 1030°C, cubic crystals (spinels) >>> T_L between 1030°C and 1107°C
- HROM ThS, 1058°C: cubic crystals (spinels) >>> T_L between 1058°C and 1107°C
- HROM ThS, 1074°C: small cubic crystals (spinels) >>> T_L between 1074°C and 1107°C
- HROM ThS, 1086°C: sample clear of spinel >>> T_L between 1074°C and 1086°C
- HROM ThS, 1082°C: some features in agglomerates appear to be cubic at base, large black agglomerates of noble metals >>> T_L between 1082°C and 1086°C
- **T_L = 1084°C**

US-13:

- HROM ThS, 1157°C: homogeneous >>> lower temperature
- LROM, 1108°C: few white agglomerates on surface, few black agglomerates of noble metals in bulk >>> heat treatment between 1108°C and 1157°C
- HROM ThS, 1131°C: black agglomerates of noble metals in bulk >>> lower temperature
- HROM ThS, 1106°C: black agglomerates of noble metals in bulk >>> lower temperature
- HROM ThS, 1005°C: cubic crystals (spinels) >>> T_L between 1005°C and 1106°C
- HROM ThS, 1056°C: black agglomerates of noble materials in bulk >>> T_L between 1005°C and 1056°C
- HROM ThS, 1040°C: black agglomerates of noble metals >>> T_L between 1005°C and 1040°C
- HROM ThS, 1015°C: several cubic crystals (spinels) throughout bulk, black agglomerates of noble metals >>> T_L between 1015°C and 1040°C
- HROM ThS, 1029°C: black agglomerates of noble metals, no spinel >>> T_L between 1015°C and 1029°C
- HROM ThS, 1022°C: several small cubes (spinel), black agglomerates of noble metals >>> T_L between 1022°C and 1029°C
- **T_L = 1026°C**

US-14:

- HROM ThS, 901°C: big black agglomerates of noble metals at bottom and in the bulk, needle-like crystals that often agglomerate to stars >>> higher temperature
- HROM ThS, 1005°C: few black agglomerates of noble metals >>> lower temperature
- HROM ThS, 952°C: many tiny needles >>> T_L between 952°C and 1005°C
- HROM ThS, 980°C: small needles everywhere in bulk >>> T_L between 980°C and 1005°C
- HROM ThS, 994°C: needles everywhere >>> T_L between 994°C and 1005°C
- HROM ThS, 1000°C: several black agglomerates of noble metals, lots of small undissolved needles >>> T_L between 994°C and 1005°C
- HROM ThS, 861°C: lots of small cubic crystals (spinels) at base, lots of needles, black agglomerates of noble metals >>> T_L between 861°C and 901°C
- HROM ThS, 879°C: needles everywhere, black agglomerates of noble metals (discoloration in sample – possibly redox) >>> T_L between 861°C and 879°C
- HROM ThS, 869°C: black agglomerates of noble metals in bulk at base, needles throughout bulk lots of undissolved particles throughout, small cubic crystals (spinels) in bulk and throughout base >>> T_L between 869°C and 879°C
- **T_L = 874°C**

US-15:

- LROM, 1121°C, 1136°C, 1156°C, 1176°C, 1236°C: big black amorphous agglomerates at bottom, glass becomes darker with increasing temperature >>> SEM
- HROM ThS, 1386°C: homogeneous
- SEM-EDS, 1236°C: big black amorphous agglomerates at bottom are RuO_2 >>> lower temperature to detect other crystals besides RuO_2
- HROM ThS, 1005°C: black agglomerates of noble metals >>> lower temperature
- HROM ThS, 901°C: needles >>> higher temperature
- HROM ThS, 954°C: few needles >>> T_L between 954°C and 1005°C
- HROM ThS, 982°C: black agglomerates of noble metals >>> T_L between 954°C and 982°C
- HROM ThS, 861°C: lots of hematite, black agglomerates of noble metals, needles everywhere >>> T_L between 861°C and 901°C
- HROM ThS, 879°C: hematite everywhere, black agglomerates of noble metals, needles throughout, undissolved particles throughout >>> T_L between 879°C and 901°C
- HROM ThS, 890°C: several hematite crystals, black agglomerates of noble metals, lots of undissolved material throughout >>> T_L between 890°C and 901°C
- **T_L = 895°C**

US-16:

- LROM, 1402°C: brown crystal surface layer, fractured surface clear black
- HROM ThS, 1199°C: some undissolved materials (appears that they are all noble metals) >>> T_L < 1199°C
- HROM ThS, 1247°C: sample appears to be clear of crystals but does contain noble metals >>> T_L < 1199°C
- HROM ThS, 1000°C: sample full of undissolved materials (spinels and noble metals) >>> T_L between 1000°C and 1199°C
- HROM ThS, 1098°C: lots of undissolved materials (small and large spinels, some noble metals) >>> T_L between 1098°C and 1199°C
- HROM ThS, 1126°C: no spinel, some undissolved materials present >>> T_L between 1099°C and 1126°C
- HROM ThS, 980°C: sample full of undissolved materials (noble metals and spinels), some hematite at base of sample >>> T_L between 1099°C and 1126°C [XRD sample]
- HROM ThS, 1113°C: spinel at base, noble metals along base >>> T_L between 1113°C and 1126°C
- HROM ThS, 1120°C: spinel at base, noble metals along base >>> T_L between 1120°C and 1126°C
- **T_L = 1124°C**

US-17:

- HROM ThS, 1056°C: black agglomerates of noble metals >>> lower temperature
- HROM ThS, 1005°C: cubic crystals (spinels) >>> T_L between 1005°C and 1056°C
- HROM ThS, 1030°C: cubic crystals (spinels) >>> T_L between 1030°C and 1056°C
- HROM ThS, 1040°C: black agglomerates of noble metals, lots of little cubic crystals (spinels) at walls and bottom corner >>> T_L between 1040°C and 1057°C
- HROM ThS, 1049°C: black agglomerates of noble metals throughout bulk >>> T_L between 1040°C and 1049°C
- **T_L = 1045°C**

US-18:

- HROM ThS, 1005°C: few tiny needles >>> higher temperature
- HROM ThS, 1056°C: black agglomerates of noble metals >>> T_L between 1005°C and 1056°C
- HROM ThS, 1030°C: black agglomerates of noble metals >>> T_L between 1005°C and 1030°C
- HROM ThS, 1015°C: needles everywhere >>> T_L between 1005°C and 1015°C
- HROM ThS, 861°C: surface crystallization
- HROM ThS, 954°C: needles everywhere, several small cubic crystals (spinel) at base >>> T_L between 954°C and 1005°C
- HROM ThS, 982°C: a few large spinel agglomerates at base, needles throughout, RuO_2 agglomerates >>> T_L between 982°C and 1005°C
- HROM ThS, 994°C: lots of needles, few RuO_2 agglomerates >>> T_L between 982°C and 994°C
- **T_L = 988°C**

US-19:
- HROM ThS, 1056°C: black agglomerates of noble metals in bulk >>> lower temperature
- HROM ThS, 954°C: cubic crystals (spinels) >>> T_L between 954°C and 1056°C
- HROM ThS, 1007°C: tiny black spots around edges (maybe crystals) >>> T_L between 1007°C and 1056°C
- HROM ThS, 1040°C: black agglomerates of noble metals in bulk >>> T_L between 1007°C and 1040°C
- HROM ThS, 1015°C: black agglomerates of noble metals >>> T_L between 1007°C and 1015°C
- HROM ThS, 1029°C: small spinel cluster at bottom, black agglomerates of noble metals >>> T_L between 1029°C and 1040°C
- **T_L = 1035°C**

US-20:
- HROM ThS, 1056°C: black agglomerates of noble metals at bottom and in bulk >>> lower temperature
- HROM ThS, 954°C: cubic crystals >>> higher temperature
- HROM ThS, 1007°C: black agglomerates of noble metals >>> T_L between 954°C and 1007°C
- HROM ThS, 981°C: many cubic crystals in bulk of sample >>> T_L between 982°C and 1007°C
- HROM ThS, 995°C: black agglomerates of noble metals, lots of spinel in bulk, few needles >>> T_L between 995°C and 1007°C
- HROM ThS, 1001°C: black agglomerates of noble metals, submicron particles in areas (maybe spinels) >>> T_L between 1001°C and 1007°C
- **T_L = 1004°C**

US-21:
- HROM ThS, 1056°C: small cubic crystals >>> higher temperature
- HROM ThS, 1106°C: black agglomerates of noble metals >>> T_L between 1056°C and 1106°C
- HROM ThS, 1080°C: several large black agglomerates of noble metals in bulk, no spinels >>> T_L between 1056°C and 1080°C
- HROM ThS, 1067°C: black agglomerates of noble metals, very few small spinel >>> T_L between 1067°C and 1080°C
- HROM ThS, 1074°C: several black agglomerates of noble metals, no spinels >>> T_L between 1067°C and 1074°C
- HROM ThS, 1070°C: a few small black agglomerates of noble metals at bottom – some appear to spinel and the rest are RuO_2 >>> T_L between 1070°C and 1074°C
- **T_L = 1072°C**

US-22:
- HROM ThS, 1056°C: small cubic crystals >>> higher temperature
- HROM ThS, 1106°C: black agglomerates of noble metals >>> T_L between 1056°C and 1106°C
- HROM ThS, 1080°C: spinel present (some large, some small) >>> T_L between 1080°C and 1106°C
- HROM ThS, 1095°C: black agglomerates of noble metals at base, no crystals present >>> T_L between 1080°C and 1095°C
- HROM ThS, 1086°C: few clusters of spinel at bottom corner, black agglomerates of noble metals >>> T_L between 1086°C and 1095°C
- HROM ThS, 1066°C: several spinels at base, small and large (other undissolved materials) >>> T_L between 1086°C and 1095°C [XRD sample]
- **T_L = 1091°C**

US-23:
- HROM ThS, 1056°C: black agglomerates of noble metals in bulk >>> lower temperature
- HROM ThS, 1007°C: cubic crystals (spinels) >>> T_L between 1007°C and 1056°C
- HROM ThS, 1030°C: very few cubic crystals (spinels) >>> T_L between 1030°C and 1056°C
- HROM ThS, 1040°C: black agglomerates of noble metals >>> T_L between 1030°C and 1040°C
- HROM ThS, 1035°C: black agglomerates of noble metals, no spinels >>> T_L between 1030°C and 1035°C
- **T_L = 1032°C**

US-24:
- HROM ThS, 1056°C: black agglomerates of noble metals in bulk >>> lower temperature
- HROM ThS, 954°C: cubic crystals (spinels) >>> higher temperature
- HROM ThS, 1007°C: cubic crystals (spinels) >>> T_L between 1007°C and 1056°C
- HROM ThS, 1030°C: cubic crystals (spinels) >>> T_L between 1030°C and 1056°C
- HROM ThS, 1040°C: black agglomerates of noble metals in bulk, lots of little cubic crystals (spinel) throughout sample >>> T_L between 1040°C and 1056°C
- HROM ThS, 1049°C: clusters of very small cubic crystals (spinels) throughout the sample, black agglomerates of noble metals >>> T_L between 1049°C and 1056°C
- **T_L = 1052°C**

US-25:
- HROM ThS, 1007°C and 1056°C: cubic crystals (spinel) >>> higher temperature
- HROM ThS, 1106°C: black agglomerates of noble metals >>> T_L between 1056°C and 1106°C
- HROM ThS, 1080°C: lots of cubic crystals (spinel), lots of smaller undefined crystals >>> T_L between 1080°C and 1106°C
- HROM ThS, 1095°C: black agglomerates of noble metals >>> T_L between 1080°C and 1095°C
- HROM ThS, 1086°C: black agglomerates of noble metals >>> T_L between 1080°C and 1086°C
- **T_L = 1083°C**

US-26:
- HROM ThS, 1107°C: many tiny cubic crystals (spinel) mostly at crucible bottom >>> higher temperature
- HROM ThS, 1205°C: cubic crystals (spinels) >>> higher temperature
- HROM ThS, 1254°C: black agglomerates of noble metals >>> T_L between 1205°C and 1254°C
- HROM ThS, 1232°C: black agglomerates of noble metals >>> T_L between 1205°C and 1232°C
- HROM ThS, 1217°C: sample clear >>> T_L between 1205°C and 1217°C
- HROM ThS, 1206°C: black agglomerates of noble metals at base of sample >>> T_L between 1205°C and 1206°C
- **T_L = 1206°C**

US-27:

- HROM ThS, 1056°C: few cubic crystals (spinels) and black agglomerates of noble metals in bulk >>> higher temperature
- HROM ThS, 1095°C: sample clear >>> T_L between 1056°C and 1095°C
- HROM ThS, 1086°C: sample clear >>> T_L between 1056°C and 1086°C
- HROM ThS, 1070°C: a few small cubic crystals (spinels) at base, black agglomerates of noble metals at base of sample >>> T_L between 1070°C and 1086°C
- HROM ThS, 1079°C: sample volatilized out of crucible a lot; layer on bottom of agglomerates, appear to have cubic shape (possibly spinel), some black agglomerates of noble metals in bulk >>> T_L between 1079°C and 1086°C
- **T_L = 1082°C**

US-28:

- HROM ThS, 1006°C: black agglomerates of noble metals >>> lower temperature
- HROM ThS, 903°C: few needles >>> T_L between 903°C and 1006°C
- HROM ThS, 952°C: black agglomerates of noble metals, several small sets of needles >>> T_L between 952°C and 1006°C
- HROM ThS, 980°C: small needles through out bulk, black agglomerates of noble metals >>> T_L between 980°C and 1006°C
- HROM ThS, 994°C: small needles throughout sample, black agglomerates of noble metals throughout bulk >>> T_L between 994°C and 1006°C
- HROM ThS, 1000°C: black agglomerates of noble metals throughout, small needles throughout, undissolved particles throughout >>> T_L between 994°C and 1006°C
- HROM ThS, 861°C: black agglomerates of noble metals throughout, small needles throughout >>> T_L <861°C
- HROM ThS, 812°C: black agglomerates of noble metals, small spinel everywhere, some hematite, also clear cubic crystals everywhere >>> T_L between 812°C and 861°C
- HROM ThS, 840°C: black agglomerates of noble metals, lots of needles >>> T_L between 812°C and 840°C
- HROM ThS, 826°C: a few hematite crystals, a few small spinels in bulk >>> T_L between 826°C and 840°C
- HROM ThS, 831°C: black agglomerates of noble metals, needles throughout, small undissolved particles in bulk >>> T_L between 826°C and 831°C
- **T_L = 829°C**

US-29:

- HROM ThS, 952°C: very few needles >>> higher temperature
- HROM ThS, 1006°C: possible homogeneous >>> T_L between 952°C and 1006°C
- HROM ThS, 981°C: few black agglomerates of noble metals >>> T_L between 952°C and 981°C
- HROM ThS, 812°C: black agglomerates of noble metals, needles everywhere, undissolved material everywhere >>> T_L <812°C
- HROM ThS, 879°C: spinel everywhere, black agglomerates of noble metals >>> T_L between 879°C and 903°C
- HROM ThS, 890°C: a few black agglomerates of noble metals, needles everywhere >>> T_L between 879°C and 890°C
- **T_L = 885°C**

US-30:

- LROM, 1402°C: brown crystal striations in bulk
- HROM ThS, 1426°C: sample clear >>> T_L < 1426°C
- HROM ThS, 1405°C: lots of small crystals, looks like they all formed during cooling >>> T_L < 1426°C
- HROM ThS, 1350°C: sample clear >>> T_L 1350< °C
- HROM ThS, 1304°C: a few small undissolved agglomerates at base of sample, possible some spinel near one of the agglomerates (5 cubic structures)
- HROM ThS, 1247°C: several clusters of noble metals throughout sample, possibly some spinel
- HROM ThS, 1218°C: quite a few spinels throughout bulk, some other undissolved materials (noble metals) >>> T_L between 1218°C and 1247°C
- HROM ThS, 1074°C: lots of undissolved materials (noble metals and spinels) >>> T_L between 1218°C and 1247°C [XRD sample]
- HROM ThS, 1017°C: lots of undissolved materials (noble metals and spinels) >>> T_L between 1218°C and 1247°C [XRD sample]
- HROM ThS, 1232°C: few spinels and other undissolved noble metals >>> T_L between 1232°C and 1247°C
- HROM ThS, 1235°C: few spinels and other undissolved noble metals >>> T_L between 1235°C and 1247°C
- **T_L = 1241°C**

US-31:

- HROM ThS, 1056°C: cubic crystals (spinels) and red rhombic crystals (hematite) >>> higher temperature
- HROM ThS, 1107°C: black agglomerates of noble metals at bottom, some agglomerates are cubic (spinel) >>> higher temperature
- HROM ThS, 1153°C: black agglomerates of noble metals >>> lower temperature
- HROM ThS, 1130°C: sample looks clear >>> T_L between 1107°C and 1130°C
- HROM ThS, 1095°C: black agglomerates of noble metals, several clusters of round and cubic spinel along bottom perimeter of sample >>> T_L between 1107°C and 1130°C
- HROM ThS, 1118°C: sample clear >>> T_L between 1107°C and 1118°C
- **T_L = 1113°C**

US-32:

- HROM ThS, 903°C: some very tiny needles, very difficult to see, verification advisable >>> lower temperature
- HROM ThS, 952°C: some very tiny needles, very difficult to see, verification advisable >>> lower temperature
- HROM ThS, 1006°C: possibly homogeneous >>> lower temperature
- HROM ThS, 981°C: black agglomerates of noble metals and needles throughout the sample >>> lower temperature
- HROM ThS, 995°C: black agglomerates of noble metals, few small needles in bulk >>> lower temperature
- HROM ThS, 1001°C: black agglomerates of noble metals throughout, needles in bulk >>> lower temperature
- HROM ThS, 861°C: needles everywhere >>> lower temperature
- HROM ThS, 812°C: black agglomerates of noble metals, undissolved material everywhere, needles throughout >>> lower temperature
- HROM ThS, 764°C: surface crystallization, black agglomerates of noble metals, undissolved material >>> T_L <764°C
- HROM ThS, 704°C: surface crystallization; some spinel in bulk, lots of clear rectangular prism-like crystals with different shapes (some flat plates, some rods), black agglomerates of noble metals >>> T_L between 704°C and 764°C
- HROM ThS, 731°C: large hematite crystals, few cubic crystals (spinel), few triangle-like crystals, lots of small undissolved particles >>> T_L between 731°C and 764°C
- HROM ThS, 753°C: large spinel at top, streaks of needles throughout bulk, undissolved materials (noble metals) >>> T_L between 753°C and 764°C
- **T_L = 759°C**

US-33:

- HROM ThS, 1157°C and 1206°C: small, black agglomerates of noble metals >>> repeat treatment at 1206°C for obtaining bigger sample
- HROM ThS, 1203°C: few black agglomerates of noble metals >>> lower temperature
- HROM ThS, 1007°C: homogeneous in small sample, black agglomerates of noble metals >>> lower temperature
- HROM ThS, 854°C: cubic crystals (spinel) >>> T_L between 854°C and 1007°C
- HROM ThS, 902°C: lots of small cubic crystals (spinel), several prism/faceted crystals >>> T_L between 902°C and 1007°C
- HROM ThS, 954°C: spinel everywhere >>> T_L between 954°C and 1007°C
- HROM ThS, 980°C: spinel everywhere >>> T_L between 980°C and 1007°C
- HROM ThS, 995°C: extremely large quantity of noble metal agglomerates >>> T_L between 995°C and 1007°C
- HROM ThS, 1001°C: lots of spinels and black agglomerates of noble metals >>> T_L between 1001°C and 1007°C
- **T_L = 1004°C**

US-34:

- HROM ThS, 854°C: many needle-like crystals in bulk >>> lower temperature
- HROM ThS, 903°C: some needle-like crystals in bulk >>> lower temperature
- HROM ThS, 954°C: small needles in bulk >>> lower temperature
- HROM ThS, 1095°C: sample appears to be amorphous >>> lower temperature
- HROM ThS, 994°C: one black agglomerate of noble metals – sample appears to be amorphous >>> lower temperature
- HROM ThS, 1015°C: sample clear >>> lower temperature
- HROM ThS, 861°C: needles everywhere >>> lower temperature
- HROM ThS, 854°C: needles everywhere >>> lower temperature
- HROM ThS, 812°C: lots of large spinel, some hematite >>> T_L between 812°C and 854°C
- HROM ThS, 840°C: lots of undissolved material everywhere, needles throughout >>> T_L between 812°C and 840°C
- HROM ThS, 828°C: sample too opaque to see through, even when polished really thin >>> T_L is between 828°C and 840°C
- **T_L = 832°C**

US-35:

- LROM, 1200°C (as received sample from SRNL): many black crystal agglomerates in bulk
- LROM, 1397°C: brown crystal surface layer, many white spots on fractured surface
- HROM ThS, 1350°C: small crystals formed upon cooling, a few clusters of semi-transparent orange cubic crystals at base with light halo surrounding (possibly undissolved noble metals)
- HROM ThS, 1247°C: several spinel throughout bulk, other undissolved materials >>> T_L > 1247°C
- HROM ThS, 1218°C: several spinel throughout bulk, other undissolved materials >>> T_L > 1247°C
- HROM ThS, 1074°C: lots of undissolved materials >>> T_L > 1247°C [XRD sample]
- HROM ThS, 1017°C: lots of undissolved materials >>> T_L > 1247°C [XRD sample]
- HROM ThS, 1318°C: some undissolved materials at base (most likely noble metals and not spinel >>> T_L is between 1247°C and 1318°C
- HROM ThS, 1278°C: some undissolved materials at base (noble metals), probably not spinel >>> T_L is between 1278°C and 1318°C
- HROM ThS, 1301°C: few spinels and some other undissolved materials (noble metals) >>> T_L is between 1301°C and 1318°C
- HROM ThS, 1309°C: undissolved materials, appears to be a few cubic structures (spinels?) >>> T_L is between 1309°C and 1318°C
- **T_L = 1312°C**

US-36:

- LROM, 1150°C (as received sample from SRNL): many black crystal agglomerates in bulk
- LROM, 1401°C: brown crystal striations on surface, many white spots on fractured surface
- HROM ThS, 1426°C: redox in sample, small crystals from cooling but no large crystals >>> T_L < 1426°C
- HROM ThS, 1405°C: lots of small crystals, looks like they all formed during cooling >>> T_L < 1405°C
- HROM ThS, 1350°C: small crystals formed upon cooling, doesn't appear to contain any large crystals >>> T_L < 1350°C
- HROM ThS, 1304°C: samples appears to be clear >>> T_L < 1304°C
- HROM ThS, 1328°C: one small black structure with a light halo around it (might be spinel or a different crystal) >>> T_L < 1304°C
- HROM ThS, 1199°C: a few spinel throughout bulk, some undissolved noble metals >>> T_L is between 1199°C and 1304°C
- HROM ThS, 1247°C: crystallized upon cooling, glass matrix has a light brown color >>> T_L is between 1199°C and 1247°C
- HROM ThS, 1000°C: large quantities of spinel and other undissolved materials >>> T_L is between 1199°C and 1247°C [XRD sample]
- HROM ThS, 1098°C: several spinel throughout bulk, other undissolved materials (noble metals) >>> T_L is between 1199°C and 1247°C [XRD sample]
- HROM ThS, 1164°C: several crystals throughout bulk, some noble metals at base >>> T_L is between 1199°C and 1247°C [XRD sample]
- HROM ThS, 1225°C: spinels in sample >>> T_L is between 1225°C and 1247°C
- HROM ThS, 1235°C: lots of little spinels (formed from cooling), possibly one actual spinel (formed during HT) triangle with halo in bulk >>> T_L is between 1235°C and 1247°C
- **T_L = 1238°C**

US-37:

- HROM ThS, 1007°C: black agglomerates of noble metals >>> lower temperature
- HROM ThS, 952°C: cubic crystals (spinels) >>> T_L between 952°C and 1007°C
- HROM ThS, 981°C: black agglomerates of noble metals at bottom, tiny needles throughout the sample >>> T_L between 981°C and 1007°C
- HROM ThS, 995°C: needles throughout sample, black agglomerates of noble metals >>> T_L between 995°C and 1007°C
- HROM ThS, 1001°C: lots of cubic crystals (spinels) and some black agglomerates of noble metals >>> T_L between 1001°C and 1007°C
- HROM ThS, 1021°C: undissolved materials (all noble metals?) >>> T_L between 1001°C and 1007°C
- **T_L = 1004°C**

US-38:

- HROM ThS, 1056°C: very few cubic crystals and black agglomerates of noble metals in bulk >>> higher temperature
- HROM ThS, 1095°C: a few black agglomerates of noble metals >>> T_L between 1056°C and 1095°C
- HROM ThS, 1086°C: sample clear >>> T_L between 1056°C and 1086°C
- HROM ThS, 1070°C: one small, black agglomerate of noble metals >>> T_L between 1056°C and 1070°C
- HROM ThS, 1067°C: sample is clear of crystals >>>T_L between 1056°C and 1067°C
- HROM ThS, 1036°C: a few 4-pronged stars; like sharp-cornered spinels at top and bottom borders >>> T_L between 1056°C and 1067°C
- **T_L = 1062°C**

US-39:

- HROM ThS, 1056°C: many tiny cubic crystals, especially at crucible bottom >>> higher temperature
- HROM ThS, 1107°C: few cubic crystals >>> higher temperature
- HROM ThS, 1130°C: very few black agglomerates of noble metals in bulk >>> T_L between 1107°C and 1130°C
- HROM ThS, 1118°C: black agglomerates of noble metals, no spinel >>> T_L between 1107°C and 1118°C
- HROM ThS, 1110°C: black agglomerates of noble metals at base of sample, no spinel >>> T_L between 1107°C and 1110°C
- **T_L = 1109°C**

US-40:

- Didn't form glass upon initial melting so this glass was rejected as a candidate for testing

US-41:

- HROM ThS, 1108°C: black agglomerates of noble metals, few cubic crystals (spinel) >>> higher temperature
- HROM ThS, 1157°C: small, black agglomerates of noble metals, appears to be no spinel >>> repeat treatment at 1157°C for obtaining bigger sample
- HROM ThS, 1159°C: black agglomerates of noble metals at base, some needle-like crystals at bottom with brown coloring surrounding them >>> SEM
- SEM-EDS, 1159°C: black agglomerates of noble metals >>> lower temperature
- HROM ThS, 1058°C: red hexagons (hematite) >>> higher temperature
- HROM ThS, 1108°C: black agglomerates of noble metals >>> T_L between 1058°C and 1108°C
- HROM ThS, 1080°C: black agglomerates of noble metals >>> T_L between 1058°C and 1080°C
- HROM ThS, 1067°C: black agglomerates of noble metals >>> T_L between 1058°C and 1067°C
- **T_L = 1063°C**

US-42:

- LROM, 1302°C and 1401°C: grey crystal cover on surface, clear brown fractured surface, bulk may be homogeneous
- HROM ThS, 1405°C: bulk is clear/glassy (no redox) strange structures around top and base (maybe crystals) >>> T_L < 1405°C
- HROM ThS, 1350°C: sample looks clear aside from strange transparent diamond/cubic structures at base of sample >>> T_L < 1350°C
- HROM ThS, 1304°C: sample clear >>> T_L < 1304°C
- HROM ThS, 1199°C: sample appears to be clear >>> T_L < 1199°C
- HROM ThS, 1247°C: no spinel, possibly some undissolved noble metals >>> T_L < 1199°C
- HROM ThS, 1000°C: spinel throughout bulk and other undissolved materials >>> T_L is between 1000°C and 1199°C
- HROM ThS, 1098°C: sample clear >>> T_L is between 1000°C and 1098°C
- HROM ThS, 1035°C: sample clear of crystals >>> T_L is between 1000°C and 1035°C
- HROM ThS, 1052°C: sample clear >>> T_L is between 1000°C and 1035°C
- HROM ThS, 925°C: sample full of undissolved materials (spinel, noble metals, possibly nepheline) >>> T_L is between 1000°C and 1035°C
- HROM ThS, 1017°C: lots of undissolved materials, some spinels >>> T_L is between 1017°C and 1035°C
- HROM ThS, 1028°C: no spinel, some undissolved materials present >>> T_L is between 1017°C and 1028°C
- **T_L = 1023°C**

US-43:

- HROM ThS, 1402°C: homogeneous >>> lower temperature
- HROM ThS, 1282°C: homogeneous >>> lower temperature
- HROM ThS, 1197°C: crystals at crucible bottom, very few of them appear to be cubic >>> T_L between 1197°C and 1282°C
- HROM ThS, 1232°C: sample is clear of crystals >>> T_L between 1197°C and 1232°C
- HROM ThS, 1217°C: small round crystals at base, black agglomerates of noble metals >>> T_L between 1217°C and 1232°C
- HROM ThS, 1225°C: some of the sample bubbled out of the crucible, sample looks free of crystals >>> T_L between 1217°C and 1225°C
- HROM ThS, 1085°C: lots of undissolved transparent material in bulk, undissolved opaque materials at base (noble metals) >>> T_L between 1217°C and 1225°C [XRD sample]
- **T_L = 1221°C**

US-44:

- HROM ThS, 1058°C: cubic crystals >>> higher temperature
- HROM ThS, 1108°C: black agglomerates of noble metals >>> T_L between 1058°C and 1108°C
- HROM ThS, 1080°C: cubic crystals >>> T_L between 1080°C and 1108°C
- HROM ThS, 1095°C: small spinel clumps at bottom, black agglomerates of noble metals >>> T_L between 1095°C and 1108°C
- HROM ThS, 1101°C: small, black agglomerates of noble metals >>> T_L between 1095°C and 1101°C
- **T_L = 1098°C**

US-45:

- HROM ThS, 1058°C: few cubic crystals in bulk >>> higher temperature
- HROM ThS, 1108°C: black agglomerates of noble metals >>> T_L between 1058°C and 1108°C
- HROM ThS, 1080°C: black agglomerates of noble metals >>> T_L between 1058°C and 1080°C
- HROM ThS, 1067°C: large and small spinels throughout sample, black agglomerates of noble metals >>> T_L between 1067°C and 1080°C
- HROM ThS, 1074°C: sample clear >>> T_L between 1067°C and 1074°C
- HROM ThS, 1070°C: a few small agglomerates at bottom – some are spinel and the rest are black agglomerates of noble metals >>> T_L between 1070°C and 1074°C
- **T_L = 1072°C**

Appendix B

Crystal Fraction Summary Table

Table B-1. Summary of crystalline phases for different heat treated specimens for all glasses along with the data fit information – slope, intercept (or calculated T_L), and correlation coefficient (R^2) – and the primary phase (listed as "Prim. Ph.") identified.

Crystalline phases, listed in the table as wt% abundance, are abbreviated as follows: Trev. = trevorite, Neph. = nepheline, Nos. = nosean, Zirc. = zircon, Hem. = hematite. The term "(OP)" listed after some of the primary phases means that the measured T_L for the crystal fraction method for that particular glass is listed as being below the detection limit in Table 5-7 due to a lack of sufficient crystal fraction data.

Glass	Temp. (°C)	Trev.	Neph.	NiO	Nos.	Zirc.	Hem.	Li_2SiO_3	Slope	Int.	R^2	Prim. Ph.
US-01	905	1							-110.74	1019	0.997	Spinel
US-01	854	1.5										
US-01	954	0.6										
US-02	854								N/A	N/A	N/A	Baddelyite (OP)
US-02	905											
US-02	954											
US-02	1006											
US-03	854	1.1							-148.28	1018	0.996	Spinel
US-03	954	0.4										
US-03	904	0.8										
US-03	1006	0.1										
US-04	954	0.1							-62.67	956	0.984	Spinel
US-04	861	1.5										
US-04	904	0.9										
US-04	931	0.3										
US-05	854						4.6		-37.99	1025	0.984	Hematite
US-05	904						2.9					
US-05	954						2.1					
US-05	1006	0.2					0.5					
US-06	854	3							-39.39	968	0.945	Spinel
US-06	904	1.3										
US-06	954	0.6										
US-07	954	1.7							-37.76	1018	1.000	Spinel
US-07	1006	0.3										
US-07	1015	0.1										
US-08	854	2.4							-52.60	981	1.000	Spinel
US-08	903	1.5										
US-08	954	0.5										
US-09	854						0.5		-510.00	1091	0.917	Hematite
US-09	903						0.3					
US-09	1058						0.1					
US-10	854	3.5							-42.09	998	0.966	Spinel
US-10	903	2										
US-10	954	1.2										
US-11	854	1.6					2.8		-79.29	976	0.764	Spinel

Glass	Temp. (°C)	Trev.	Neph.	NiO	Nos.	Zirc.	Hem.	Li_2SiO_3	Slope	Int.	R^2	Prim. Ph.
US-11	980	0.3										
US-11	903	0.5					1.7					
US-12	854	5.2							-39.99	1062	1.000	Spinel
US-12	903	4										
US-12	954	2.7										
US-13	854	2.6							-69.26	1034	0.999	Spinel
US-13	901	1.9										
US-13	954	1.2										
US-13	1005	0.4										
US-14	861	0.5							-40.00	880	0.750	Spinel
US-14	861	0.4										
US-14	869	0.3										
US-15	854	0.5							-117.50	913	1.000	Spinel
US-15	901	0.1										
US-16	954						3.7		-47.67	1136	0.964	Hematite
US-16	1005						3.1					
US-16	1000						2.6					
US-16	1000						2.8					
US-16	1056						1.8					
US-16	1106						0.6					
US-17	903	2.2							-58.39	1031	0.994	Spinel
US-17	974	0.9										
US-17	999	0.6										
US-18	901	2.1							-60.62	1026	0.992	Spinel
US-18	954	1.1										
US-18	1005	0.4										
US-19	852	1.6							-118.03	1052	0.950	Spinel
US-19	954	1										
US-19	1007	0.3										
US-20	852	1.5							-97.09	1006	0.954	Spinel
US-20	902	1.2										
US-20	954	0.5										
US-21	852	2.2							-96.13	1071	0.987	Spinel
US-21	902	1.8										
US-21	954	1.3										
US-21	1007	0.6										
US-22	852	3.6							-53.81	1050	0.977	Spinel
US-22	895	2.7										
US-22	902	3										
US-22	1007	0.8										
US-23	852	1.4							-129.25	1032	1.000	Spinel
US-23	902	1										
US-23	954	0.6										
US-23	1007	0.2										

Glass	Temp. (°C)	Trev.	Neph.	NiO	Nos.	Zirc.	Hem.	Li_2SiO_3	Slope	Int.	R^2	Prim. Ph.
US-24	852	2.8							-58.55	1024	0.987	Spinel
US-24	902	2.2										
US-24	954	1.3										
US-24	1007	0.2										
US-25	954	1.9							-61.79	1074	0.986	Spinel
US-25	994	1.4										
US-25	1007	1										
US-25	1056	0.3										
US-26	855	1.3							-236.29	1167	0.967	Spinel
US-26	903	1.2										
US-26	952	0.8										
US-26	1107	0.3										
US-27	903	1.2							-153.00	1077	0.959	Spinel
US-27	952	0.7										
US-27	1056	0.2										
US-28	752	1			0.6		0.2		-61.11	813	1.000	Spinel
US-28	807	0.1			0.9							
US-29	903	1					0		N/A	N/A	N/A	Spinel(OP)
US-29	700	1			0.7		0.2					
US-30	855	1.4				0.1			-277.91	1251	0.996	Spinel
US-30	952	1.1				0.2						
US-30	1006	0.9										
US-30	1056	0.7										
US-30	1107	0.5										
US-31	903						5.6		-39.59	1125	1.000	Hematite
US-31	952						4.4					
US-31	1006						3					
US-32	704	0.1							N/A	N/A	N/A	Spinel(OP)
US-32	731	0.1										
US-33	854	1			1.9				-163.33	1017	1.000	Spinel
US-33	902	0.7			1.5							
US-33	952	0.4										
US-34	828	11.2							N/A	N/A	N/A	Spinel(OP)
US-34	854											
US-34	902											
US-35	952	3.6							-114.02	1310	0.880	Spinel
US-35	1007	2										
US-35	1205	0.8										
US-35	1247	0.7										
US-35	1328	0.4										
US-35	1017	2.7										
US-35	1074	1.4										
US-35	1218	0.6										
US-35	1278	0.4										

Glass	Temp. (°C)	Trev.	Neph.	NiO	Nos.	Zirc.	Hem.	Li_2SiO_3	Slope	Int.	R^2	Prim. Ph.
US-35	1301	0.3										
US-36	902	1.9							-196.84	1253	0.804	Spinel
US-36	952	1.2										
US-36	1007	0.8										
US-36	1199	0.4										
US-36	1205	0.5										
US-36	1000	1.5										
US-36	1098	0.7										
US-36	1164	0.6										
US-37	854	2.3	3.9						-80.59	1036	0.996	Spinel
US-37	902	1.6										
US-37	952	1										
US-37	1007	0.4										
US-38	854	2.6		0.4	0.7				-71.32	1038	0.968	Spinel
US-38	902	1.7		0.5								
US-38	952	1.4		0.7								
US-38	1007	0.4		1.1								
US-39	854	5.4							-46.68	1105	0.999	Spinel
US-39	902	4.3				0.2						
US-39	952	3.3				0.3						
US-39	1007	2.1				0.2						
US-41	855						3.7		-49.04	1046	0.982	Hematite
US-41	905						3.1					
US-41	956						1.9					
US-41	1008						0.7					
US-42	925	3.1	35.3						-36.56	1037	0.982	Spinel
US-42	1035	0.3										
US-42	1017	0.4										
US-42	1000	0.9										
US-43	895	2.6				1.5		4.1	-217.69	1245	0.910	Zircon
US-43	994	0.8				1.3		2.1				
US-43	1085					0.7		0.7				
US-44	905	1							-203.42	1112	0.988	Spinel
US-44	956	0.8										
US-44	1008	0.5										
US-45	905	0.8							-203.42	1072		Spinel
US-45	956	0.6										
US-45	1008	0.3										

Appendix C

Report on Fabrication and Testing of KRI Test Matrix Glasses
(SRNS-OS-2008-00001)

Subcontract AC 55551T

Task 6:

Improved Retention of Aluminum, Chromium, and Sulfate in U.S. Waste Glasses

Deliverable 6 on Sub-Task T6-12a

Report on Fabrication and Testing of KRI Test Matrix Glasses

(crucible scale)

S. Petersburg
2007

TABLE OF CONTENTS

LIST OF ABBREVIATIONS

HLW	High-level waste
U.S. DOE	United States Department of Energy
KRI	Khlopin Radium Institute
DWPF	Defense Waste Processing Facility at Savannah River Site
WTP	Waste Treatment Plant at Hanford
SNF	spent nuclear fuel
PNNL	Pacific North-West National Laboratory
SRNL	Savannah River National Laboratory
EPMA	electron probe microanalysis
PCT	product consistency test (glass leach tests for B, Li, Na, and SI leaching)
XRDA	X-ray diffraction analysis
SEM	scanning electron microscopy
TCLP	Toxicity Characteristics Leaching Procedure
CCC	Canister Centerline Cooling
TC	thermocouple

Introduction

The U.S. Department of Energy (DOE) is currently processing (or planning to process) high-level waste (HLW) through Joule-heated melters at the Savannah River Site (SRS) and Hanford. The process combines the HLW sludge with a prefritted or mined mineral glass forming additives which are subsequently melted and pouring the molten glass in stainless steel canisters to create the final waste form.

Development of strategies at both the SRS and Hanford have identified high Al_2O_3 waste streams that are scheduled to be processed through their respective HLW vitrification facilities. These streams have Al_2O_3 concentrations between approximately 25 – 40 wt. %, Na_2O - between ~ 22 – 26 wt%, and SO_4 - between ~ 0.8 – 1.6 wt. Current Hanford projections suggest the Al_2O_3 concentrations in sludge could be much greater than those currently projected for DWPF with Al_2O_3 concentrations as high as 80 wt%

While it is well known that the addition of small amounts of Al_2O_3 to borosilicate glasses generally enhances the durability of the waste form (through creation of network-forming tetrahedral Na^+-$[AlO_{4/2}]^-$ pairs), nepheline ($NaAlSiO_4$) formation, which depends in part on the Al_2O_3 content, can result in a severe deterioration of the chemical durability of the slowly cooled glass near the center of the canister through residual glass compositional changes. The primary driver for the reduction in durability is the fact that nepheline removes three moles of glass forming oxides (Al_2O_3 and $2SiO_2$) per each mole of Na_2O from the continuous glass phase. Therefore, nepheline formation produces an Al_2O_3 and SiO_2 deficient continuous glass matrix (relative to the same composition which is void of crystals) which reduces the durability of the final product. The magnitude of the reduction ultimately depends on the extent (e.g., volume %) of crystallization and on the initial glass composition.

The formation of nepheline and/or other aluminum/silicon-containing crystals is a potential for both DWPF and Hanford due to the projected compositional views recently evaluated coupled with the frit development strategy (e.g., higher alkali frits have lead to enhanced melt rates at DWPF for those sludge batches). Although durability is obvious a critical constraint that the HLW glass must meet, other process related issues are equally important. Additionally, the addition of higher concentrations of Al_2O_3 will generally increase the liquidus temperature of the melt and decrease the processing rate.

The objective of this task is to develop glass formulations for specific DOE waste streams to avoid nepheline formation while maintaining or meeting waste loading and/or waste throughput expectations as well as satisfying critical process and product performance related constraints. Secondary objectives of this are to assess the SO_4 solubility limit for the DWPF composition and spinel settling for the PNNL composition.

1. Fabrication of Glasses under Laboratory Conditions (Crucible Scale)

Thirty glass compositions were selected for studies at KRI, and all these glass compositions were synthesized with appropriate ratios of metal oxides, carbonates, H_3BO_3, and salts to assure sufficient quantities for subsequent testing (usually ~ 300 grams).
Table 1 lists chemicals that were utilized for feed preparation. The original materials were thoroughly mixed and placed into a platinum crucible. The crucible was then placed into a muffle furnace to be heated to 1,150°C. After being isothermically held at 1,150°C for two hours, the glass was poured onto a clean stainless steel plate for quenching.

Fig. 1 shows a photograph of KRI-07 glass being poured from the Pt crucible. Fig. 2 shows a cooled glass on the stainless steel plate. Table 2 provides compositions of the synthesized glasses.

Table 1. Oxides and Chemicals Utilized for Feed Preparation

Oxides	Chemicals	Grade
Al_2O_3	$Al(OH)_3$	Pure for analysis
B_2O_3	H_3BO_3	Chemically pure
CaO	CaO	Pure for analysis
Cr_2O_3	Cr_2O_3	Pure
Fe_2O_3	Fe_2O_3	Pure for analysis
K_2O	K_2CO_3	Chemically pure
Li_2O	Li_2CO_3	Chemically pure
MgO	MgO	Chemically pure
MnO	MnO_2	Pure
Na_2O	Na_2CO_3	Chemically pure
NiO	NiO	Pure
PbO	PbO	Pure for analysis
SO_3	Na_2SO_4	Chemically pure
SiO_2	SiO_2	Pure
SrO	$SrCO_3$	Pure for analysis
TiO_2	TiO_2	Pure
ZnO	ZnO	Pure
ZrO_2	ZrO_2	Pure

Fig. 1. Glass pouring

Fig.2. Quenched glass

Table 2. Compositions of Synthesized Glasses

		Al2O3	B2O3	CaO	Cr2O3	Fe2O3	K2O	Li2O	MgO	MnO	Na2O	NiO	PbO	SO3	SO4	SiO2	SrO	TiO2	UO3	ZnO	ZrO2
US-08	**KRI-01**	15.196	9.557	0.000	0.000	9.749	1.000	4.865	0.000	2.438	9.816	0.001	0.099	0.499	0.599	45.781	0.000	1.000	0.000	0.000	0.000
US-19	**KRI-02**	14.476	14.404	0.700	0.069	8.230	0.777	3.638	0.333	1.988	10.804	0.209	0.070	0.277	0.333	42.817	0.061	0.805	0.000	0.067	0.275
US-20	**KRI-03**	14.476	14.404	0.700	0.069	8.230	0.777	3.638	0.333	1.988	10.804	0.209	0.070	0.277	0.333	42.817	0.061	0.805	0.000	0.067	0.275
US-24	**KRI-04**	14.499	12.252	0.749	0.081	7.789	0.749	3.001	0.374	2.249	11.576	0.501	0.079	0.374	0.449	44.441	0.079	0.749	0.000	0.079	0.379
US-35	**KRI-05**	10.018	19.962	1.000	0.518	11.354	0.000	2.000	0.500	4.000	7.943	0.000	0.000	0.000	0.000	38.003	2.703	0.000	0.000	2.000	0.000
US-44	**KRI-06**	12.805	12.589	0.555	0.305	8.862	0.640	4.050	0.253	1.834	12.731	0.359	0.667	0.222	0.267	39.556	1.620	0.465	0.000	1.024	1.464
US-45	**KRI-07**	12.805	12.589	0.555	0.305	8.862	0.640	4.050	0.253	1.834	12.731	0.359	0.667	0.222	0.267	39.556	1.620	0.465	0.000	1.024	1.464
	KRI-08	12.694	16.250	0.250	0.467	8.000	0.750	3.000	0.380	3.000	10.029	0.812	0.750	0.130	0.156	39.487	0.750	0.750	0.000	1.500	1.000
	KRI-09	13.309	14.337	0.250	0.405	8.000	0.250	3.000	0.380	1.000	11.208	0.750	0.750	0.130	0.156	40.231	0.750	0.750	0.000	1.500	3.000
	KRI-10	12.500	9.378	0.750	0.610	8.000	0.750	3.112	0.130	1.143	12.803	0.750	0.250	0.130	0.156	45.583	1.789	0.250	0.000	1.072	1.000
	KRI-11	15.785	13.987	0.251	0.251	9.910	0.447	4.083	0.131	1.002	10.664	0.751	0.251	0.131	0.157	39.851	0.751	0.251	0.000	0.501	1.001
	KRI-12	12.817	14.089	0.750	0.256	8.483	0.750	3.875	0.130	3.000	9.086	0.870	0.250	0.130	0.156	39.514	2.250	0.250	0.000	0.500	3.000
	KRI-13	12.500	10.788	0.251	0.389	8.000	0.750	3.000	0.130	3.000	11.795	0.750	0.750	0.380	0.456	41.520	0.750	0.750	0.000	1.500	2.997
	KRI-14	13.117	15.460	0.250	0.345	8.000	0.250	5.000	0.380	3.000	8.764	1.097	0.750	0.380	0.456	39.286	0.750	0.750	0.000	1.422	1.000
	KRI-15	16.235	13.682	0.250	0.251	8.001	0.750	3.317	0.131	1.109	10.355	0.751	0.551	0.331	0.397	41.565	0.770	0.250	0.000	0.702	1.000
	KRI-16	12.500	8.750	0.250	0.250	8.000	0.250	4.922	0.130	1.000	9.016	0.750	0.750	0.380	0.456	46.250	2.250	0.750	0.000	1.500	2.302
	KRI-17	12.859	12.399	0.750	0.250	8.591	0.366	3.882	0.380	1.821	10.328	0.751	0.377	0.380	0.456	40.866	2.250	0.250	0.000	0.500	3.000
	KRI-18	13.383	14.830	0.750	0.318	8.913	0.547	3.521	0.131	2.031	10.365	0.830	0.750	0.380	0.456	38.750	0.750	0.250	0.000	0.500	3.000
	KRI-19	13.536	11.125	0.250	0.353	9.810	0.250	4.371	0.130	3.000	12.513	1.032	0.250	0.130	0.156	38.750	2.250	0.750	0.000	0.500	1.000
	KRI-20	14.404	14.791	0.750	0.322	8.645	0.250	3.000	0.380	1.000	11.618	0.781	0.750	0.130	0.156	39.181	2.250	0.250	0.000	0.500	1.000
	KRI-21	13.516	11.831	0.750	0.263	9.063	0.437	3.293	0.207	1.267	12.592	1.050	0.470	0.380	0.456	40.171	0.820	0.320	0.000	0.570	3.000
	KRI-22	15.745	11.519	0.250	0.250	8.000	0.250	5.000	0.130	1.000	11.078	0.751	0.250	0.380	0.456	38.897	2.250	0.750	0.000	0.500	3.000
	KRI-23	16.262	12.599	0.250	0.252	8.001	0.250	3.000	0.352	1.000	12.204	0.751	0.250	0.380	0.456	40.948	0.750	0.250	0.000	1.500	1.000
	KRI-24	12.653	9.693	0.749	0.251	8.304	0.749	3.767	0.131	1.883	10.236	0.751	0.749	0.379	0.455	43.724	1.177	0.607	0.000	1.198	2.999
	KRI-25	15.058	13.510	0.282	0.251	11.231	0.683	3.750	0.131	1.118	11.510	0.751	0.251	0.187	0.224	38.785	0.751	0.251	0.000	0.501	1.001
	KRI-26	10.480	10.193	1.000	0.000	11.141	0.000	6.000	0.000	0.000	13.542	3.000	0.000	0.500	0.600	39.588	3.000	0.000	1.557	0.000	0.000
	KRI-27	10.440	17.200	1.000	0.847	9.870	0.000	5.733	0.500	0.659	10.229	0.468	1.000	0.500	0.600	35.562	0.000	1.000	0.992	0.000	4.000
	KRI-28	18.349	6.126	0.000	1.000	5.000	0.000	5.718	0.000	3.854	18.520	0.000	1.000	0.500	0.600	36.504	0.000	1.000	2.429	0.000	0.000
	KRI-29	14.268	11.383	0.000	0.000	5.646	1.000	2.000	0.500	0.000	20.000	3.000	1.000	0.000	0.000	35.000	2.203	1.000	3.000	0.000	0.000
	KRI-30	20.000	15.297	0.750	0.000	5.511	0.000	5.794	0.500	0.000	7.238	0.000	1.000	0.500	0.600	35.736	3.000	0.000	2.675	2.000	0.000

2. Research and Data Processing Methods

2.1 X-Ray Diffraction Analysis (XRDA)

For XRD analysis, KRI used the DRON-UM1 diffractometer with CuK_α irradiation. The X-ray tube had the voltage of 35 kV and the current of 2 mA. JCPDS data sets were used to assure a high quality analysis.

KRI used the PDWIN software application for a quantitative analysis of crystalline phases, i.e., sample analysis with the known mass absorption coefficient. Magnetite (Fe_3O_4) with the spinel structure, α-quartz (SiO_2), and nepheline ($NaAlSiO_4$) were used as standard phases.

Since the sensitivity of the XRD method for identifying spinel was, in our case, 1 mass %, we used SEM photographs for evaluating the spinel content in those glass samples that contained less than 1 mass % of spinel. This analysis is shown below using KRI-15 sample as an example.

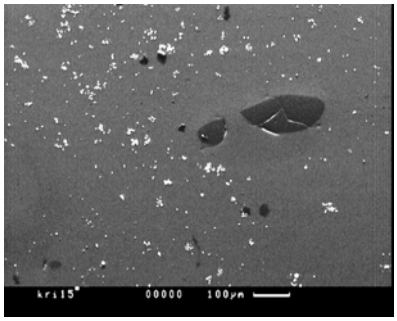

Fig. 3. Original image. White inclusions – spinel. Magnification ~1000x

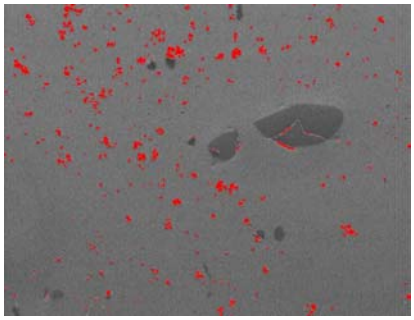

Fig. 4. Digitized image. Red dots are spinel.

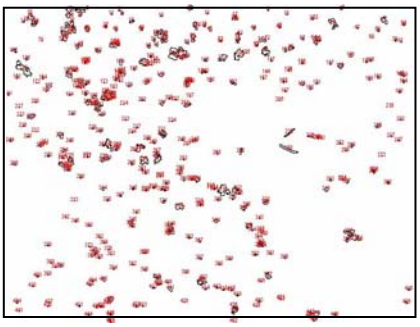

Fig. 5. Processed image with each spinel particle recorded and numbered

Image Analysis Results: quantity of particles: 453; total Area: 16,102.97 μm^2; average size: 35.55 μm^2; area fraction: 2.14%. For statistics**:** processing of another photograph of the same sample gives 2.11% of the area fraction. We used a similar technique for evaluating all compositions that contained crystalline phase spinel inclusions.

2.2 Chemical and Phase Composition Glass Homogeneity Studies

For glass homogeneity studies, we applied scanning microscopy and electron probe microanalysis (EPMA) using CAMSCAN-4DV with the semiconductor spectrometer LINK AN-10000 (UK). The studies included the following phases:

1. Prepare glass samples. We polished glass sample fragments and coated them with carbon to create a conductive layer using a carbon rod thermal evaporation method.
2. Evaluate glass sample homogeneity and inclusions by analyzing scanning microscopy images in back scattered electrons. The phases with a higher atomic number could be seen as lighter

phases, e.g., spinel inclusions in glass. Obtained images could be recorded as colored photographs with magnification from x20 to x10000.

3. Perform electron probe microanalysis to determine glass chemical composition with the detection limit of about 0.1 mass % for most elements. The area analysis with the minimal magnification of x20 gives an average glass composition in the area of a few mm^2. To analyze sample homogeneity, we analyzed 5 sample areas, 0.01 mm^2 each. For major macroelements, we calculated mean square deviations associated with non-homogeneity (Er). We determined the non-homogeneity coefficient as the ratio of Er and the measurement error (Re). If Er/Re <2, the element distribution in the sample bulk was considered homogenous.

3. Chemical and Phase Composition Glass Homogeneity Studies

Using XRD, SEM, and EPMA, KRI studied the following characteristics of the synthesized glasses: homogeneity, chemical and phase compositions . Attachments 1, 2, and 3 contain data obtained by using EPMA, SEM, and XRD for the KRI matrix glasses from KRI-1 through KRI-30.

Table 3 provides phase compositions of the synthesized glasses and their crystalline phases determined by using XRD and SEM. Table 4 contains chemical compositions of the spinel in glass samples KRI-05, KRI-08, KRI-09, KRI-10, and KRI-11. As KRI-08 and KRI-09 shows, the same glass can have spinels of various chemical compositions.

Table 3. Phase Compositions of Quenched KRI Glasses

Sample #	Crystalline phase, XRD	Content, mass %, XRD	Content, vol.%, SEM	Size, , μm
KRI–01	n/d	n/d	–	–
KRI–02	n/d	n/d	–	–
KRI–03	n/d	n/d	–	–
KRI–04	n/d	n/d	–	–
KRI–05	spinel	3.5	2.8	1.2
KRI–06	n/d	n/d	–	–
KRI–07	n/d	n/d	–	–
KRI–08	spinel	1.5	6.6	11
KRI–09	spinel	2.4	1.5	13
KRI–10	n/d	n/d	0.9	2.2
KRI–11	spinel	3	2.5	4.3
KRI–12	spinel	2	1.2	15.8
KRI–13	spinel	2	2.2	11.3
KRI–14	spinel	2.5	1.5	12.3
KRI–15	spinel	3.5	2,7	9.5
KRI–16	n/d	n/d	0,5	2.8
KRI–17	n/d	n/d	0,91	2.8
KRI–18	spinel	2.5	2.3	10.0
KRI–19	n/d	n/d	0,2	10
KRI–20	n/d	n/d	0,34	5.9
KRI–21	n/d	n/d	0,6	8.5
KRI–22	n/d	n/d	0,2	7.3
KRI–23	spinel	3.2	2,8	7.6
KRI–24	n/d	n/d	0,58	7.7
KRI–25	n/d	n/d	0,78	6.1
KRI–26	n/d	n/d	n/d	–
KRI–27	spinel	1	0.8	4.2
KRI–28	n/d	n/d	–	–
KRI–29	n/d	n/d	–	–
KRI–30	n/d	n/d	–	–

Table 4. Spinel Chemical Compositions (mass %) in Quenched KRI Matrix Glasses (EPMA Data)

	Al2O3	Cr2O3	FeO	Fe2O3	MnO	NiO	TiO2	ZnO	Total
KRI-05 SP1	10.09	17.81	41.70		16.53	0.00	0.00	13.57	99.79
KRI-08 SP1	1.13	7.89	1.63	60.09	17.83	0.00	0.00	11.45	100.03
KRI-08 SP2	10.09	17.81	42.29		16.04	0.00	0.00	13.57	99.79
KRI-09 SP1	2.08	13.01	1.19	50.43	4.13	21.00	0.67	6.72	99.24
KRI -09 SP2	2.27	25.15	2.60	38.86	3.49	16.80	0.00	9.83	98.99
KRI-09 SP3	3.84	7.35	54.96		5.25	20.97	0.71	6.66	99.74
KRI -09 SP4	3.97	8.04	54.36		4.52	20.36	0.83	7.22	99.30
KRI -09 SP5	3.78	3.51	58.72		4.91	21.63	0.83	5.35	98.73
KRI-10 SP1	1.32	28.95	2.14	36.08	4.13	20.23	0.00	5.73	98.59
KRI-10 SP2	1.51	35.09	2.42	30.90	4.52	18.33	0.00	7.84	100.62
KRI-11 SP1	3.02	2.34	65.29		3.10	20.36	0.00	2.24	96.35

The content of the "critical elements" in the generated spinels with the gross formula $(Fe,Ni,Mn,Zn)(Fe,Cr,Al)_2O_4$ depends on the glass composition [1]. The presence of spinel crystals of various compositions in one glass can be explained by their crystallization at various temperatures during cooling of the original melt [2].

4. CCC Testing of KRI Matrix Glasses

4.1 CCC Testing and Determination of Phase Compositions for KRI Matrix Glasses

All synthesized glasses were tested for their resistance to crystallization using heat treatment to simulate cooling along the centerline of a Defense Waste Processing Facility (DWPF)-type canister. This cooling regime is commonly referred to as the canister centerline cooled (CCC) curve.

According to the recommendations, we placed the Pt crucibles with about 25 g glass samples in each crucible into the muffle furnace with an adjustable cooling/heating rate. Fig. 6 compares a temperature curve that we used in our experiments with the recommended full-scale canister cooling curve showing that our cooling curve matches the baseline fairly well.

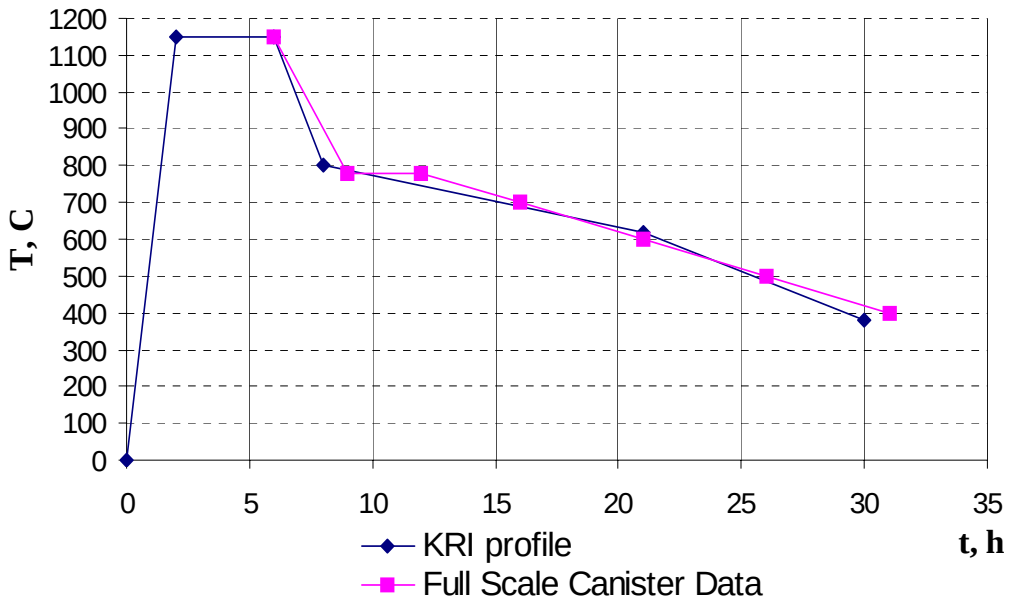

Fig.6. Thermal Heat Treatment Schedule to Simulate CCC Curve

Attachment 4 contains photographs of the glass sample surfaces after the CCC treatment. Table 5 provides visual descriptions of glass samples surfaces after the CCC treatment. Table 6 illustrates phase compositions of the CCC treated glasses, and Table 7 gives data on chemical compositions of the spinels resulting from the CCC treament. Attachment 5 contains microphotogprahs of the same samples. Attachment 6 provides data on the chemical homogeneouty obtained by EPMA. Attachment 7 contains XRD patterns of the CCC treated glasses.

Table 5. Description of CCC Treated Glass Samples

Sample #	Surface	Bulk
KRI-01	Smooth surface, semi-dull gloss, several star-shaped silver white crystals from 0.1 to 0.3 mm	Glassy shine, conchoidal transparent cross-section, several star-shaped silver white crystals from 0.1 to 0.3 mm
KRI-02	Cell-like surface, semi-dull gloss, a few star-shaped silver white crystals from 0.1 to 0.2 mm мм (more than in KRI-01)	Glassy shine, non-transparent cross-section, brown unevenly distributed color
KRI-03	Large cell-like surface, semi-dull gloss, silver white crystals throughout almost the entire surface	Glassy shine, no crystals, conchoidal transparent cross-section
KRI-04	Large cell-like surface, semi-dull gloss, silver white crystals from 0.1 to 0.4 mm throughout the entire surface, a thin torn gray film	Glassy shine, non-transparent cross-section, uneven brown color. No new formations
KRI-05	Small cell-like even surface, matte gloss, no new formations	Dull gloss, non-transparent cross section, no new formations
KRI-06	Large cell-like surface, semi-dull gloss, silver white crystals from 1 to 2 mm	Glassy shine, conchoidal transparent cross-section, no new formations
KRI-07	Large cell-like surface, semi-dull gloss, silver white crystals throughout almost the entire surface	Conchoidal transparent cross-section, semi-dull gloss, no new formations
KRI-08	Small cell-like even surface, semi-dull gloss, tiny silver white crystals (< 0.01 mm) throughout the entire surface	Non-transparent cross section, a radial seam on the cross-section, semi-dull gloss, tiny (<0,01 mm) crystals
KRI-09	Small cell-like surface, semi-glassy shine, tiny (< 0.01 mm) silver white crystals throughout the entire surface	Conchoidal non-transparent cross-section, semi-dull gloss, tiny (<0,01мм) crystals
KRI-10	Fibrous surface, glassy shine, few silver white crystals (0.1-0.2 mm)	Conchoidal cross-section with a radial seam. Tiny (<0.01mm) silver white crystals on the cross section radius
KRI-11	Small cell-like even surface, semi-glassy shine, tiny (< 0.01 mm) silver white crystals on the entire surface	Semi-dull gloss, small cell-like non-transparent cross-section, tiny (< 0.01 mm) silver white crystals are distributed throughout the entire bulk
KRI-12	Large cell-like surface, semi-dull gloss. Silver white crystal rounded agglomerations up to 8 mm in size are observed on 40% of the surface .	Semi-dull gloss, uneven color of the cross section (black inclusions in clear brown glass). Long (up to 50 mm) needle-like randomly oriented agglomerations
KRI-13	Small cell-like surface, semi-glassy shine, tiny (< 0.01 mm) silver white crystals on the entire surface	Small cell-like surface of the cross-section, tiny (< 0.01 mm) silver white crystals are distributed throughout the entire bulk
KRI-14	Small cell-like surface, semi-dull gloss, tiny (< 0.01 mm) silver white crystals on the entire surface	Semi-dull gloss, small cell-like non-transparent cross-section, tiny (< 0.01 mm) silver white crystals are distributed throughout the entire bulk
KRI-15	Most surface smooth, glassy shine, a thin gray film near the edge of the crucible, tiny (< 0.01 mm) silver white crystals on the entire surface	Semi-dull gloss, small cell-like non-transparent cross-section, tiny (< 0.01 mm) silver white crystals are distributed throughout the entire bulk
KRI-16	Illarge cell-like surface, uneven color of the glass, black dented inclusions in the brown glass, tiny crystals in the dents. 20% of the surface is covered with silver white crystalline round agglomerates up to 50 mm in size	Glassy shine, conchoidal transparent cross section, no new formations observed
KRI-17	Uneven surface, dull gloss, practically all surface is covered with a gray film	Non-transparent small cell-like cross-section, no crystals observed

KRI-18	Large cell-like surface, semi-glassy shine, 10-15% of the surface is covered with unevenly distributed separate white rounded crystalline agglomerates	Conchoidal cell-like cross-section, crystals (< 0.01 mm) are evenly distributed in the bulk and located in the cells
KRI-19	Large cell-like surface, glassy shine, tiny crystals are observed on the bottom of the cells. 10% of the surface is covered with few silver white crystalline rounded agglomerates	Glassy shine, conchoidal cell-like cross-section, Crystals (< 0.01 mm) are evenly distributed in the bulk.
KRI-20	Cell-like surface, semi-dull gloss, tiny (<0.01 mm) silver white crystals on the surface .	Semi-glassy shine, small cell-like transparent cross-section, tiny (<0.01 mm) silver white crystals are distributed in the entire bulk
KRI-21	Large cell-like surface, semi-dull gloss, tiny crystals on the bottom of the cells, 40% of the surface is covered with few silver white round crystalline agglomerates (10 mm in size), Uneven color of the glass. Black inclusions on the brown glass	Semi-glassy shine, small cell-like cross-section, tiny (<0.01 mm) silver white crystals are distributed throughout the entire bulk
KRI-22	Large cell-like surface, semi-dull gloss, small crystals on the bottom of the cells. Dense crystalline agglomerates (10 mm in size) occupy 50% of the surface	Semi-glassy shine, small cell-like transparent cross-section, tiny (<0.01 mm) silver white crystals are distributed in the entire bulk
KRI-23	Most of the surface is smooth, glassy shine, a torn thin gray film near the edge of the crucible. Tiny (<0.01 mm) silver white crystals are evenly distributed on the surface	Semi-glassy shine, small cell-like transparent cross-section, tiny (<0.01 mm) silver white crystals are distributed in the entire bulk
KRI-24	Large cell-like surface, glassy shine, tiny crystals on the bottom of the cells, 20% of the surface is covered with a few silver white crystalline round agglomerates	Semi-glassy shine, small cell-like transparent cross-section, tiny (<0.01 mm) silver white crystals are distributed in the entire bulk
KRI-25	Small cell-like surface. Glassy shine, crystals of various sizes on the bottom of the cells	Semi-glassy shine, small cell-like transparent cross-section, tiny (<0.01 mm) silver white crystals are distributed in the entire bulk
KRI-26	80% of the surface is covered with silver white crystals of various shapes. Needle-like 0.01-1 mm long round crystalline agglomerates	Semi-glassy shine, small cell-like transparent and uneven cross-section, tiny (<0.01 mm) silver white crystals are distributed in the entire bulk
KRI-27	Glassy shine, silver white unevenly distributed crystals (0.01 – 0.5 mm)	Semi-glassy shine, small cell-like transparent cross-section, tiny (<0.01 mm) silver white crystals are distributed in the entire bulk
KRI-28	Homogenous dense silver-colored film covers the surface from the edge to the center of the crucible. There is an irregularly shaped area (0.8 – 0.5 cm) in the center covered with a less dense film. Greenish crystals are observed on the border of the area. Caverns are observed in the area, with greenish crystals on the edges.	Dull gloss, uneven color
KRI-29	Uneven surface completely covered with a loose murky film.	Dull gloss, small (0.01 mm) and large (10 mm) tan inclusions are observed.
KRI-30	Large cell-like surface, with the cells evenly distributed on the surface. There is a three-pointed star-shaped crystal (0.1 – 0.5 mm) on the bottom of each cell. Dark gray and brown spots are observed in the bulk in the center of the crucible	Glassy shine, uneven color (brown and black)

Table 6. Phase Compositions of CCC Treated KRI Matrix Glasses

Sample #	Crystalline phase, XRD	Content, mass %, XRD	Content, vol. .%, SEM	Size, μm
KRI-01	--	< 1	0.3	
KRI-02	spinel	1	0.8	
KRI-03	--	< 1	0.2	
KRI-04	--	< 1	0.3	
KRI-05	spinel	8	7.3	8.8
KRI-06	spinel	1.5	1.2	
KRI-07	spinel	<1	0.2	
KRI-08	spinel	15	15	15
KRI-09	spinel	4	3.1	5.1
KRI-10	spinel	<1	0.94	4.1
KRI-11	spinel	6	5.3	3.7
KRI-12	spinel	3	2.5	1.0
KRI-13	spinel	3.5	2.8	11.3
KRI-14	spinel	4.5	3.8	12.3
KRI-15	spinel	5	4.3	9.5
KRI-16	spinel	1	0.6	3.3
KRI-17	spinel	3	2.0	3.2
KRI-18	spinel	3.5	3.6	10.2
KRI-19	spinel	3	2.3	32.5
KRI-20	spinel	3	2.6	17.7
KRI-21	spinel	3.5	2.5	14.0
KRI-22	spinel	3	2.8	4.7
KRI-23	spinel	3	2.6	11.1
KRI-24	spinel	4	3.5	5.0
KRI-25	spinel	2	2.2	25.0
KRI-26	spinel	6	4.5	16.5
KRI-27	spinel	2	1.9	27.0
KRI-28	nepheline $NaAlSiO_4$ (#19-1176) Li_2SiO_3 (#29-828) $Na_8Al_6Si_6O_{24}SO_4$ (#21-1099) spinel	40 33 24 3		
KRI-29	nepheline $NaAlSiO_4$	10	2.0	10.2
KRI-30	spinel	3	1.4	10.9

Table 7. Chemical Compositions of Spinels (mass %) in CCC Treated KRI Matrix Glasses (EPMA Data)

Sample	TiO2	Al2O3	FeO	Fe2O3	Cr2O3	NiO	ZnO	MnO	Total
KRI-11 SP	nd	2.08	8.58	44.36	19.44	16.67	3.24	3.10	97.48
2 SP	nd	nd	7.84	51.34	14.47	16.29	2.99	3.75	96.67
KRI-12 SP	nd	nd	0.00	50.47	15.20	21.25	1.87	7.88	96.67
2 SP	nd	nd	0.00	58.62	6.43	22.78	1.49	7.24	96.56
KRI-13 SP	nd	nd	0.00	39.32	23.68	15.02	7.34	9.69	95.05
2 SP	0.67	nd	0.00	38.03	24.27	14.38	7.84	9.82	95.01
KRI-14 SP	0.50	2.08	0.66	41.44	21.20	19.34	5.48	6.85	97.55
2 SP	nd	2.46	1.84	37.99	25.00	16.93	6.47	6.72	97.40
KRI-16 SP	3.17	6.43	0.00	52.18	1.02	24.94	5.85	5.43	99.03
2 SP	1.67	nd	0.00	58.19	3.36	28.00	3.61	2.97	97.80
KRI-17 SP	0.67	1.89	53.80	0.00	1.46	25.45	1.99	7.11	92.37
2 SP	nd	2.84	2.19	51.18	12.13	22.78	1.62	5.17	97.91
KRI-18 SP	nd	2.08	0.00	55.90	6.29	23.42	1.37	8.27	97.32
2 SP	0.50	1.89	0.00	53.19	7.89	23.29	1.87	8.40	97.03
KRI-19 SP	0.50	1.70	0.00	53.90	9.80	23.16	1.74	7.49	98.30
2 SP	0.67	1.89	0.00	57.62	3.22	24.56	1.37	8.40	97.72
3 SP	1.17	nd	0.00	57.76	3.51	23.67	1.62	8.79	96.51
KRI-20 SP	nd	2.08	3.71	43.20	20.91	22.40	2.86	2.97	98.13
2 SP	nd	nd	3.39	42.13	23.83	22.14	2.86	2.97	97.33
KRI-21 SP	nd	nd	1.15	49.33	16.96	24.94	1.74	3.49	97.62
2 SP	nd	nd	0.28	59.59	7.02	27.11	0.87	2.97	97.84
3 SP	nd	nd	1.25	51.65	14.62	25.07	1.87	3.10	97.56
KRI-22 SP	0.83	nd	0.00	59.91	4.97	28.25	1.74	2.45	98.16
2 SP	2.50	2.08	0.00	56.19	1.46	31.56	1.37	3.10	98.26
KRI-23 SP	nd	3.02	1.88	47.66	15.50	22.78	3.61	3.88	98.33
2 SP	nd	3.21	3.24	48.16	14.62	21.76	3.11	3.88	97.98
KRI-24 SP	0.67	nd	0.00	51.90	11.26	23.03	4.23	5.68	96.77
2 SP	0.83	1.51	0.00	57.05	4.39	25.32	2.99	5.68	97.78
KRI-25 SP	nd	1.70	5.33	47.69	17.40	21.00	2.37	3.23	98.71
2 SP	nd	nd	3.26	57.14	8.63	22.78	2.12	2.71	96.63

5. Liquidus Temperature (T_L) Measurements for KRI Matrix

5.1 Muffle Furnace Calibrations and T_L Measurements for SRM-773 Reference Standard

We used furnace UMEGA SNOL 7.2/1300 for liquidus (T_L) temperature measurements of the glass samples. This furnace was fabricated in December, 2006, and it meets the low-voltage (73/23/EEC) and electromagnetic compatibility (89/336/EEC) requirements of the Directives of the European Union. The dimensions of the working chamber are 284 x 208 x 112 mm. The furnace has five heating surfaces. Prior to T_L measurements, we calibrated the furnace consistence between the required heating temperature (t_1) and the actual temperature in the heat area (t_0).

For verification that the actual temperature in the work zone of the heat area of the furnace (t_0) matched the required heating temperature (t_1) (the temperature setting of the furnace controller), the certified reference standard thermocouple was placed inside the furnace along the axis of the heat area, with the hot junction point of the thermocouple being placed down from the axis (FIg. 7). The differences in the furnace temperature readings and the temperature values measured by the reference standard thermocouple (t_0) were recorded. In the temperature range of 850-1,200°C, the t_0-t_1 value remained constant and was equal to 8 ^{0}C. Upon reaching the required temperature, the holding time was approximately 10 hours.

To reduce the temperature gradient in the furnace, we used a Pt boat with the volume of approximately ~ 300 mL with a tightly fitting lid. The temperature gradient in the Pt boat was measured using temperature rings. For the temperatures of 850°C and 1050°C, we used rings PTCR-ETH manufactured by KEMA, dmc^2, For the temperature of 1150°C, we used rings PTCR-STH manufactured by KEMA, Ferro received from Dr. Alexander Fluegel, PNNL. Upon completion of the experiments, we measured the diameters of the rings and determined the temperature difference. The temperature field homogeneity inside the Pt boat was ±2°C, which was confirmed for different temperatures by the temperature rings placed into the Pt boat. Up to 8 Pt alloy crucibles with studied glass samples can be placed into the Pt boat.

The next phase of the furnace calibration was to determine T_L for the SRM773 glass reference standard. Fig. 7 shows Pt crucibles with lids containing the previously prepared standard samples placed into the Pt boat.

To prepare the standard samples, they were crushed, and a piece of the sample of approximately 3 grams with the particle size of 0.425-4.0 mm was taken for the measurements. This 3 g piece was triple washed with ethanol in the ultrasound bath and then dried. After drying, the glass was placed into the Pt crucible, and then into the Pt boat with a lid where the glass was held for 24 hours at the required temperature.

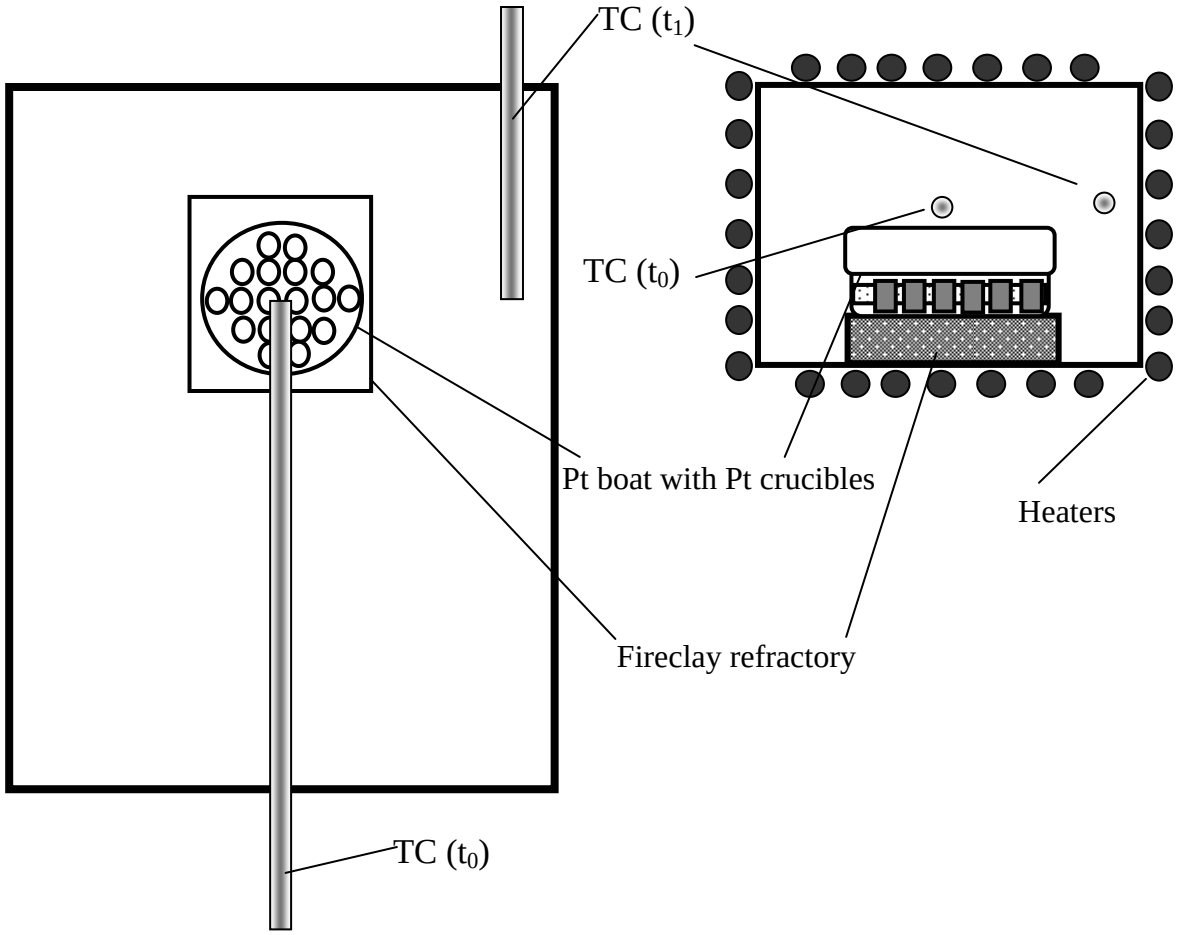

Fig. 7. Liquidus Temperature Measurements Using Pt Boat

Pt crucible

D= 23 mm

H= 8 mm

Glass mass = 3 grams

Fig. 8. View and Parameters of Pt Crucible

After holding for 24 hours followed by quenching, the glass samples were analyzed to determine the crystalline phase volume using SEM. To measure T_L, the SRM773 standard samples were held at the following temperatures: 1008°C, 989°C, and 981°C.

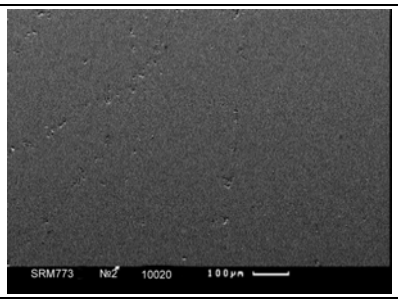

1008°C

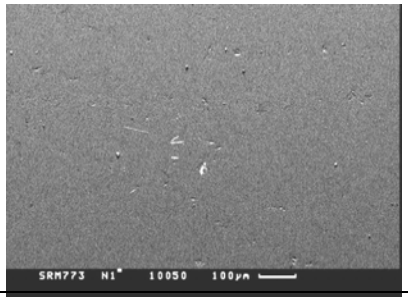

989°C

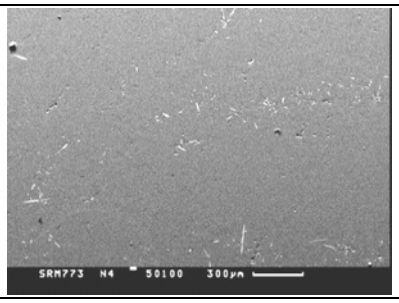

981°C

Fig. 9 Microphotos of SRM773 Standard Glasses Held at Various Temperatures

The SEM and XRD data showed that the SRM773 glass sample held at 1008°C had no inclusions and the glass was X-ray amorphous. According to the SEM, the SRM773 glass sample held at 989°C contained less than 0.1 vol.% of wollastonite. According to the SEM and XRD data, the SRM773 glass sample held at 981°C contained the crystalline phase of wollastonite, $CaSiO_3$. The average content of wollastonite was 0.7 vol.%.

Therefore, according to our experimental results, the liquidus temperature for the SRM773 standard glass was 989±2°C.

5.2 T_L Measurements for KRI Matrix Glasses

Table 8 provides SEM data on quantities of the primary crystalline phase (vol. %) at various heat treatment temperatures for KRI matrix glasses. The obtained data were used to establish the occurrence temperature interval and minimum temperature interval for T_L measurements. The minimum temperature interval (occurrence interval) was determined as the difference between two temperatures: the first is the temperature at which the glass has a crystalline phase, and the second is the temperature at which the glass is amorphous. Then the temperature occurrence interval was narrowed. For this purpose, the volume percentage of the crystalline phase formed within 24 hours of heat treatment at a certain temperature was measured. The analysis of quantities and types of crystalline particles in the glass at the minimal volume percentage of the generated crystalline phase made it possible to narrow the temperature interval to 10°C. (the minimum temperature interval). The liquidus temperature is defined as the temperature at which 1-3 crystalline particles are formed in the glass sample volume at the minimal volume percentage of the primary crystalline phase (less than 0.1 vol. %). The liquidus temperatures are given in Table 9.

The data show that for KRI-01, KRI-02, KRI-03, KRI-06, KRI-07, KRI-28,, and KRI-30, the T_L values are in the range of 958-1100°C. Samples KRI-05, KRI-08, KRI-09, KRI-10, KRI-13, KRI-15, and KRI-23 have high T_L values in the range of 1180-1270°C. For the remaining compositions, T_L values exceeded the melting temperature (1150°C) by 10-20 degrees C.

Table 8. Primary Crystalline Phase in KRI Matrix Glasses after CCC Treatment

	Spinel content, vol. %, SEM										
	1258^{0}C	1208^{0}C	1183^{0}C	1158^{0}C	1133^{0}C	1108^{0}C	1083^{0}C	1058^{0}C	1033^{0}C	1008^{0}C	**958^{0}C**
KRI-01	-	-	-	-	-	0.0	-	0.0	0.0	0.04	0.23
KRI-02	-	-	-	-	-	0.0	0.0	0.07	0.69	-	-
KRI-03	-	-	-	-	-	0.0	0.0	0.03	0.37	-	-
KRI-04	-	-	-	0.0	0.0	0.13	0.58	0.66	-	-	-
KRI-05	0.17	0.24	-	0.31	-	-	-	-	-	-	-
KRI-06	-	-	-	0.0	-	0.0	0.14	0.73	1.12	-	-
KRI-07	-	-	-	0.0	-	0.0	0.0	0.08	0.24	-	-
KRI-08	-	0.0	0.0	0.28	-	-	-	-	1.12	-	-
KRI-09	-	0.0	0.15	0.70	-	-	-	-	-	-	-
KRI-10	0.0	1.12	-	1.25	-	1.50	1.61	-	-	-	-
KRI-11	-	0.0	0.0	0.06	-	0.65	-	0.68	-	-	-
KRI-12	-	0.0	0.0	0.13	-	-	-	-	1.95	-	-
KRI-13	-	0.0	0.04	0.42	-	-	-	1.55	-	-	-
KRI-14	-	0.0	0.0	0.38	-	-	-	-	1.42	-	-
KRI-15	-	0.0	0.10	0.52	-	2.1	-	-	-	-	-
KRI-16	-	0.0	0.0	0.16	-	0.55	-	0.77	-	-	-
KRI-17	-	0.0	0.0	0.02	-	0.80	-	-	-	-	-
KRI-18	-	0.0	0.0	0.09	-	-	-	-	1.52	-	-
KRI-19	-	0.0	0.0	0.32	-	1.45	-	-	-	-	-
KRI-20	-	0.0	0.0	0.13	-	1.05	-	-	-	-	-
KRI-21	-	0.0	0.0	0.17	-	0.80	-	-	-	-	-
KRI-22	-	0.0	-	0.0	0.05	0.95	-	-	-	-	-
KRI-23	-	0.0	0.0	0.50	-	0.65	-	-	-	-	-
KRI-24	-	-	0.0	0.07	-	0.75	-	-	-	-	-
KRI-25	-	0.0	0.0	0.20	-	0.80	-	-	-	-	-
KRI-26	-	0.0	-	0	0.0	0.50	-	-	-	-	-
KRI-27	-	0.0	0.0	0.07	-	0.8	-	-	1.16	-	-
KRI-28	-	-	-	0.0	-	0.0	-	0.0	1.1	-	-
KRI-29	-	-	-	-	0.0	0.05	0.08	0.21	0.23	-	-
KRI-30	-	-	-	-	-	0.0	-	0.0	-	0.0	0.03

Table 9. Liquidus Temperatures Determined by SEM

Glass	Temperatures, ^{0}C		
	Occurrence interval	Minimum temperature interval	T_L
KRI-01	1008-1033	1008	1008
KRI-02	1058-1083	1058-1068	1063
KRI-03	1058-1083	1058	1058
KRI-04	1108-1133	1108-1118	1113
KRI-05	1258-1283	1258-1268	1263
KRI-06	1083-1108	1093-1098	1095
KRI-07	1058-1083	1068-1073	1071
KRI-08	1158-1183	1173-1183	1173-1183
KRI-09	1183-1208	1183-1193	1183-1193
KRI-10	1208-1258	1248-1258	1248-1258
KRI-11	1158-1183	1158-1168	1158-1168
KRI-12	1158-1183	1168-1173	1168-1173
KRI-13	1158-1208	1183	1183
KRI-14	1158-1183	1173-1183	1173-1183
KRI-15	1183-1208	1183-1193	1183-1193
KRI-16	1158-1183	1158-1163	1158-1163
KRI-17	1158-1183	1158	1158
KRI-18	1158-1183	1168-1178	1168-1178
KRI-19	1158-1183	1173-1183	1173-1183
KRI-20	1158-1183	1158-1168	1158-1168
KRI-21	1158-1183	1168-1173	1168-1173
KRI-22	1133-1158	1133	1133
KRI-23	1158-1183	1168-1173	1168-1173
KRI-24	1158-1183	1158-1168	1158-1168
KRI-25	1158-1183	1168-1178	1168-1178
KRI-26	1108-1133	1118-1123	1118-1123
KRI-27	1158-1183	1158-1168	1158-1168
KRI-28	1033-1058	1043-1048	1043-1048
KRI-29	1108-1133	1108	1108
KRI-30	958-1108	958	958

The data in Table 9 show that the increase of Cr_2O_3, NiO, Al_2O_3, and Fe_2O_3 content in the KRI matrix glasses leads to increase of the liquidus temperatures. The increase of Na_2O and Li_2O concentrations reduce the liquidus temperature [2]. Boron and silicon oxids do not significantly affect T_L. For KRI-05, KRI-08, KRI-09, KRI-10, KRI-13, KRI-15, and KRI-23, the T_L values are significantly higher than the recommended temperature for synthesis, i.e., 1150°C, which makes it impossible to use these glasses on a larger scale. KRI-11, KRI-12, KRI-16, KRI-17, KRI-18, KRI-20, KRI-24, and KRI-26 have crystalline inclusions over 1 vol. % at the synthesis temperature. The liquidus temperatures for KRI-01, KRI-02, KRI-03, KRI-06, KRI-07, and KRI-30 are 50-100°C lower than the glass melting temperature. These compositions can be considered promising for subsequent testing at SMK and EP-5 systems.

6. PCT Evaluations of Quenched and CCC Treated KRI Matrix Glasses

We used PCT-A procedure for leaching KRI matrix glasses. A sample of each glass was crushed in a titanium mill (Fig. 10) and sieved the powders through Fritsch sieves (Fig.11). One gram of the appropriate glass (0.074-0.149 mm fraction sluiced in water and alcohol and then purified by ultrasound (Fig.12) and dried) was placed into a stainless steel or polytetrafluoroethylene vessel (Figs. 13 and 14) where 10 grams of deionized water were added. We used apyrogenic deeply demineralized water (brand name "Ultraaqua") with the resistance of 22.7 MΩ /cm.

Each series of testing included three samples of each KRI glass, three samples of the ARM standard glass and one blank sample. The airtight vessels were held for 7 days at 90°C. 0.445 μm membrane filters were used for sampling leachates to measure elements concentrations using ICP-AE.

Fig. 10. Mill for Glass Crushing

Fig. 11 Set of Sieves FRITSCH TEST SIEVE ASTM E 11

Fig.12 Ultrasound Bath UZV7-0.063/37

Fig.13. Stainless steel vessel, disassembled

Fig. 14. Vessels in Oven

Table 10 provides data on tuning ICP-AE spectrometer using multi-element ICP standard (manufactured in the U.S.). Tables 11 and 12 provide elements concentrations in the blank samples and ARM glass standard leachates.

Table 10. Tuning ICP-AE Spectrometer Using ICP Standard

Series	mg/L			
	B (20)	Li (10)	Na (81)	Si (50)
1	20	10	81	50
	20	10	81	50
	20	10	81	50
2	19.9	10.1	80.9	49.7
	19.3	10.1	79.6	48.5
3	19.5	10.0	80	49.5
	19	10.0	79.4	49.0
4	19	10	84	47
5	19	9.9	77	50
	18	9.8	75	48
6	20	9.9	82	49
	20	9.7	82	48

Table 11. ARM Standard Leaching

Series	Vessel material	PH of leachates	Elements concentrations in leachates (average values), mg/L			
			B	Li	Na	Si
			Reference values, mg/L			
			10.80- 16.32	12.87- 22.65	28.86- 43.58	49.03 - 74.43
1	Teflon	9.61	15	12	34	52
2	steel	10.14	16	12.8	34.5	56.2
3	Teflon	9.59	14	13	32	51
4	Teflon	9.55	13	13	33	49.6
5	Teflon	9.96	16	14	35	51
6	steel	10.33	16	13	34	53

Table 12. Elements Concentrations in Blank Samples

Series	pH upon completion of test	Concentrations upon completion of test, mg/L			
		B	Li	Na	Si
1	5.80	<0.01	<0.01	<0.10	<0.064
2	6.68	0.033	<0.01	0.16	0.12
3	6.65	0.012	0.029	0.18	0.085
4	6.28	0.029	0.013	0.24	0.13
5	н/а	<0.01	<0.001	0.05	<0.05
6	6.52	<0.01	<0.0037	0.12	0.11

Table 13 provides elements concentrations in water normalized for weight percentage of this element in the glass (NL, g/L), as well as Log NL[El_i(g/L).

Table 13. KRI Glasses Leaching Data

Glass #	NL, g/L									Log NL[El_i(g/L)]							
	quenched				CCC treated					quenched				CCC treated			
	B	Li	Na	Si	B	Li	Na	Si	U	B	Li	Na	Si	B	Li	Na	Si
KRI-01	0.39	0.53	0.32	0.32	0.42	0.55	0.32	0.36	—	-0.41	-0.28	-0.50	-0.50	-0.38	-0.30	-0.50	-0.44
KRI-02	0.53	0.65	0.37	0.30	0.40	0.53	0.31	0.29	—	-0.28	-0.19	-0.43	-0.52	-0.40	-0.28	-0.51	-0.54
KRI-03	0.36	0.52	0.30	0.26	0.40	0.53	0.33	0.31	—	-0.45	-0.28	-0.52	-0.59	-0.40	-0.28	-0.48	-0.51
KRI-04	0.37	0.53	0.36	0.28	0.41	0.55	0.35	0.30	—	-0.43	-0.27	-0.44	-0.55	-0.39	-0.26	-0.46	-0.52
KRI-05	0.87	0.96	0.70	0.23	2.95	3.31	2.57	0.23	—	-0.06	-0.02	-0.15	-0.65	0.47	0.52	0.41	-0.64
KRI-06	0.47	0.52	0.47	0.28	0.47	0.56	0.42	0.27	—	-0.33	-0.28	-0.33	-0.55	-0.33	-0.25	-0.38	-0.57
KRI-07	0.74	0.74	0.68	0.33	0.47	0.55	0.42	0.27	—	-0.13	-0.13	-0.17	-0.49	-0.33	-0.26	-0.38	-0.57
KRI-08	2.34	1.44	1.19	0.16	3.11	2.94	2.03	0.17	—	0.37	0.16	0.08	-0.79	0.49	0.47	0.31	-0.77
KRI-09	0.37	0.60	0.29	0.23	0.42	0.51	0.36	0.22	—	-0.43	-0.22	-0.54	-0.64	-0.38	-0.29	-0.44	-0.66
KRI-10	0.30	0.46	0.33	0.22	0.28	0.44	0.39	0.20	—	-0.53	-0.34	-0.48	-0.66	-0.55	-0.36	-0.41	-0.70
KRI-11	0.40	0.54	0.42	0.27	0.48	0.58	0.52	0.27	—	-0.39	-0.27	-0.38	-0.57	-0.32	-0.24	-0.28	-0.57
KRI-12	0.45	0.58	0.32	0.21	0.43	0.56	0.34	0.29	—	-0.34	-0.23	-0.50	-0.69	-0.37	-0.25	-0.47	-0.54
KRI-13	0.39	0.58	0.35	0.26	0.28	0.46	0.29	0.22	—	-0.41	-0.24	-0.45	-0.59	-0.55	-0.34	-0.54	-0.66
KRI-14	0.58	0.67	0.39	0.31	0.27	0.48	0.21	0.19	—	-0.23	-0.18	-0.41	-0.51	-0.57	-0.32	-0.68	-0.72
KRI-15	0.40	0.62	0.28	0.23	0.39	0.65	0.22	0.22	—	-0.40	-0.21	-0.55	-0.64	-0.41	-0.19	-0.66	-0.66
KRI-16	0.34	0.55	0.32	0.22	0.28	0.44	0.25	0.18	—	-0.47	-0.26	-0.49	-0.66	-0.55	-0.36	-0.60	-0.75
KRI-17	0.36	0.53	0.38	0.19	0.34	0.54	0.36	0.20	—	-0.44	-0.28	-0.42	-0.71	-0.47	-0.27	-0.44	-0.70
KRI-18	0.38	0.63	0.33	0.18	0.42	0.56	0.29	0.21	—	-0.42	-0.20	-0.48	-0.75	-0.38	-0.25	-0.54	-0.68
KRI-19	0.39	0.45	0.47	0.24	0.38	0.47	0.50	0.28	—	-0.41	-0.35	-0.33	-0.62	-0.42	-0.33	-0.30	-0.55
KRI-20	0.36	0.53	0.38	0.19	0.38	0.55	0.39	0.21	—	-0.44	-0.27	-0.42	-0.72	-0.42	-0.26	-0.41	-0.68
KRI-21	0.38	0.54	0.43	0.22	0.43	0.62	0.52	0.26	—	-0.42	-0.27	-0.37	-0.66	-0.37	-0.21	-0.29	-0.58
KRI-22	0.36	0.52	0.35	0.23	0.97	1.07	0.57	0.25	—	-0.44	-0.29	-0.46	-0.63	-0.01	0.03	-0.24	-0.60
KRI-23	0.41	0.67	0.22	0.23	0.39	0.79	0.27	0.35	—	-0.37	-0.17	-0.65	-0.63	-0.41	-0.05	-0.57	-0.46
KRI-24	0.32	0.52	0.30	0.22	0.34	0.51	0.31	0.23	—	-0.50	-0.29	-0.53	-0.66	-0.47	-0.29	-0.51	-0.64
KRI-25	0.39	0.56	0.38	0.26	0.40	0.54	0.39	0.27	—	-0.41	-0.25	-0.42	-0.59	-0.40	-0.27	-0.41	-0.57
KRI-26	0.63	0.73	0.86	0.40	0.64	0.82	0.87	0.41	0.12	-0.20	-0.13	-0.66	-0.40	-0.19	-0.09	-0.06	-0.39
KRI-27	1.04	1.11	0.72	0.29	1.29	1.28	0.93	0.34	0.05	0.02	0.04	-0.14	-0.54	0.11	-0.11	-0.03	-0.47
KRI-28	0.74	0.70	1.20	0.55	6.99	1.19	2.40	2.75	0.30	-0.13	-0.16	0.08	-0.26	0.84	0.08	0.38	0.44
KRI-29	0.71	0.49	0.77	0.32	7.99	6.86	4.27	0.85	0.07	-0.15	-0.31	-0.11	-0.49	0.90	0.84	0.63	-0.07
KRI-30	0.34	0.48	0.27	0.22	0.42	0.41	0.80	0.27	0.42	-0.47	-0.32	-0.57	-0.65	-0.38	-0.39	-0.10	-0.57

The NL(i) values show that all glasses leach incongruently. Practically for all glasses, with the exception of KRI-28 and KRI-29, all NL(i) values are in the following row: NL(Li)>NL(B)>NL(Na)>NL(Si). In a number of cases, we observed deviations from the overall similar leaching pattern. For example, glasses KRI-05, KRI-08, and KRI-27, with the highest B_2O_3 concentration (19.96 wt.%, 16.25 wt.%, and 17.20 wt.%), are characterized by a higher dissolution rate for all three elements, i.e., boron, lithium, and sodium. If the alkaline metal content (R_2O) increases in the glasses KRI-08 and KRI-27, NL of these elements further increases. A high R_2O content in the glasses KRI-26, KRI-28, and KRI-29 leads to the same results.

Tables 14 and 15 show NL of elements for glasses US-08, US-19, US-20, US-24, US-35, US-44, and US-45 with the compositions identical to glasses KRI-01, KRI-02, KRI-03, KRI-04, KRI-05, KRI-06, and KRI-07. The glass leaching results obtained in the United States and at KRI are fairly close.

Table 14. Leach Data for KRI and US Quenched Glasses with Identical Compositions

Glasses with identical compositions		Log NL[El_i(g/L)]							
		KRI				US			
		B	Li	Na	Si	B	Li	Na	Si
KRI-01	US-08	-0.41	-0.28	-0.50	-0.50	-0.36	-0.22	-0.49	-0.42
KRI-02	US-19	-0.28	-0.19	-0.43	-0.52	-0.35	-0.24	-0.46	-0.49
KRI-03	US-20	-0.44	-0.28	-0.52	-0.59	-0.35	-0.23	-0.45	-0.51
KRI-04	US-24	-0.43	-0.28	-0.44	-0.55	-0.40	-0.25	0.47	-0.54
KRI-05	US-35	-0.60	-0.02	-0.16	-0.64	-0.10	-0.04	-0.20	-0.68
KRI-06	US-44	-0.33	-0.28	-0.33	-0.55	-0.28	-0.25	-0.30	-0.55
KRI-07	US-45	-0.13	-0.13	-0.17	-0.49	-0.32	-0.25	-0.31	-0.54

Table 15. Leach Data for KRI and US CCC Treated Glasses

Glasses with identical compositions		Log NL[El_i(g/L)]							
		KRI				US			
		B	Li	Na	Si	B	Li	Na	Si
KRI-01	US-08	-0.38	-0.30	-0.50	-0.44	-0.39	-0.27	-0.49	-0.45
KRI-02	US-19	-0.40	-0.28	-0.51	-0.54	-0.38	-0.27	-0.47	-0.53
KRI-03	US-20	-0.40	-0.28	-0.48	-0.51	-0.38	-0.26	-0.46	-0.52
KRI-04	US-24	-0.39	-0.26	-0.46	-0.52	-0.39	-0.26	-0.45	-0.53
KRI-05	US-35	0.47	0.52	0.41	-0.64	0.60	0.55	0.40	-0.66
KRI-06	US-44	-0.33	-0.25	-0.38	-0.57	-0.29	-0.25	-0.31	-0.54
KRI-07	US-45	-0.33	-0.26	-0.38	-0.57	-0.34	-0.26	-0.34	-0.55

7. TCLP Leaching

7.1 Selection of Appropriate Extraction Fluid

Glasses KRI-02, KRI-05, KRI-07, KRI-10, KRI-28, and KRI-30 were tested using TCLP Procedure, method 1311. The extraction fluid selection was performed in accordance with Section 7.1.4 of the TCLP Procedure. According to the data given in Table 14, for extraction of the toxic elements from all tested glasses, extraction fluid # 1 (Buffer #1 acidity) should be used. The buffer prepared according to Section 5.7.1 of the TCLP procedure had the pH value of 4.91±0.05.

Table 16. Selection of Appropriate Extraction Fluid

Glass ID	pH (section 7.1.4.1–7.1.4.2 of TCLP test)	pH (section 7.1.4.3-7.1.4.4 of TCLP test)	Type (number) of extraction fluid
KRI-02	8.92	1.68	#1
KRI-05	7.04	1.63	#1
KRI-07	8.83	1.72	#1
KRI-10	8.49	1.76	#1
KRI-28	9.70	1.80	#1
KRI-30	8.74	1.78	#1

7.2 TCLP Glass Testing

The glasses of six compositions were crushed. For each glass, we leached glass fractions below 10 mm placing 2 g of the glass followed by 40 ml of the extraction fluid #1 into polystyrene vessels. After sealing the vessels, we agitated them for 18 hours. Upon completion of the extraction, the TCLP extracts were filtered using a 0.45μm membrane filter. The average pH values of the TCLP extracts were recorded as 4.87.

The TCLP extract samples were prepared for measuring concentrations of toxic elements using mass spectrometry with inductively coupled plasma (MS-ICP) as follows: for each glass, 10 mL of the filtered extract were acidified by 0.1 mL of nitric acid (reagent grade). We observed for all tested glasses that, upon acidification of the extracts, no precipitation occurred. The blank sample was prepared directly from 10 mL of extraction fluid # 1 acidified by 0.1 mL of HNO_3. MS-ICP toxic concentrations values for the extracts ($X_{unspiked}$) were given in Table 17. All concentrations values are adjusted relatively to the blank values. Table 17 shows that none of the toxic concentrations in the TCLP-extracts exceeds the allowable limits. If a concentration of a toxic element in the glass increases, its concentration also increases in the TCLP-extract.

Table 17. Concentrations of Toxic Elements in TCLP-Extracts

#	$X_{unspiked}$, mg/L			
	Cr	Mn	Pb	Zn
US EPA's TCLP limit	5	N/L	5	25
(Blank)	*(0.0018)*	*(0.0026)*	*(0.0068)*	*(0.015)*
KRI-02	0.0092	0.4370	0.0880	0.037
KRI-05	0.0082	0.7774	N/A	0.365
KRI-07	0.0051	0.1270	0.0410	0.095
KRI-10	0.0112	0.0574	0.1130	0.060

KRI-28	0.6380	2.8970	1.0930	N/A
KRI-30	N/D	N/A	1.393	1.985

7.3. TCLP Testing Quality Assurance

According to Section 5.8 of the TCLP Procedure, we prepared an analytical chromium and lead standard that was used as standard additives for the TCLP-extracts samples.

First of all, we prepared a reference standard. For this purpose, 0.03312 g of the analytical standard was added to extraction fluid # 1 acidified with 0.1 mL HNO_3. Cr and Pb concentrations were measured in this reference standard using MS-ICP. Table 18 provides calculated and MS-ICP measured Cr and Pb concentrations in the reference standard, as well as their average values.

Table 18. Cr and Pb Concentrations in the Reference Standard

Cr			Pb		
Concentration, mg/L			Concentration, mg/L		
Calculated value	MS-ICP measured value	Average value	Calculated value	MS-ICP measured value	Average value
0.0556	0.0452	0.0504±10.3%	0.126	0.0922	0.109±15.5%

Then we used a *method of precise additions*, adding exact portions of Cr and Pb analytical standard to 10 mL of the TCLP-extracts acidified by 0.1 mL HNO_3. We calculated Cr and Pb concentrations in the TCLP-extracts that will correspond to the introduced exact portions (K_{known}, Table 19). After the analytical standard was added, samples of the TCLP-extracts wer analyzed for toxic elements using MS-ICP. The MS-ICP data for Cr and Pb concentrations (X_{spiked}) are given in Table 19.
Table 19 contains %R (% recovery) values. The following equation was used for %R calculations:

$$\%R = 100\ (X_{spiked} - X_{unspiked}) / K_{known} \qquad (1)$$

Table 19. TCLP Testing Quality Assurance Using a *Method of Precise Additions*

Glass #	Analytical standard, g	[Cr], mg/L				[Pb], mg/L			
		X spiked	X unspiked	K known	% release	X spiked	X unspiked	K known	% release
Reference standard	0.03312	(0.0452)	-	0.0452	100.0	(0.0922)	-	0.0922	100.0
KRI-02	0.03240	0.0552	0.0092	0.0442	104.1	0.193	0.088	0.0902	116.4
KRI-05	0.03080	0.0552	0.0082	0.0420	111.9	N/A	N/A	N/A	-
KRI-07	0.03432	0.0592	0.0051	0.0468	115.6	0.183	0.041	0.0955	148.7
KRI-10	0.03573	0.0632	0.0112	0.0488	106.6	0.233	0.113	0.0995	120.6
KRI-28	0.03513	0.6680	0.6380	0.0479	62.6	1.193	1.093	0.0978	102.2
KRI-30	0.03410	0.0563	N/D	0.0465	121.1	1.493	1.393	0.0949	105.4

Table 19 makes it possible to conclude that the TCLP testing of the glasses provided a sufficient level of data validity since the average release of the toxic elements of concern, i.e., Cr and Pb, is 111.5 % (with the exception of Pb in KRI-07 and Cr in KRI-28). A low Cr release in KRI-28 is

related to the fact that, for that glass, K_{known} value is in the range of the X_{spiked} measurement uncertainty.

8. Uranium and Iron Oxidation States

For melting of glasses that contain a large number of elements with variable oxidation states, the equilibrium between their oxidation states is very important. Some elements can be present in the glass in different oxidation states functioning as modifiers or entering the glass array, for example, Mn(3+) and Mn(2+); Fe(3+) and Fe(2+); Cr(6+) and Cr(3+); U(4+) and U(6+). In case of iron, we need to consider reversibility of the $Fe_2O_3 \leftrightarrow 2FeO+1/2O_2$ reaction at high temperatures. Higher manganese oxides (MnO_2) contribute to converting FeO into Fe_2O_3 due to its decomposition associated with heating and oxygen release. In addition, the presence of such compounds as carbonates and sulfates in the feed may affect the oxidation states of multivalent cations.

Taking into account these factors, we studied the oxidation states of iron using Mossbauer spectroscopy and the oxidation states of uranium using optical spectrometry in quenched glasses. The results of these preliminary studies are described below.

To study the oxidation states of iron and uranium, we selected those glasses (Table 20), the feed for which contained various concentrations of carbonates and did not contain the crystalline phase (spinel).

Table 20. Glass Compositions Evaluated by Mossbauer Spectroscopy

	Al_2O_3	B_2O_3	CaO	Cr_2O_3	Fe_2O_3	K_2O	Li_2O	MgO	MnO	Na_2O	NiO	PbO	SO_3	SO_4	SiO_2	SrO	TiO_2	ZnO	ZrO_2	UO_3
KRI-01	15.19	9.55	0.00	0.00	9.74	1.00	4.86	0.00	2.43	9.81	0.001	0.09	0.49	0.59	45.78	0.00	1.00	0.00	0.00	0.00
KRI-06	12.80	12.58	0.55	0.305	8.86	0.64	4.05	0.25	1.83	12.73	0.359	0.66	0.22	0.26	39.55	1.62	0.46	1.02	1.46	0.00
KRI-28	18.34	6.12	0.00	1.00	5.00	0.00	5.71	0.00	3.85	18.52	0.00	1.00	0.50	0.60	36.50	0.00	1.00	0.00	0.00	2.42
KRI-30	20.00	15.29	0.75	0.00	5.51	0.00	5.79	0.50	0.00	7.23	0.00	1.00	0.50	0.60	35.73	3.00	0.00	0.00	2.00	2.67

8.1. Uranium Oxidation State in KRI-28 and KRI-30

Uranium oxidation state in glasses KRI-28 and KRI-30 was determined using spectrometric and luminescent methods. Uranium was introduced as U_3O_8 into the feed. Since the glasses contained elements with a high absorption (U,Fe,Cr), they were practically non-transparent in the visible and shorter wavelength region of the spectrum. Therefore, we chemically dissolved the samples without interfering with the uranium oxidation state. We performed the dissolution as described below.

We placed ~1g samples of the KRI-28 and KRI-30 glasses into Teflon bottles with plugs and added 0.5 mL concentrated phosphoric acid and 0.3 mL of 40% hydrofluoric acid. Then the bottles were simmered in "sand bath" for 5 hours at 80-100^{o}C, followed by HF distillation. We added 1 mL of water to the sample and sampled 0.6 mL of the generated solution that was placed into a standard quartz vial. The spectrum was taken in the 300-800 nm range using the spectrometer UV-3101. As a reference standard, we used the similarly prepared standardized U_3O_8 solution.

Similar treatment of uranium dioxide did not result in generation of U(6+). U(4+) and U(6+) absorptions do not overlap in the visible part of the spectrum. As analytical bands, we selected the following: 420 nm for uranyl and 640 nm for U(4+) – 640 nm. From the U_3O_8 spectrum, we determined absorption coefficients calculated for 1 mg of uranium (K_i), and these coefficients

were 0.0161 and 0.0155 for 420 nm and 640 nm, respectively. The A_i / K_i ratio gives the content of this oxidation state of uranium in the sample in mg. Table 21 provides the measurements results.

Table 21. U(6+) and U(4+) Content ion Glasses KRI-28 and KRI-30

Composition	Absorption, A_i		Content		
	420 nm	640 nm	U(6+), mg	U(4+), mg	U(IV),%
U_3O_8	0.334	0.161	20.8	10.4	33.3
KRI-28	0.30	Not detectable	19.0	Not detectable	0
KRI-30	0.140	0.037	8.7	2.4	21,5

In the KRI-28 sample, the U(4+)- 640 nm absorption band overlapped with the chromium absorption band, therefore, we had to perform an additional luminescent analysis of the sample before and after its oxidation with strong nitric acid, to determine a relative uranium content.

Our studies showed an equal U(6+) intensity before and after the oxidation, which made us conclude that the KRI-28 glass sample had uranium in the oxidation state of U(6+). We plan to continue work with other uranium-containing glasses.

8.2 Iron Oxidation State in Glasses KRI-01, KRI-06, and KRI-28

We used Mossbauer spectroscopy to determine the oxidation state of iron in the glass samples KRI-01, KRI-06, and KRI-28. Mossbauer spectra were taken using the spectro-photometer VS 1101E in the mode of constant accelerations at room temperature. The gamma resonance pair $^{57}Co(Cr)$ source, detector RSD 112, and converter $K_2Mg^{57}Fe(CN)_6$ were used to measure absorption spectra.

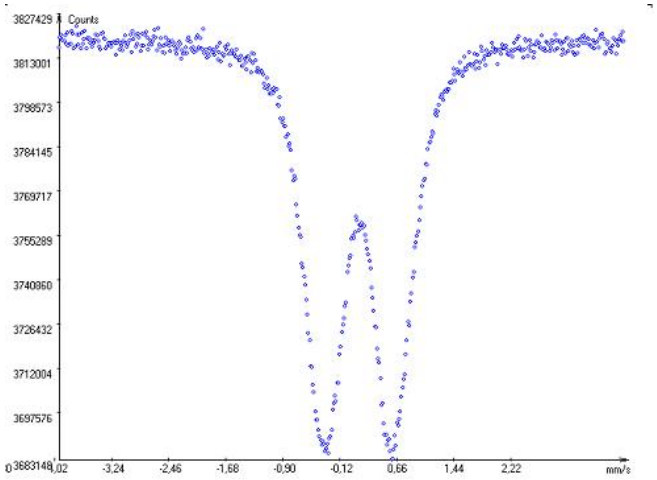

Fig. 15. Mossbauer Spectra for KRI-01 Glass

For data processing, we used a standard spectra Lorentz line shape processing code. The isomeric shift was given relatively to α-Fe. We only determined Fe(3+) in the glasses. The KRI-01, KRI-06, and KRI-28 glass samples had iron in one octahedral position, i.e., a doublet: isomeric shift (I.S) = 0.2 mm/s; quadruple split (Q.S.)= 0.96 mm/s (Fig.15).

9. Viscosity Measurements for Selected KRI Matrix Glasses

9.1. Viscosity Measurement Procedure

We measured viscosity of the melts using a vibration viscosimeter and also a viscosimeter that is based on a platinum ball immersion into the melt. Fig. 16 shows a schematic of the vibration viscosimeter. The principle of its operation and description are given below.

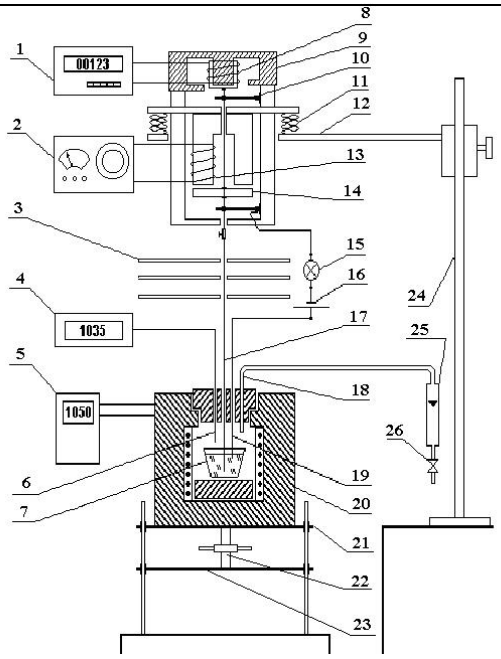

Fig.16. Schematic of Vibration Viscosimeter

DC from the sound generator ZG-10 (2) is supplied to the vibrator coil (13). The variable magnetic field of the vibrator interacts with the anchor (14) and forces the mobile system of the viscosimeter to oscillate. Apart from the anchor, the mobile system of the viscosimeter includes the following: rod (17), springs (10), and coil (8). For viscosity measurements, the lower part of the rod is immersed into the crucible with liquid or melt (7). The buffers (11) between the body of the viscosimeter and the support bar (12) prevent transfer of oscillations from the viscosimeter to the support bar. When the mobile system oscillates, and an electromotive force is induced in the coil (8) that maximizes at the resonance, i.e., when the frequency of the viscosimeter oscillations coincides with the frequency of the forced oscillations. The milli-voltmeter Sctch-4501 (1) records the electromotive force (E) induced in the coil (8).

When the rod is immersed into the liquid or melt, the oscillations amplitude will decrease with the viscosity increase, thereby making it possible to determine the viscosity by measuring the electromotive force E.

To measure viscosity in the melts, scientists use platinum, molybdenum, or tungsten 1-2 mm diameter and 300-400 mm long wire for the rods, depending on the properties of the measured melt, as well as temperature and media of the measurements.

Legend for Fig. 16

1 – digital milli-voltmeter, 2 – sound generator ZG-10, 3 – heat screens,
4 – potentiometer PITs-5T, 5 – temperature regulator RIT-23, 6 - thermocouple,
7 – crucible with melt, 8 – measuring coil, 9 – permanent magnet,
10 - springs, 11 - buffers, 12 – support bar, 13 – vibrator coil,
14 – vibrator anchor, 15 – indicating light, 16 – power supply, 17 – tungsten wire rod,
18 – ceramic tube for inert gas supply,
19 – additional tungsten wire, 20 – shaft furnace,
21 – upper platform, 22 – fine-adjustment screw, 23 – lower platform,
24 – tripod, 25 - rotameter, 26 – vent for argon feed

This viscosimeter uses a 350 mm long tungsten wire with the diameter of 1.2 mm. The wire is immersed 15 mm deep into the liquid or melt . When the rod touches the melt surface, the indicating light (15) turns on, and, for this purpose, an additional tungsten rod (19) is immersed into the glass melt .

We use alundum or porcelain 25 mm high crucibles with the upper diameter of 35 mm and place them into the small-scale shaft furnace PP-1.2 (20). The temperature in the furnace is regulated by the temperature regulator RIT-23 (5). The chromel/alumel thermocouple (6) and the digital potentiometer PITs-5T (4) monitor the melt temperature.

Argon is fed into the furnace headspace through the ceramic tube (18) to prevent oxidation of the tungsten wire rods. The rotameter RM-A (25) monitors and regulates the argon flow rate. The body of the viscosimeter is installed on the tripod (21).

9.2. Viscosity Parameters for Studied Glasses

Fig. 17 shows data for comparison of viscosity values for the DWPG glass standard obtained by different methods. Fig 17 shows a satisfactory precision of the DWPF viscosity values measured by the vibrating viscosimeter in the temperature range of 850-1,000 °C. Afterwards, in the 1,000-1,150°C temperature range, the values start to significantly diverge, and at the temperature of 1,150 °C, our values significantly exceed the reference values.

For the viscosity values obtained by the platinum ball immersion based viscosimeter, the values diverge at the entire temperature range of 850-1,200 °C. The immersion method measured data (KRI-2) have a temperature dependence similar to the round-robin results, but they are located slightly higher. It may likely be explained by the fact that different frit batches were used for our measurements and the round-robin measurements.

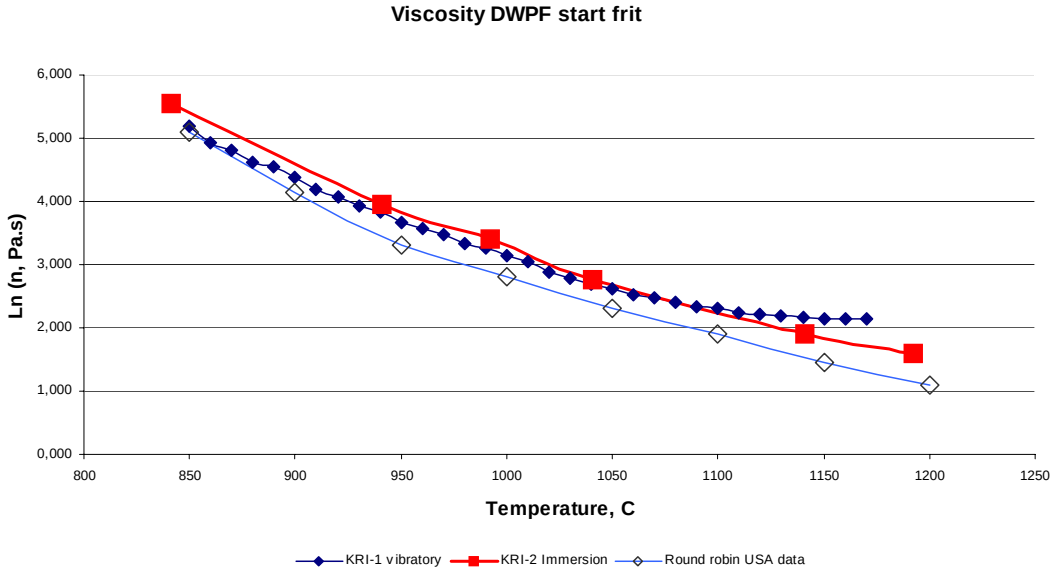

Fig. 17. Comparison of Viscosity Data for DWPF Standard vs Data Obtained Using Vibration and Immersion Viscosimeters

Since the viscosity data for the DWPF standard significantly differ from the U.S. data, the KRI viscosity measurements at KRI were only performed for several selected compositions, but not for all 30 compositions. Table 22 provides viscosity values for KRI-01, KRI-03, KRI-04, KRI-07, KRI-11, KRI-20, KRI-24, and KRI-30 obtained using the vibration viscosimeter. Glasses

KRI-01,KRI- 03, and KRI-07 correspond to US-08, US-20, and US-45. Previously submitted reports provided more detailed data on the viscosity of glasses. KRI-01, KRI-03, KRI-04, KRI-07, KRI-11, KRI-20, KRI-24, and KRI- 30.

Table 22. Viscosity Values for KRI Matrix Glasses

T, °C	Viscosity, Pa s							
	KRI-01	KRI-03	KRI-04	KRI-07	KRI-11	KRI-20	KRI-24	KRI-30
950	135.83	70.45	92.02	19.70	93.32	62.99	155.08	33.09
1000	74.00	40.61	47.70	10.88	43.92	33.22	65.87	19.31
1050	41.61	24.53	30.33	6.31	23.70	21.49	35.95	13.18
1100	26.30	16.39	21.10	4.36	15.23	16.22	21.27	10.01
1150	15.36	11.72	17.01	3.60	12.35	13.45	16.28	8.51

10. Selection of Optimal KRI Matrix Glasses

Table 23 provides all data on crystalline phases and leaching for KRI matrix glasses both quenched and CCC treated, as well as T_L values. We used the following criteria to select glasses with the optical properties: NL values (PCT) are not supposed to exceed 1 g/L, T_L values are not supposed to exceed 1050ºC, and the melt viscosity values are not supposed to exceed 5-7 Pa·s.

Table 23. Characterization Data Summary for KRI Matrix Glasses

Glass #	Quenched KRI glasses					CCC Treated KRI glasses					T_L
	Crystallinity, vol. .%	NL, g/L				Crystallinity, vol. .%	NL, g/L				
		B	Li	Na	Si		B	Li	Na	Si	
KRI-01	N/d	0.39	0.53	0.32	0.32	0.3	0.42	0.55	0.32	0.36	1008
KRI-02	N/d	0.53	0.65	0.37	0.30	0.8	0.40	0.53	0.31	0.29	1063
KRI-03	N/d	0.36	0.52	0.30	0.26	0.2	0.40	0.53	0.33	0.31	1058
KRI-04	N/d	0.37	0.53	0.36	0.28	0.3	0.41	0.55	0.35	0.30	1113
KRI-05	2.8	0.87	0.96	0.70	0.23	7.3	2.95	3.31	2.57	0.23	1263
KRI-06	N/d	0.47	0.52	0.47	0.28	1.2	0.47	0.56	0.42	0.27	1095
KRI-07	N/d	0.74	0.74	0.68	0.33	0.2	0.47	0.55	0.42	0.27	1071
KRI-08	6.6	2.34	1.44	1.19	0.16	15.0	3.11	2.94	2.03	0.17	1178
KRI-09	1.5	0.37	0.60	0.29	0.23	3.1	0.42	0.51	0.36	0.22	1188
KRI-10	0.9	0.30	0.46	0.33	0.22	0.94	0.28	0.44	0.39	0.20	1253
KRI-11	2.5	0.40	0.54	0.42	0.27	5.3	0.48	0.58	0.52	0.27	1162
KRI-12	1.2	0.45	0.58	0.32	0.21	2.5	0.43	0.56	0.34	0.29	1168
KRI-13	2.2	0.39	0.58	0.35	0.26	2.8	0.28	0.46	0.29	0.22	1183
KRI-14	1.5	0.58	0.67	0.39	0.31	3.8	0.27	0.48	0.21	0.19	1178
KRI-15	2.7	0.40	0.62	0.28	0.23	4.3	0.39	0.65	0.22	0.22	1183
KRI-16	0.5	0.34	0.55	0.32	0.22	0.6	0.28	0.44	0.25	0.18	1160
KRI-17	0.91	0.36	0.53	0.38	0.19	2.0	0.34	0.54	0.36	0.20	1158
KRI-18	2.3	0.38	0.63	0.33	0.18	3.6	0.42	0.56	0.29	0.21	1173
KRI-19	0.2	0.39	0.45	0.47	0.24	2.3	0.38	0.47	0.50	0.28	1178
KRI-20	0.34	0.36	0.53	0.38	0.19	2.6	0.38	0.55	0.39	0.21	1166
KRI-21	0.6	0.38	0.54	0.43	0.22	2.5	0.43	0.62	0.52	0.26	1171
KRI-22	0.2	0.36	0.52	0.35	0.23	2.8	0.97	1.07	0.57	0.25	1133
KRI-23	2.8	0.41	0.67	0.22	0.23	2.6	0.39	0.79	0.27	0.35	1170
KRI-24	0.58	0.32	0.52	0.30	0.22	3.5	0.34	0.51	0.31	0.23	1164
KRI-25	0.78	0.39	0.56	0.38	0.26	2.2	0.40	0.54	0.39	0.27	1175
KRI-26	0.5	0.63	0.73	0.86	0.40	4.5	0.64	0.82	0.87	0.41	1121
KRI-27	N/d	1.04	1.11	0.72	0.29	1.9	1.29	1.28	0.93	0.34	1163
KRI-28	N/d	0.74	0.70	1.20	0.55	100	6.99	1.19	2.40	2.75	1045
KRI-29	N/d	0.71	0.49	0.77	0.32	2.0	7.99	6.86	4.27	0.85	1108
KRI-30	N/d	0.34	0.48	0.27	0.22	1.4	0.42	0.41	0.80	0.27	958

Table 24 shows the glasses and their properties that can be considered the most appropriate for testing in SMK-1 and EP-5 systems. KRI-07 and KRI-30 are of a special interest.

Table 24. Optimal KRI Matrix Glass Compositions

Glass #	Quenched KRI matrix glasses					CCC treated KRI matrix glasses					T_L	Viscosity, Pa s (1150^0C)
	Crystallinity, vol. .%	NL, g/L				Crystallinity, vol. .%	NL, g/L					
		B	Li	Na	Si		B	Li	Na	Si		
KRI-01	N/d	0.39	0.53	0.32	0.32	0.3	0.42	0.55	0.32	0.36	1008	15.36
KRI-03	N/d	0.36	0.52	0.30	0.26	0.2	0.40	0.53	0.33	0.31	1058	11.72
KRI-07	N/d	0.74	0.74	0.68	0.33	0.2	0.47	0.55	0.42	0.27	1071	3.60
KRI-26	0.5	0.63	0.73	0.86	0.40	4.5	0.64	0.82	0.87	0.41	1121	-
KRI-30	N/d	0.34	0.48	0.27	0.22	1.4	0.42	0.41	0.80	0.27	958	8.51

11. Conclusions

1. KRI completed crucible scale fabrication of 30 KRI matrix compositions in the muffle furnace at 1150ºC. All KRI matrix glasses underwent CCC treatment experiments.

2. The synthesized glasses and CCC treated glasses were tested for chemical homogeneity and crystallization using SEM, EPMA, and XRD. The synthesized glasses KRI-01 – KRI-04, KRI-06, KRI-07, KRI-26, and KRI-28 – KRI-30 are homogenous regarding their main components and free from crystalline inclusions. Glasses KRI-10, KRI-16, KRI-17, KRI-19, KRI-20, KRI-21, KRI-22, KRI-24, KRI-25, and KRI-27 contain less than 1 vol. % of the spinel crystalline phase.

3. The ARM glass standard was tested using the PCT procedure. The leaching parameters were also identified for KRI matrix quenched and CCC treated glasses. All studied glasses were shown to have a high chemical durability, wit the exception of KRI-05, KRI-08, KRI-22, and KRI-27- KRI-29. The NL(i) values fall in the following row: NL(Li)>NL(B)>NL(Na)>NL(Si). Glasses KRI-02, KRI-05, KRI-07, KRI-10, KRI-28, and KRI-30 were tested using the TCLP procedure. All toxic concentrations in the extracts do not exceed the allowable limits.

4. The liquidus temperature values were determined for the SRM 733 glass standard and all 30 KRI matrix compositions using the certified furnace SNOL 7.2/1300 manufactured by UMEGA. The increase of Cr_2O_3, NiO, Al_2O_3 and Fe_2O_3 concentrations in the KRI matrix glasses leads to the increase of the liquidus temperatures. The increase of Na_2O and Li_2O concentrations decreases the liquidus temperature. Boron and silicon oxides do not significantly affect the liquidus temperature.

5. The viscosity as a function of temperature data were obtained for KRI-01, KRI-03, KRI-04, KRI-07, KRI-11, KRI-20, KRI- 24, and KRI-30.

6. Taking into account all physical and chemical characteristics of the KRI matrix glasses, KRI recommended compositions KRI-06 (KRI-07) and KRI-30 for further studies under the ongoing task.

12 References

1 M. Mika, M.J. Schweiger, J.D. Vienna, P. Hrma. Liquidus Temperature of Spinel Precipitating High-Level Waste Glasses, Mat. Res. Symp. Proc.V.465, 1997, pp-71-78.

2 Pavel Hrma, John Vienna, Jarrod Crum, Greg Piepel, Martin Mika. Liquidus Temperature of High-Level Waste Borosilicate Glasses with Spinel Primary Phase", Mat. Res. Symp. Proc.V.608, 2000, pp-671-676.

Attachment 1. EPMA Data on Chemical Homogeneity of Glasses

Sample KRI 01

	SiO2	TiO2	Al2O3	Fe2O3	MnO	Na2O	K2O	SO3	B2O3	Li2O	Total
1	44.60	0.91	15.74	8.78	2.47	11.61	0.88	0.59	9.50	4.90	100.00
2	42.27	1.04	16.97	9.82	2.63	11.54	0.84	0.47	9.50	4.90	100.00
3	42.69	1.11	15.67	10.36	2.58	11.83	0.90	0.47	9.50	4.90	100.00
4	42.79	1.06	15.94	10.28	2.65	11.48	0.95	0.45	9.50	4.90	100.00
5	43.08	1.03	16.08	9.81	2.58	11.62	0.89	0.50	9.50	4.90	100.00
Average	43.09	1.03	16.08	9.81	2.58	11.62	0.89	0.50	9.50	4.90	100.00

Sample KRI 02

	Al2O3	CaO	Fe2O3	K2O	MgO	MnO	Na2O	NiO	SO3	SiO2	TiO2	ZrO2	B2O3	Li2O	
1	13.43	0.42	7.82	0.62	0.03	1.92	9.85	0.05	0.24	46.65	0.75	0.19	14.40	3.64	100.00
2	15.57	0.61	8.82	0.64	0.00	2.24	10.82	0.05	0.32	41.72	0.88	0.28	14.40	3.64	100.00
3	15.79	0.49	9.30	0.65	0.12	2.10	11.00	0.19	0.32	40.63	0.99	0.39	14.40	3.64	100.00
4	15.70	0.64	8.79	0.68	0.11	2.34	11.09	0.12	0.38	40.89	0.97	0.25	14.40	3.64	100.00
5	15.69	0.51	8.49	0.60	0.17	2.31	10.84	0.28	0.38	41.43	0.94	0.32	14.40	3.64	100.00
Average	15.23	0.53	8.64	0.64	0.09	2.18	10.72	0.14	0.33	42.27	0.91	0.28	14.40	3.64	100.00
Er/Re	4.00	4.40	2.80	0.50	0.80	1.7	1.0	0.7	2.10	3.40	1.40	1.50			

Sample KRI 03

	Al2O3	CaO	Fe2O3	K2O	MnO	Na2O	SO3	SiO2	TiO2	B2O3	Li2O	Total
1	16.38	0.577	8.99	0.7	2.39	10.85	0.51	40.44	1.032	14.4	3.64	100
2	15.69	0.424	8.57	0.7	2.20	10.64	0.50	42.19	1	14.4	3.64	100
3	11.85	0.532	7.46	0.6	2.09	10.11	0.47	48.22	0.633	14.4	3.64	100
4	16.15	0.580	9.29	0.6	2.40	10.58	0.51	40.93	0.866	14.4	3.64	100
5	16.47	0.554	8.91	0.6	2.42	11.87	0.49	39.64	0.99	14.4	3.64	100
Average	15.31	0.533	8.64	0.7	2.30	10.81	0.50	42.28	0.904	14.4	3.64	100
Skin around SiO_2	6.24	0.28	6.14	0.8	2.07	6.87	0	66.6	0.5			
Er/Re	6.4	20.2	4.7	1	1.3	1.1	0.1	15.8	28.5			

Sample KRI 04

	Al2O3	CaO	Fe2O3	K2O	MgO	MnO	Na2O	NiO	SO3	SiO2	TiO2	ZrO2	B2O3	Li2O	
1	14.37	0.64	7.84	0.69	0.03	2.20	11.2	0.7	0.2	45.81	0.71	0.37	12.25	3	100
2	13.85	0.56	7.46	0.63	0.07	2.10	11.27	0.3	0.47	46.97	0.6	0.44	12.25	3	100
3	11.36	0.39	7.54	0.63	0.09	2.33	10.26	0.6	0.21	50.42	0.5	0.45	12.25	3	100
4	16.49	0.62	8.46	0.63	0.25	2.54	11.62	0.6	0.36	42.04	0.68	0.44	12.25	3	100
5	16.63	0.67	8.72	0.67	0.04	2.77	11.83	0.5	0.49	41.03	0.88	0.47	12.25	3	100
Average	14.54	0.58	8.01	0.65	0.09	2.39	11.23	0.5	0.35	45.26	0.68	0.43	12.25	3	100
Er/Re	8.4	4.4	2.8	0.5	0.8	1.7	1	0.7	2.1	3.4	1.4	1.5			

Sample KRI 05

	Al2O3	CaO	Cr2O3	Fe2O3	K2O	MnO	Na2O	SiO2	SrO*	ZnO	B2O3	Li2O	Сумма
1	13.81	0.91	0.32	12.62	1.84	5.07	9.70	38.99	2.70	2.04	10.00	2.00	100.00
2	13.35	1.06	0.32	12.57	1.83	5.05	10.54	38.15	2.70	2.43	10.00	2.00	100.00
3	12.67	0.89	0.31	12.46	1.79	4.54	9.61	40.78	2.70	2.25	10.00	2.00	100.00
4	14.05	0.92	0.32	12.96	1.84	5.08	8.99	39.09	2.70	2.04	10.00	2.00	100.00
5	13.45	0.90	0.47	12.93	1.82	5.29	9.15	39.00	2.70	2.28	10.00	2.00	100.00
Average in area	13.46	0.94	0.35	12.71	1.83	5.01	9.60	39.21	2.70	2.21	10.00	2.00	100.00
Average	11.08	0.82	0.29	11.03	1.53	4.42	8.16	40.38	2.70	2.31	10.00	2.00	100.29
Er/Re	1.2			1.3	0	2	0.8	5.7					

Sample KRI 06

	SiO2	TiO2	Al2O3	Cr2O3	Fe2O3	MnO	CaO	Na2O	K2O	NiO	ZnO	ZrO2	PbO	SrO	B2O3*	Li2O*	Total
1	40.24	0.43	13.30	0.35	8.73	1.86	0.37	13.90	0.47	0.35	1.02	1.12	0.61	0.58	12.58	4.10	100.00
2	40.23	0.43	12.43	0.33	8.10	1.83	0.39	14.11	0.53	0.28	0.96	1.10	0.39	2.20	12.58	4.10	100.00
3	40.45	0.43	13.25	0.34	8.33	1.93	0.40	13.94	0.53	0.31	1.09	1.03	0.66	0.64	12.58	4.10	100.00
4	41.04	0.45	13.09	0.31	8.41	1.97	0.38	13.71	0.43	0.41	1.14	0.87	0.70	0.41	12.58	4.10	100.00
5	39.30	0.52	13.75	0.31	8.68	1.96	0.43	14.02	0.58	0.32	1.07	1.25	0.48	0.66	12.58	4.10	100.00
Average	40.51	0.45	13.14	0.32	8.40	1.89	0.40	13.74	0.50	0.34	1.04	1.06	0.62	0.91			

Sample KRI 07

	Al2O3	CaO	Cr2O3	Fe2O3	K2O	MgO	MnO	Na2O	NiO	PbO	SiO2	SrO*	TiO2	ZnO	ZrO2	B2O3*	Li2O*	Total
1.00	12.31	0.13	0.40	7.47	0.67	0.00	2.96	9.52	0.70	0.88	37.52	2.70	0.77	1.37	0.62	20.00	2.00	100.00
2.00	13.10	0.26	0.40	7.03	0.55	0.00	3.06	9.09	0.82	0.69	37.67	2.70	0.77	1.25	0.62	20.00	2.00	100.00
3.00	14.14	0.00	0.39	7.51	0.65	0.00	3.10	10.44	0.68	0.86	34.51	2.70	0.75	1.44	0.85	20.00	2.00	100.00
4.00	13.21	0.13	0.41	8.14	0.67	0.00	3.33	9.78	0.81	0.79	35.04	2.70	0.76	1.60	0.63	20.00	2.00	100.00
5.00	10.13	0.12	0.39	6.40	0.53	0.00	2.61	8.40	0.79	0.67	42.88	2.70	0.59	1.20	0.60	20.00	2.00	100.00
Average in area	11.75	0.25	0.40	6.82	0.54	0.00	2.91	8.37	0.80	0.97	39.55	2.70	0.75	1.46	0.73	20.00	2.00	100.00
Average	12.58	0.13	0.40	7.31	0.61	0.00	3.01	9.45	0.76	0.78	37.53	2.70	0.73	1.37	0.66	20.00	2.00	100.00
Er/Re	5.00	28.10		4.40	0.90		2.20	1.10			15.20		13.60		0.40			

Sample KRI 08

	Al2O3	CaO	Cr2O3	Fe2O3	K2O	MnO	Na2O	NiO	PbO	SiO2	SrO*	TiO2	ZnO	ZrO2	B2O3*	Li2O*	Total
1	13.08	0.14	0.43	7.93	0.70	3.15	10.11	0.74	0.94	39.85	0.75	0.81	1.46	0.66	16.25	3.00	100.00
2	13.92	0.27	0.42	7.47	0.58	3.25	9.66	0.86	0.73	40.03	0.75	0.81	1.33	0.65	16.25	3.00	100.00
3	15.02	0.00	0.41	7.97	0.68	3.30	11.09	0.72	0.92	36.66	0.75	0.79	1.53	0.89	16.25	3.00	100.00
4	14.03	0.14	0.43	8.65	0.71	3.53	10.40	0.87	0.84	37.23	0.75	0.82	1.70	0.66	16.25	3.00	100.00
5	10.76	0.13	0.41	6.80	0.56	2.77	8.93	0.83	0.70	45.56	0.75	0.62	1.28	0.63	16.25	3.00	100.00
Average in area	12.48	0.27	0.42	7.25	0.58	3.09	8.90	0.85	1.03	42.01	0.75	0.80	1.55	0.78	16.25	3.00	100.00
Average	13.36	0.13	0.42	7.77	0.65	3.20	10.04	0.81	0.83	39.86	0.75	0.77	1.46	0.70	16.25	3.00	100.00
Er/Re	5.0	28.1		4.4	0.9	2.2	1.1			15.2		14		0			

Sample KRI 09

	Al2O3	CaO	Cr2O3	Fe2O3	K2O	MnO	Na2O	NiO	PbO	SiO2	SrO*	TiO2	ZnO	ZrO2	B2O3	Li2O	Total
1	15.14	0.13	0.28	7.77	0.23	1.10	11.7	0.48	0.82	39.21	0.75	0.95	1.67	2.45	14.3	3	100
2	16.09	0.13	0.27	8.24	0.23	1.22	12.5	0.48	0.82	37.08	0.75	0.79	1.53	2.56	14.3	3	100
3	15.72	0.13	0.28	8.33	0.34	1.10	11.86	0.48	1.03	37.48	0.75	0.8	1.67	2.71	14.3	3	100
4	16.06	0.27	0.28	7.63	0.23	1.10	12.22	0.6	1.03	37.42	0.75	0.95	1.55	2.58	14.3	3	100
5	14.62	0.14	0.29	7.97	0.24	1.13	10.03	0.62	0.84	41.12	0.75	0.82	1.46	2.65	14.3	3	100
Average in area	14.26	0.13	0.278	7.54	0.23	1.09	11.18	0.6	1.12	40.78	0.75	0.78	1.41	2.55	14.3	3	100
Average	15.53	0.16	0.281	7.99	0.25	1.14	11.66	0.54	0.91	38.46	0.75	0.86	1.57	2.59	14.3	3	100
Er/Re	2.1	18.3		2.1	0.7	0.4	1.4			8		14.3		0.4			
Spinel 1	3.84	0	7.35	53.81	0	5.25	0	21	0	1.15	0	0.71	6.66	0	0	0	99.74
Spinel 2	3.97	0	8.04	53.29	0	4.52	0	20.4	0	1.07	0	0.83	7.22	0	0	0	99.3
Spinel 3	3.78	0	3.51	57.86	0	4.91	0	21.6	0	0.86	0	0.83	5.35	0	0	0	98.73

Sample KRI 10

	Al2O3	CaO	Cr2O3	Fe2O3	K2O	MnO	Na2O	NiO	PbO	SiO2	SrO*	TiO2	ZnO	ZrO2	B2O3	Li2O	Total
1	13.27	0.52	0.409	7.3931	0.67	1.197	12.32	0.82	0	47.67	1.79	0.31	1.15	0	9.38	3.11	100
2	13.3	0.65	0.412	7.5083	0.68	1.094	12.9	0.71	0	47.01	1.8	0.16	1.28	0	9.38	3.11	100
3	12.944	0.67	0.554	7.6109	0.69	1.23	12.18	0.6	0	48.05	1.8	0	1.18	0	9.38	3.11	100
4	12.877	0.53	0.415	7.7042	0.57	1.225	12.24	0.72	0.61	46.8	1.81	0.31	1.06	0.64	9.38	3.11	100
5	12.325	0.65	0.409	7.4527	0.56	1.086	12.42	0.71	0.6	47.66	1.78	0.31	0.93	0.63	9.38	3.11	100
Average in area	13.111	0.54	0.427	7.7118	0.69	1.241	12.08	0.73	0.31	47.25	1.78	0.16	0.96	0.52	9.38	3.11	100
Average	12.946	0.6	0.442	7.5267	0.63	1.164	12.41	0.71	0.24	47.44	1.8	0.22	1.12	0.25	9.38	3.11	100
Spinel	1.89	nd	33.63	3.93	27.9	nd	4.78	nd	16.7	nd	0.86	nd	nd	7.97	nd	97.66	
Er/Re	1.3			0.5	0.9	0.6	0.5			3.3		24		1.5			

Sample KRI 11

	Al2O3	CaO	Cr2O3	Fe2O3	K2O	MnO	Na2O	NiO	SO3	SiO2	TiO2	ZnO	ZrO2	SrO	PbO	B2O3	Li2O	Total
1	15.147	0	0	8.0231	0.4	0.849	11.13	0.32	0	43.16	0.29	0.41	1.12	1.08	0	13.99	4.08	100
2	17.673	0.23	0.24	10.31	0.3	1.059	11.94	0.94	0.21	35.83	0.3	0.51	1.33	1.07	0	13.99	4.08	100
3	15.866	0.14	0	8.7026	0.4	0.959	10.2	0.31	0.41	41.58	0.26	0.41	1.33	1.36	0	13.99	4.08	100
4	16.128	0.11	0	8.8235	0.29	0.949	10.95	0.31	0.2	41.06	0.24	0.51	1.21	1.15	0	13.99	4.08	100
5	17.649	0	0	9.4043	0.4	0.969	11.46	0.42	0	38.74	0.28	0.52	1.01	1.08	0	13.99	4.08	100
Average	16.492	0.1	0.05	9.0501	0.36	0.959	11.14	0.46	0.16	40.07	0.28	0.47	1.2	1.15	0	13.99	4.08	100
Average in area	15.969	0	0.299	9.0169	0.49	0.918	10.15	0.52	0	42.72	0.17	0	0.96	0.72	0	13.99	4.08	100
Er/Re	3.41			3.43			0.54			7.15								

Sample KRI 12

	Al2O3	CaO	Cr2O3	Fe2O3	K2O	MnO	Na2O	NiO	SO3	SiO2	TiO2	ZnO	ZrO2	SrO	B2O3	Li2O	Totql
1	13.62	0.41	0.00	7.90	0.59	3.06	10.25	0.63	0.25	39.10	0.33	0.49	2.93	2.45	14.09	3.88	100.0
2	11.93	0.40	0.14	7.10	0.58	2.72	9.28	0.73	0.00	43.63	0.32	0.60	2.46	2.15	14.09	3.88	100.0
3	13.48	0.56	0.00	7.60	0.60	2.98	7.85	0.63	0.25	41.50	0.34	0.38	3.12	2.73	14.09	3.88	100.0
4	13.68	0.41	0.29	8.66	0.59	3.29	9.48	1.12	0.00	38.73	0.33	0.73	2.64	2.08	14.09	3.88	100.0
5	12.29	0.40	0.00	7.24	0.58	2.72	8.50	0.60	0.00	44.21	0.16	0.71	2.71	1.92	14.09	3.88	100.0
Average	13.00	0.44	0.09	7.70	0.58	2.95	9.07	0.74	0.10	41.44	0.30	0.58	2.77	2.27	14.09	3.88	100.0
Average in area	13.07	0.55	0.00	7.37	0.58	2.89	7.61	0.62	0.25	40.24	0.33	0.37	3.02	2.65	14.09	3.88	-
Er/Re	2.58			2.54			0.79			6.17							

Sample KRI 13

	Al2O3	Cr2O3	Fe2O3	K2O	MnO	Na2O	NiO	PbO	SO3	SiO2	TiO2	ZnO	ZrO2	SrO	B_2O_3	Li_2O	Total
1	12.57	0.31	7.39	0.76	2.86	12.24	0.67	0.80	0.00	43.63	0.71	1.45	1.57	1.25	10.79	3.00	100.00
2	13.37	0.16	7.77	0.66	3.09	12.47	0.55	1.17	0.00	41.72	0.73	1.35	1.62	1.54	10.79	3.00	100.00
3	12.63	0.32	8.29	0.53	2.83	12.11	0.56	0.83	0.00	43.39	0.73	1.50	1.33	1.17	10.79	3.00	100.00
4	13.61	0.31	7.52	0.52	2.78	12.46	0.55	0.93	0.54	42.34	0.72	1.47	1.45	1.02	10.79	3.00	100.00
5	12.80	0.31	7.25	0.64	2.73	12.98	0.40	0.80	0.53	43.04	0.71	1.32	1.57	1.13	10.79	3.00	100.00
Average	13.00	0.28	7.65	0.62	2.86	12.45	0.55	0.90	0.21	42.83	0.72	1.42	1.51	1.22	10.79	3.00	100.00
Average in area	13.11	0.31	7.65	0.63	2.85	12.18	0.67	0.57	0.53	42.52	0.70	1.57	1.56	1.37	10.79	3.00	100.00
Er/Re	1.2		1.40			0.20				1.60							

Sample KRI 14

	Al2O3	CaO	Cr2O3	Fe2O3	K2O	MnO	Na2O	NiO	PbO	SO3	SiO2	TiO2	ZnO	ZrO2	SrO	B2O3	Li2O	Total
1	12.09	0.14	0.00	6.92	0.23	2.75	9.27	0.86	0.63	0.00	42.74	0.65	1.21	0.92	1.15	15.46	5.00	100.00
2	13.33	0.14	0.00	7.45	0.25	3.04	10.61	0.78	0.88	0.00	38.74	0.85	1.27	1.10	1.09	15.46	5.00	100.00
3	13.58	0.14	0.30	7.77	0.25	2.92	8.99	1.18	0.66	0.51	38.45	0.69	1.53	1.25	1.33	15.46	5.00	100.00
4	13.45	0.14	0.30	7.41	0.24	3.02	9.59	0.91	0.77	0.00	39.62	0.68	1.52	0.69	1.20	15.46	5.00	100.00
5	12.03	0.28	0.44	6.96	0.24	2.57	9.11	0.89	0.75	0.00	41.95	0.83	0.99	1.21	1.29	15.46	5.00	100.00
Average	12.90	0.17	0.21	7.30	0.24	2.86	9.51	0.92	0.74	0.10	40.30	0.74	1.30	1.03	1.21	15.46	5.00	100.00
Average in area	13.00	0.00	0.28	7.33	0.23	2.75	9.66	0.86	0.73	0.48	39.81	0.65	1.21	1.18	1.37	15.46	5.00	100.00
Er/Re	1.9			1.2			1.7				3.9							

Sample KRI 15

	Al_2O_3	Cr_2O_3	Fe_2O_3	K_2O	MnO	Na_2O	NiO	PbO	SO_3	SiO_2	TiO_2	ZnO	ZrO_2	SrO	B_2O_3	Li_2O	Total
1	17.03	0.00	8.77	0.49	1.19	10.48	0.78	0.66	0.26	39.67	0.17	0.64	1.38	1.33	13.68	3.32	100.00
2	17.58	0.00	8.34	0.73	1.18	11.45	0.77	0.65	0.00	39.19	0.34	0.50	0.96	1.31	13.68	3.32	100.00
3	19.17	0.31	9.95	0.63	1.22	10.71	0.67	0.00	0.00	37.38	0.00	0.65	0.85	1.48	13.68	3.32	100.00
4	12.81	0.29	7.48	0.71	1.02	9.40	0.62	0.53	0.00	47.32	0.00	0.49	1.06	1.28	13.68	3.32	100.00
5	17.96	0.00	8.65	0.49	1.04	12.39	0.51	0.00	0.25	38.30	0.34	0.50	1.23	1.19	13.68	3.32	100.00
Average	16.91	0.12	8.64	0.61	1.13	10.89	0.67	0.37	0.10	40.37	0.17	0.56	1.10	1.32	13.68	3.32	100.00
Average in area	15.57	0.29	8.44	0.61	1.17	11.24	0.64	0.00	0.50	41.52	0.00	0.50	1.09	1.43	13.68	3.32	100.00
Er/Re	6.1		3.0			0.7				8.0							

Sample KRI 16

	Al2O3	CaO	Cr2O3	Fe2O3	K2O	MnO	Na2O	NiO	PbO	SO3	SiO2	TiO2	ZnO	ZrO2	SrO*	B2O3*	Li2O*	Total
1	13.32	0.12	0.25	7.83	0.21	1.01	9.87	0.66	0.75	0.43	41.16	0.73	1.41	2.58	2.25	12.50	4.92	100.00
2	13.25	0.14	0.00	8.27	0.12	1.18	9.24	0.65	0.77	0.51	41.11	0.85	1.64	2.61	2.25	12.50	4.92	100.00
3	11.68	0.13	0.28	7.47	0.23	0.86	8.89	0.73	0.51	0.48	44.18	0.63	1.30	2.95	2.25	12.50	4.92	100.00
4	12.77	0.13	0.27	7.51	0.23	0.97	10.53	0.72	0.71	0.47	41.20	0.63	1.40	2.79	2.25	12.50	4.92	100.00
5	13.13	0.27	0.28	7.89	0.11	1.11	10.08	0.73	0.82	0.48	40.55	0.64	1.42	2.83	2.25	12.50	4.92	100.00
Average in area	12.10	0.12	0.26	7.51	0.21	1.02	8.74	0.78	0.94	0.66	42.99	0.73	1.42	2.84	2.25	12.50	4.92	100.00
Average	12.83	0.16	0.22	7.79	0.18	1.03	9.72	0.70	0.71	0.47	41.64	0.69	1.44	2.75	2.25	12.50	4.92	100.00
Er/Re	2.2			1.4			0.5				3.4							

Sample KRI-17

	Al2O3	CaO	Cr2O3	Fe2O3	K2O	MnO	Na2O	NiO	SiO2	SrO*	TiO2	ZnO	ZrO2	B2O3*	Li2O*	Total
1	12.25	0.41	0.29	7.85	0.35	1.78	9.26	0.50	45.61	2.25	0.16	0.49	2.52	12.40	3.88	100.00
2	11.48	0.41	0.00	7.56	0.35	1.65	9.77	0.50	46.58	2.25	0.16	0.49	2.51	12.40	3.88	100.00
3	11.21	0.54	0.28	7.38	0.23	1.73	11.35	0.49	45.89	2.25	0.16	0.36	2.58	12.40	3.88	100.00
4	13.67	0.56	0.15	9.04	0.36	2.08	10.01	0.51	41.71	2.25	0.17	0.50	2.71	12.40	3.88	100.00
5	11.97	0.54	0.00	7.79	0.35	1.76	9.19	0.37	46.08	2.25	0.16	0.48	2.76	12.40	3.88	100.00
Average	12.12	0.49	0.14	7.92	0.33	1.80	9.92	0.47	45.18	2.25	0.16	0.46	2.62	12.40	3.88	
Average in area.	13.34	0.564	0	8.5	0.24	1.82	10.32	0.4	43.17	2.25	0.17	0.5	2.45	12.40	3.88	100.00
Er/Re	2.9			2.6			0.7		5.9							

Sample KRI-18

	Al2O3	CaO	Cr2O3	Fe2O3	K2O	MnO	Na2O	NiO	SiO2	TiO2	ZnO	ZrO2	SrO	B2O3	Li2O	Сумма
1	4.22	0.00	0.00	3.57	0.00	0.58	6.13	0.00	64.02	0.30	0.89	1.20	0.74	14.83	3.52	100.0
2	14.79	0.14	0.30	7.84	0.25	1.05	11.78	0.52	40.03	0.85	1.52	2.61	0.00	14.83	3.52	100.0
3	15.79	0.14	0.30	8.00	0.12	1.05	12.21	0.64	37.07	0.85	1.64	2.75	1.08	14.83	3.52	100.0
4	8.19	0.00	0.14	5.12	0.23	0.85	9.39	0.36	53.85	0.32	1.17	2.04	0.00	14.83	3.52	100.0
5	16.35	0.14	0.31	8.18	0.25	1.08	12.08	0.53	37.50	0.87	1.69	2.67	0.00	14.83	3.52	100.0
Average	11.87	0.08	0.21	6.54	0.17	0.92	10.32	0.41	46.49	0.64	1.38	2.25	0.36	14.83	3.52	
Average in area	14.81	0.14	0.30	8.00	0.25	1.05	10.84	0.64	39.25	0.85	1.64	3.03	0.84	14.83	3.52	100.0
Er/Re	16.25			8.3			2.16		30.31							

Sample KRI 19

	Al2O3	CaO	Cr2O3	Fe2O3	K2O	MnO	Na2O	NiO	SiO2	TiO2	ZnO	ZrO2	SrO*	B2O3*	Li2O*	Total
1	13.65	0.00	0.00	9.21	0.23	2.74	13.92	0.61	38.96	0.64	0.60	1.69	2.25	11.12	4.37	100.00
2	13.24	0.14	0.28	9.03	0.23	3.02	13.70	0.99	39.79	0.65	0.00	1.18	2.25	11.12	4.37	100.00
3	13.47	0.27	0.29	9.48	0.24	2.77	12.66	0.75	39.72	0.81	0.49	1.32	2.25	11.12	4.37	100.00
4	13.78	0.00	0.14	9.01	0.24	2.80	13.76	0.88	39.67	0.66	0.00	1.33	2.25	11.12	4.37	100.00
5	13.50	0.27	0.00	8.80	0.24	3.03	13.78	0.87	39.17	0.65	0.49	1.45	2.25	11.12	4.37	100.00
Average in area	13.84	0.14	0.14	9.33	0.24	2.94	12.82	0.76	39.18	0.66	0.62	1.60	2.25	11.12	4.37	100.00
Average	13.53	0.14	0.14	9.11	0.23	2.87	13.56	0.82	39.46	0.68	0.31	1.40	2.25	11.12	4.37	100.00
Er/Re	0.6			1.1			0.4		0.8							

Sample KRI-20

	Al2O3	CaO	Cr2O3	Fe2O3	K2O	MnO	Na2O	NiO	PbO	SiO2	SrO*	TiO2	ZnO	ZrO2	B2O3*	Li2O*	Total
1	16.85	0.56	0.29	9.30	0.24	1.29	11.20	0.51	0.54	38.16	2.25	0.17	0.00	0.85	14.79	3.00	100.00
2	16.61	0.57	0.15	9.34	0.25	1.19	11.01	0.65	0.00	38.94	2.25	0.34	0.00	0.91	14.79	3.00	100.00
3	16.14	0.42	0.29	9.36	0.24	1.28	11.11	0.63	0.53	38.27	2.25	0.33	0.49	0.85	14.79	3.00	100.00
4	15.70	0.41	0.14	9.04	0.24	1.15	11.86	0.50	0.00	40.03	2.25	0.00	0.00	0.87	14.79	3.00	100.00
5	16.41	0.42	0.15	9.37	0.24	1.30	11.29	0.51	0.00	38.70	2.25	0.17	0.50	0.88	14.79	3.00	100.00
Average	16.34	0.47	0.2	9.28	0.24	1.24	11.3	0.56	0.21	38.82	2.3	0.2	0.2	0.873	14.79	3.00	
Average in area.	16.17	0.54	0.00	9.44	0.12	1.13	11.79	0.62	0.00	38.71	2.25	0.32	0.36	0.77	14.79	3.00	100.00
Er/Re	1.1			0.5			0.4			2.4							

Sample KRI 21

	Al2O3	CaO	Fe2O3	K2O	MnO	Na2O	NiO	PbO	SO3	SiO2	TiO2	ZnO	ZrO2	SrO*	B2O3*	Li2O*	Total
1	14.84	0.56	8.03	0.36	1.30	13.18	0.90	0.43	0.50	39.44	0.34	0.50	3.67	0.82	11.83	3.29	100.00
2	14.31	0.54	7.40	0.35	0.99	14.82	0.73	0.62	0.00	39.61	0.32	0.60	3.50	0.82	11.83	3.29	100.00
3	14.53	0.55	7.61	0.48	1.27	14.25	0.88	0.53	0.49	39.05	0.33	0.49	3.59	0.82	11.83	3.29	100.00
4	14.22	0.41	7.79	0.35	1.39	14.37	0.87	0.53	0.49	38.90	0.33	0.73	3.69	0.82	11.83	3.29	100.00
5	14.54	0.55	7.99	0.36	1.40	14.50	0.88	0.74	0.00	38.42	0.33	0.61	3.73	0.82	11.83	3.29	100.00
Average in area	14.17	0.55	7.99	0.36	1.27	14.38	1.00	0.53	0.49	38.64	0.33	0.61	3.73	0.82	11.83	3.29	100.00
Average	14.49	0.52	7.77	0.38	1.27	14.22	0.85	0.57	0.30	39.08	0.33	0.59	3.64	0.82	11.83	3.29	
Er/Re	0.8		1.1			0.5				1.1							

Sample KRI 22

	Al2O3	CaO	Cr2O3	Fe2O3	K2O	MnO	Na2O	NiO	SO3	SiO2	TiO2	ZnO	ZrO2	SrO*	B2O3*	Li2O*	Total
1	15.47	0.13	0.00	7.66	0.11	0.97	12.17	0.84	0.47	38.47	0.79	0.59	3.56	2.25	11.52	5.00	100.00
2	16.38	0.13	0.00	8.21	0.22	1.06	13.15	0.58	0.46	36.14	0.76	0.57	3.57	2.25	11.52	5.00	100.00
3	16.17	0.27	0.00	8.14	0.23	1.10	12.93	0.85	0.48	36.22	0.79	0.47	3.59	2.25	11.52	5.00	100.00
4	16.34	0.26	0.27	8.23	0.22	1.08	13.02	0.83	0.46	35.42	0.62	0.46	4.02	2.25	11.52	5.00	100.00
5	16.01	0.26	0.27	8.29	0.11	1.07	13.40	0.59	0.46	36.28	0.77	0.00	3.73	2.25	11.52	5.00	100.00
Average in area	15.29	0.26	0.27	7.92	0.23	1.09	10.55	0.72	0.47	39.66	0.63	0.70	3.43	2.25	11.52	5.00	100.00
Average	16.07	0.21	0.11	8.11	0.18	1.06	12.94	0.74	0.47	36.50	0.75	0.42	3.69	2.25	11.52	5.00	100.00
Er/Re	1.2			1.1			0.4			2.8							

Sample KRI 23

	Al2O3	CaO	Fe2O3	K2O	MnO	Na2O	NiO	PbO	SO3	SiO2	TiO2	ZnO	ZrO2	SrO*	B2O3*	Li2O*	Total
1	18.20	0.00	7.57	0.70	1.12	11.64	0.37	0.52	0.72	40.21	0.32	0.72	1.56	0.75	12.60	3.00	100.00
2	19.12	0.27	7.84	0.70	1.12	12.13	0.49	0.62	0.48	38.16	0.32	0.96	1.43	0.75	12.60	3.00	100.00
3	18.83	0.14	7.89	0.71	1.15	11.31	0.50	0.74	0.49	39.49	0.33	0.74	1.33	0.75	12.60	3.00	100.00
4	18.58	0.13	7.71	0.81	1.12	12.61	0.61	0.73	0.48	38.38	0.32	0.72	1.43	0.75	12.60	3.00	100.00
5	18.26	0.00	7.89	0.71	1.15	11.31	0.50	0.74	0.25	40.74	0.16	0.61	1.33	0.75	12.60	3.00	100.00
Average in area	17.40	0.13	8.36	0.69	1.24	10.40	0.61	0.72	0.24	40.86	0.32	0.84	1.55	0.75	12.60	3.00	99.72
Average	18.60	0.11	7.78	0.73	1.13	11.80	0.49	0.67	0.49	39.40	0.29	0.75	1.42	0.75	12.60	3.00	100.00
Er/Re	1.3		0.6			0.5				2.6							

Sample KRI24

	Al2O3	CaO	Cr2O3	Fe2O3	K2O	MnO	Na2O	NiO	SiO2	SrO*	TiO2	ZnO	ZrO2	B2O3*	Li2O*	Total
1	13.65	0.42	0.15	8.88	0.60	2.07	11.08	0.64	43.38	1.18	0.50	1.00	2.98	9.69	3.77	100.00
2	14.16	0.57	0.00	8.68	0.61	2.22	9.96	0.52	44.23	1.18	0.68	1.01	2.74	9.69	3.77	100.00
3	13.92	0.42	0.15	8.22	0.61	2.09	10.74	0.51	44.72	1.18	0.51	0.88	2.59	9.69	3.77	100.00
4	13.48	0.57	0.00	8.00	0.61	1.97	9.33	0.39	46.45	1.18	0.51	1.01	3.03	9.69	3.77	100.00
5	12.52	0.43	0.00	7.86	0.74	1.84	8.79	0.52	48.42	1.18	0.34	0.89	3.03	9.69	3.77	100.00
Average	13.55	0.48	0.06	8.33	0.63	2.04	9.98	0.51	45.44	1.18	0.51	0.96	2.87	9.69	3.77	100.00
Average in area	12.21	0.42	0.29	7.81	0.72	2.05	9.78	0.51	47.66	1.18	0.50	0.74	2.68	9.69	3.77	100.00
Er/Re	2.3			2				0.8				4.5				

Sample KRI 25

	Al2O3	CaO	Cr2O3	Fe2O3	K2O	MnO	Na2O	NiO	SiO2	SrO*	TiO2	ZnO	ZrO2	B2O3*	Li2O*	Total
1	16.02	0.28	0.15	10.68	0.60	1.16	11.56	0.38	40.78	0.75	0.00	0.37	0.00	13.51	3.75	100.00
2	13.77	0.14	0.00	9.56	0.71	1.14	9.42	0.50	45.52	0.75	0.16	0.00	1.06	13.51	3.75	100.00
3	15.65	0.00	0.00	11.11	0.48	1.16	11.83	0.00	40.79	0.75	0.17	0.00	0.81	13.51	3.75	100.00
4	15.88	0.14	0.00	10.41	0.61	1.18	10.36	0.26	42.03	0.75	0.17	0.00	0.96	13.51	3.75	100.00
5	14.66	0.14	0.00	10.38	0.47	1.14	11.51	0.37	42.25	0.75	0.00	0.00	1.06	13.51	3.75	100.00
Average	15.19	0.14	0.03	10.43	0.58	1.16	10.94	0.30	42.28	0.75	0.10	0.07	0.78	13.51	3.75	100.00
Average in area	15.60	0.14	0.00	10.82	0.59	1.13	11.78	0.37	40.76	0.75	0.32	0.48	0.00	13.51	3.75	100.00
Er/Re	2.80			2.30					0.90			5.40				

Sample KRI 26

	Al2O3	CaO	Fe2O3	Na2O	NiO	SO3	SiO2	SrO	UO3	B2O3	Li2O	Total
1	10.05	0.64	10.47	13.59	3.15	0.46	40.43	3.03	1.98	10.19	6.00	100.00
2	10.15	0.79	10.50	13.46	3.00	0.71	41.16	2.34	1.70	10.19	6.00	100.00
3	10.64	0.77	10.28	14.30	2.94	0.46	40.12	2.73	1.55	10.19	6.00	100.00
4	10.30	0.76	10.50	13.21	2.54	0.68	40.62	3.33	1.85	10.19	6.00	100.00
5	10.18	0.64	10.69	13.77	3.02	0.68	40.25	2.59	1.97	10.19	6.00	100.00
Average in area	10.52	0.77	10.17	13.90	2.67	0.46	40.65	2.80	1.86	10.19	6.00	100.00
Average	10.26	0.72	10.49	13.67	2.93	0.60	40.52	2.80	1.81	10.19	6.00	100.00
Er/Re	0.7		0.8	0.5			1.3					

Sample KRI 27

	Al2O3	CaO	Cr2O3	Fe2O3	MnO	Na2O	NiO	PbO	SO3	SiO2	TiO2	UO3	ZrO2	B2O3	Li2O	Total
1	10.63	0.75	0.26	9.69	0.81	10.82	0.00	1.44	0.00	36.49	0.89	0.86	4.46	17.20	5.73	100.00
2	10.54	0.75	0.66	10.02	0.58	10.06	0.34	0.87	0.67	35.63	1.05	1.30	4.62	17.20	5.73	100.00
3	9.71	0.84	0.50	9.05	0.66	10.62	0.44	1.01	0.86	35.39	0.86	1.34	4.97	17.20	5.73	100.00
4	10.22	0.64	0.54	9.56	0.71	10.63	0.00	1.38	0.00	37.89	1.07	0.00	4.46	17.20	5.73	100.00
5	10.91	0.76	0.66	9.92	0.58	9.85	0.46	1.17	0.68	35.93	1.05	0.87	4.26	17.20	5.73	100.00
Average in area	10.53	0.73	0.64	9.70	0.67	10.68	0.66	1.13	0.44	35.42	1.31	0.84	4.35	17.20	5.73	100.00
Average	10.40	0.75	0.52	9.65	0.67	10.39	0.25	1.18	0.44	36.27	0.99	0.87	4.55	17.20	5.73	100.00
Er/Re	1.3			2.0		0.5				3.1						

Sample KRI 28

	Al2O3	CaO	Cr2O3	Fe2O3	MnO	Na2O	NiO	PbO	SO3	SiO2	SrO	TiO2	UO3	B2O3	Li2O	Total
1	18.03	0.00	0.90	5.25	4.18	18.16	0.00	1.04	0.66	36.54	0.00	0.88	2.52	6.13	5.72	100.00
2	17.34	0.00	0.93	4.93	4.11	16.89	0.00	1.37	0.68	37.73	0.00	1.21	2.95	6.13	5.72	100.00
3	17.59	0.00	0.50	4.92	4.23	18.93	0.00	1.02	0.65	36.71	0.00	1.01	2.59	6.13	5.72	100.00
4	17.81	0.00	0.91	5.21	4.36	18.21	0.00	1.05	0.44	36.55	0.00	1.04	2.56	6.13	5.72	100.00
5	17.78	0.00	1.21	4.72	4.14	18.38	0.00	1.00	0.52	36.51	0.00	1.04	2.86	6.13	5.72	100.00
Average in area	17.67	0.00	0.92	5.39	4.41	17.44	0.00	1.07	0.45	37.15	0.00	1.05	2.59	6.13	5.72	100.00
Average	17.71	0.00	0.89	5.01	4.20	18.11	0.00	1.10	0.59	36.81	0.00	1.03	2.70	6.13	5.72	100.00
Er/Re	0.8			1.2		1.0				1.6						

Sample KRI 29

	Al2O3	Fe2O3	K2O	MgO	Na2O	NiO	PbO	SiO2	SrO	TiO2	UO3	B2O3	Li2O	Total
1	14.47	5.61	0.87	0.00	20.21	3.03	1.00	35.43	1.59	1.04	3.36	11.38	2.00	100.00
2	13.83	5.51	0.98	0.00	19.99	3.10	0.98	35.24	2.04	1.02	3.91	11.38	2.00	100.00
3	13.21	5.64	0.85	0.00	19.25	3.22	1.31	35.14	2.16	1.18	4.63	11.38	2.00	100.00
4	13.88	5.81	0.72	0.99	20.06	2.78	1.18	34.85	1.99	0.99	3.34	11.38	2.00	100.00
5	14.22	5.89	0.87	0.00	19.03	3.28	1.00	35.75	1.95	1.03	3.59	11.38	2.00	100.00
Average in area	14.27	5.91	0.87	0.00	17.98	3.16	0.89	36.31	2.20	1.04	3.98	11.38	2.00	100.00
Average	13.92	5.69	0.86	0.20	19.71	3.08	1.09	35.28	1.95	1.05	3.76	11.38	2.00	100.00
Er/Re	1.4	0.8			0.7			1.0						

Sample KRI 30

	Al2O3	CaO	Fe2O3	Na2O	PbO	SO3	SiO2	ZnO	SrO	UO3	B2O3	Li2O	
1	18.60	0.55	5.06	7.03	1.06	0.25	39.82	1.71	2.09	2.72	15.30	5.79	100.00
2	19.61	0.55	5.22	7.85	1.06	0.49	37.65	1.97	1.63	2.85	15.30	5.79	100.00
3	19.60	0.56	5.47	7.06	1.08	0.50	38.16	2.13	1.43	2.90	15.30	5.79	100.00
4	20.03	0.55	5.38	7.48	1.07	0.74	36.48	1.97	2.46	2.74	15.30	5.79	100.00
5	19.72	0.55	5.34	7.30	0.95	0.49	37.30	1.96	2.44	2.84	15.30	5.79	100.00
Average in area	19.61	0.54	5.40	7.97	1.15	0.00	36.96	2.05	2.41	2.80	15.30	5.79	100.00
Average	19.51	0.55	5.29	7.34	1.05	0.50	37.88	1.95	2.01	2.81	15.30	5.79	100.00
Er/Re	4.15		1.05	0.57			6.23						

Attachment 2. SEM Photographs of Quenched Glasses

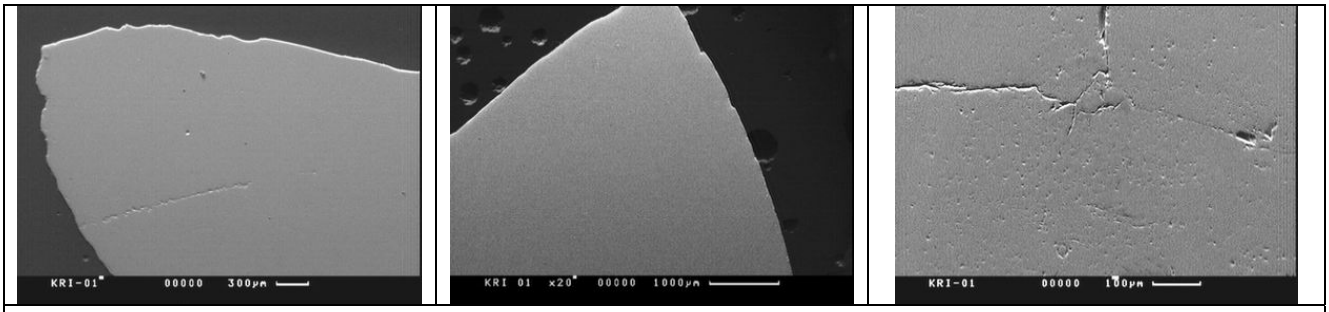

KRI-01

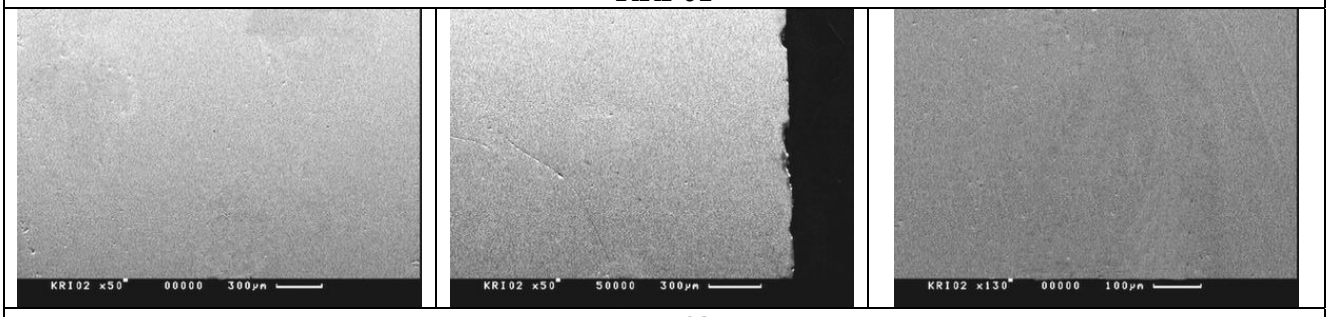

KRI-02

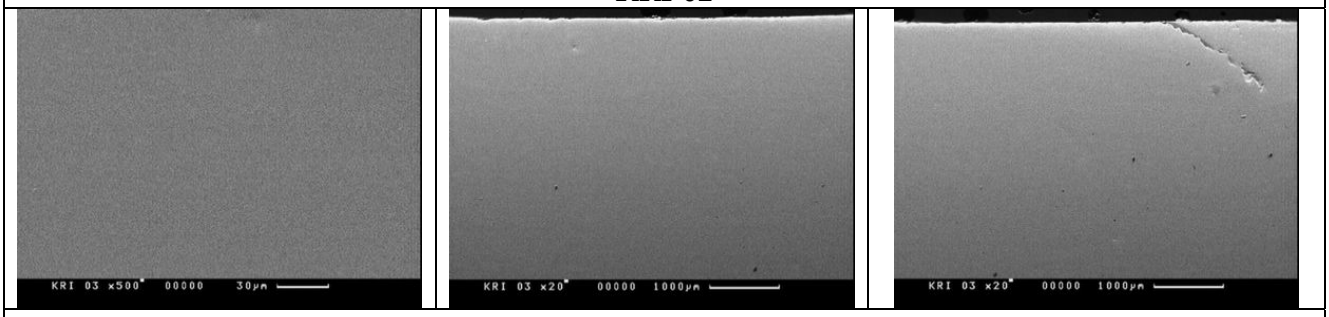

KRI-03

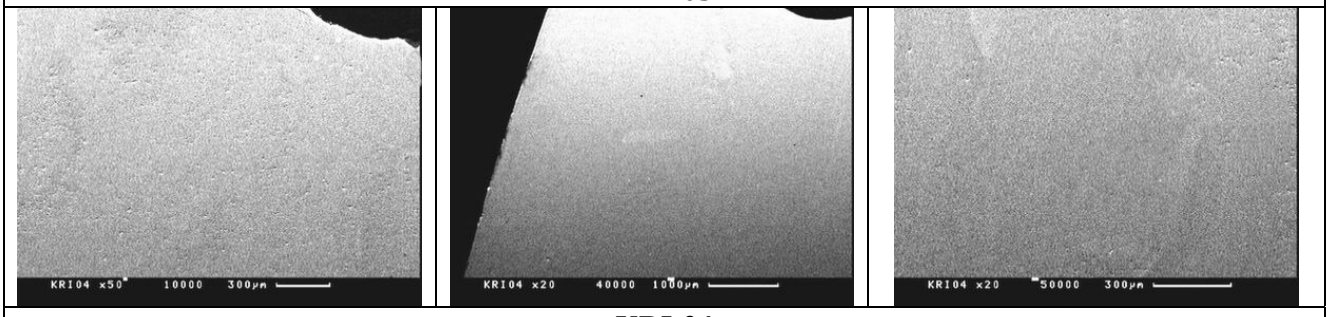

KRI-04

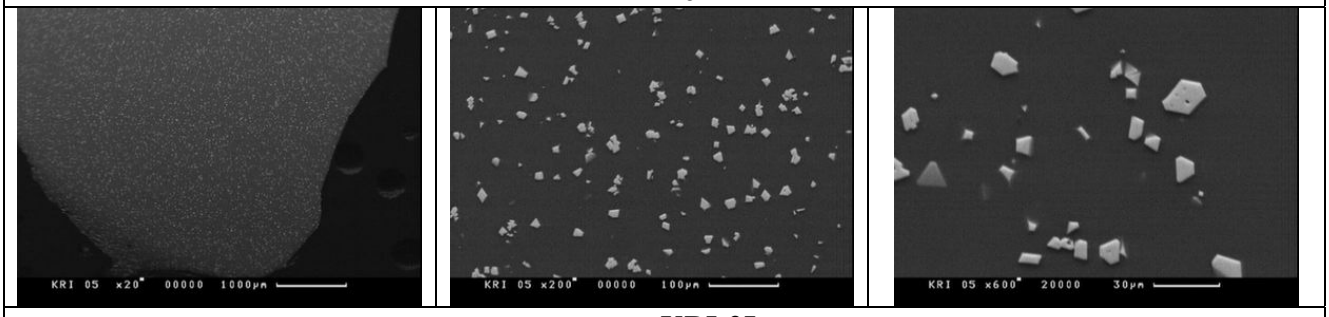

KRI-05

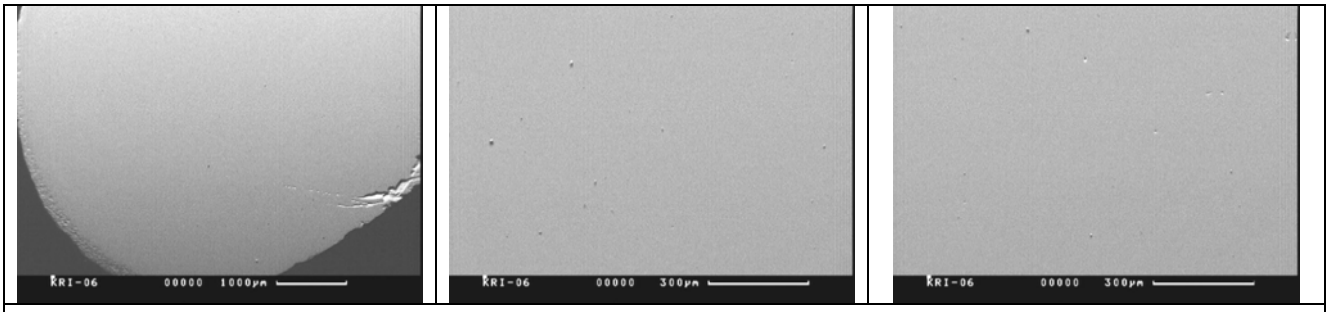

KRI-06

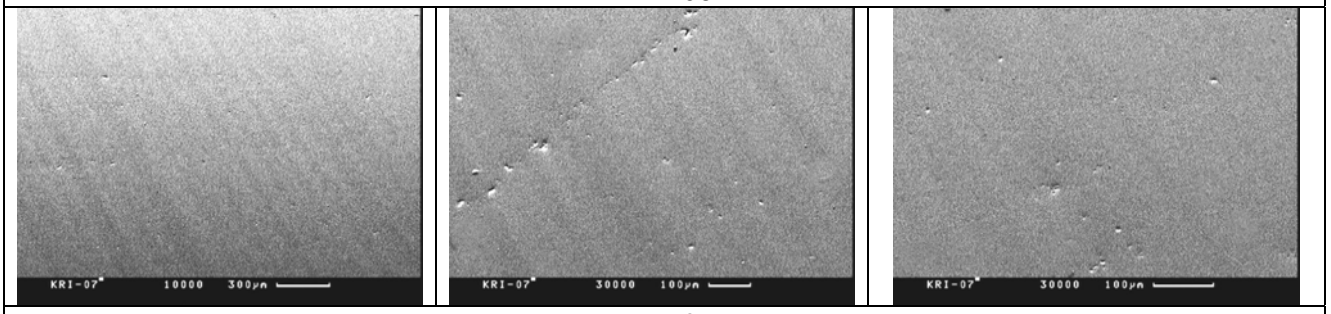

KRI-07

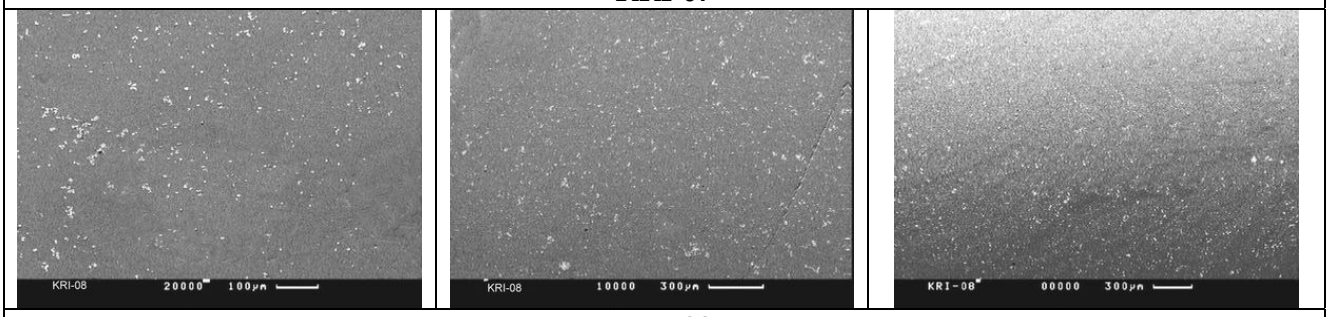

KRI-08

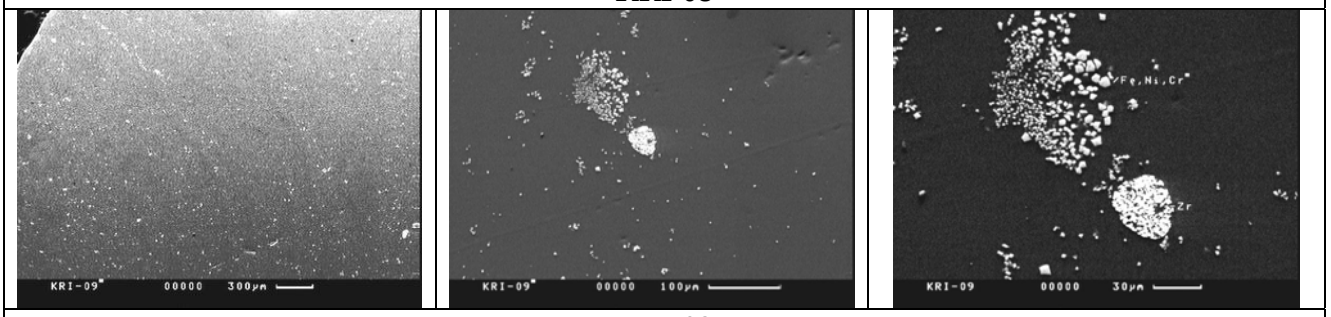

KRI-09

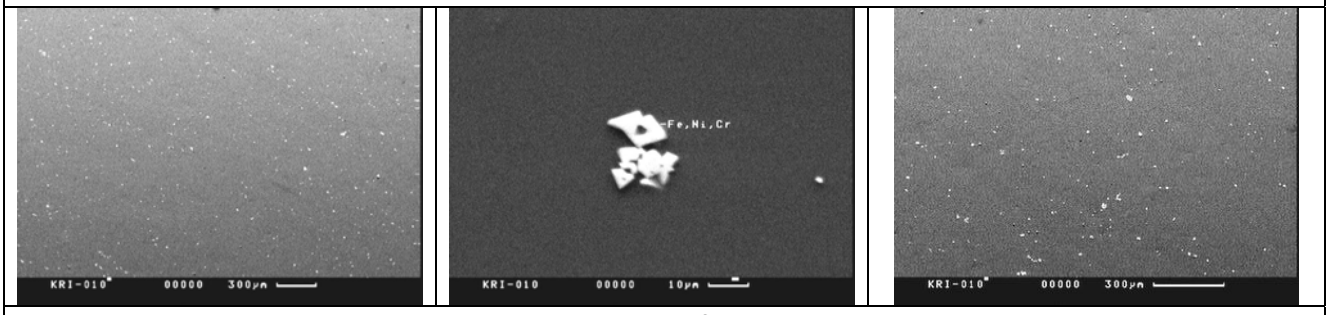

KRI-10

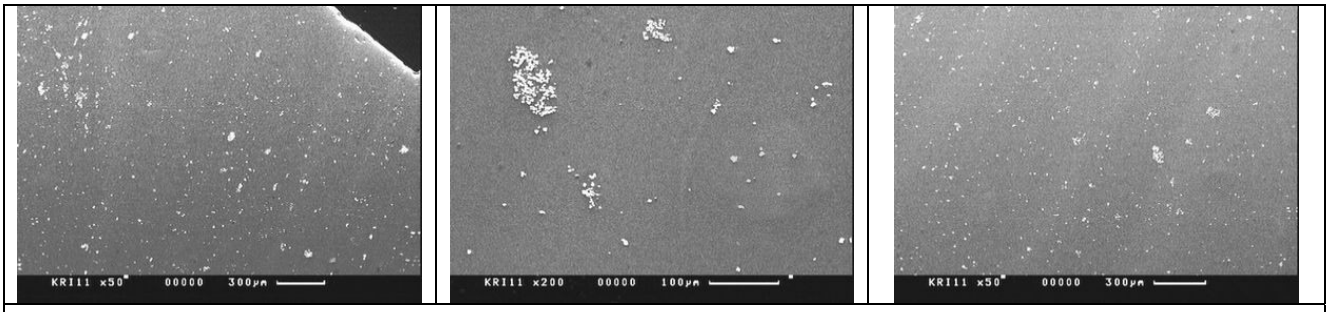

KRI-11

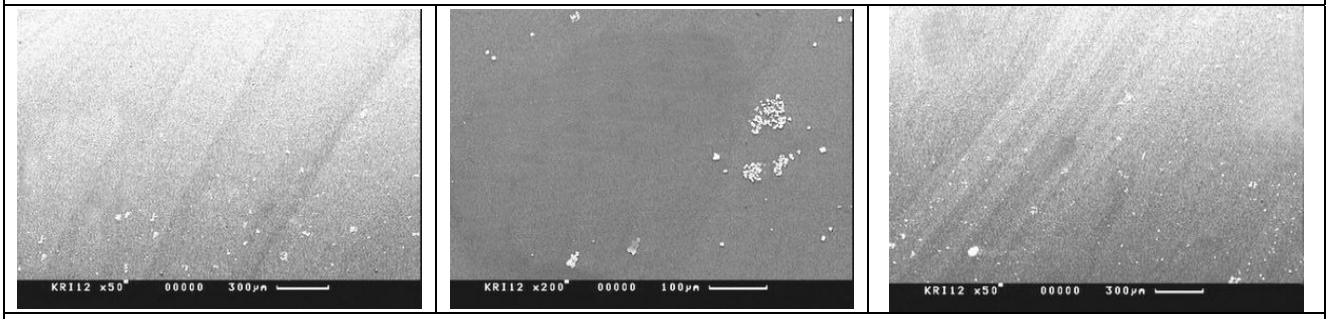

KRI-12

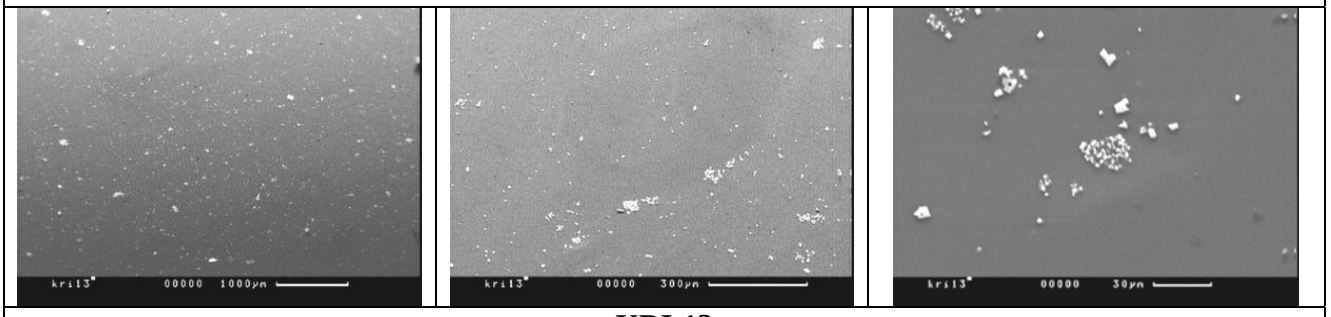

KRI-13

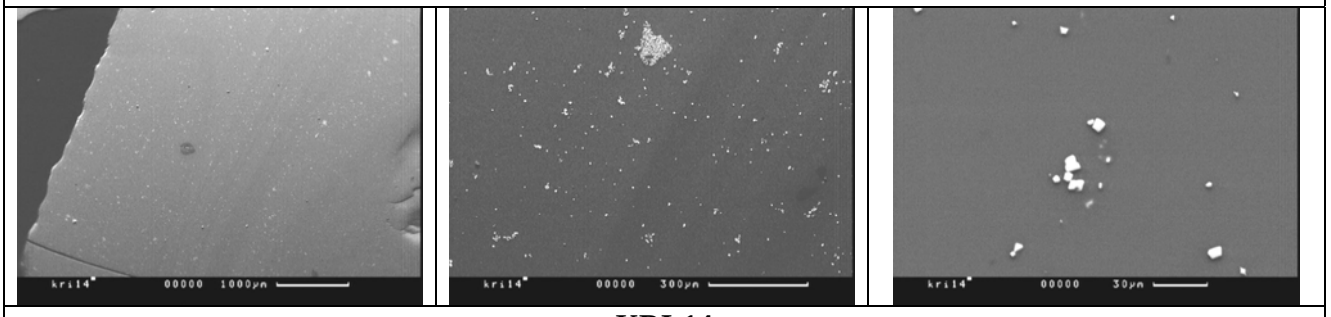

KRI-14

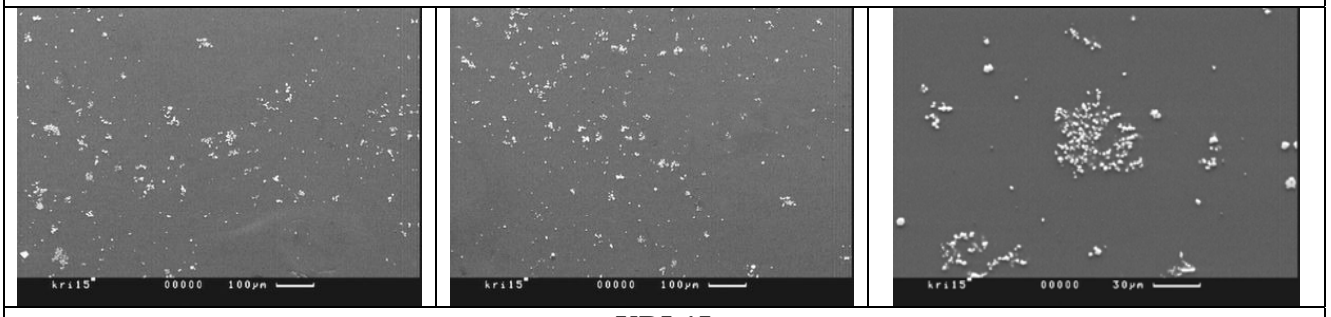

KRI-15

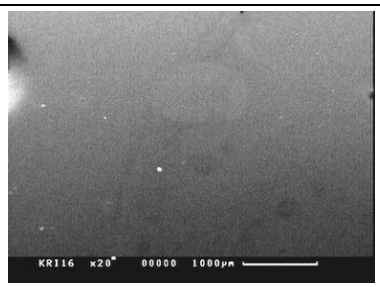
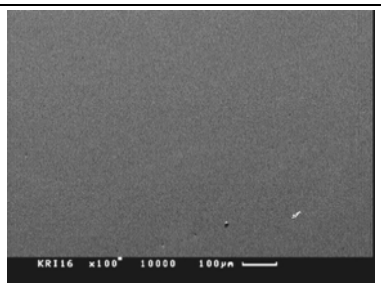
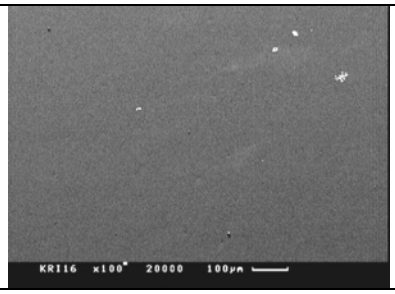

KRI-16

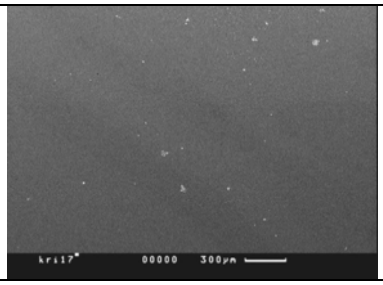
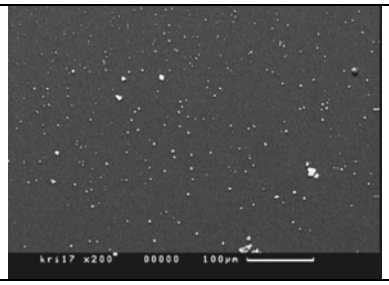
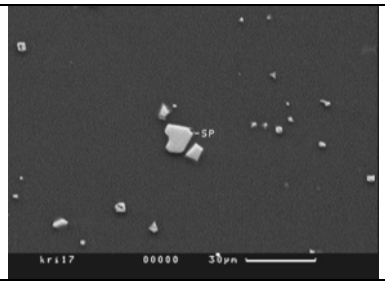

KRI-17

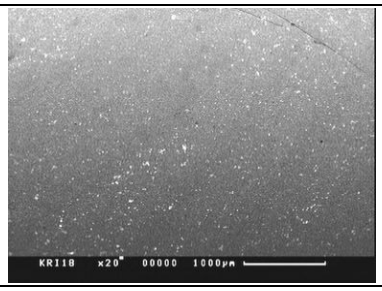
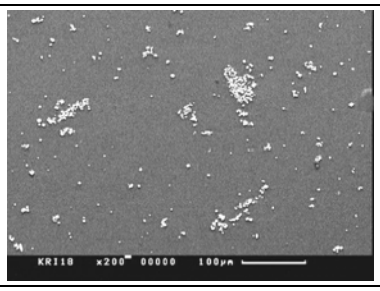
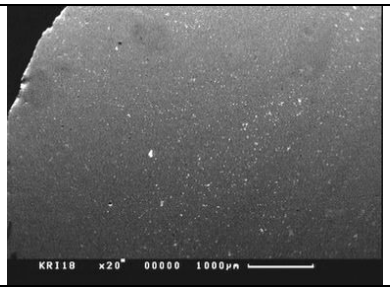

KRI-18

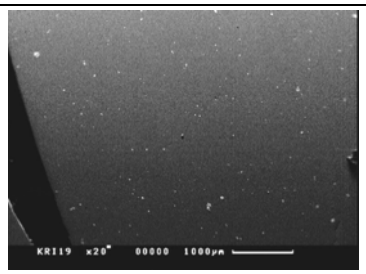
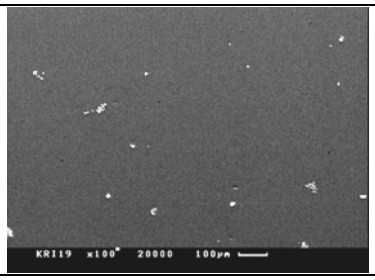
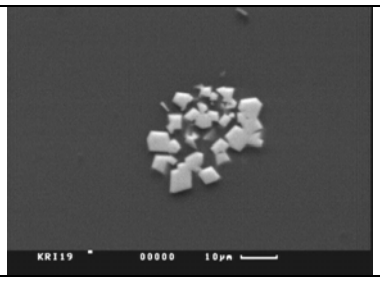

KRI-19

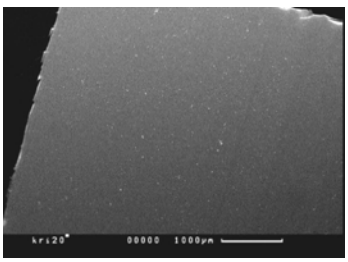
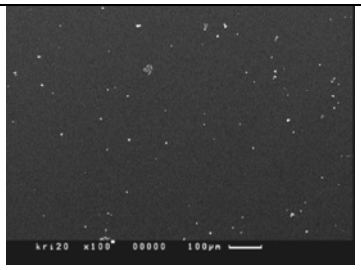
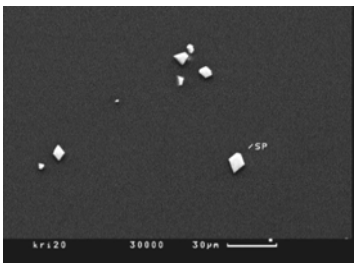

KRI-20

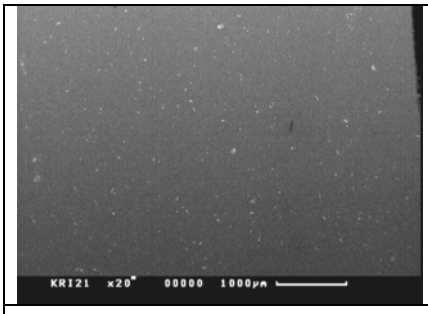

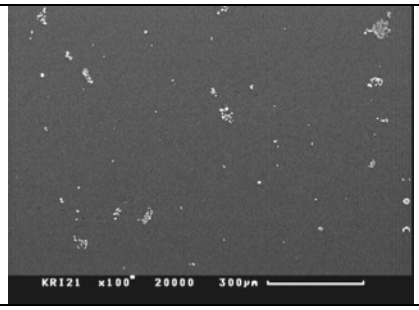

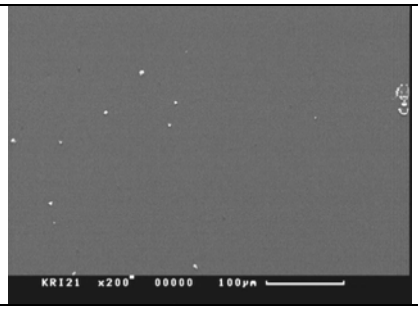

KRI-21

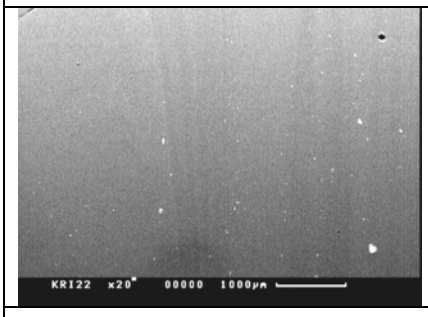

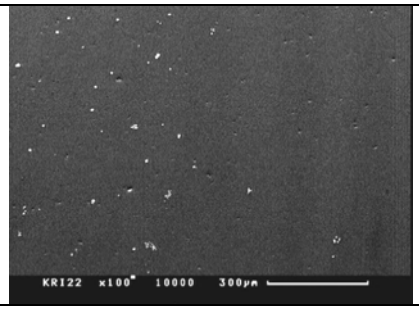

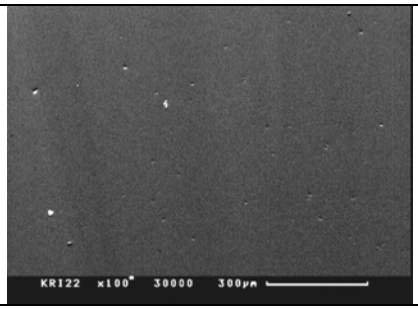

KRI-22

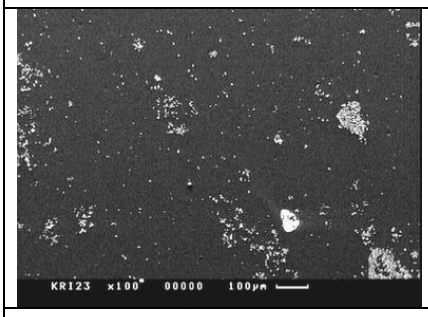

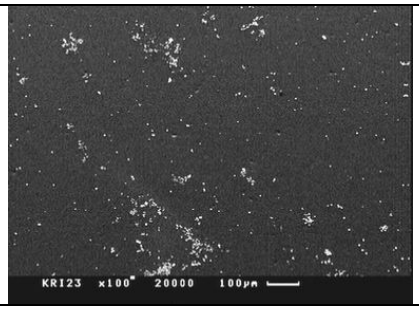

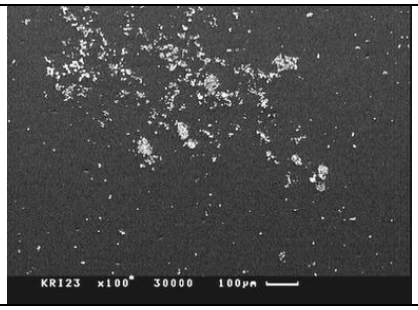

KRI-23

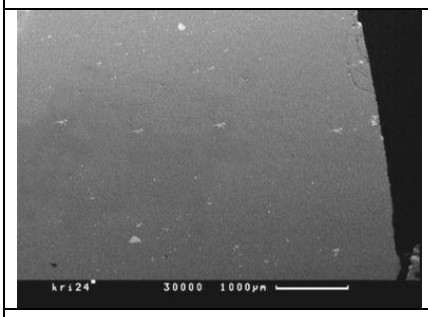

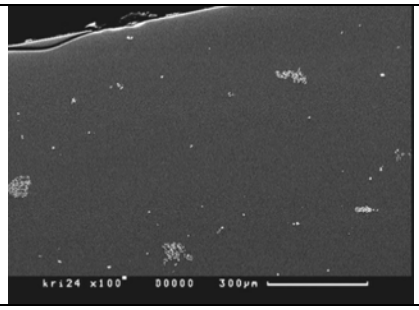

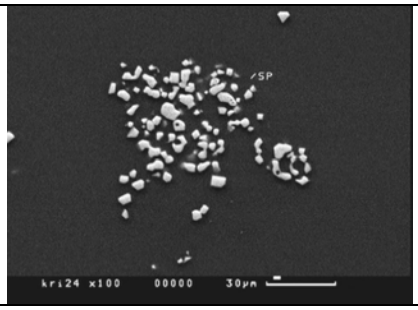

KRI-24

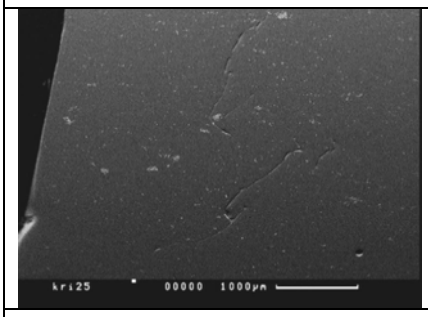

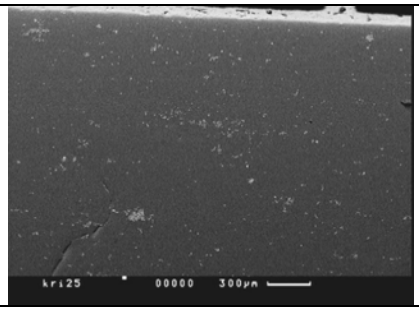

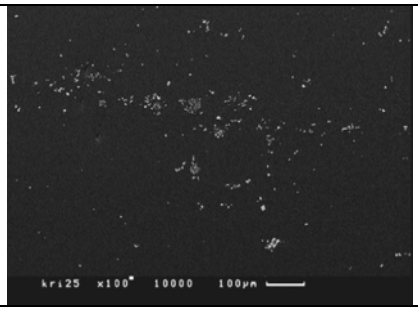

KRI-25

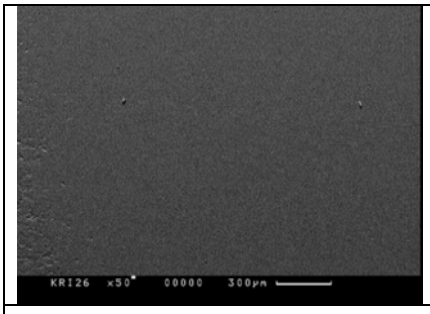

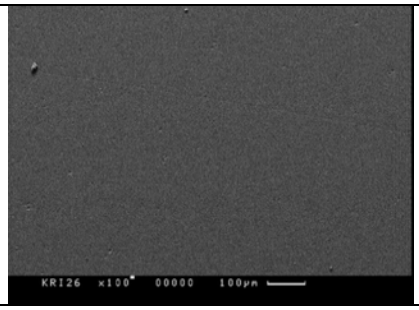

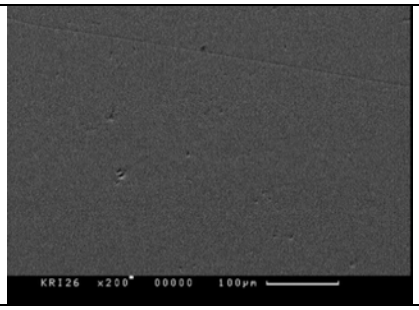

KRI-26

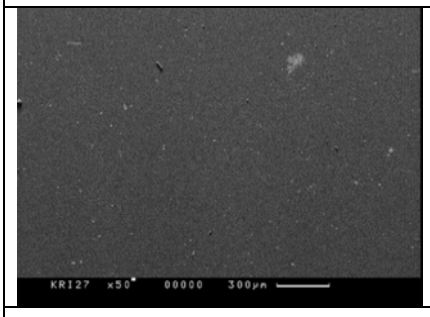

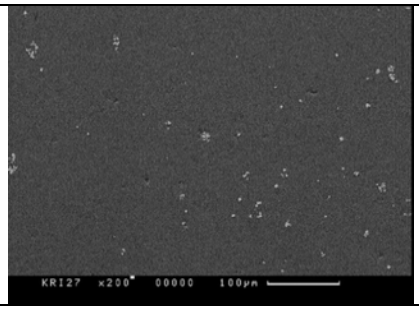

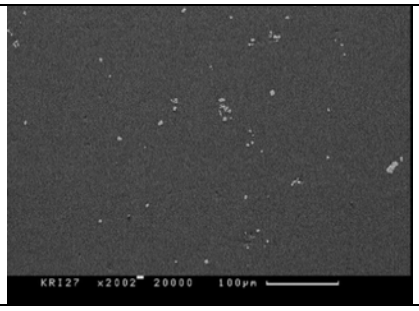

KRI-27

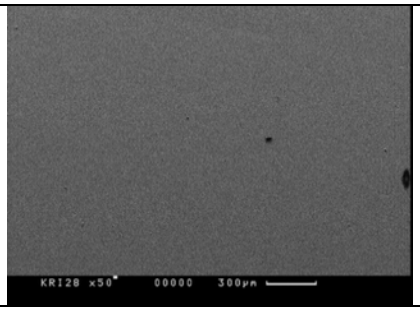

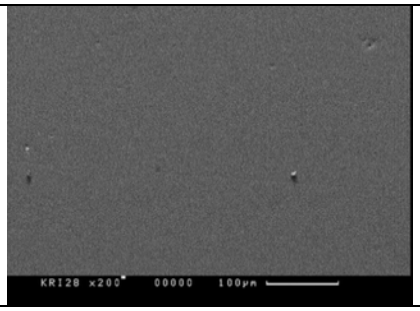

KRI-28

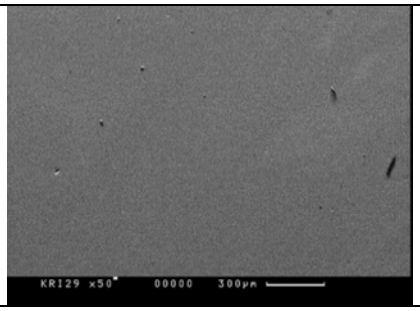

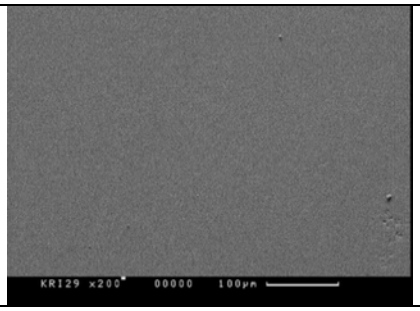

KRI-29

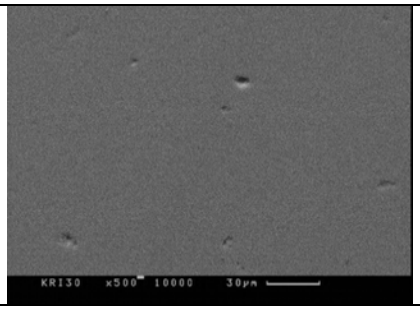

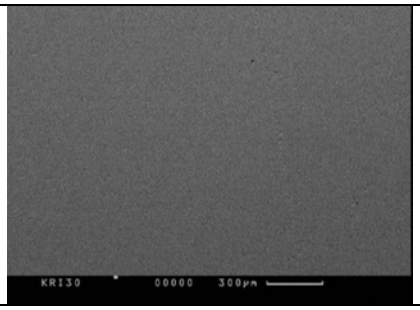

KRI-30

Attachment 3. XRD Data for Quenched Glasses

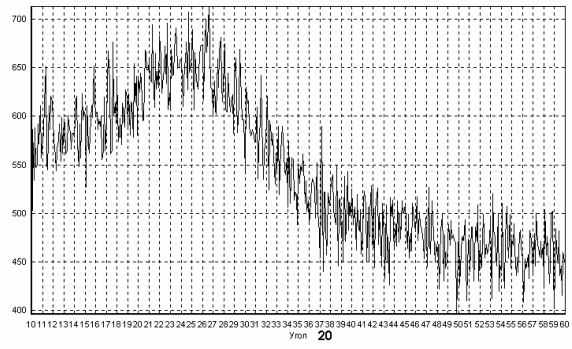

KRI-01

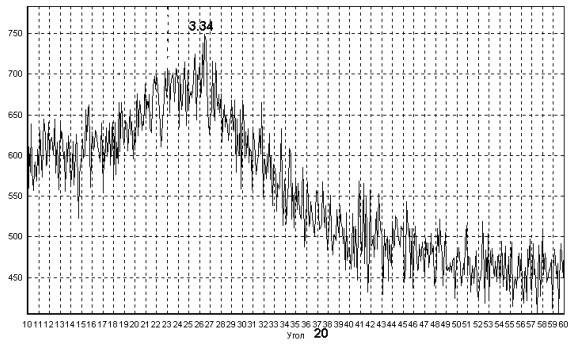

KRI-02

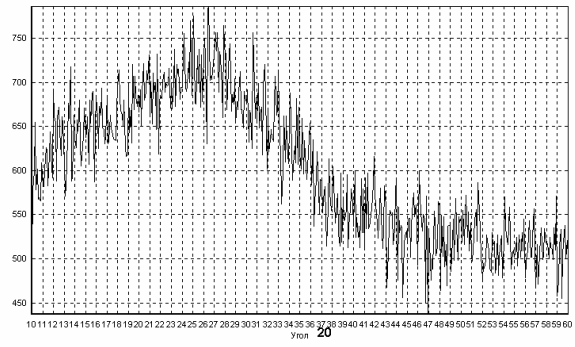

KRI-03

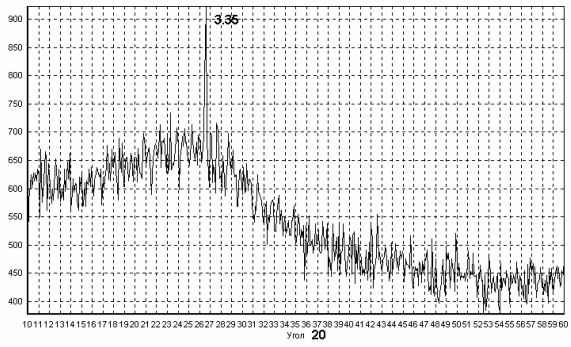

KRI-04

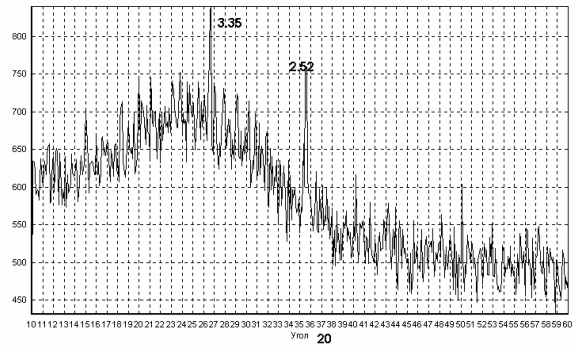

KRI-05

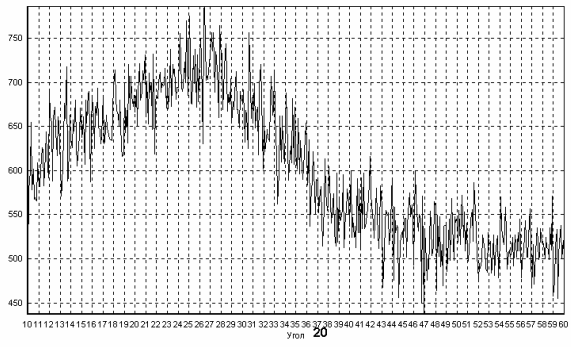

KRI-06

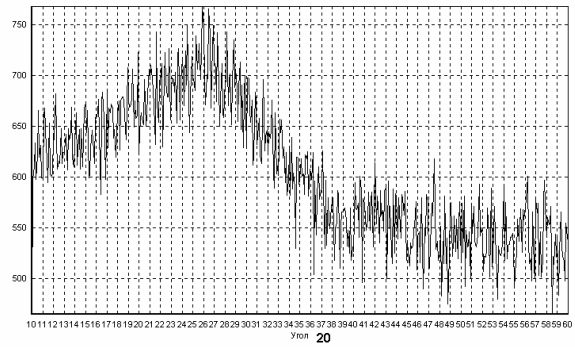

KRI-07

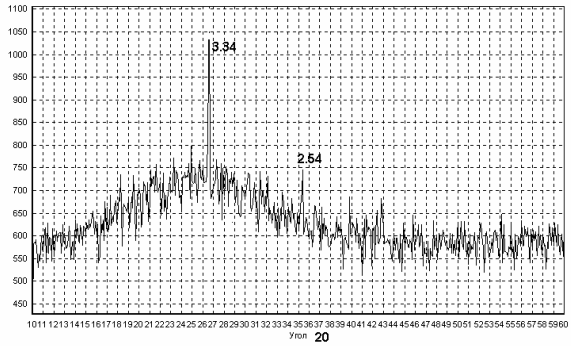

KRI-08

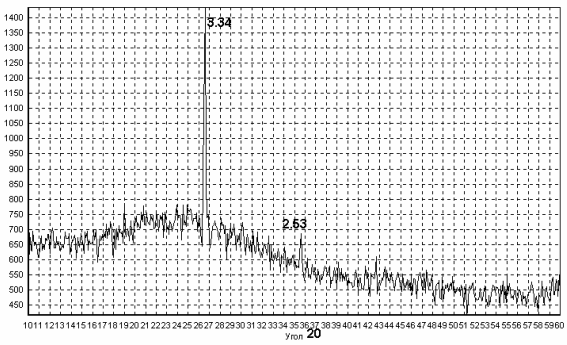

KRI-09

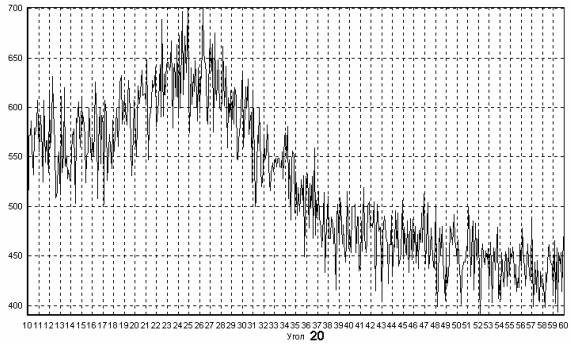

KRI-10

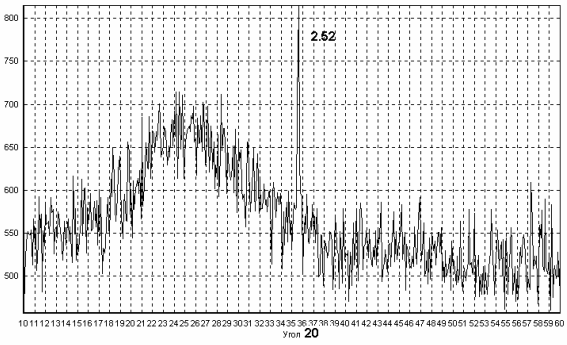

KRI-11

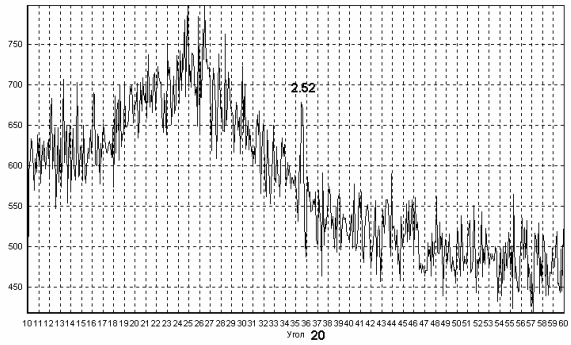

KRI-12

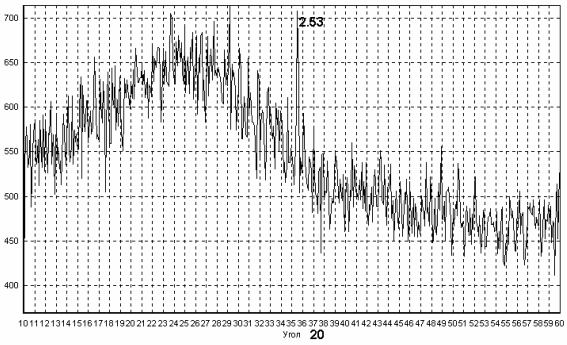

KRI-13

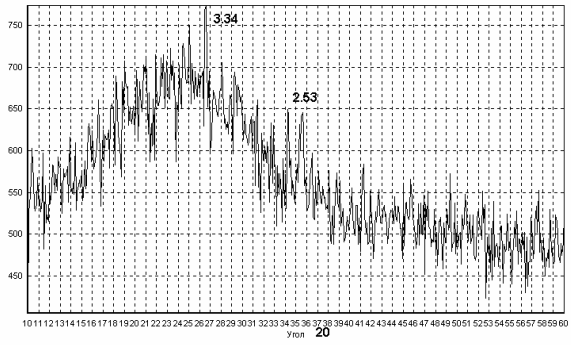

KRI-14

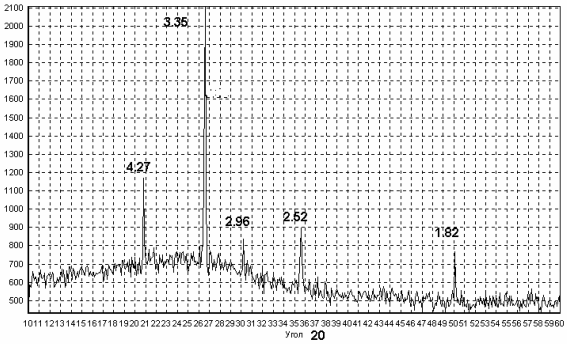

KRI-15

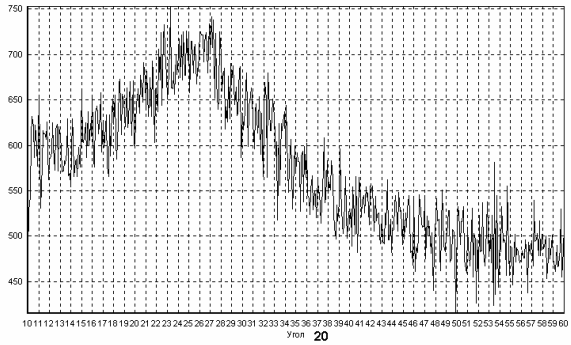

KRI-16

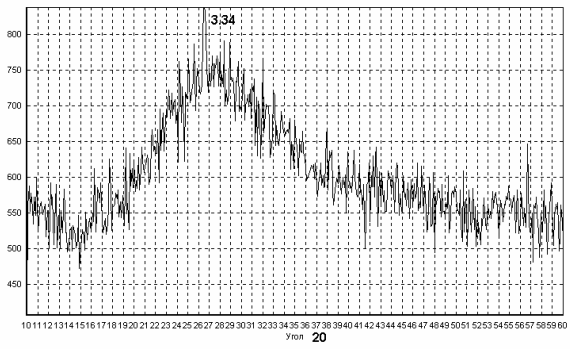

KRI-17

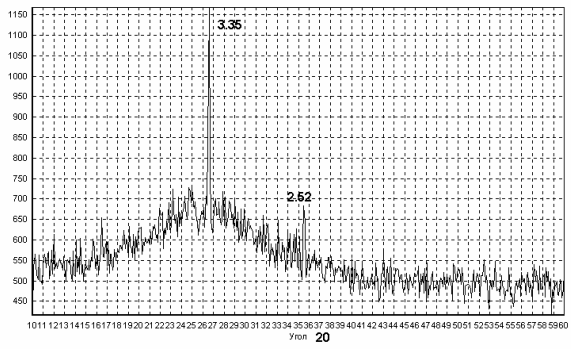

KRI-18

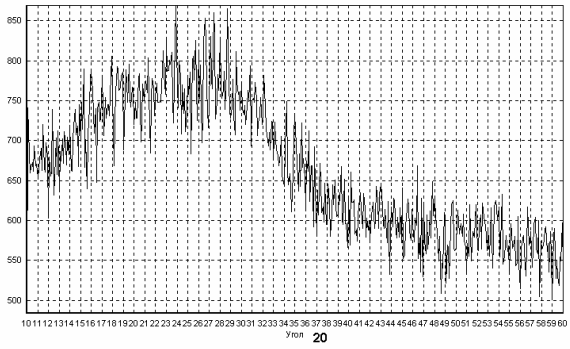

KRI-19

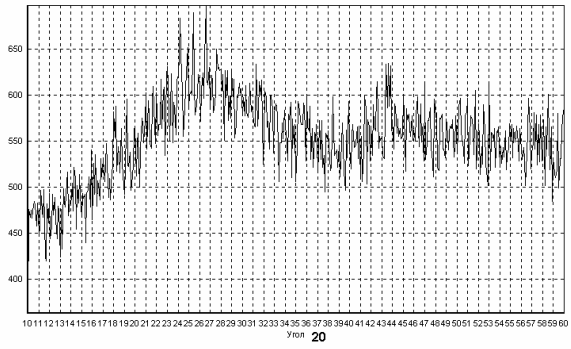

KRI-20

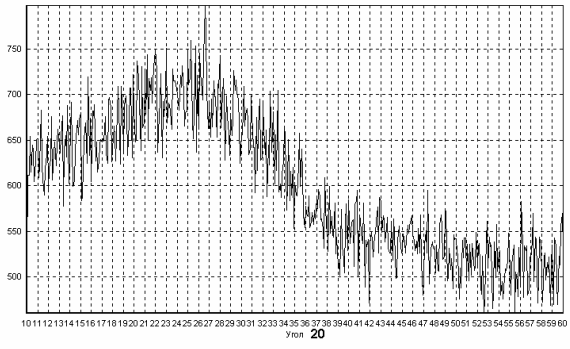

KRI-21

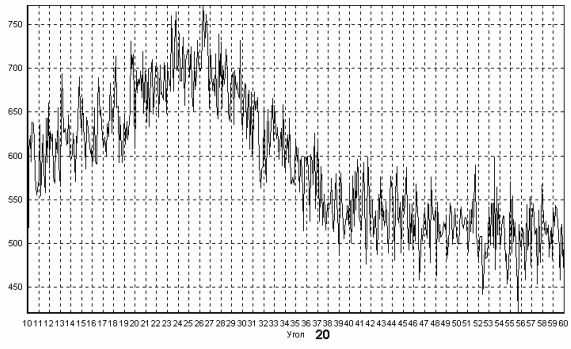

KRI-22

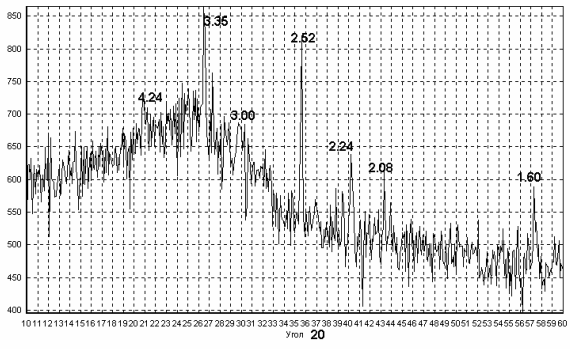

KRI-23

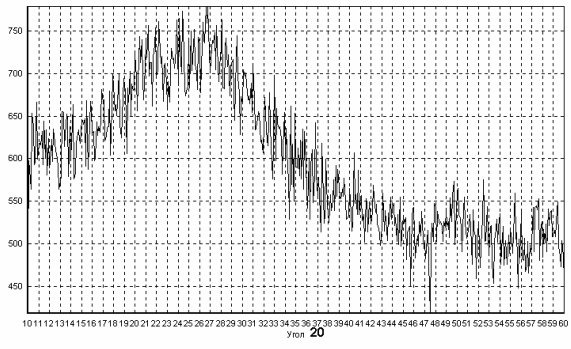

KRI-24

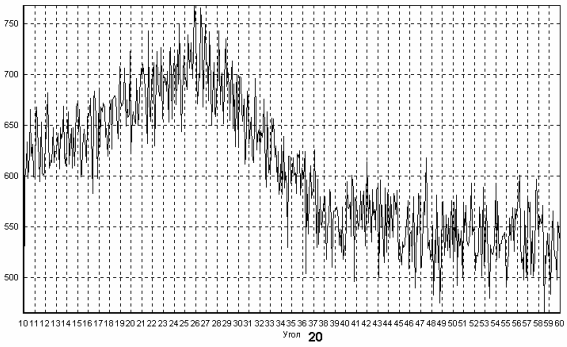

KRI-25

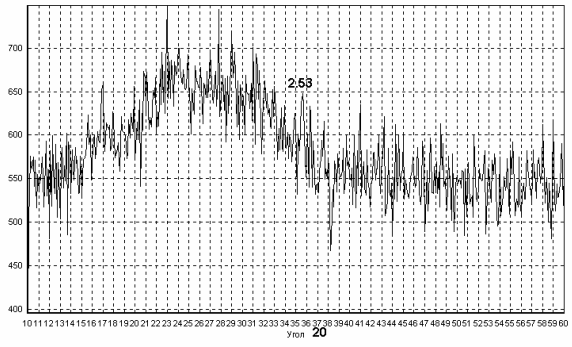

KRI-26

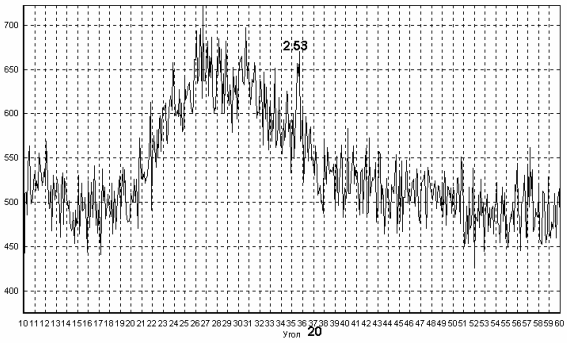

KRI-27

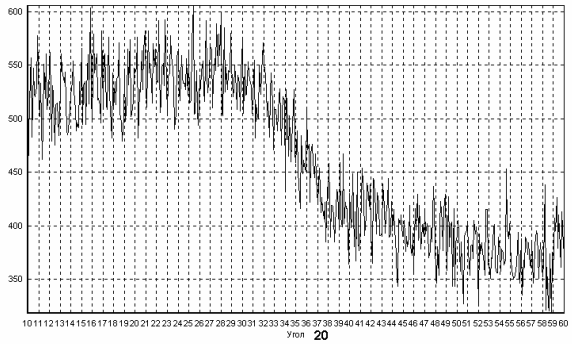

KRI-28

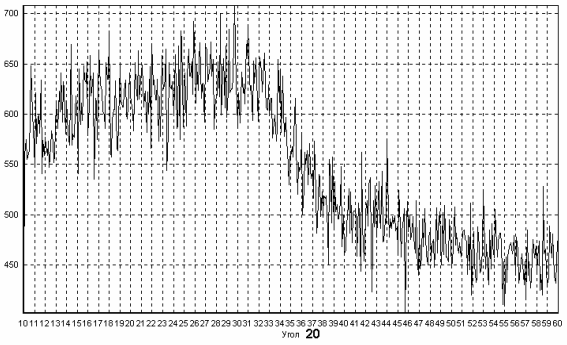

KRI-29

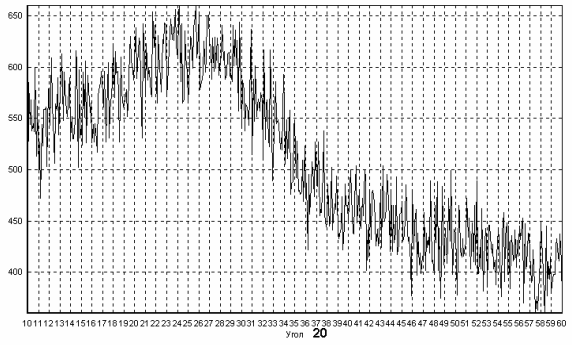

KRI-30

Attachment 4 Surface of KRI Glasses after CCC Treatment

KRI-01 CCC

KRI-02 CCC

KRI-03 CCC

KRI-04 CCC

KRI-05 CCC

KRI-06 CCC

KRI-07 CCC

KRI-08 CCC

KRI-09 CCC

KRI-10 CCC

KRI-011 CCC

KRI-12 CCC

KRI-13 CCC

KRI-14 CCC

KRI-15 CCC

KRI-21 CCC

KRI-22 CCC

KRI-23 CCC

KRI-24 CCC

KRI-25 CCC

KRI-26 CCC

KRI-27 CCC

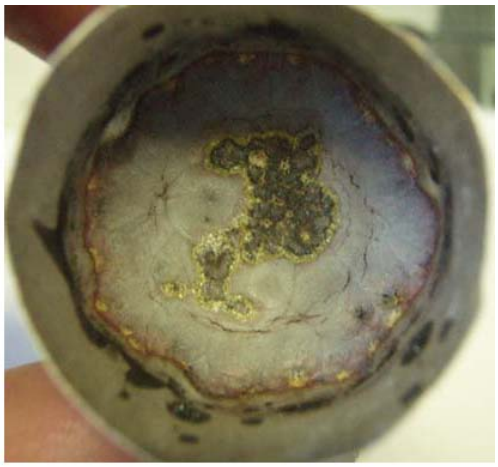

KRI-28 CCC

KRI-29 CCC

KRI-30 CCC

Attachment 5. SEM Photographs of Glass Samples after CCC Treatment

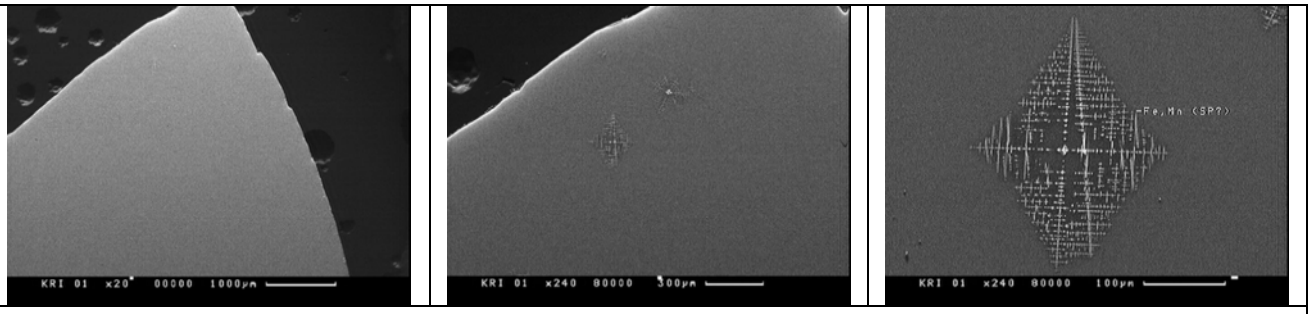

KRI-01 CCC

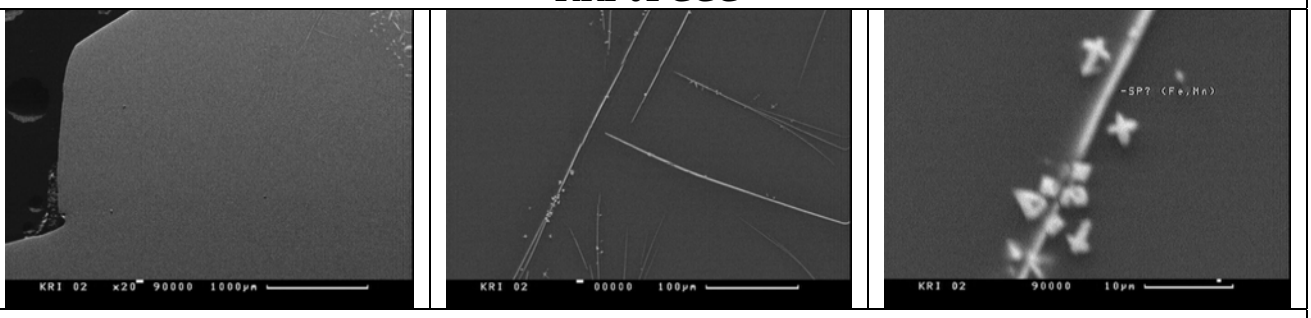

KRI-02 CCC

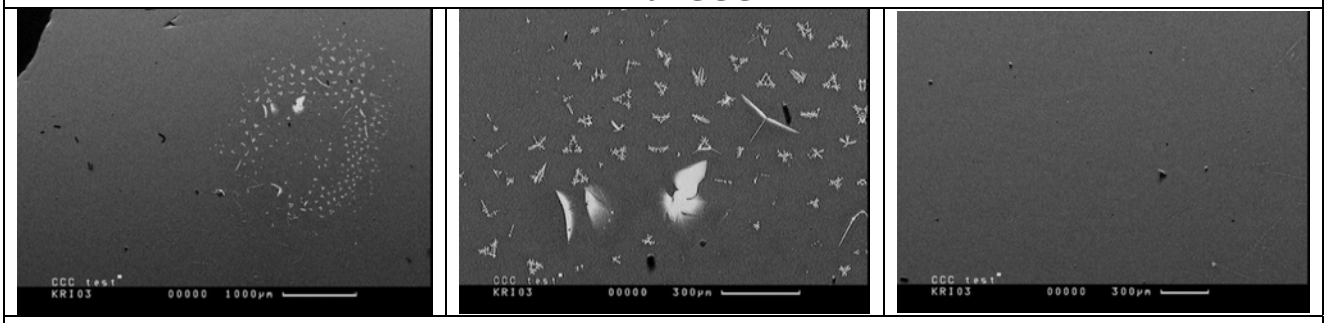

KRI-03 CCC

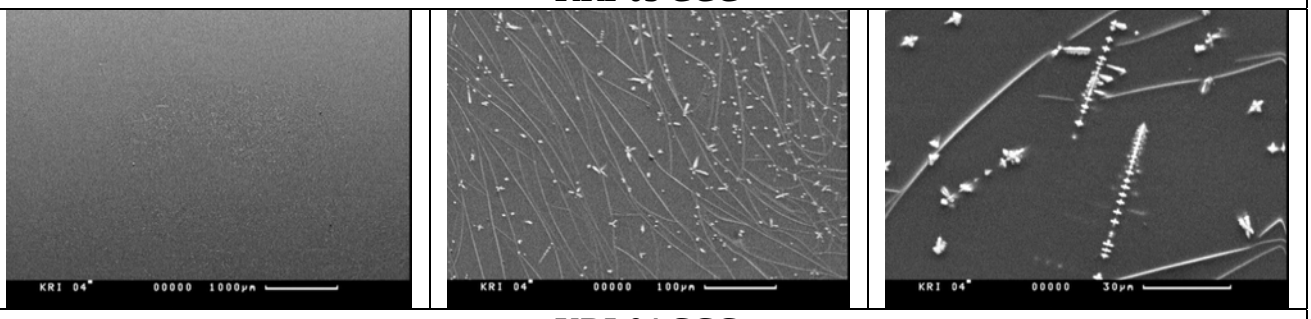

KRI-04 CCC

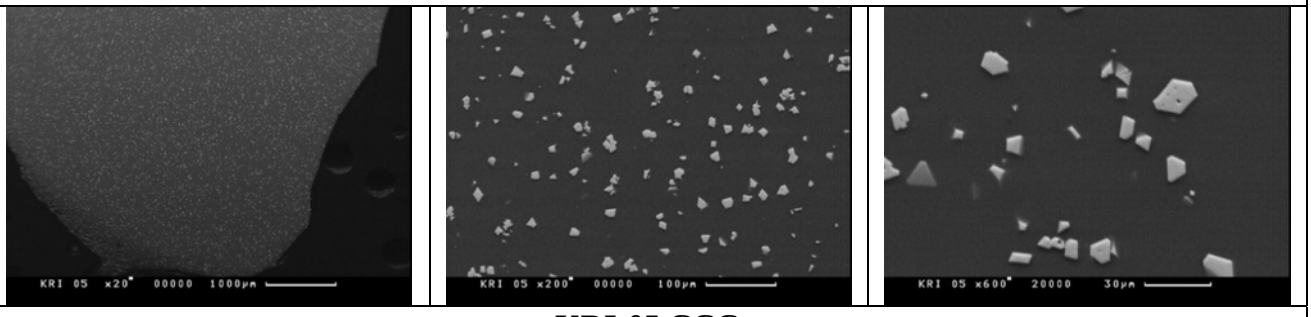

KRI-05 CCC

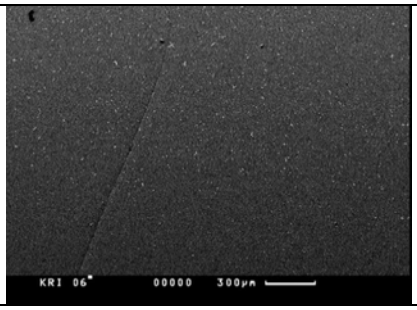

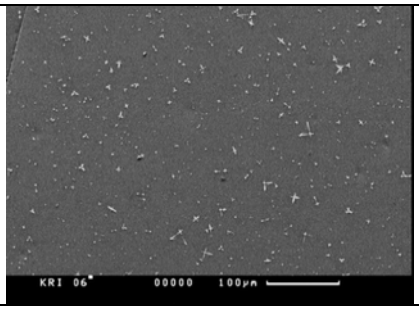

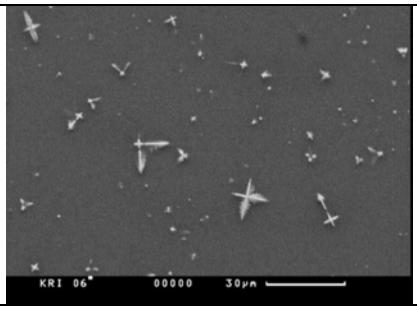

KRI-06 CCC

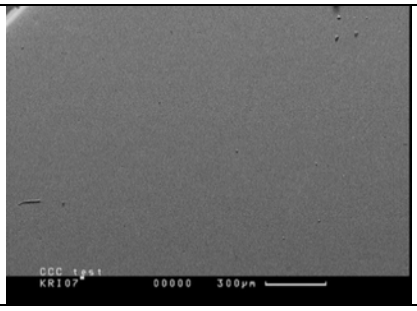

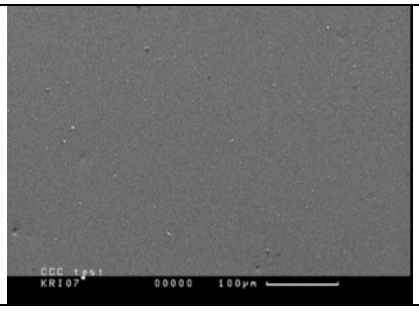

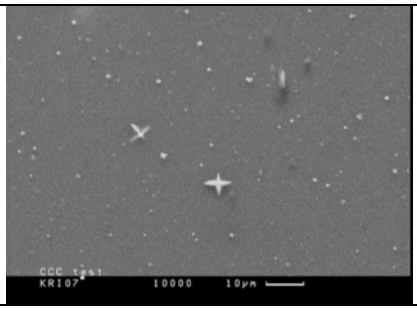

KRI-07 CCC

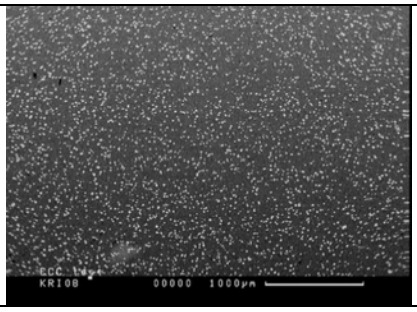

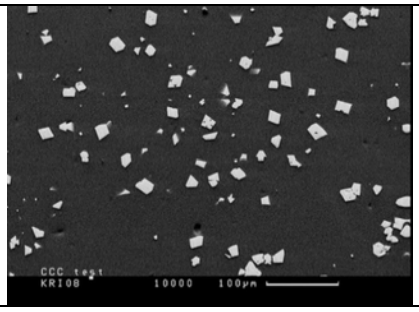

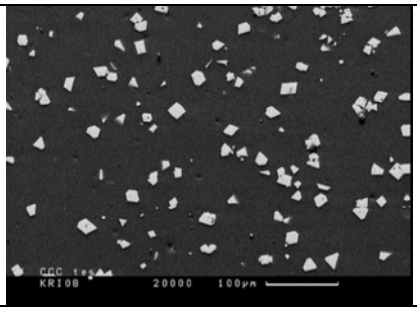

KRI-08 CCC

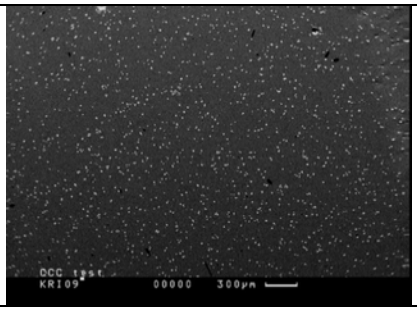

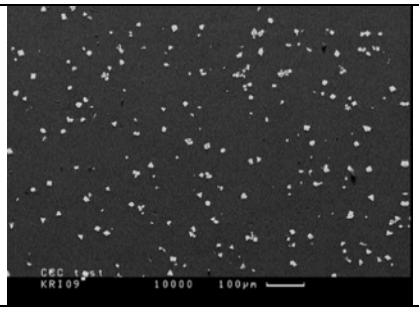

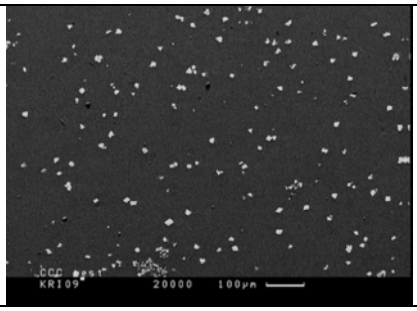

KRI-09 CCC

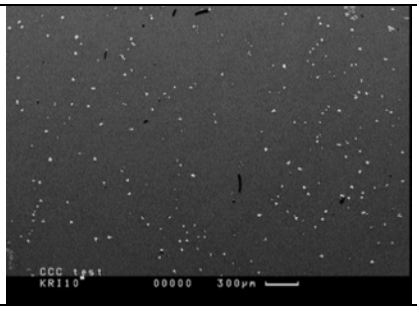

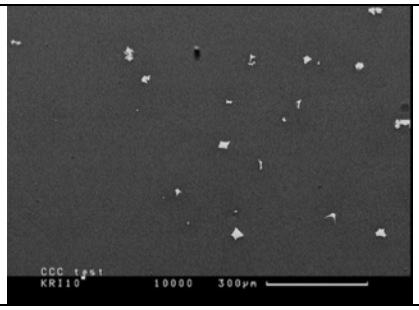

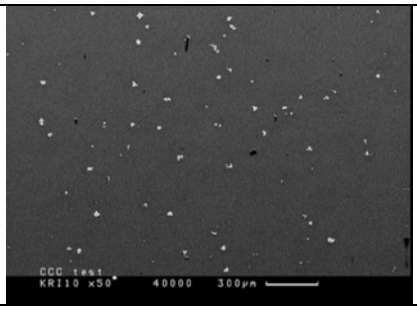

KRI-10 CCC

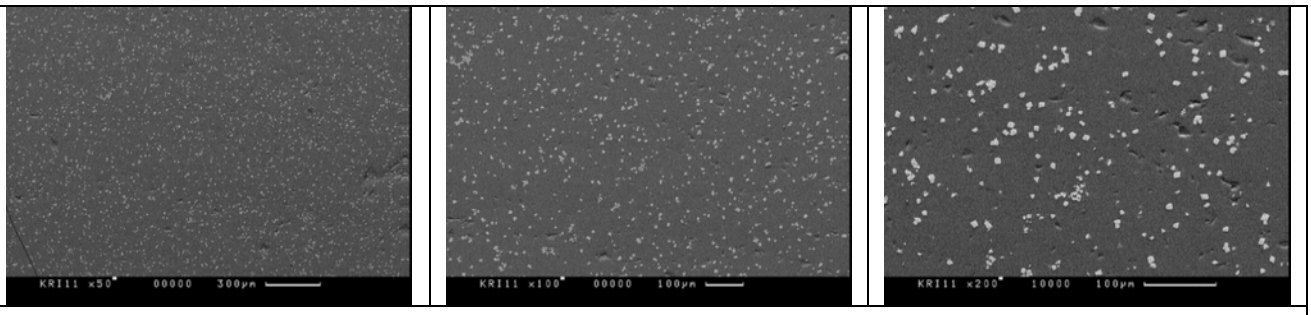

KRI-11 CCC

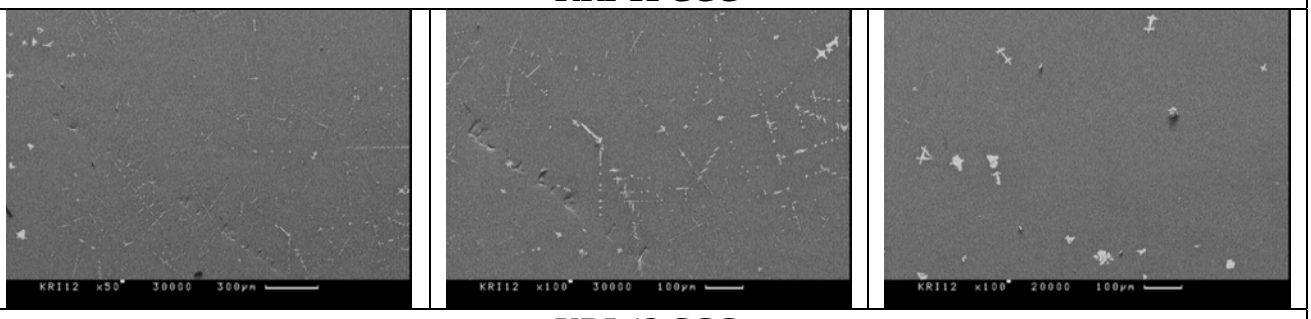

KRI-12 CCC

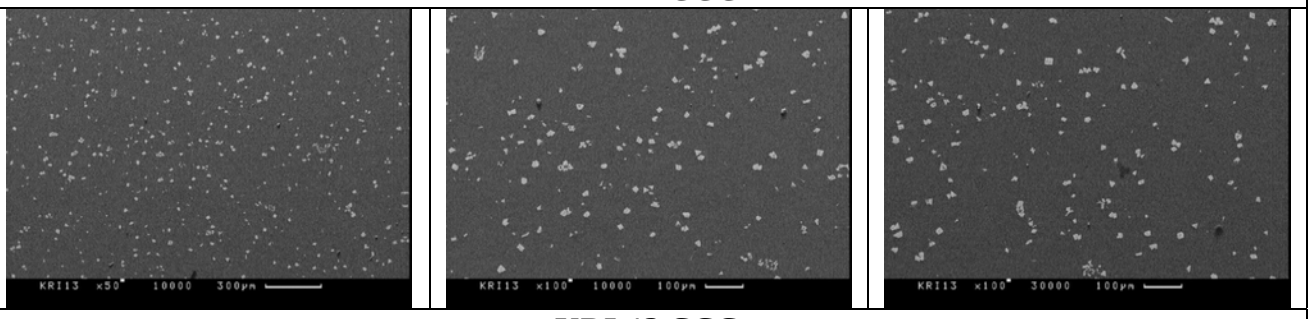

KRI-13 CCC

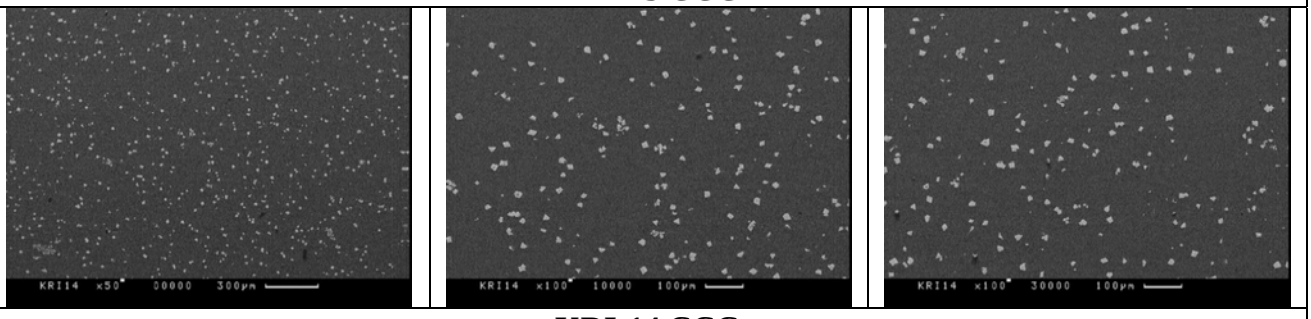

KRI-14 CCC

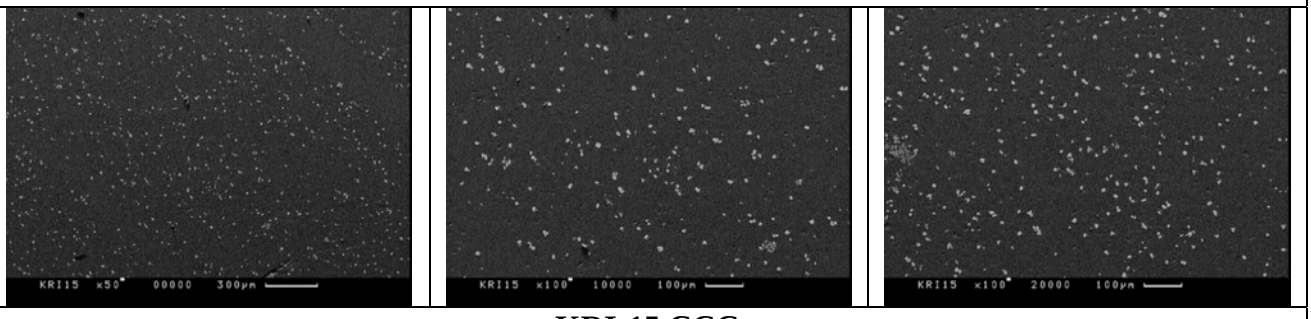

KRI-15 CCC

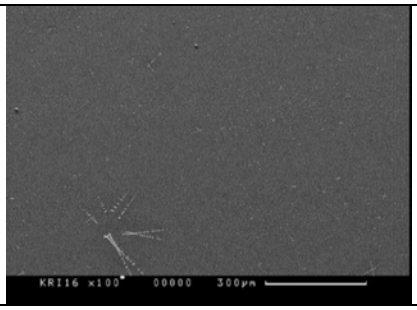

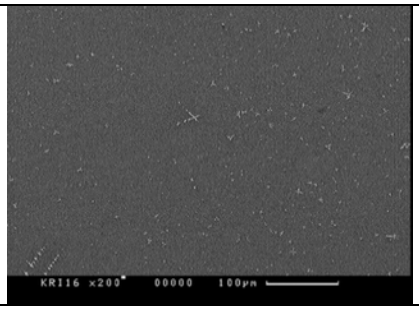

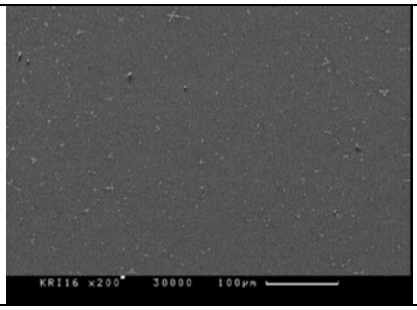

KRI-16 CCC

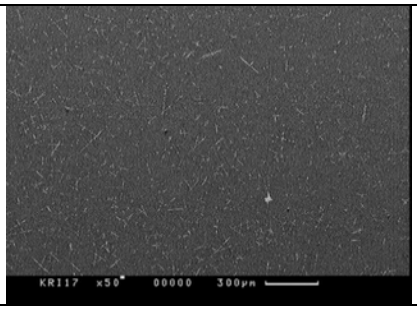

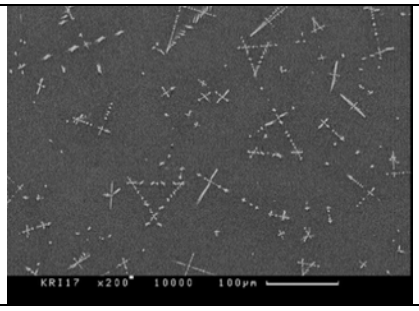

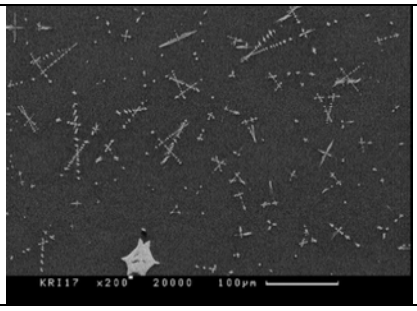

KRI-17 CCC

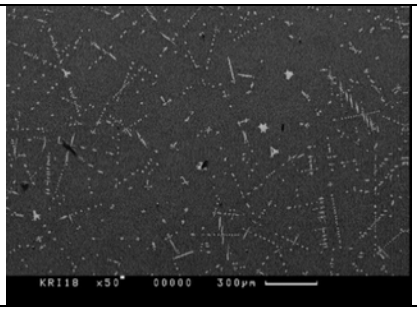

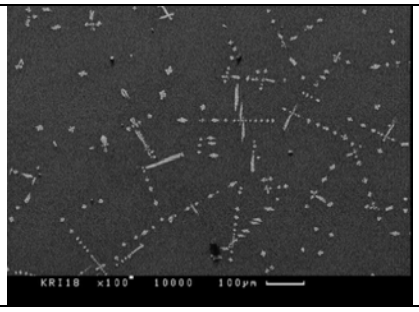

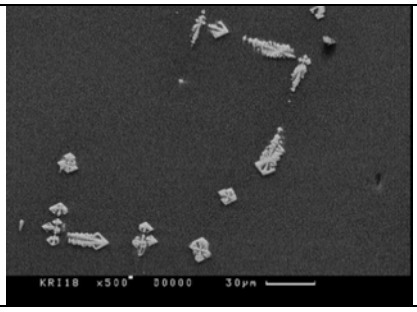

KRI-18 CCC

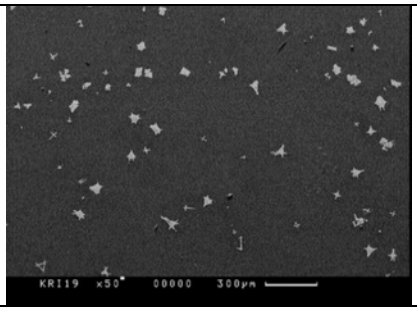

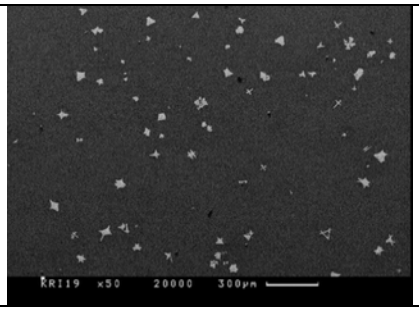

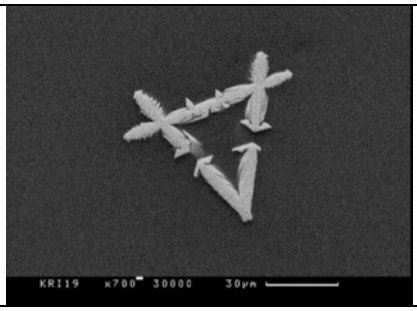

KRI-19 CCC

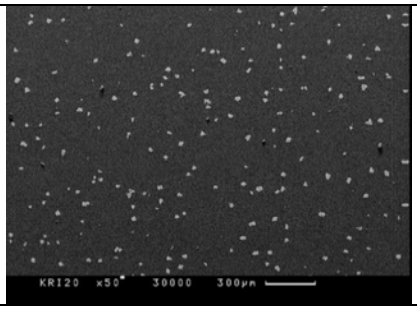

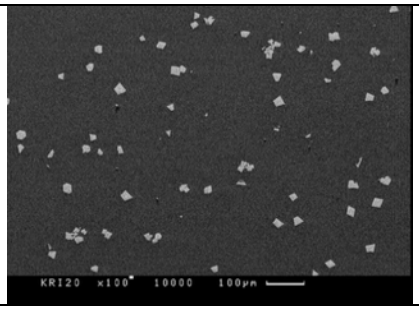

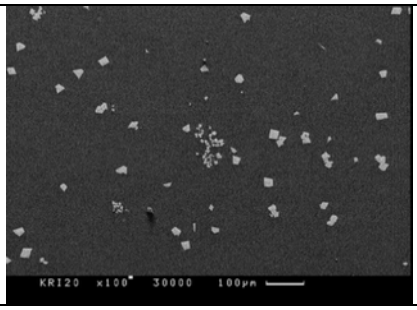

KRI-20 CCC

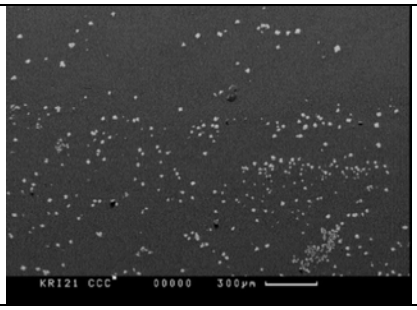

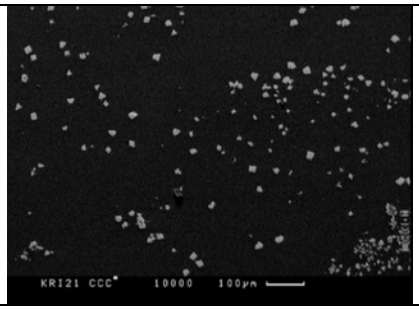

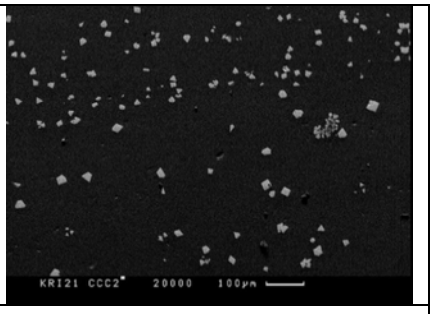

KRI-21 CCC

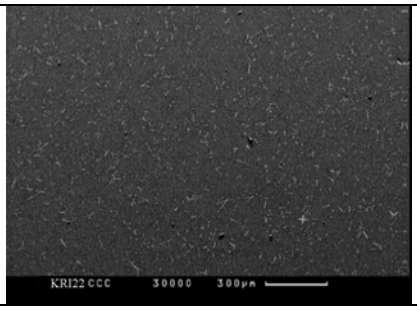

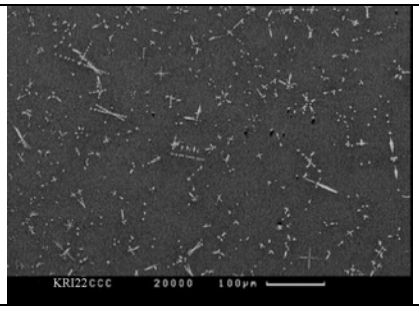

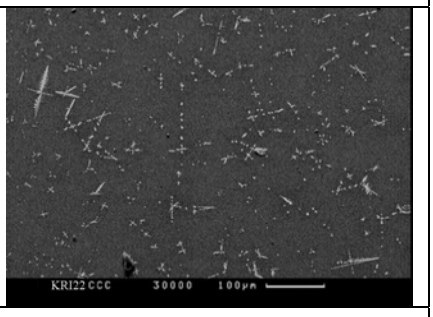

KRI-22 CCC

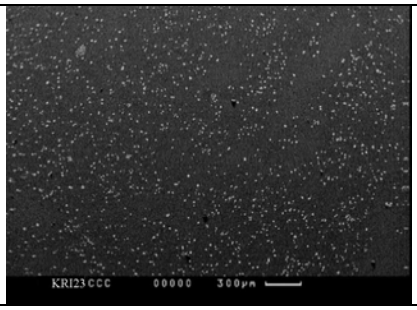

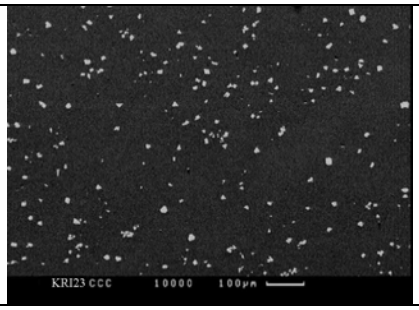

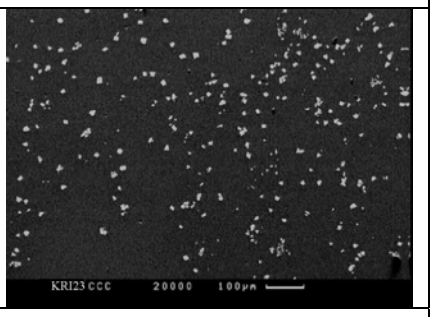

KRI-23 CCC

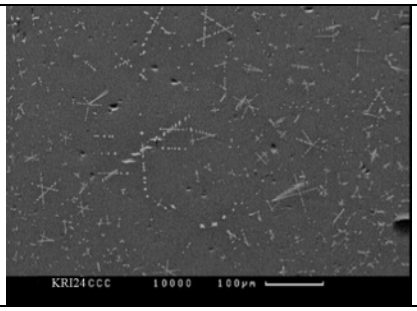

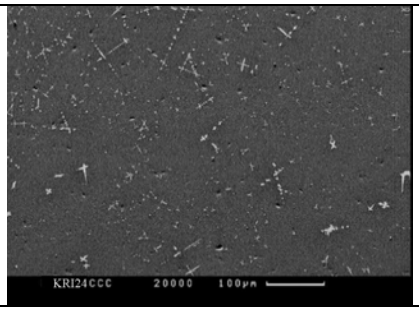

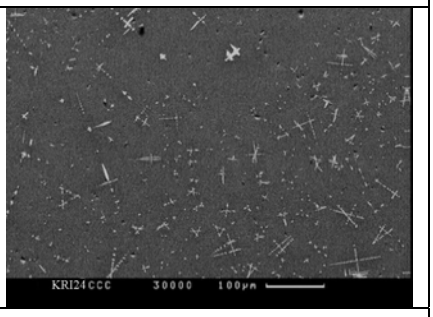

KRI-24 CCC

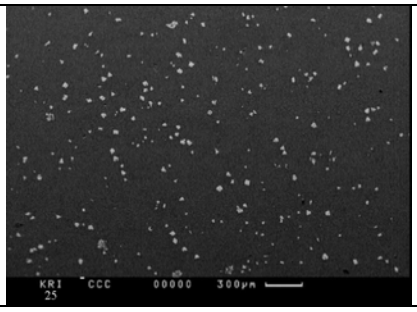

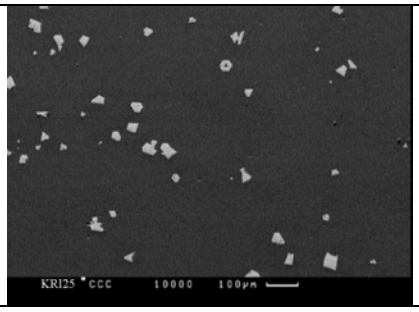

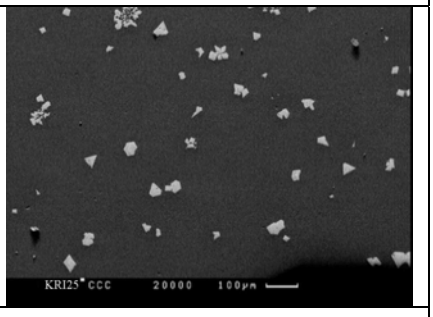

KRI-25 CCC

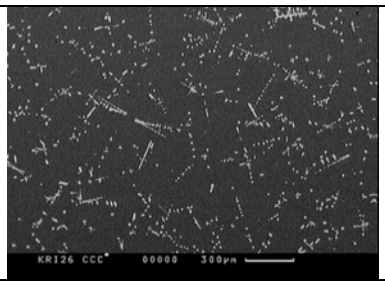

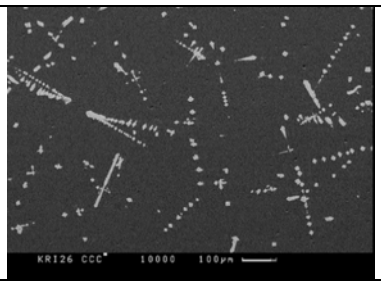

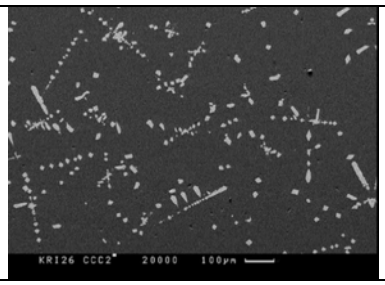

KRI-26 CCC

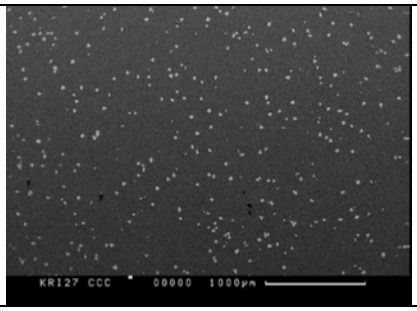

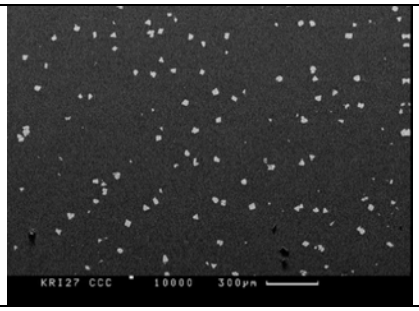

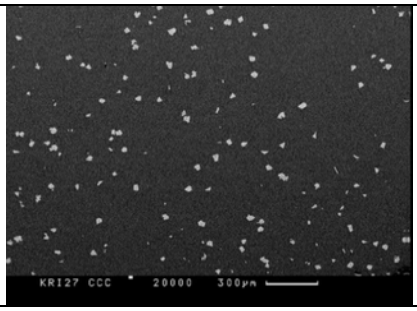

KRI-27 CCC

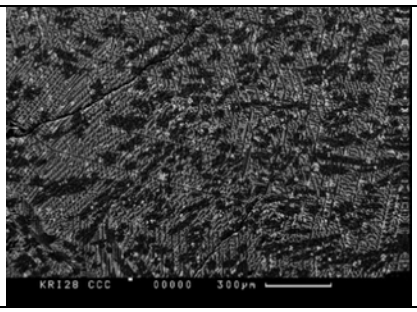

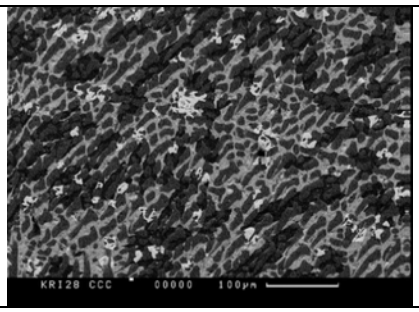

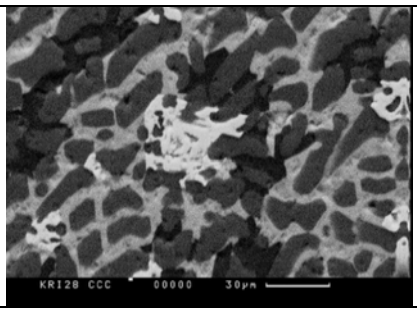

KRI-28 CCC

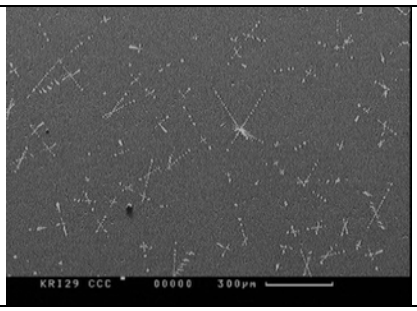

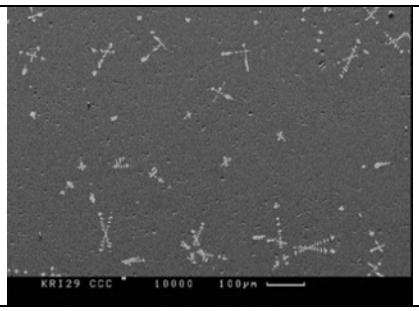

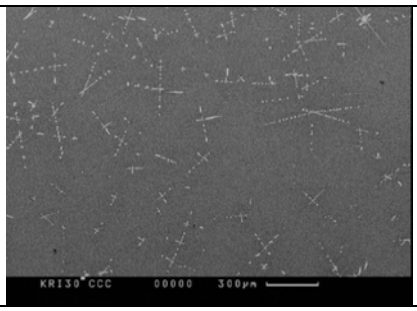

KRI-29 CCC

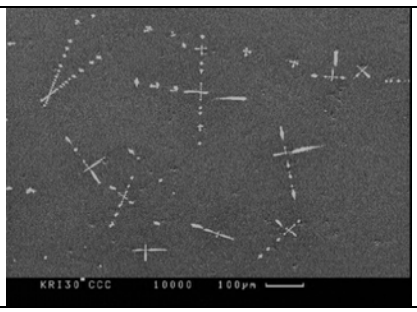

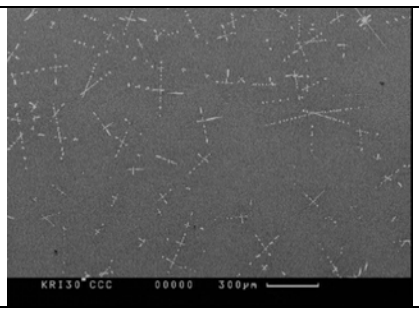

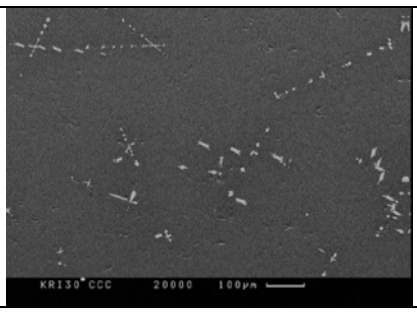

KRI-30 CCC

Attachment 6. EPMA Data on Chemical Homogeneity of Glasses After CCC Treatment

Sample KRI-01 CCC

	Al2O3	Fe2O3	K2O	MnO	Na2O	SO3	SiO2	TiO2	B2O3	Li2O	Total
1	14.93	9.54	0.68	2.55	11.15	0.24	45.71	0.78	9.56	4.86	100.00
2	14.91	10.04	0.69	2.33	10.24	0.24	46.18	0.95	9.56	4.86	100.00
3	14.97	9.94	0.81	2.37	9.11	0.24	47.16	0.97	9.56	4.86	100.00
4	15.04	9.76	0.68	2.66	10.59	0.23	45.69	0.94	9.56	4.86	100.00
5	14.65	9.75	0.78	2.50	10.94	0.23	45.64	1.08	9.56	4.86	100.00
Average	14.90	9.81	0.73	2.48	10.41	0.24	46.08	0.94	9.56	4.86	100.00
Average in area	14.96	9.83	0.79	2.68	10.54	0.24	45.60	0.94	9.56	4.86	100.00
Er/Re	0.43	0.71			0.64		1.41				

Sample KRI-02 CCC

	Al2O3	CaO	Fe2O3	K2O	MnO	Na2O	NiO	SO3	SiO2	TiO2	B2O3	Li2O	Total
1	14.38	0.40	8.26	0.58	1.99	10.26	0.25	0.48	44.76	0.64	14.40	3.64	100.00
2	14.88	0.54	8.47	0.47	2.01	10.48	0.00	0.00	44.33	0.81	14.40	3.64	100.00
3	14.23	0.41	8.66	0.59	2.02	10.02	0.00	0.49	44.60	0.98	14.40	3.64	100.00
4	14.18	0.27	8.52	0.46	2.11	11.40	0.00	0.00	44.26	0.80	14.40	3.64	100.00
5	14.33	0.27	8.61	0.70	1.88	11.13	0.00	0.00	44.11	0.97	14.40	3.64	100.00
Average	14.40	0.38	8.50	0.56	2.00	10.66	0.05	0.19	44.41	0.84	14.40	3.64	100.00
Average in area	14.47	0.41	8.86	0.58	2.13	10.06	0.00	0.48	44.20	0.81	14.40	3.64	100.00
Er/Re	0.83		0.57			0.47			0.58				

Sample KRI-03 CCC

	Al2O3	CaO	Fe2O3	K2O	MnO	Na2O	NiO	SiO2	TiO2	B2O3	Li2O	Total
1	14.79	0.53	8.35	0.68	1.83	10.67	0.00	43.81	0.79	14.40	3.64	100.00
2	14.78	0.54	8.41	0.70	1.75	10.28	0.00	44.86	0.64	14.40	3.64	100.00
3	14.75	0.53	8.29	0.69	1.84	10.90	0.36	43.80	0.79	14.40	3.64	100.00
4	14.91	0.53	8.42	0.57	1.96	10.76	0.24	43.76	0.79	14.40	3.64	100.00
5	14.49	0.56	8.11	0.60	1.93	9.39	0.00	46.05	0.83	14.40	3.64	100.00
Average	14.75	0.54	8.32	0.65	1.86	10.41	0.12	44.44	0.77	14.40	3.64	100.00
Average in area	14.70	0.52	8.43	0.68	1.94	10.48	0.00	43.53	0.94	14.40	3.64	100.00
Er/Re	0.8		0.6			1.0		2.5				

Sample KRI-04 CCC

	Al2O3	CaO	Fe2O3	K2O	MnO	Na2O	NiO	SO3	SiO2	TiO2	B2O3	Li2O	Total
1	14.27	0.54	7.60	0.58	2.25	12.39	0.25	0.48	45.58	0.81	12.25	3.00	100.00
2	14.51	0.54	7.81	0.46	2.36	11.64	0.37	0.00	46.43	0.64	12.25	3.00	100.00
3	14.30	0.68	7.90	0.47	2.26	11.37	0.00	0.00	47.14	0.65	12.25	3.00	100.00
4	14.78	0.53	7.81	0.57	2.31	11.56	0.36	0.00	46.21	0.63	12.25	3.00	100.00
5	14.20	0.41	8.36	0.59	2.27	10.92	0.37	0.00	46.81	0.81	12.25	3.00	100.00
Average	14.41	0.54	7.90	0.53	2.29	11.57	0.27	0.10	46.43	0.71	12.25	3.00	100.00
Average in area	14.41	0.52	7.30	0.56	2.28	12.78	0.47	0.00	45.18	0.62	12.25	3.00	100.00
Er/Re	0.70		1.04			0.43			1.30				

Sample KRI-05 CCC

	Al_2O_3	CaO	Fe_2O_3	K_2O	MnO	Na_2O	PbO	SiO_2	TiO_2	ZnO	ZrO_2	SrO	B_2O_3	Li_2O	Total
1	13.08	0.27	5.96	0.68	2.45	10.60	0.82	41.59	0.63	0.94	1.02	0.00	19.96	2.00	100.00
2	13.62	0.26	4.14	0.68	2.18	10.34	0.60	42.88	0.62	0.93	1.01	0.77	19.96	2.00	100.00
3	13.25	0.26	4.33	0.57	2.57	10.34	0.82	43.20	0.63	1.18	0.90	0.00	19.96	2.00	100.00
4	13.17	0.26	4.04	0.57	2.43	11.42	0.71	42.75	0.63	1.17	0.89	0.00	19.96	2.00	100.00
5	13.27	0.00	4.15	0.56	2.42	10.60	0.71	42.29	0.63	1.05	1.26	1.11	19.96	2.00	100.00
Average	13.28	0.21	4.52	0.61	2.41	10.66	0.73	42.54	0.63	1.05	1.02	0.38	19.96	2.00	100.00
Average in area	13.07	0.26	6.54	0.56	2.90	10.45	0.91	41.00	0.62	0.93	0.76	0.00	19.96	2.00	99.95
Er/Re	0.61		2.96			0.36		1.36							

Sample KRI-06 CCC

	Al2O3	CaO	Cr2O3	Fe2O3	K2O	MnO	Na2O	NiO	PbO	SO3	SiO2	TiO2	ZnO	ZrO2	SrO	B2O3	Li2O	Total
1	12.40	0.26	0.27	8.70	0.45	1.69	12.50	0.00	0.50	0.00	41.53	0.31	0.93	2.03	1.77	12.59	4.05	100.00
2	12.50	0.40	0.00	9.03	0.35	1.98	11.88	0.00	0.62	0.00	42.26	0.48	1.07	1.42	1.36	12.59	4.05	100.00
3	12.53	0.40	0.28	8.64	0.46	1.74	12.68	0.00	0.41	0.00	42.37	0.48	0.72	1.17	1.48	12.59	4.05	100.00
4	12.38	0.27	0.28	8.68	0.46	1.96	12.15	0.24	0.72	0.00	42.07	0.32	1.06	1.67	1.12	12.59	4.05	100.00
5	12.69	0.27	0.28	8.63	0.46	1.86	11.89	0.00	0.52	0.00	42.30	0.48	0.95	1.55	1.47	12.59	4.05	100.00
Average	12.50	0.32	0.22	8.74	0.44	1.85	12.22	0.05	0.55	0.00	42.11	0.41	0.95	1.57	1.44	12.59	4.05	100.00
Average in area	12.50	0.39	0.27	8.52	0.45	1.93	12.30	0.24	0.60	0.00	40.89	0.47	1.04	1.89	1.87	12.59	4.05	100.00
Er/Re	0.37			0.62			0.29				0.75							

Sample KRI-07 CCC

	Al2O3	CaO	Cr2O3	Fe2O3	K2O	MnO	Na2O	NiO	PbO	SiO2	TiO2	ZnO	ZrO2	SrO	B2O3	Li2O	Total
1	12.76	0.39	0.27	8.85	0.45	1.91	12.58	0.35	0.80	39.79	0.46	0.92	1.75	2.08	12.60	4.05	100.00
2	13.30	0.40	0.28	8.81	0.46	1.74	12.08	0.00	0.52	41.26	0.48	0.84	1.69	1.48	12.60	4.05	100.00
3	13.05	0.40	0.00	9.04	0.58	1.86	11.37	0.00	0.72	41.28	0.48	1.19	1.55	1.81	12.60	4.05	100.00
4	12.81	0.39	0.28	9.01	0.45	1.82	12.05	0.48	0.61	40.50	0.47	0.94	1.65	1.89	12.60	4.05	100.00
5	12.93	0.39	0.14	8.57	0.56	1.94	12.63	0.00	0.81	40.34	0.47	1.05	1.52	1.99	12.60	4.05	100.00
Average	12.97	0.40	0.19	8.86	0.50	1.85	12.14	0.17	0.69	40.63	0.47	0.99	1.63	1.85	12.60	4.05	100.00
Average in area	13.16	0.40	0.28	8.99	0.57	1.72	12.60	0.00	0.72	40.84	0.48	0.83	1.29	1.47	12.60	4.05	100.00
Er/Re	1.1			0.9			0.8			1.6							

Sample KRI-08 CCC

	Al2O3	CaO	Fe2O3	K2O	MnO	Na2O	SiO2	ZnO	SrO	B2O3	Li2O	Total
1	12.75	0.99	5.61	1.82	2.86	9.36	42.67	1.25	3.45	16.25	3.00	100.00
2	12.76	1.00	5.41	1.85	2.91	9.51	42.92	1.02	3.38	16.25	3.00	100.00
3	13.34	1.00	5.40	1.85	2.91	9.92	41.81	1.02	3.50	16.25	3.00	100.00
4	13.35	1.00	5.26	2.10	2.64	9.79	42.07	1.27	3.27	16.25	3.00	100.00
5	13.63	0.86	5.30	1.86	2.53	10.13	42.13	0.90	3.41	16.25	3.00	100.00
Average	13.16	0.97	5.40	1.89	2.77	9.74	42.32	1.09	3.40	16.25	3.00	100.00
Average in area	12.66	0.83	9.57	1.66	3.82	9.29	38.16	1.23	3.26	16.25	3.00	100.00
Er/Re	2.0		0.7			0.5	1.1					

Sample KRI 09-CCC

	Al2O3	CaO	Fe2O3	K2O	MnO	Na2O	PbO	SiO2	TiO2	ZnO	ZrO2	SrO	B2O3	Li2O	Total
1	14.17	0.13	6.01	0.22	0.71	12.20	0.89	42.09	0.61	1.14	3.21	1.30	14.34	3.00	100.00
2	14.42	0.13	5.65	0.23	0.73	11.42	0.91	43.35	0.63	1.17	2.80	1.22	14.34	3.00	100.00
3	14.22	0.13	5.65	0.23	0.87	11.05	0.94	44.41	0.64	0.96	2.87	0.68	14.34	3.00	100.00
4	14.44	0.00	5.32	0.23	0.86	11.58	0.93	43.54	0.80	0.95	3.22	0.79	14.34	3.00	100.00
5	14.12	0.13	5.94	0.23	0.86	12.36	0.71	43.33	0.63	0.94	2.94	0.00	14.34	3.00	100.00
Average	14.27	0.11	5.71	0.23	0.81	11.72	0.87	43.34	0.66	1.03	3.01	0.80	14.34	3.00	100.00
Average in area	13.91	0.00	6.79	0.22	0.96	11.17	0.70	42.09	0.78	1.39	3.02	0.99	14.34	3.00	100.00
Er/Re	0.7		1.4			0.9		2.1							

Sample KRI-10 CCC

	Al2O3	CaO	Cr2O3	Fe2O3	K2O	MnO	Na2O	NiO	SiO2	TiO2	ZnO	ZrO2	SrO	B2O3	Li2O	Total
1	12.87	0.58	0.30	7.66	0.75	1.07	12.93	0.53	47.50	0.00	1.03	0.84	1.46	9.38	3.11	100.00
2	12.62	0.56	0.29	7.54	0.60	1.16	13.56	0.63	46.30	0.17	1.12	1.08	1.88	9.38	3.11	100.00
3	12.93	0.58	0.30	7.40	0.75	0.94	12.71	0.00	48.16	0.00	1.03	0.98	1.72	9.38	3.11	100.00
4	12.99	0.57	0.45	7.77	0.62	0.93	12.44	0.26	47.45	0.34	1.02	0.97	1.70	9.38	3.11	100.00
5	12.95	0.57	0.30	7.60	0.74	1.06	12.13	0.26	47.97	0.00	1.27	0.97	1.69	9.38	3.11	100.00
Average	12.87	0.57	0.33	7.60	0.69	1.03	12.76	0.34	47.47	0.10	1.09	0.97	1.69	9.38	3.11	100.00
Average in area	12.75	0.65	0.41	7.66	0.67	1.19	12.71	0.59	46.90	0.31	0.81	1.12	1.75	9.38	3.11	100.00
Er/Re	0.7			0.7			0.9		1.8							

Sample KRI-11 CCC

	Al2O3	CaO	Fe2O3	K2O	MnO	Na2O	SiO2	TiO2	ZrO2	SrO	B2O3	Li2O	Total
1	16.94	0.00	7.26	0.33	0.84	11.58	42.93	0.31	1.25	0.00	13.99	4.08	100.00
2	17.58	0.14	5.09	0.24	0.64	10.53	44.91	0.00	1.60	1.17	13.99	4.08	100.00
3	17.08	0.26	5.24	0.34	0.61	11.67	43.94	0.00	1.53	1.22	13.99	4.08	100.00
4	17.17	0.27	5.38	0.35	0.62	11.72	44.89	0.32	1.17	0.00	13.99	4.08	100.00
5	17.46	0.00	5.39	0.48	0.64	9.77	46.36	0.33	1.48	0.00	13.99	4.08	100.00
Average in area	16.64	0.26	7.76	0.45	0.73	10.47	41.90	0.31	1.39	1.11	13.99	4.08	100.00
Average	17.25	0.13	5.67	0.35	0.67	11.05	44.61	0.19	1.41	0.48	13.99	4.08	100.00
Er/Re	1.33		8.1			1.1	4.2						

Sample KRI-12 CCC

	Al2O3	CaO	Fe2O3	K2O	MnO	Na2O	SiO2	TiO2	ZrO2	SrO	B2O3	Li2O	Total
1	13.59	0.54	7.67	0.69	2.97	9.04	40.83	0.32	3.49	2.27	14.10	3.88	100.00
2	13.22	0.39	7.62	0.66	2.85	10.04	39.79	0.31	3.73	3.04	14.10	3.88	100.00
3	14.16	0.41	6.95	0.59	3.02	8.26	42.49	0.32	3.28	2.53	14.10	3.88	100.00
4	14.47	0.40	5.88	0.69	2.47	9.55	42.22	0.32	3.62	2.38	14.10	3.88	100.00
5	14.61	0.54	5.24	0.70	2.62	9.64	42.82	0.00	3.65	2.17	14.10	3.88	100.00
Average in area	13.86	0.54	7.72	0.58	3.12	8.97	41.53	0.00	3.39	2.28	14.10	3.88	100.00
Average	14.01	0.45	6.67	0.67	2.79	9.30	41.63	0.25	3.56	2.48	14.10	3.88	100.00
Er/Re	2.97		9.8			0.9	4.3						

Sample KRI 13-CCC

	Al2O3	CaO	Fe2O3	K2O	MnO	Na2O	PbO	SiO2	TiO2	ZnO	ZrO2	SrO	B2O3	Li2O	Total
1	13.62	0.00	5.84	0.70	2.39	12.20	0.84	46.90	0.81	1.45	1.45	0.86	10.79	3.00	100.00
2	13.54	0.00	6.17	0.59	2.41	12.56	0.74	46.86	0.66	1.34	1.33	0.86	10.79	3.00	100.00
3	13.87	0.27	5.99	0.69	2.59	11.69	0.92	46.33	0.64	1.07	1.67	0.86	10.79	3.00	100.00
4	13.93	0.00	6.51	0.58	2.63	11.37	0.73	46.93	0.49	1.45	1.57	0.86	10.79	3.00	100.00
5	13.68	0.00	5.87	0.59	2.40	11.60	0.74	47.75	0.65	1.34	1.59	0.86	10.79	3.00	100.00
Average in area	13.19	0.26	6.43	0.55	2.73	13.74	0.89	44.63	0.46	1.37	1.49	0.86	10.79	3.00	100.00
Average	13.73	0.05	6.08	0.63	2.48	11.88	0.79	46.95	0.65	1.33	1.52	0.86	10.79	3.00	100.00
Er/Re	0.84		2.5			0.6		1.7							

Sample KRI-14 CCC

	Al2O3	Fe2O3	K2O	MnO	Na2O	PbO	SiO2	TiO2	ZnO	ZrO2	SrO	B2O3	Li2O	Total
1	14.08	4.15	0.23	2.63	8.35	0.83	44.54	0.65	1.32	1.44	1.14	15.46	5.00	100.00
2	14.13	4.73	0.23	2.44	9.18	0.92	43.75	0.79	0.94	1.28	1.12	15.46	5.00	100.00
3	14.30	4.24	0.35	2.72	9.42	0.93	44.70	0.48	1.19	1.16	0.00	15.46	5.00	100.00
4	13.64	5.09	0.23	2.79	9.10	0.81	43.15	0.78	1.28	1.27	1.11	15.46	5.00	100.00
5	13.85	4.08	0.23	2.58	8.98	1.02	44.62	0.64	1.07	1.54	0.90	15.46	5.00	100.00
Average in area	13.44	6.46	0.11	2.62	8.83	0.89	42.50	0.77	1.03	1.12	0.98	15.46	5.00	100.00
Average	14.00	4.46	0.25	2.63	9.00	0.90	44.15	0.67	1.16	1.34	0.85	15.46	5.00	
Er/Re	1.28	4.0			0.5		2.3							

Sample KRI-15 CCC

	Al2O3	Fe2O3	K2O	MnO	Na2O	PbO	SO3	SiO2	SrO	ZnO	ZrO2	B2O3	Li2O	Total
1	15.86	5.66	0.56	0.83	10.19	0.70	0.00	45.60	1.31	0.80	1.25	13.68	3.32	100.00
2	15.44	6.84	0.57	1.09	10.00	0.71	0.70	45.04	1.33	0.00	1.27	13.68	3.32	100.00
3	16.95	5.85	0.82	1.13	10.37	0.00	0.00	47.15	0.00	0.73	0.00	13.68	3.32	100.00
4	16.02	5.60	0.55	0.94	10.32	0.69	0.00	46.05	1.29	0.57	0.98	13.68	3.32	100.00
5	15.11	6.75	0.66	0.94	10.65	0.88	0.00	45.72	0.00	0.68	1.35	13.68	3.32	100.00
Average in area	15.55	6.53	0.66	1.30	11.09	0.98	0.00	45.02	0.00	0.57	0.99	13.68	3.32	100.00
Average	15.88	6.14	0.63	0.99	10.31	0.59	0.14	45.91	0.79	0.56	0.97	13.68	3.32	100.00
Er/Re	2.0	3.3			0.3			2.5						

Sample KRI-16 CCC

	Al2O3	CaO	Cr2O3	Fe2O3	K2O	MnO	Na2O	NiO	PbO	SO3	SiO2	TiO2	ZnO	ZrO2	SrO	B2O3	Li2O	Total
1	13.00	0.00	0.28	8.08	0.23	0.97	9.40	0.48	0.00	0.47	46.21	0.79	1.41	2.55	2.45	8.75	4.92	100.00
2	12.97	0.13	0.00	8.08	0.00	0.84	9.88	0.59	1.10	0.46	45.48	0.77	1.04	2.76	2.19	8.75	4.92	100.00
3	12.41	0.13	0.00	8.06	0.22	1.08	10.35	0.59	0.80	0.46	44.96	0.62	1.38	2.62	2.62	8.75	4.92	100.00
4	12.64	0.13	0.41	7.80	0.23	0.85	10.28	0.72	1.01	0.00	46.39	0.94	1.06	2.16	1.67	8.75	4.92	100.00
5	12.93	0.00	0.27	7.90	0.00	0.97	9.98	0.48	0.71	0.00	46.15	0.78	1.17	2.53	2.44	8.75	4.92	100.00
Average in area	12.70	0.26	0.27	7.73	0.22	1.08	9.93	0.47	1.11	0.00	45.55	0.62	1.51	2.52	2.32	8.75	4.92	100.00
Average	12.79	0.08	0.19	7.98	0.14	0.94	9.98	0.57	0.72	0.28	45.84	0.78	1.21	2.52	2.27	8.75	4.92	100.00
Er/Re	1.28			1.1			0.5				2.0							

Sample KRI-17 CCC

	Al2O3	CaO	Cr2O3	Fe2O3	K2O	MnO	Na2O	NiO	SiO2	TiO2	ZrO2	SrO	B2O3	Li2O	Total
1	13.68	0.53	0.00	8.16	0.23	1.72	11.42	0.00	42.62	0.00	2.96	2.36	12.40	3.88	100.00
2	13.57	0.54	0.43	8.04	0.35	1.63	10.33	0.00	43.41	0.32	3.01	2.06	12.40	3.88	100.00
3	13.52	0.51	0.00	8.12	0.33	1.90	12.85	0.58	40.83	0.00	3.22	1.84	12.40	3.88	100.00
4	13.37	0.51	0.27	8.14	0.33	1.54	11.14	0.00	41.11	0.31	3.35	2.82	12.40	3.88	100.00
5	13.40	0.65	0.00	7.86	0.45	1.57	11.69	0.00	41.56	0.00	3.28	2.54	12.40	3.88	100.00
Average in area	13.49	0.52	0.27	8.21	0.22	1.68	11.24	0.47	41.07	0.31	3.25	2.52	12.40	3.88	100.00
Average	13.51	0.55	0.14	8.06	0.34	1.67	11.49	0.12	41.91	0.13	3.16	2.33	12.40	3.88	100.00
Er/Re	0.63			1.1			1.1		3.6						

Sample KRI-18 CCC

	Al2O3	CaO	Fe2O3	K2O	MnO	Na2O	NiO	SiO2	TiO2	ZnO	ZrO2	SrO	B2O3	Li2O	Total
1	14.00	0.40	8.10	0.70	2.73	9.07	0.00	40.35	0.32	0.00	3.25	2.73	14.83	3.52	100.00
2	14.12	0.55	7.02	0.71	2.79	9.14	0.00	42.08	0.33	0.00	3.05	1.86	14.83	3.52	100.00
3	13.79	0.54	6.11	0.59	2.76	9.31	0.00	41.44	0.32	0.61	3.42	2.76	14.83	3.52	100.00
4	14.30	0.54	6.70	0.69	2.60	8.91	0.00	41.83	0.00	0.60	3.10	2.38	14.83	3.52	100.00
5	14.04	0.53	6.53	0.69	2.34	9.11	0.00	40.98	0.32	0.83	3.09	2.59	14.83	3.52	100.00
Average in area	14.33	0.57	7.94	0.61	3.00	8.45	0.51	40.70	0.00	0.00	3.14	2.39	14.83	3.52	100.00
Average	14.05	0.51	6.89	0.67	2.65	9.11	0.00	41.34	0.26	0.41	3.18	2.46	14.83	3.52	100.00
Er/Re	0.93		6.8			0.2		2.3							

Sample KRI-19 CCC

	Al2O3	CaO	Fe2O3	K2O	MnO	Na2O	SiO2	TiO2	ZnO	ZrO2	SrO	B2O3	Li2O	Total
1	13.68	0.00	7.59	0.33	2.49	14.32	41.39	0.61	0.57	1.24	2.27	11.12	4.37	100.00
2	13.63	0.00	8.96	0.23	2.90	13.63	41.11	0.78	0.00	1.26	1.99	11.12	4.37	100.00
3	14.05	0.27	8.99	0.23	2.71	12.59	41.63	0.48	0.00	1.42	2.14	11.12	4.37	100.00
4	14.26	0.00	8.38	0.22	2.53	14.31	41.68	0.78	0.58	0.00	1.76	11.12	4.37	100.00
5	14.22	0.27	8.82	0.23	2.49	12.87	42.33	0.64	0.00	0.91	1.71	11.12	4.37	100.00
Average in area	14.32	0.26	8.52	0.23	2.69	11.49	41.98	0.79	0.00	1.02	2.58	11.12	4.37	100.00
Average	13.97	0.11	8.55	0.25	2.62	13.54	41.63	0.66	0.23	0.97	1.98	11.12	4.37	100.00
Er/Re	1.48		5.3			1.0	1.5							

Sample KRI-20 CCC

	Al2O3	CaO	Fe2O3	K2O	MnO	Na2O	NiO	PbO	SiO2	TiO2	ZnO	ZrO2	SrO	B2O3	Li2O	Total
1	15.14	0.53	7.08	0.23	0.99	13.36	0.00	0.82	39.80	0.00	0.59	1.29	2.37	14.79	3.00	100.00
2	15.85	0.53	7.13	0.23	0.85	12.32	0.00	1.01	39.95	0.00	0.59	1.40	2.34	14.79	3.00	100.00
3	15.95	0.69	7.57	0.24	0.89	11.77	0.00	0.85	40.77	0.33	0.00	1.06	2.09	14.79	3.00	100.00
4	16.14	0.54	6.99	0.23	0.87	13.06	0.00	0.72	40.68	0.00	0.00	1.04	1.93	14.79	3.00	100.00
5	15.53	0.54	7.32	0.23	1.00	12.51	0.00	1.15	40.16	0.32	0.00	1.04	2.40	14.79	3.00	100.00
Average in area	15.68	0.53	8.21	0.34	0.97	12.20	0.36	1.02	39.76	0.31	0.00	1.15	1.67	14.79	3.00	100.00
Average	15.72	0.56	7.22	0.23	0.92	12.60	0.00	0.91	40.27	0.13	0.24	1.17	2.22	14.79	3.00	100.00
Er/Re	1.98		2.1			0.8			1.4							

Sample KRI-21 CCC

	Al2O3	CaO	Fe2O3	K2O	MnO	Na2O	NiO	PbO	SO3	SiO2	TiO2	ZnO	ZrO2	SrO	B2O3	Li2O	Total
1	13.47	0.65	8.59	0.45	1.32	13.72	0.00	0.00	0.00	41.02	0.31	0.69	3.38	1.31	11.83	3.29	100.02
2	14.17	0.67	7.14	0.35	1.12	13.86	0.00	0.00	0.00	43.01	0.00	0.00	3.12	1.48	11.83	3.29	100.02
3	13.99	0.52	7.09	0.45	0.85	13.13	0.00	0.00	0.47	42.74	0.31	0.70	3.42	1.22	11.83	3.29	100.02
4	13.64	0.54	7.70	0.35	1.24	12.84	0.00	0.62	0.00	42.44	0.32	0.00	3.51	1.71	11.83	3.29	100.02
5	13.62	0.52	6.95	0.34	1.09	13.74	0.00	0.60	0.00	42.87	0.31	0.70	3.16	1.00	11.83	3.29	100.02
Average in area	13.97	0.54	8.20	0.35	1.38	12.19	0.37	0.00	0.00	43.31	0.32	0.00	2.89	1.38	11.83	3.29	100.02
Average	13.78	0.58	7.49	0.39	1.12	13.46	0.00	0.25	0.09	42.41	0.25	0.42	3.32	1.34	11.83	3.29	100.02
Er/Re	1.5		3.4			0.7				4.0							

Sample KRI-22 CCC

	Al2O3	CaO	Fe2O3	K2O	MnO	Na2O	SiO2	TiO2	ZnO	ZrO2	SrO	B2O3	Li2O	Total
1	16.20	0.27	7.29	0.23	0.87	10.77	41.23	0.64	0.48	3.12	2.39	11.52	5.00	100.02
2	15.86	0.27	7.25	0.24	0.76	10.78	41.57	0.81	0.00	3.43	2.54	11.52	5.00	100.02
3	15.73	0.27	6.63	0.23	0.87	11.60	41.22	0.81	0.60	3.01	2.52	11.52	5.00	100.02
4	15.95	0.27	7.26	0.00	0.87	11.11	41.07	0.64	0.00	3.50	2.83	11.52	5.00	100.02
5	15.97	0.27	6.99	0.00	0.99	11.51	41.11	0.80	0.00	3.24	2.61	11.52	5.00	100.02
Average in area	15.53	0.26	7.42	0.00	0.85	11.33	40.45	0.79	0.71	3.44	2.23	11.52	5.00	100.02
Average	15.94	0.27	7.08	0.14	0.87	11.16	41.24	0.74	0.22	3.26	2.58	11.83	3.29	100.02
Er/Re	0.86		1.39			0.66	0.99							

Sample KRI-23 CCC

	Al2O3	CaO	Fe2O3	K2O	MnO	Na2O	PbO	SO3	SiO2	TiO2	ZnO	ZrO2	SrO	B2O3	Li2O	Total
1	18.09	0.00	5.38	0.61	0.92	9.19	0.99	0.00	45.99	0.00	0.63	1.51	1.08	12.60	3.00	100.00
2	18.11	0.14	5.78	0.59	0.89	11.44	0.74	0.00	43.13	0.33	0.00	1.60	1.63	12.60	3.00	100.00
3	17.56	0.00	4.84	0.58	0.87	11.73	0.73	0.00	44.12	0.32	0.60	1.44	1.60	12.60	3.00	100.00
4	17.99	0.00	5.55	0.82	1.13	10.73	0.00	0.49	43.46	0.32	0.60	1.71	1.61	12.60	3.00	100.00
5	18.61	0.00	4.49	0.73	1.05	11.08	0.00	0.51	46.07	0.00	0.63	1.23	0.00	12.60	3.00	100.00
Average in area	17.23	0.27	7.42	0.59	1.01	10.56	0.63	0.00	43.85	0.00	0.73	1.06	1.04	12.60	3.00	100.00
Average	18.07	0.03	5.21	0.67	0.97	10.84	0.49	0.20	44.55	0.20	0.49	1.50	1.18	11.83	3.29	100.00
Er/Re	1.87		2.65			1.66			6.97							

Sample KRI-24 CCC

	Al2O3	CaO	Fe2O3	K2O	MnO	Na2O	NiO	PbO	SiO2	TiO2	ZnO	ZrO2	SrO	B2O3	Li2O	Total
1	13.00	0.40	7.91	0.58	1.85	10.30	0.36	0.62	44.18	0.48	1.07	3.61	2.14	9.69	3.77	100.00
2	13.03	0.40	7.11	0.58	1.48	11.22	0.00	0.82	44.88	0.48	0.83	3.62	2.04	9.69	3.77	100.00
3	13.48	0.40	6.25	0.69	1.47	11.27	0.00	0.82	45.39	0.63	1.18	3.34	1.57	9.69	3.77	100.00
4	13.02	0.54	6.93	0.58	1.63	9.93	0.00	0.94	46.31	0.65	0.97	3.28	1.72	9.69	3.77	100.00
5	12.82	0.41	7.30	0.59	1.78	9.93	0.00	0.85	46.51	0.49	1.10	3.32	1.39	9.69	3.77	100.00
Average in area	12.56	0.39	7.51	0.56	1.79	11.81	0.47	0.99	43.86	0.62	0.92	3.24	1.53	9.69	3.77	100.00
Average	13.07	0.43	7.10	0.60	1.64	10.53	0.07	0.81	45.46	0.55	1.03	3.43	1.77	11.83	3.29	100.02
Er/Re	1.22		3.02			1.12			4.89							

Sample KRI-25 CCC

	Al2O3	CaO	Fe2O3	K2O	MnO	Na2O	SiO2	TiO2	ZnO	ZrO2	SrO	B2O3	Li2O	Total
1	16.24	0.26	6.80	0.68	1.21	12.84	40.99	0.31	0.00	1.77	1.66	13.50	3.75	100.00
2	15.91	0.00	9.06	0.72	0.90	12.28	42.42	0.00	0.00	1.47	0.00	13.50	3.75	100.00
3	15.84	0.27	9.05	0.59	1.13	12.08	41.53	0.33	0.61	1.32	0.00	13.50	3.75	100.00
4	15.49	0.27	8.26	0.70	0.87	13.90	41.90	0.32	0.00	1.04	0.00	13.50	3.75	100.00
5	15.87	0.27	8.82	0.58	1.00	11.32	41.54	0.32	0.00	1.43	1.60	13.50	3.75	100.00
Average in area	15.76	0.26	9.66	0.67	1.08	12.86	39.47	0.31	0.00	1.38	1.31	13.50	3.75	100.00
Average	15.87	0.21	8.40	0.65	1.02	12.48	41.68	0.26	0.12	1.41	0.65	11.83	3.29	100.02
Er/Re	1.34		4.74			1.60	2.63							

Sample KRI-26 CCC

	Al2O3	CaO	Fe2O3	Na2O	SO3	SiO2	SrO	UO3	B2O3	Li2O	Total
1	11.35	0.79	6.30	15.94	0.23	44.61	2.66	1.92	10.19	6.00	100.00
2	11.28	0.86	6.32	15.67	0.00	45.16	2.80	1.73	10.19	6.00	100.00
3	11.63	0.85	6.34	14.82	0.50	45.58	2.15	1.94	10.19	6.00	100.00
4	11.47	0.96	6.57	14.91	0.24	44.65	3.01	2.00	10.19	6.00	100.00
5	11.47	0.83	6.54	14.61	0.25	45.37	2.70	2.03	10.19	6.00	100.00
Average in area	11.04	0.77	9.13	14.64	0.46	42.02	2.27	1.87	10.19	6.00	100.00
Average	11.44	0.86	6.41	15.19	0.25	45.07	2.66	1.92	10.19	6.00	100.00
Er/Re	1.04		0.86	0.96		2.16					

Sample KRI-27 CCC

	Al2O3	CaO	Fe2O3	MnO	Na2O	PbO	SiO2	TiO2	ZnO	ZrO2	UO3	B2O3	Li2O	
1	10.97	0.83	7.45	0.51	10.74	0.95	38.97	1.31	0.00	4.39	0.95	17.20	5.73	100.00
2	10.97	0.79	7.76	0.60	11.74	1.01	37.50	1.41	0.00	4.17	1.13	17.20	5.73	100.00
3	11.29	0.84	7.40	0.51	11.00	1.18	38.16	1.33	0.00	4.17	1.20	17.20	5.73	100.00
4	10.92	0.84	7.54	0.51	10.61	1.07	38.61	1.33	0.00	4.44	1.20	17.20	5.73	100.00
5	10.96	0.84	7.42	0.52	10.77	1.18	38.52	1.33	0.00	4.32	1.20	17.20	5.73	100.00
Average in area	10.74	0.79	8.66	0.61	10.72	1.02	37.50	1.26	0.00	3.96	1.02	17.20	5.73	100.00
Average	11.02	0.82	7.51	0.53	10.97	1.08	38.35	1.34	0.00	4.30	1.13	17.20	5.73	100.00
Er/Re	1.16		0.98		0.75		2.80							

Sample KRI 28 CCC

# in photo		Al2O3	CaO	Cr2O3	FeO	Fe2O3	MnO	Na2O	NiO	PbO	SO3	SiO2	TiO2	ZnO	ZrO2	SrO	UO3	Total
T	Average	18.71	nd	0.44	3.86	0.00	2.97	18.46	nd	1.29	0.25	38.33	1.17	nd	nd	nd	2.40	87.89
1	spinel	0.76	nd	14.77	0.00	37.46	43.28	nd	nd	nd	nd	nd	4.51	nd	nd	nd	nd	100.77
5	spinel	1.13	nd	11.26	30.37	0.00	38.89	nd	nd	nd	nd	nd	4.17	nd	nd	nd	nd	85.83
2	white phase	1.51	nd	nd	4.12	0.00	3.49	10.92	nd	3.88	1.75	20.56	3.34	nd	nd	nd	10.82	60.38
8	white phase	2.84	nd	nd	4.25	0.00	3.49	14.02	nd	3.88	2.00	23.13	3.34	nd	nd	nd	9.98	66.91
3	nepheline	33.84	nd	nd	2.32	0.00	nd	19.95	nd	nd	nd	41.54	nd	nd	nd	nd	nd	97.64
6	nepheline н	31.00	nd	nd	2.57	0.00	nd	19.41	nd	nd	nd	39.61	nd	nd	nd	nd	nd	92.60
7	black – SiO2	nd	nd	nd	0.39	0.00	0.52	nd	nd	nd	nd	73.45	nd	nd	nd	nd	nd	74.35

Sample KRI-29 CCC

	Al2O3	Fe2O3	K2O	Na2O	NiO	PbO	SiO2	TiO2	SrO	UO3	B2O3	Li2O	Total
1	14.89	5.56	0.84	20.56	0.51	0.86	37.58	1.17	1.65	3.00	11.38	2.00	100.00
2	14.55	5.36	0.83	20.75	0.63	1.17	37.20	1.15	1.63	3.32	11.38	2.00	100.00
3	14.89	5.49	0.83	20.44	0.88	1.06	36.69	1.15	1.86	3.31	11.38	2.00	100.00
4	14.51	5.84	0.84	20.42	0.63	1.18	37.14	1.16	1.89	2.99	11.38	2.00	100.00
5	14.97	5.45	0.82	20.42	0.62	1.16	36.84	1.31	1.50	3.52	11.38	2.00	100.00
Average in area	15.12	5.44	0.82	19.59	1.74	0.74	36.77	1.14	1.73	3.52	11.38	2.00	100.00
Average	14.76	5.54	0.83	20.52	0.65	1.09	37.09	1.19	1.71	3.23	11.38	2.00	100.00
Er/Re	1.64	1.22		0.24			1.72						

Sample KRI-30 CCC

	Al2O3	CaO	Fe2O3	K2O	Na2O	NiO	PbO	SO3	SiO2	TiO2	ZnO	SrO	UO3	B2O3	Li2O	Total
1	16.71	0.27	3.29	0.35	12.82	0.00	1.35	0.00	37.86	0.48	0.72	1.70	3.35	15.30	5.79	100.00
2	16.85	0.39	4.38	0.34	13.01	0.00	1.00	0.00	36.18	0.62	1.04	2.08	3.01	15.30	5.79	100.00
3	17.30	0.40	5.09	0.35	11.16	0.37	0.93	0.24	36.71	0.32	1.20	1.94	2.89	15.30	5.79	100.00
4	16.96	0.26	5.13	0.34	12.47	0.84	1.12	0.00	35.39	0.47	1.06	2.01	2.84	15.30	5.79	100.00
5	17.07	0.27	5.16	0.34	11.66	0.60	1.23	0.00	36.03	0.48	0.83	2.02	3.20	15.30	5.79	100.00
Average in area	16.89	0.40	5.02	0.34	11.27	0.85	0.92	0.24	36.22	0.48	0.95	2.25	3.08	15.30	5.79	100.00
Average	16.98	0.32	4.61	0.34	12.23	0.36	1.13	0.05	36.44	0.47	0.97	1.95	3.06	15.30	5.79	100.00
Er/Re	1.71		5.36		1.31				4.62							

Attachment 7. XRD Data for Glasses after CCC Treatment

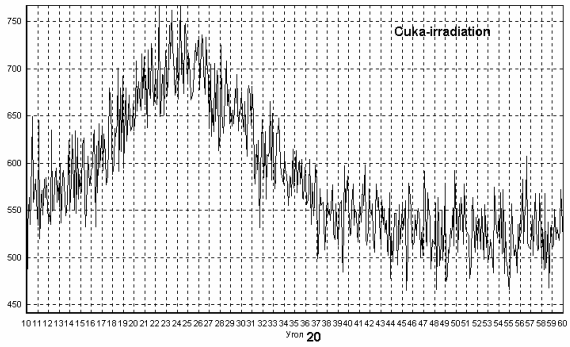

KRI-01 CCC

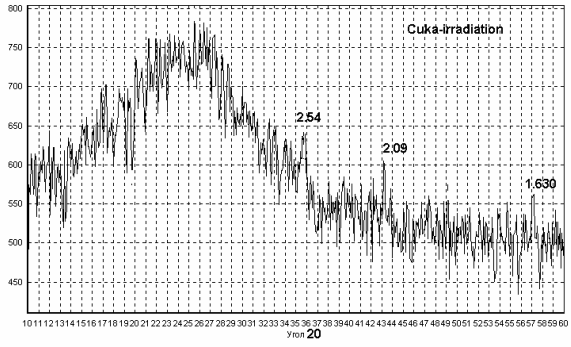

KRI-02 CCC

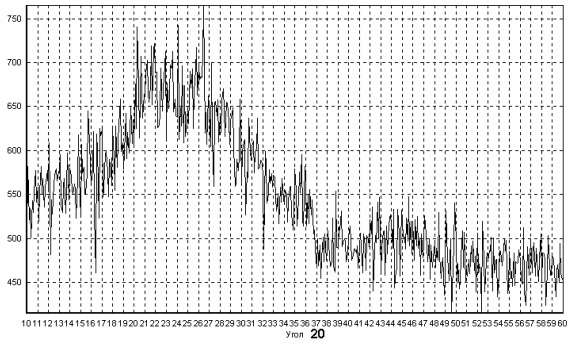

KRI-03 CCC

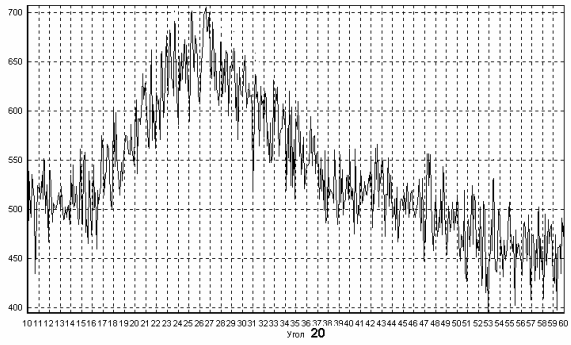

KRI-04 CCC

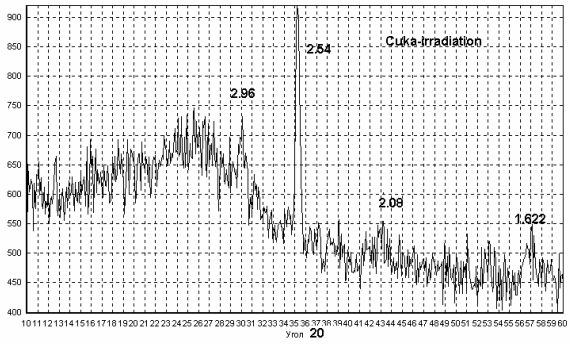

KRI-05 CCC

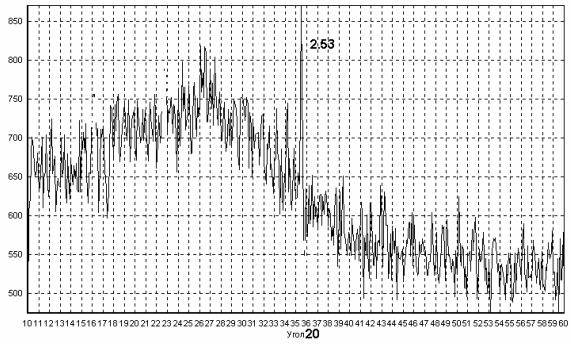

KRI-06 CCC

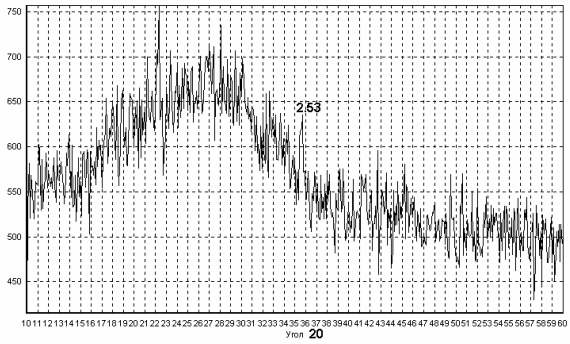

KRI-07 CCC

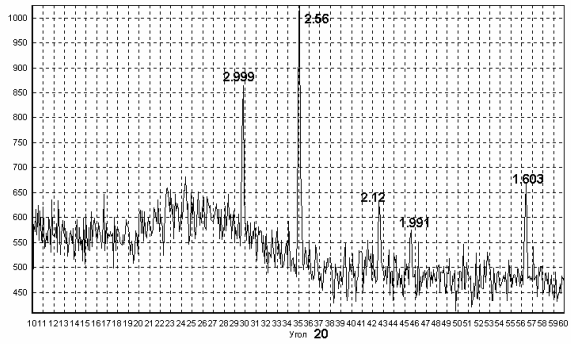

KRI-08 CCC

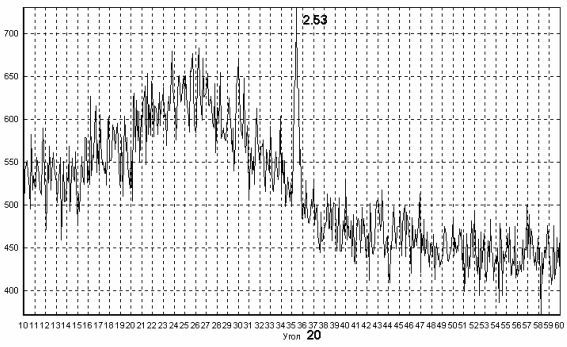

KRI-09 CCC

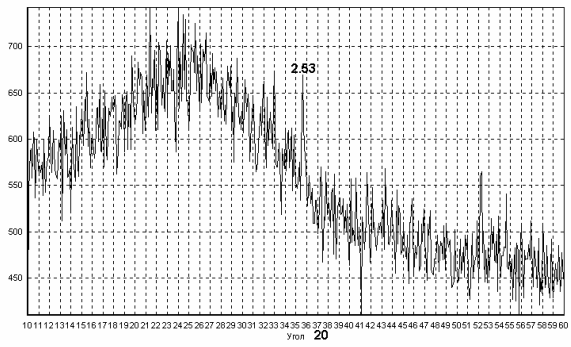

KRI-10 CCC

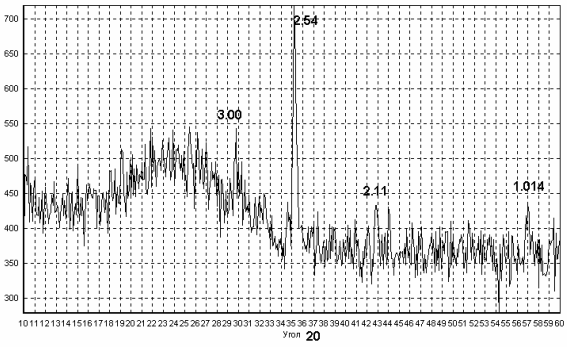

KRI-11 CCC

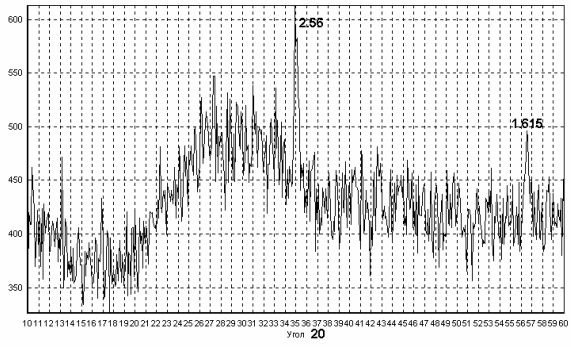

KRI-12 CCC

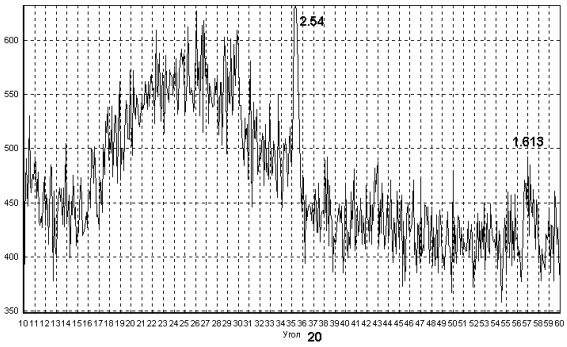

KRI-13-CCC

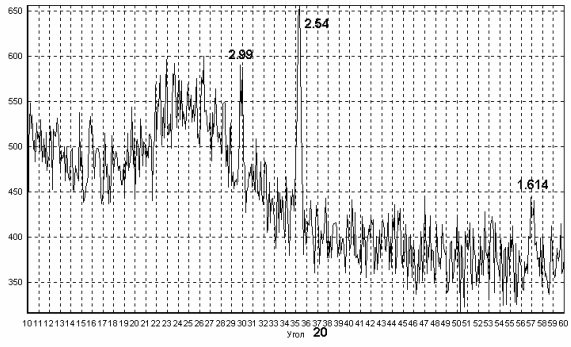

KRI-14-CCC

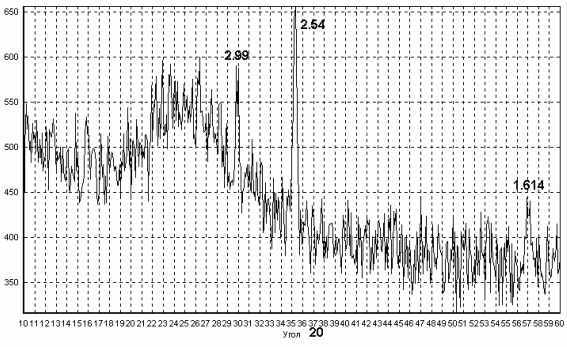

KRI-15 CCC

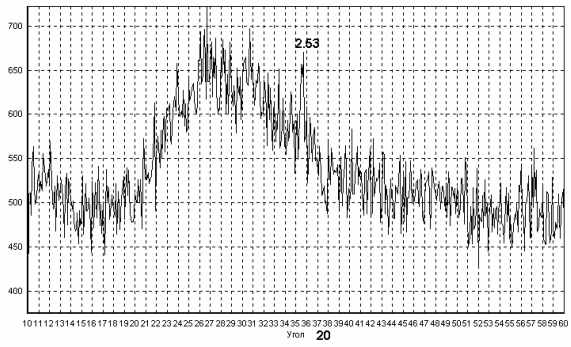

KRI-16 CCC

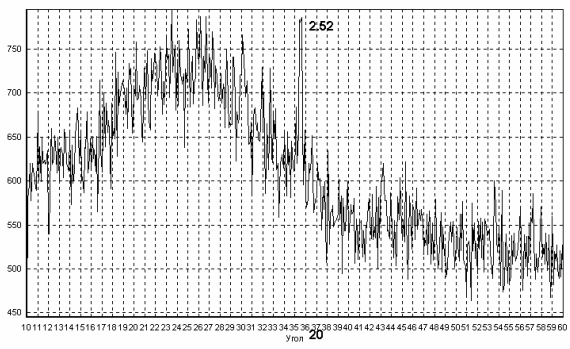

KRI-17 CCC

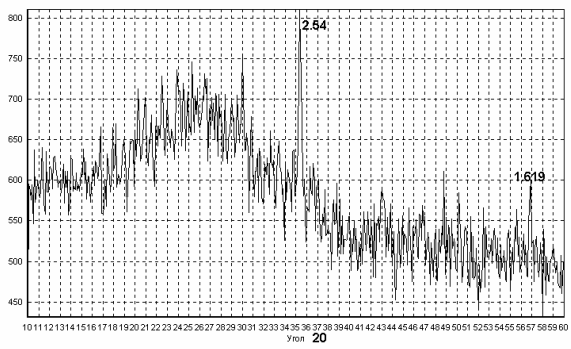

KRI-18 CCC

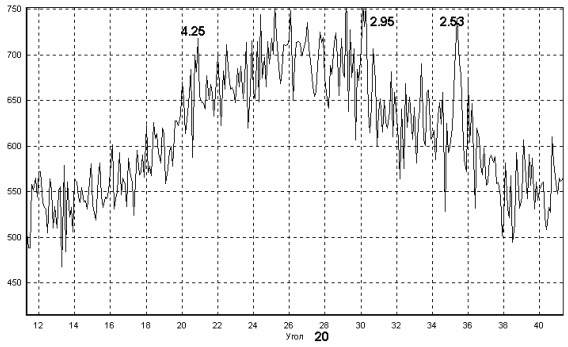

KRI-19 CCC

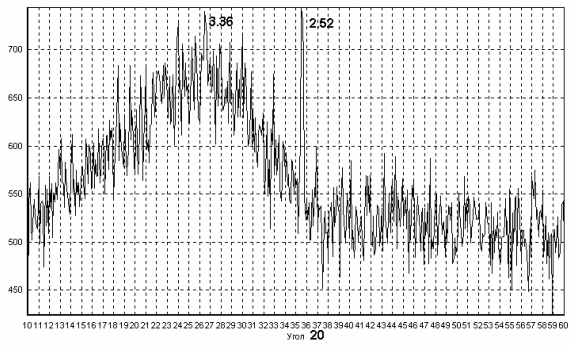

KRI-20 CCC

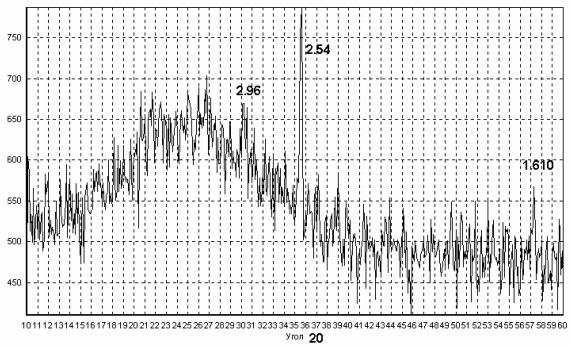

KRI-21 CCC

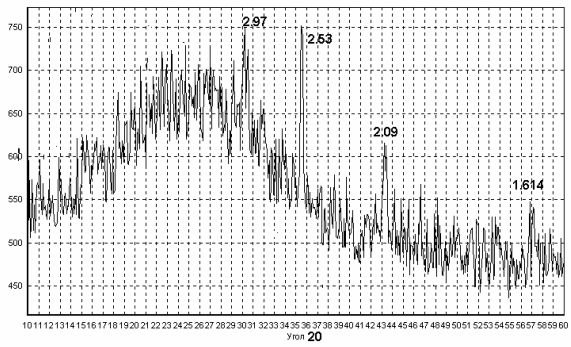

KRI-22 CCC

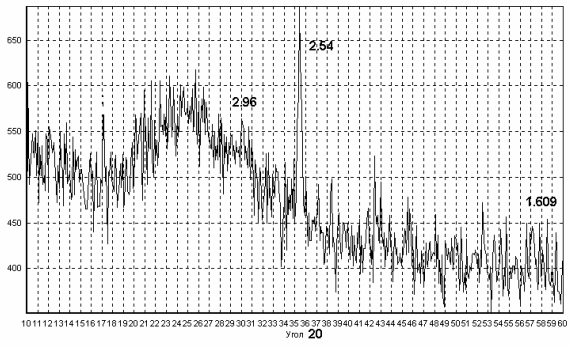

KRI-23 CCC

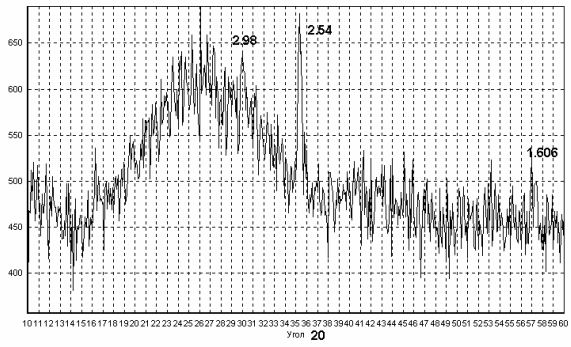

KRI-24 CCC

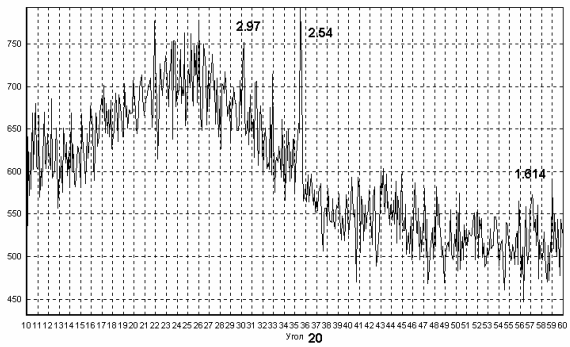

KRI-25 CCC

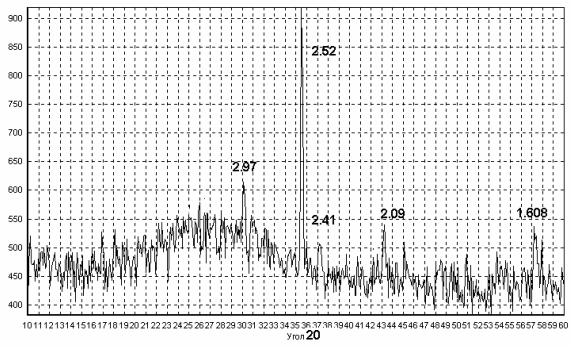

KRI-26 CCC

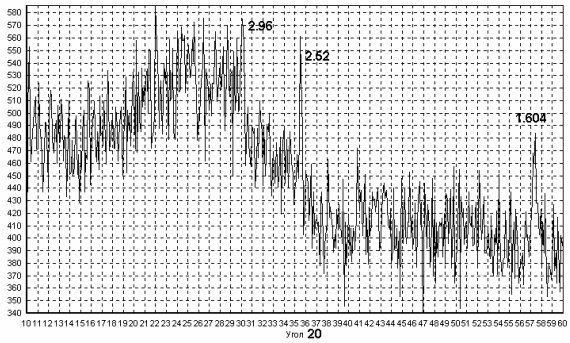

KRI-27 CCC

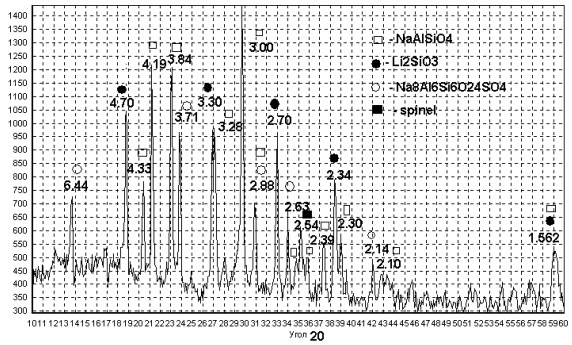

KRI-28 CCC

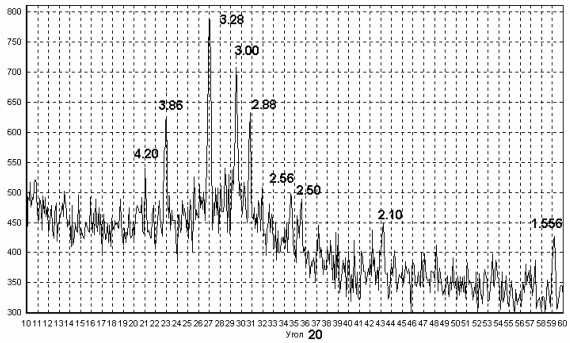

KRI-29 CCC

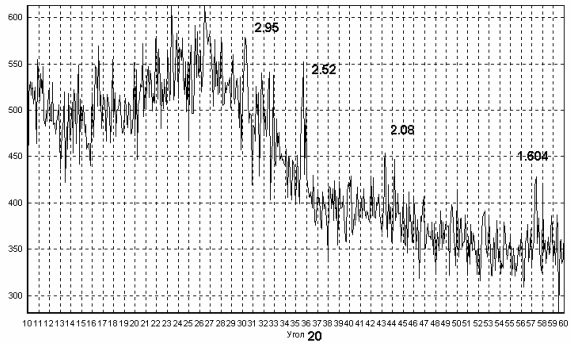

KRI-30 CCC